

# **Mango (*Mangifera indica* L.) Flavor Biogenesis: Metabolic Profiling and Molecular Analysis**

Thesis Submitted to AcSIR  
for the Award of the Degree of

**Doctor of Philosophy**

In

**BIOLOGICAL SCIENCES**



By

***Deshpande Ashish Balwant***

10BB11J26126

Under the guidance of

**Dr. Vidya S. Gupta (Research supervisor)**

**Dr. Ashok P. Giri (Research co-supervisor)**



Biochemical Sciences Division  
CSIR-National Chemical Laboratory

Pune 411008, India

2017



*Dedicated to my parents*

*and*

*All researchers who  
contributed to the field of  
plant metabolomics and  
molecular biology*







सीएसआईआर - राष्ट्रीय रासायनिक प्रयोगशाला

(वैज्ञानिक तथा औद्योगिक अनुसंधान परिषद)

डॉ. होमी भाभा मार्ग, पुणे - 411 008. भारत



CSIR - NATIONAL CHEMICAL LABORATORY

(Council of Scientific & Industrial Research)

Dr. Homi Bhabha Road, Pune - 411 008. India

## Certificate

This is to certify that the work incorporated in this Ph.D. thesis entitled “**Mango (*Mangifera indica* L.) Flavor Biogenesis: Metabolic Profiling and Molecular Analysis**” submitted by **Mr. Deshpande Ashish Balwant** to Academy of Scientific and Innovative Research (AcSIR) in fulfillment of the requirements for the award of the Degree of **Doctor of Philosophy**, embodies original research work under our guidance. We further certify that this work has not been submitted to any other University or Institution in part or full for the award of any degree or diploma. Research material obtained from other sources has been duly acknowledged in the thesis. Any text, illustration, table etc., used in the thesis from other sources, have been duly cited and acknowledged.

Deshpande Ashish Balwant  
(Student)

Dr. Ashok P. Giri  
(Research co-supervisor)

Dr. Vidya S. Gupta  
(Research supervisor)

Date: 23/03/2017

Place: Pune



## **Declaration by Research Scholar**

I hereby declare that thesis entitled “**Mango (*Mangifera indica* L.) Flavor Biogenesis: Metabolic Profiling and Molecular Analysis**” submitted by me for the Degree of Doctor of Philosophy to Academy of Scientific and Innovative Research (AcSIR) is the record of work carried out by me at Biochemical Sciences Division, CSIR-National Chemical Laboratory, Pune-411008, India, under the supervision of Dr. Vidya S. Gupta. The work is original and has not formed the basis for the award of any degree, diploma, associateship and/or fellowship titles in this or any other University or Institution. I further declare that the material from other sources has been duly acknowledged in the thesis.

Deshpande Ashish Balwant

(Student)

Date: 23/03/2017

Place: Pune





## Acknowledgement



I would like to express my special appreciation and thanks to my research advisor Dr. Vidya S. Gupta, she has been a fabulous mentor for me. I would like to thank her for her guidance, support, encouragement and the freedom that she gave me to think and work throughout my doctoral studies, which helped me to grow as a better researcher. Her advice on both research as well as on my career have been priceless.



I would also like to thank Dr. Ashok Giri my research co-advisor, and Dr. Narendra Kadoo for their advice in planning the research and constant encouragement during my work.



My special thanks to Ms. Anamika and Mr. Vinit Jha (Persistent System Ltd., Pune, India) for their help during transcriptomic analysis. Also, I would like to thank Dr. Aarti Desai for her initial inputs and Dr. Abhay Jere for his support during the discussion regarding bioinformatic data analysis.



I thank Dr. K. H. Pujari and Mr. Kiran Malashe (Dr. Balasaheb Sawant Kokan Krishi Vidyapeeth) for their generous help in mango sample collection.

I am grateful to Dr. Shantakumari and Dr. Mahesh Kulkarni for their help during various experiments.

I would also like to thank my Doctoral Advisory Committee members, Dr. G. J. Sanjayan, Dr. Archana Pundle and Dr. C. G. Suresh for serving as my

committee members and for their brilliant comments and timely suggestions.

My sincere thanks also goes to Prof. Kothadiya, Prof. Sujata, Ms Harshini, Mr. Maradkar and all my respected teachers for inspiring me throughout my education.





Ashwini Kumar Nangia, Director and Dr. Saurav Pal, Ex- Director, CSIR-NCL for providing me the research facilities. I am thankful to staff of SAC office and Biochemical Sciences Division at CSIR-NCL for their help during AcSIR documentation.

I would like to offer my special thanks to my dear project mates, Ram and Hemangi for their constant help, support and inputs in deciding my thesis objectives. My deepest appreciation goes to Pranjali for her constant support filled with energy and supplemented with entertainment during various experiments. My special thanks to Pranjali, Gouri and Amol for making my hectic tissue collection trips easy and enjoyable.

I am grateful to U.G.C. for my research fellowship and CSIR for research grant. I also feel happy to express my thanks to Prof.

Very special thanks to my friends Sheon, Rahul, Gouri, Amey, Aditi, Sachin, Tejas and Reema for their support all the time. It is impossible to forget our enjoyed moments during trips, cooking and of course while working in lab. I would like to also thank my batch mates Sheon, Ruchira, Sayli, Deepak and Priya for all the information, course work, CSIR-800 and AcSIR document preparation. With a special mention to Sheon, it was wonderful sharing table with her while writing thesis and working on a word template which made my thesis writing very easy.

It is a  
pleasure to  
thank all  
my  
labmates  
Dr. Vishal  
Dawkar,

Dr.

Bhushan

Dholakia,

Dr. Ashwini

Rajwade,

Dr. Gayatri

Gurjar, Dr.

Rasika

Bhagwat,

Dr.

Yashwant

Kumar, Dr.

Ramya, Dr.

Purushotta

m, Amey,

Sheon,

Rahul,

Neha K.,

Neha M.,

Manasi,

Medha,

Priya, Ajit,

Tejas, Pranjali, Sonal, Balkrishna, Sucheta,  
Smriti, Swapnil, Vaishnavi, Bhakti, Neha J.,  
Nidhi, Rakesh, Yojana, Ranjit, Saleem,  
Ramesha, Gayatri, Santosh, Gauri, Gopal,  
Radhika, Amol K, Amol J, Uma and all other lab  
members, it was great sharing PMB laboratory  
with all of them.



Words cannot express the feelings I have for my parents (Aai and Baba) and my Dada-Vahini for their constant unconditional emotional, spiritual and financial support. I would also like to thank my grandparents and whole family for their support all the time.

Ashish

A big  
“Thank  
you!” also  
goes out to  
my dear  
friends  
Kunal,  
Vishal and  
Priyank  
who have  
been there  
for any  
kind of help  
since last  
13 years.



# Table of Contents

## Contents

### Certificate 5

Declaration by Research Scholar -----	7
Acknowledgement -----	9
List of Tables -----	18
List of Figures -----	19
List of Accompanying Material -----	21
List of Abbreviations -----	23
Chapter 1 General Introduction and Review of Literature-----	27
1.1 Flavor: A combined perception -----	27
1.2 Aroma compounds and their perception -----	28
1.3 Fruit ripening -----	30
1.3.1 Biochemical changes -----	31
1.3.2 Changes in fruit physiology -----	32
1.3.3 Generation of aroma volatiles -----	33
1.4 Mango: The king of fruits-----	35
1.5 Biochemical characterization of mango flavor -----	38
1.5.1 Deciphering the volatile diversity of mango cultivars -----	38
1.5.2 Development and ripening of mango: A flavouring volatile perspective -----	40
1.6 Molecular characterization of mango genes-----	42
1.6.1 Differential expression of genes during development and ripening of mango-----	42
1.6.2 Aroma volatile biosynthesis in mango-----	44
Genesis of thesis and its organization -----	50
Chapter 2 Changes in fatty acid composition during fruit development and ripening of three mango cultivars (Alphonso, Pairi and Kent) varying in lactone content -----	53
2.1 Introduction -----	53
2.2 Materials and methods-----	55
2.2.1 Plant material -----	55
2.2.2 Transesterification of fatty acids-----	55
2.2.3 Extraction of aroma volatiles-----	56
2.2.4 Gas chromatography analysis -----	56
2.2.5 Statistical analysis-----	57
2.3 Results -----	58
2.3.1 Fatty acid composition of mango pulp and skin -----	58
2.3.2 Variation in total fatty acid content of three mango cultivars -----	58

2.3.3	Saturated fatty acids -----	64
2.3.4	Unsaturated fatty acids -----	65
2.3.5	Principle component analysis-----	68
2.3.6	Lactone content of three cultivars at ripe stage -----	70
2.4	Discussion-----	71
2.4.1	Origin of unusual fatty acids-----	71
2.4.2	Fatty acids from mango fruit and their nutritional significance -----	72
2.4.3	Fatty acid content and flavor qualities of mango cultivars -----	73
2.5	Conclusion -----	76
Chapter 3	Isolation and characterization of <i>9-lipoxygenase</i> and <i>epoxide hydrolase 2</i> genes: Insight into lactone biosynthesis in mango fruit ( <i>Mangifera indica</i> L.)-----	79
3.1	Introduction -----	79
3.2	Materials and methods-----	81
3.2.1	Plant material -----	81
3.2.2	RNA isolation and cDNA synthesis -----	81
3.2.3	Isolation of open reading frames of <i>Mi9LOX</i> , <i>MiHPL</i> , <i>MiPGX1</i> , <i>MiEH2</i> and <i>MiACO</i> -----	82
3.2.4	Quantitative real-time PCR -----	83
3.2.5	Cloning and recombinant expression of <i>Mi9LOX</i> and <i>MiEH2</i> in <i>E. coli</i> ----	83
3.2.6	Enzyme assays of recombinant <i>Mi9LOX</i> and <i>MiEH2</i> -----	85
3.2.7	Transient over expression of <i>Mi9LOX</i> and <i>MiEH2</i> in Alphonso mango fruits-----	86
3.2.8	Qualitative and quantitative analysis of metabolites -----	87
3.2.9	Statistical analysis-----	88
3.3	Results -----	88
3.3.1	<i>In silico</i> analysis of isolated genes from <i>Mangifera indica</i> L.-----	88
3.3.2	Expression of <i>Mi9LOX</i> , <i>MiHPL</i> , <i>MiPGX1</i> , <i>MiEH2</i> and <i>MiACO</i> in fruits of three mango cultivars-----	89
3.3.3	Heterologous expression and catalytic activities of proteins encoded by <i>Mi9LOX</i> and <i>MiEH2</i> -----	93
3.3.4	Transient over-expression of <i>Mi9LOX</i> and <i>MiEH2</i> resulted in elevated lactone levels in mango fruit-----	99
3.4	Discussion-----	101
3.4.1	<i>Mi9LOX</i> and <i>MiEH2</i> reveal catalytic properties similar to those of other plant 9LOX and EH2 enzymes-----	101
3.4.2	Role of <i>Mi9LOX</i> and <i>MiEH2</i> in biosynthesis of lactones in Alphonso mango-----	102



3.4.3	Temporal expression of <i>Mi9LOX</i> , <i>MiHPL</i> , <i>MiPGXI</i> , <i>MiEH2</i> and <i>MiACO</i> genes correlates with variable lactone content in fruit of mango cultivars-----	103
3.4.4	Proposed lactone biosynthesis pathway in mango -----	104
3.5	Conclusion -----	105
Chapter 4	Transcriptional transitions in Alphonso mango ( <i>Mangifera indica</i> L.) during fruit development and ripening explain distinct aroma and shelf life characteristics -----	109
4.1	Introduction -----	109
4.2	Materials and methods-----	110
4.2.1	Plant material -----	110
4.2.2	RNA isolation and cDNA synthesis-----	111
4.2.3	Library preparation and sequencing-----	111
4.2.4	Bioinformatic data analysis-----	112
4.2.5	Quantitative real-time PCR-----	113
4.3	Results -----	113
4.3.1	Alphonso mango transcriptome-----	113
4.3.2	Transcriptome changes through flower to fruit and fruit development to ripening -----	117
4.3.3	Spatial changes in transcriptome at 90 DAP -----	123
4.3.4	Genes involved in the flavor biogenesis in Alphonso mango -----	124
4.3.5	Glycosidases and cell wall degrading enzymes from Alphonso mango ----	132
4.3.6	Transcriptome analysis identified novel enzyme inhibitors from Alphonso mango -----	133
4.3.7	Transcriptome validation through qPCR -----	135
4.4	Discussion-----	138
4.4.1	Novel flavor related genes from Alphonso mango transcriptome -----	138
4.4.2	Possible role of various enzyme inhibitors in slow ripening and longer shelf life of Alphonso mango fruit-----	139
4.4.3	Defence mechanism in Alphonso from flower to fruit -----	142
4.5	Conclusion -----	142
	Summary and Future Directions -----	143
	Bibliography -----	149
	Appendices-----	168
	Curriculum Vitae-----	182

## List of Tables

Table 1.1 Perception of aroma compounds-----	29
Table 1.2 Odor detection threshold values -----	30
Table 1.3 Examples of climacteric and non-climacteric fruits-----	32
Table 1.4 List of fruit pigments responsible for various colors-----	33
Table 2.1 Fatty acid composition of mango pulp-----	61
Table 2.2 Fatty acid composition of skin -----	62
Table 2.3 Lactone content of ripe fruit-----	70
Table 2.4 Flavor and nutritional perspective of fatty acids-----	73
Table 2.5 Correlation analysis 1-----	75
Table 2.6 Correlation analysis 2-----	76
Table 3.1 List of primers used in the study-----	84
Table 3.2 Biochemical characterization and enzyme kinetics -----	97
Table 4.1 Number of non redundant transcripts/sample -----	114
Table 4.2 Number of differentially expressed transcripts -----	118
Table 4.3 Number of distinct transcripts for a stage amid various comparisons-----	121

## List of Figures

Figure 1.1	Flavor: A combined perception-----	28
Figure 1.2	Biochemical and physiological changes during fruit ripening-----	30
Figure 1.3	Composition of aroma volatiles in various fruits -----	34
Figure 1.4	Major mango producing countries across world-----	36
Figure 1.5	Mango production and export statistics -----	36
Figure 1.6	Famous mango cultivars from different parts of India -----	37
Figure 1.7	Total volatile content of various mango cultivars -----	39
Figure 1.8	Total volatile content of various Alphonso tissues -----	41
Figure 1.9	Cytosolic and plastidial IPP and DMAPP biosynthesis pathways -----	45
Figure 1.10	Terpene biosynthesis pathway-----	45
Figure 1.11	Furanone biosynthesis -----	47
Figure 1.12	Ester biosynthesis pathway-----	48
Figure 2.1	Representative fatty acid chromatograms-----	59
Figure 2.2	MS spectra of odd chain and unusual fatty acid methyl esters-----	60
Figure 2.3	Fatty acid histogram-----	63
Figure 2.4	Radar plot representing contribution ( $\text{mgg}^{-1}$ ) of total fatty acids-----	64
Figure 2.5	Loading plot (a) and Score plot (b) of PCA -----	69
Figure 3.1	Phylogenetic analysis of <i>lipxygenase</i> and <i>epoxide hydrolase</i> genes-----	90
Figure 3.2	qPCR analysis from pulp tissue -----	91
Figure 3.3	qPCR analysis from skin tissue-----	92
Figure 3.4	Secondary structure prediction of <i>Mi9LOX</i> -----	93
Figure 3.5	Secondary structure prediction of <i>MiEH2</i> -----	94
Figure 3.6	Purified recombinant <i>Mi9LOX</i> and <i>MiEH2</i> -----	95
Figure 3.7	Recombinant enzyme activities of <i>Mi9LOX</i> -----	96
Figure 3.8	Biochemical characterisation of <i>Mi9LOX</i> and <i>MiEH2</i> -----	97
Figure 3.9	Recombinant enzyme activities of <i>MiEH2</i> -----	98
Figure 3.10	Agroinfiltration and Gus staining -----	99
Figure 3.11	Effect of transient over expression on transcripts and metabolites-----	100
Figure 3.12	Changes in the lactone content upon transient over expression -----	101
Figure 3.13	Proposed lactone biosynthesis pathway in mango fruit-----	104
Figure 4.1	Blast2GO statistics -----	115
Figure 4.2	Heatmap representing expression profiles of various gene ontologies ----	116
Figure 4.3	Enzyme code distribution -----	117
Figure 4.4	Distribution of common and distinct transcripts-----	120
Figure 4.5	Gene ontology enrichment -----	122

Figure 4.6	Phylogenetic analysis of terpene synthases -----	125
Figure 4.7	Phylogenetic analysis of transcripts encoding enone oxidoreductase-----	127
Figure 4.8	Phylogenetic analysis of transcripts encoding O-methyltransferase -----	128
Figure 4.9	Phylogenetic analysis of transcripts encoding lipoxygenase -----	129
Figure 4.10	Phylogenetic analysis of transcripts encoding epoxide hydrolase -----	130
Figure 4.11	Heat map representing differential expression of flavor related genes ----	131
Figure 4.12	Heat map representing differential expression of various inhibitors -----	134
Figure 4.13	Real time validation data of various transcripts -----	136
Figure 4.14	Real time validation of various transcripts from terpene metabolism ----	137
Figure 4.15	Balance between pectinesterase enzyme and its inhibitor -----	141

## List of Accompanying Material

All the supplemental data for Chapter 4 is provided along with this thesis in the form of soft copy in CD attached to the last page

**Annexure 1\_Supplementary file 1:** Alphonso *de novo* transcriptome assembly statistics. (.xlsx)

**Annexure 1\_Supplementary file 2:** List of differentially regulated transcripts ( $p$ -value  $\leq 0.05$ ) amid various comparisons and their annotation. (.xlsx)

**Annexure 1\_Supplementary file 3:** List of distinct transcripts identified to a stage amid various comparisons and their annotation. (.xlsx)



## List of Abbreviations

°C	Degree Celsius
µm	Micro meter
µg	Micro gram
AAT	Alcohol acyltransferase
ADH	Alcohol dehydrogenase
ALA	α-linolenic acid
ATP	Adenosine triphosphate
BHT	Butylated hydroxytoluene
DAH	Days After Harvest
DAP	Days After Pollination
DCM	Dichloromethane
DTPS	Di-terpene synthases
EH	Epoxide hydrolase
EO	Enone oxidoreductase
FAMEs	Fatty acid methyl esters
FID	Flame ionisation detector
g	Gram
GC	Gas chromatography
HCl	Hydrochloric acid
HPL	Hydrperoxide lyase
i.d.	Internal diameter
LA	Linoleic acid
LOX	Lipoxygenase
m	Meter
mg	Milli gram
ml	Milli liter

mm	Milli meter
MS	Mass spectrometry
MTPS	Mono-terpene synthase
MTS	Methyltransferase
NIST	National Institute of Standards and Technology
ODT	Odor detection threshold
PCR	Polymerase chain reaction
PE	Pectin esterase
PG	Polygalacturonase
PL	Pectate lyase
qPCR	Quantitative polymerase chain reaction
rpm	Revolutions per minute
RT	Room temperature
STPS	Sesqui- terpene synthase
TPS	Terpene synthase





# Chapter 1

General Introduction

and

Review of Literature





---

## Chapter 1      General Introduction and Review of Literature

Life on the earth was assumed to be originated by the “Abiogenesis”, that is the process wherein first living form originated from non-living organic matter about 3.8 to 4.1 billion years ago (Bell et al., 2015). Organic matter such as methane, carbon dioxide, water, ammonia, hydrogen sulphide, oxygen and phosphates present in early earth’s atmosphere (extremely reducing) got converted in to the biological monomers, such as simple amino acids, sugars, fatty acids and nitrogenous bases. According to Bernal theory (Bernal, 1951) of biopoesis (origin of life) these biological monomers were responsible for origin of biological polymers, which further evolved in to the cells. Now, we have the complex world with millions of different species all of which are originated from single living form. During the course of evolution from single cell organisms to the most complex plant species and human race, basic things remained same such as nucleic acids as genetic material, proteins as functional molecules and carbohydrates, lipids along with proteins as structural components and source of energy in a cell. Of course each species is distinct from others with respect to its anatomy, physiology, reproduction, signalling or communication and many other aspects. This uniqueness of each species is due to various complex metabolic processes other than primary metabolism and called as secondary metabolic processes and one of such is flavor biogenesis in ripening fruits.

### 1.1 Flavor: A combined perception

Flavor is a term which describes sensory perception of particular food item by means of its taste, texture, visual appearance and aroma (Figure 1.1). Out of 5 senses of human *viz.* taste, vision, sound, touch and smell, except for sound all the other are responsible for combined perception of flavor. Amid these perception of taste is through taste buds present in the oral cavity and mainly on the tongue. Sweet, salty, bitter, sour and umami are five different types of tastes and recent studies have proposed fatty as the 6<sup>th</sup> taste (Mattes, 2009b). Similarly texture of food is sensory perception of touch and can be characterised in various classes such as soft, smooth, crunchy, hard, mushy and lumpy. Texture is considered important mainly for chewing and swallowing a particular food item. Third one is visual appearance of food, which is

associated with presentation or decoration of food or particular dish, but it is assumed to be mainly associated with color of food, as a study revealed increased redness in a drink is responsible for increased perception of sweetness though all the drinks were containing 1% sucrose (Johnson and Clydesdale, 1982). The last and the most important parameter of flavor is aroma or odor or smell of a food. It is the most important parameter as aroma of food can be sensed before we eat it or even see it. Another important fact is that humans are able to discriminate more than one trillion olfactory stimuli (Bushdid et al., 2014). This olfactory ability in humans is due to diversified olfactory receptor proteins which are coded by a family of about thousand genes (Malnic et al., 2004). Further these olfactory receptors are more sensitive (3,400 times) than taste receptors (Patel, 2014). That's the reason most of the flavor related studies were focused on analysis and biosynthesis of aroma compounds.

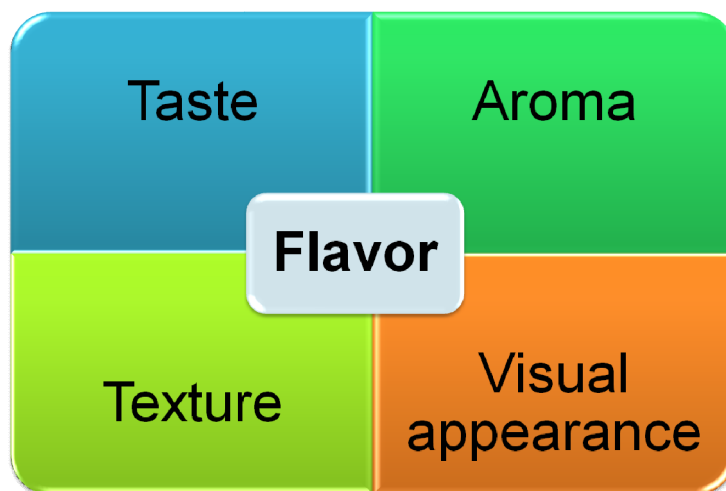


**Figure 1.1 Flavor: A combined perception**

## **1.2 Aroma compounds and their perception**

Smell is the sense of aroma compound mediated through air. Thus the basic requirement to smell a particular compound is that it should be volatile. An ability of a compound to vaporize at room temperature and mix in to the air is known as volatility, and compound is called as aroma volatile. A particular smell might be due to a single compound or group of compounds and can be described by various ways of olfactions like smell, taste or materials as described in Table 1.1. Not all volatile

compounds can be sensed and such compounds are called as anosmic, whereas others are responsible for mild to strong olfaction based on its concentration as well as odor detection threshold (ODT). ODT is a minimum concentration of a compound required to be sensed by human. Every compound has its own ODT, few examples as described in Table 1.2, lower the ODT more is the olfactory perception. Thus compounds with lower ODT are of great interest to the perfume and artificial food flavoring industries. These aroma compounds can be found in food, flower, essential oils (from spices, wood and seeds), wine and ripening fruits. Amid all these, ripening fruits show the highest diversity of aroma volatiles through various fruits and their ripening stages and always remain centre of attraction due to their commercial benefits as fresh fruits and various fruit products. Moreover, various food products with fruity aroma e.g. ice-creams, milk shakes, jams, cold drinks etc. have always remained as the first choice of consumers. Thus, scientists across the world have been working to understand biosynthesis and changes in the aroma volatile profiles of various fruits during their ripening.

**Table 1.1 Perception of aroma compounds**

Perception like	Type of smell	Examples
Smell	Fresh	Citrus fruits
	Aromatic	Gasoline
	Putrid	Old meat
	Rancid	Oxygenated fatty acids
	Foul	Decaying animals
	Stinking	Rotten fruits or leaves
Taste	Sweet	Esters, acetone
	Creamy	Delta octalactone
	Caramel	Burning sugars
	Buttery	Avocado or Shea butter
	Savory/spicy	Spices
Material/ Vision	Fruity	Various fruits
	Grassy	Green grass or leaves
	Floral	Flowers
	Woody	Smell in forest after rain
	Corky	New Furniture

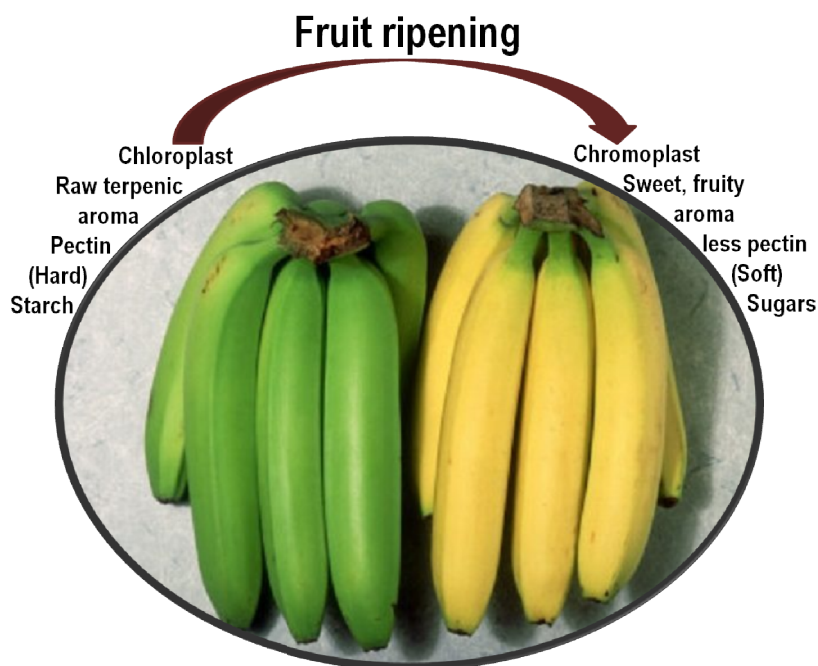
**Table 1.2 Odor detection threshold values**

Odor detection threshold values of few compounds in ppb (parts per billion)

Sr. No.	Compound	ODT value in ppb (Ho et al., 2015)
1	( <i>Z</i> )-3-hexenol	13
2	( <i>E</i> )-geraniol	3.2
3	2-Phenyl ethanol	1000
4	Hexanoic acid	890
5	Hotrienol	110
6	2,3-Butanedione	10
7	( <i>E,E</i> )-2,4-decadienal	0.16
8	Methional	0.2

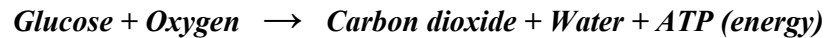
### 1.3 Fruit ripening

Fruit ripening is a very complex, irreversible but well harmonized process which involves changes in biochemical composition, physiology and organoleptic properties of fruits as summarized in Figure 1.2. These changes are finally responsible for softness, attractive color, and sweet fruity aroma of a ripe fruit (Prasanna et al., 2007).

**Figure 1.2 Biochemical and physiological changes during fruit ripening**

### 1.3.1 Biochemical changes

During fruit ripening various biochemical changes take place, which start with increased fruit respiration and ethylene production. Respiration is a biochemical process in which, cells of fruit convert glucose to carbon dioxide, water and energy (ATP) by using oxygen.



That is the reason during ripening of fruits significant increase in the carbon dioxide production is evinced in most of the fruit e.g. carbon dioxide production in Haden mango at harvest was  $20 \text{ mlKg}^{-1}\text{hr}^{-1}$  which increased 3-fold till climacteric peak to  $60 \text{ mlKg}^{-1}\text{hr}^{-1}$  (Biale et al., 1954). Carbon dioxide produced during fruit ripening is usually measured in the jars, wherein constant flow of air is maintained which further passes through a cylinder containing alkali to absorb carbon dioxide. Similarly, ethylene (a ripening gas) production in fruits is measured by its absorption in mercuric perchlorate. This simultaneously produced ethylene triggers the cascade of ripening events in fruits (Bapat et al., 2010). Ethylene is produced in all ripening fruits, but in few fruits upon harvest burst in the ethylene production is evident and this class of fruits are classified under climacteric fruits, whereas rest do not show such ethylene burst during post harvest and are known as non-climacteric fruits (Bapat et al., 2010; Bouzayen et al., 2010). Examples of few non-climacteric and climacteric fruits are summarized in Table 1.3. Ethylene act as a ripening hormone and trigger various processes in fruits such as conversion of complex structural and storage polysaccharides in to simple sugars, this is responsible for increase in the total soluble solids (TSS) and content of reducing sugars. Compositional changes studied in two guava types during ripening revealed 1.2-fold change in TSS and increase in the reducing sugars till climacteric peak in both the types (Bashir and Abu-Goukh, 2003). Further production of various organic acids like citric, malic, lactic, ascorbic and tartaric acid etc. take place which is observed through increased titratable acidity in many fruits. (Bashir and Abu-Goukh, 2003). Additionally these biochemical changes show nutritional significance by synthesis of many soluble vitamins during fruit ripening e.g. Vitamin C, Vitamin E, Carotenoids and Folic acid (Slavin and Lloyd, 2012).

**Table 1.3 Examples of climacteric and non-climacteric fruits**

<b>Climacteric fruits</b>	<b>Non-climacteric fruits</b>
Tomato	Cherry
Banana	Grape
Guava	Lemon
Kiwifruit	Litchi
Mango	Mandarin
Papaya	Melon
Passion fruit	Orange
Peach	Strawberry

### 1.3.2 Changes in fruit physiology

Once the ripening events have been triggered by ethylene it leads to various physiological changes in fruits. Significant increase in the production of diverse enzymes involved in cell wall hydrolysis have been shown in many fruits (Brady, 1987). Pectin is an important cell wall component of plants and is responsible for the fruit firmness (Brummell and Harpster, 2001). Various pectin degrading enzymes such as pectate lyase (PL), pectin esterase (PE) and polygalacturonase (PG) were found to be up regulated during ripening of various fruits. Through ripening of papaya more than 6-fold increase in the activities of PE and PG were observed along with the increased respiration and ethylene production (Paull and Chen, 1983). Similarly, cellulose and hemi-cellulose are also present in many fruits and account for insoluble fibre content and firmness of fruits (Brady, 1987; Imsabai et al., 2006). Various cellulases/glucanases degrade these insoluble fibres and play their role in fruit softening; this process was clearly observed in avocado fruit ripening, wherein firmness of the ripening fruit was inversely correlated to the cellulase activity during post-harvest span of 14 days (Pesis et al., 1978). Activities of these enzymes degrade pectin, cellulose and hemi-cellulose and are accountable for transformation of mature raw or unripe fruit to soft fruit with fleshy pulp.

Concurrently, in most of the fruits during ripening loss of green color and development of yellow, orange, red or dark blue to purple color is observed. This change is due to chloroplast degradation and chromoplast development (Egea et al.,



2010). These chromoplasts are the plastids which accumulate carotenoids and are mainly developed from pre-existing plastids (chloroplast). Various pigments such as xanthophylls, anthocyanines and carotenoids biosynthesis and accumulation take place during fruit ripening and furnish specific color characteristic to each fruit (Table 1.4). Degradation of chlorophyll (from  $50\mu\text{gg}^{-1}$  to almost null) and biosynthesis of carotene ( $10\mu\text{gg}^{-1}$  to  $200\mu\text{gg}^{-1}$ ) was reported during tomato fruit development (Fraser et al., 1994) which is responsible for transition of tomato fruit color from green to red. Altogether these physiological changes confer softness and attractive color to fruit.

**Table 1.4 List of fruit pigments responsible for various colors**

Pigment	Colour	Examples
Chlorophyll	Green	Unripe fruits, kiwifruit
Carotene	Yellow to Orange	Lemon, banana, orange
Lycopene	Red	Tomato, strawberry
Flavonoids	Yellow	Grapefruit, yellow prickly pear
Anthocyanines	Red, Blue or Purple	Blueberries, lingonberries

### 1.3.3 Generation of aroma volatiles

Generation of various aroma volatiles during fruit ripening is an important attribute from consumer point of view. Different fruits have their unique volatile profile upon ripening. Volatile compounds in fruits are diverse consisting hundreds of different chemical compounds comprising only  $10^{-7}$  to  $10^{-4}$  of the fresh fruit weight (Berger, 2007; Brückner and Wyllie, 2008). Volatile chemicals developing the fruit flavor are synthesized by means of various metabolic pathways during ripening and postharvest storage of fruit.

Volatile composition of a fruit may vary based on maturity, cultivar or variety, species, weather and pre and post-harvest handling. In general various terpenes such as mono-terpenes, sesqui-terpenes, oxygenated terpenes and hydrocarbons are major constituents in most of the fruits. Other than terpenes various esters, alcohols, aldehydes, lactones and furanones are also found to be contributing sweet, fruity, creamy and caramel like notes in ripened fruits. Each fruit has unique aroma due to perfect qualitative and quantitative blend of these volatile chemicals (Brady, 1987).



**Figure 1.3 Composition of aroma volatiles in various fruits**

Many popular fruits are mined to fetch the key aroma imparting volatiles to their ripe stages (Figure 1.3). The list includes apple (Dixon and Hewett, 2000; Flath et al., 1969; Mehinagic et al., 2006), banana (Golding et al., 1999), papaya (Almora et

al., 2004; Flath et al., 1990; Heidlas et al., 1984; Pino et al., 2003), kiwifruit (Gilbert et al., 1996), litchi (Chyau et al., 2003), grapes (Sánchez-Palomo et al., 2005), citrus fruits (Berger, 2007; Berry et al., 1983), peach (Aubert et al., 2003; Horvat et al., 1992; Narain et al., 1990), jackfruit (Maia et al., 2004; Ong et al., 2006), pineapple (Berger et al., 1985; Berger et al., 1983; Takeoka et al., 1991; Tokitomo et al., 2005), strawberry (Forney et al., 2000; Hakala et al., 2002; Sanz et al., 1994; Ulrich et al., 2007; Whitaker and Evans, 1987) and mango (Pino et al., 2005; Quijano et al., 2007). Hundreds of different volatile compounds responsible for their characteristic odor have been investigated from various fruits. Also, Aroma volatile composition of these fruits varies qualitatively and quantitatively across various fruit developmental stages.

Scientists around the world are still investigating complex ripening process and aroma volatile biosynthesis in different fruits. Aroma volatiles are diverse among various fruits and also amid numerous cultivars of single fruit/ species. There are thousands of different fruits species and each species has various cultivars or varieties with different properties. Thus, detailed study on each fruit cultivar is insinuated.

## 1.4 Mango: The king of fruits

Among all fruits, mango is highly favored and known as “The king of fruits”. Mango i.e. *Mangifera indica* L. is an Angiosperm from order Sapindales and family Anacardiaceae. It is known to be originated in south-east Asia i.e. Indo-Burma region (Ravishankar et al., 2000). It is a tropical fruit and also known as “Apple of the tropics”. There are thousands of different mango varieties across world, to example few Haden, Tommy Atkins, Alice, Ataulfo, Edward, Fazli, Keitt, Kent, Osteen, Sindhri, Alphonso, Kesar, Pairi, Dashehari, Banganpalli and Zill are famous cultivars. Mango is commercially cultivated over 103 countries of the world (Jiang et al., 2010). India, China, Thailand, Indonesia, Mexico and Pakistan are the major mango producing countries as described in Figure 1.4. In the year 2014 the world mango production was around 45.37 million metric tonnes (MMT), with India as the highest mango producing (18.43 MMT) country, which is around 40% of global mango production (Figure 1.5a). However, India held second rank in the year 2013 in mango export (0.26 MMT) after Mexico which was 0.33 MMT as shown in Figure 1.5b (<http://faostat.fao.org/>).

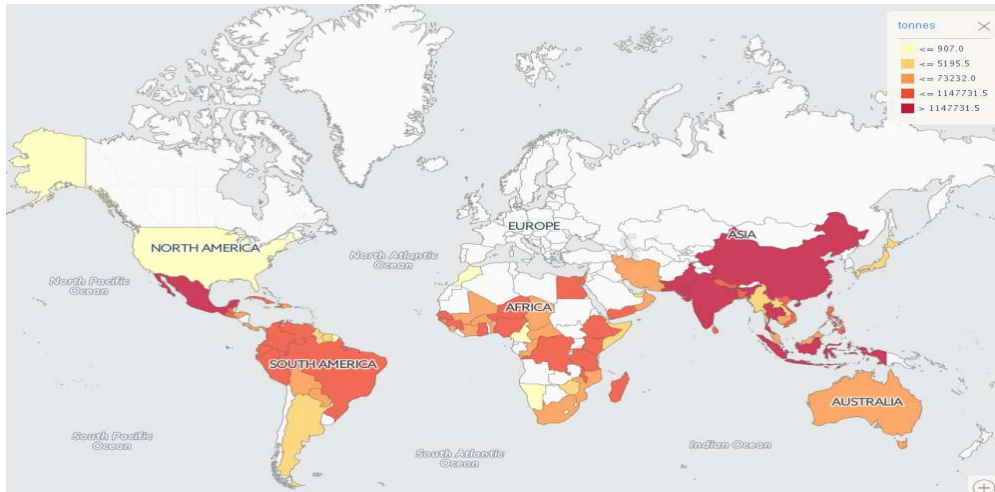


**Figure 1.4 Major mango producing countries across world**

Source: <http://www.fao.org/faostat>

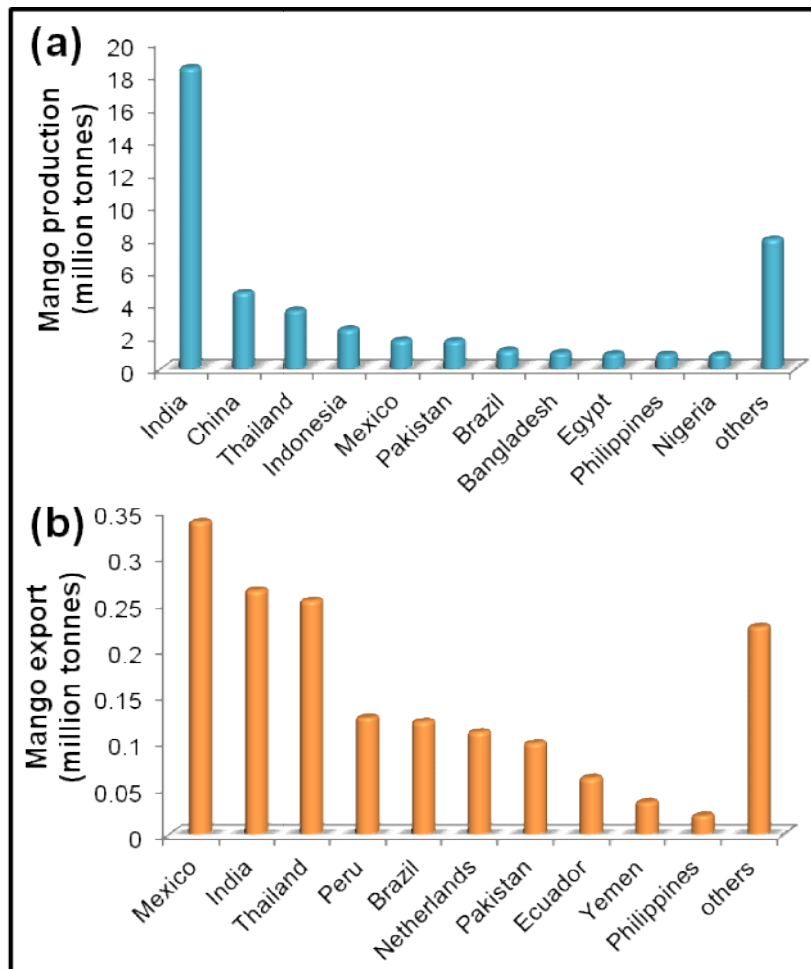


**Figure 1.5 Mango production and export statistics**

Mango production in year 2014 (a) and export in year 2013 (b) data from few top-most countries

There are thousands of mango varieties in India itself as it is the centre for diversity of mango. Various mango varieties are famous from different states of India (Figure 1.6). To list a few Alphonso, Kesar and Pairi from Maharashtra, Gujarat and Karnataka; Dashehari, Langra and Chausa are famous in North Indian states; whereas Banganapalli, Neelam and Totapuri are the favorite varieties in South-India. Amid these Alphonso is legendary mango cultivar across the world due to its unique aroma, attractive color, low fibre containing pulp and long shelf life (Tharanathan et al., 2006a). To understand the biochemical and molecular mechanisms of flavor development during mango ripening various studies have been undertaken such as analysis of aroma volatiles, genes responsible for ripening and flavor biogenesis as well as proteomic and transcriptomic analysis. These studies revealed many important findings which are summarised in following sections.



**Figure 1.6 Famous mango cultivars from different parts of India**

Source: <http://mangoworldmagazine.blogspot.in/2016/06/india-mango-that-time-forgot.html>

## 1.5 Biochemical characterization of mango flavor

Metabolites synthesized during fruit development and ripening are the actual and final indicative of molecular and physiological processes; few of them are also known to trigger other metabolic processes. Various analyses to decipher the volatile composition of number of mango cultivars all over the world indicate presence of myriad compounds, belonging to various chemical classes' viz. alcohol, aldehyde, benzenoid, ester, ketone, lactone and terpenoid, the number touching 400. The attempts have also revealed mango germplasm as the vast and the most diverse pool of volatiles. However, this vast germplasm largely remained unattended for their volatile composition sparing a few preliminary reports.

### 1.5.1 Deciphering the volatile diversity of mango cultivars

Initial work on mango volatiles dates back to 70's wherein organoleptic flavor properties of Alphonso, Langra, Rajapuri, Neelam and Totapuri mango cultivars were compared to their fatty acid composition and postulated correlation of palmitic acid to palmitoleic acid ratio and aroma intensities of these cultivars (Bandyopadhyay and Gholap, 1973c). Further, volatiles of canned Alphonso mango were analysed (Hunter et al., 1974) considering importance of the processed fruit products, closely followed by the volatile analysis of latex of Alphonso and Batali cultivars from India (Gholap and Bandyopadhyay, 1977). Both the studies implied dominance of terpene hydrocarbons in the volatile profile of mango. Earlier studies (Engel and Tressl, 1983; Idstein and Schreier, 1985) revealed a large spectrum of Alphonso volatiles and showed,  $\beta$ -myrcene and *Z*-ocimene as the main constituents of Alphonso mango flavor along with the presence of 14 different  $\gamma$ - and  $\delta$ -lactones. Further, gas chromatographic volatile analysis of Venezuelan mangoes showed eight monoterpenes dominating overall flavor and comprising 54% of the sample, amid which  $\delta$ -3-carene showed major contribution of about 26% (Macleod and Detroconis, 1982). Similarly dominance of  $\delta$ -3-carene was reported from Brazilian Haden, Tommy and Keith mango cultivars (Andrade et al., 2000) as well as from Columbian Haden, Irwin, Manila and Tommy Atkins cultivars (Quijano et al., 2007). A report from comparative analysis of volatile composition from three mango cultivars from Shri Lanka showed qualitative and quantitative differences, wherein Jaffna mango

cultivar produced mainly *cis*- $\beta$ -ocimene, whereas  $\alpha$ -terpinolene found to be dominating in Willard and Parrot mango cultivars (MacLeod and Pieris, 1984). Interestingly, Kensington Pride mango contains esters as the second major contributor (33%) to aroma volatile profile followed by monoterpenes (49%) (MacLeod et al., 1988). Green Thai mango cultivar Khieo Sawoei has been investigated to be containing higher contributions of C6 aldehydes and alcohols along with the  $\gamma$ -terpinene and (*E*)- $\beta$ -ocimene based on their odor thresholds (Tamura et al., 2001).

With the progressive advancement in the analytical techniques, more detailed analyses of mango volatiles were carried out in different parts of the world. The studies depicted major share of terpene hydrocarbons with the qualitative and quantitative variation of other classes of volatiles such as aldehydes, alcohols, esters, furanones, lactones, non-terpene hydrocarbons, nor-isoprenoids, etc. However, most of these reports targeted non-Indian cultivars leaving large mango germplasm of India unnoticed. A study which analysed and quantified the volatile profile of ripe fruits of 22 Indian and 5 non-Indian mango cultivars (Pandit et al., 2009a) was pioneering. Quantitatively, this data set generated the broadest ever range of volatile compounds wherein the highest and the lowest values were contributed by the Indian cultivars, *viz.* Langra and Chandrama, respectively (Figure 1.7).

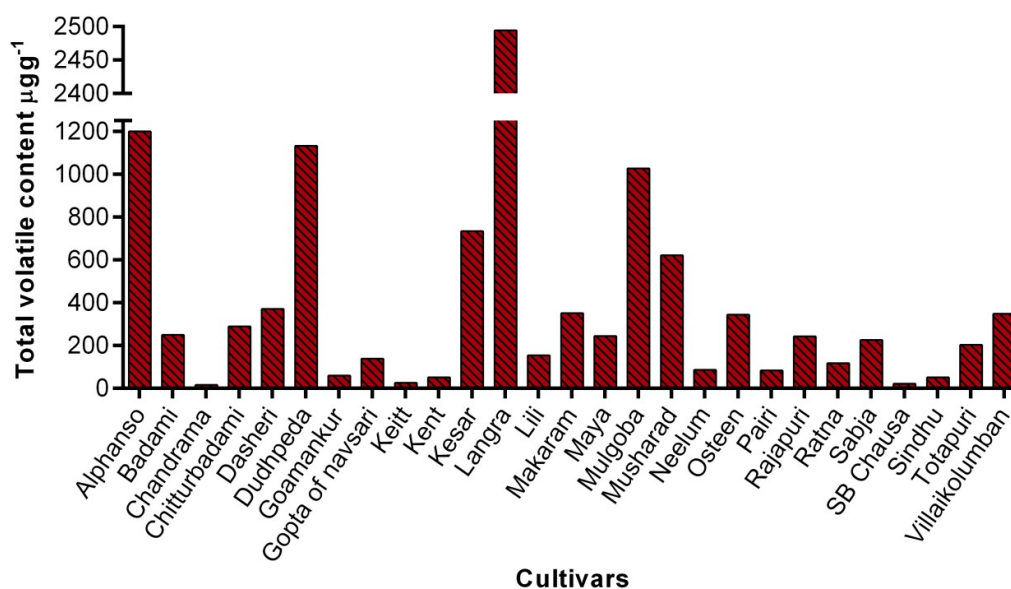


**Figure 1.7** Total volatile content of various mango cultivars

Among the set of eighty four volatile compounds identified in this analysis, the lowest number of volatiles contributed to the blend of Pairi while the blend of Alphonso flavor experienced the numerical dominance of volatile compounds. Moreover, the highest number of lactones was detected only in the fruits of Alphonso supporting the previous reports. This study also showed the dominance of terpene hydrocarbons in the volatile profile of all 27 cultivars. Moreover, monoterpene hydrocarbons,  $\beta$ -myrcene and (Z)-ocimene significantly contributed to the flavor of most of the Indian cultivars, whereas  $\delta$ -3-carene invariably dominated the blend of non-Indian cultivars. In the same study twenty cultivars formed the first group with monoterpene dominance while seven cultivars formed the sesquiterpene dominant group. This was the first report revealing sesquiterpene dominant class of mango cultivars wherein all the seven cultivars in this group were of Indian origin. India being the centre of origin and diversity of mango, such studies may be helpful in planning breeding strategies to obtain desired quality cultivars and for the food processing industry to obtain cultivar specific flavor.

### **1.5.2 Development and ripening of mango: A flavouring volatile perspective**

Aroma volatile analysis of various mango cultivars across the world suggested secondary metabolite diversity among them in terms of number of metabolites detected and their quantities. As most of the studies analysed aroma volatiles from various ripe mango cultivars, next target was to study changes in these volatile profiles during their development and ripening. Earlier study (Gholap et al., 1986) reporting olfactory analysis of various ripening stages of Alphonso mango described aroma of raw mango as more terpenic and earthy-like, whereas that of ripe stage with addition of coconut/almond like notes. Later, over-ripe stage of only two cultivars *viz.* Keitt (Macleod and Snyder, 1985) and Kensington pride (Bartley and Schwede, 1987) was monitored for their volatile content. Keitt experienced synthesis of off flavor alcohols whereas Kensington pride showed reduced levels of ethyl butanoate. Another work carried out on Kensington Pride mango showed dominance of terpene hydrocarbons with  $\alpha$ -terpenolene as a major compound of early ripening with higher share of  $\delta$ -3-carene in the late ripening stages. However, ripening of Kensington Pride mango was characterised by increased concentration of ethyl octanoate (Lalel et al.,



2003a, b). Further this study also reported synthesis of terpenes parallel to ethylene biosynthesis, whereas esters were found to be associated with fatty acid production. A comparative study of ripening stages of Cogshall, Keitt and Kent using two distinct analytical techniques also revealed important harvest maturity indices based on the volatile profile, to obtain optimum quality fruits (Lebrun et al., 2008).

Among the vast germplasm of Indian mango, Alphonso is the most popular cultivar mainly because of its highly delicious flavor, in addition to its attractive color, low fibre containing sweet pulp and long shelf life. Owing to these properties, its raw as well as ripe fruits are largely utilised in various cuisines and in food processing industries in India. With this knowledge five developing and five ripening stages of fruits, flowers and leaves of Alphonso mango along with mature raw and ripe fruits of cv. Sabja were rigorously studied for their volatile composition (Pandit et al., 2009b). This study revealed differential pattern of 55 volatile compounds throughout the analysed data set among which monoterpene hydrocarbons qualitatively and quantitatively dominated the volatile profile at all the stages followed by sesquiterpene and lactones. Interestingly, the study also confirmed the *de novo* presence of lactones and furanones at the ripening stages which could be credited for the coconut/almond like notes of ripe Alphonso fruits.

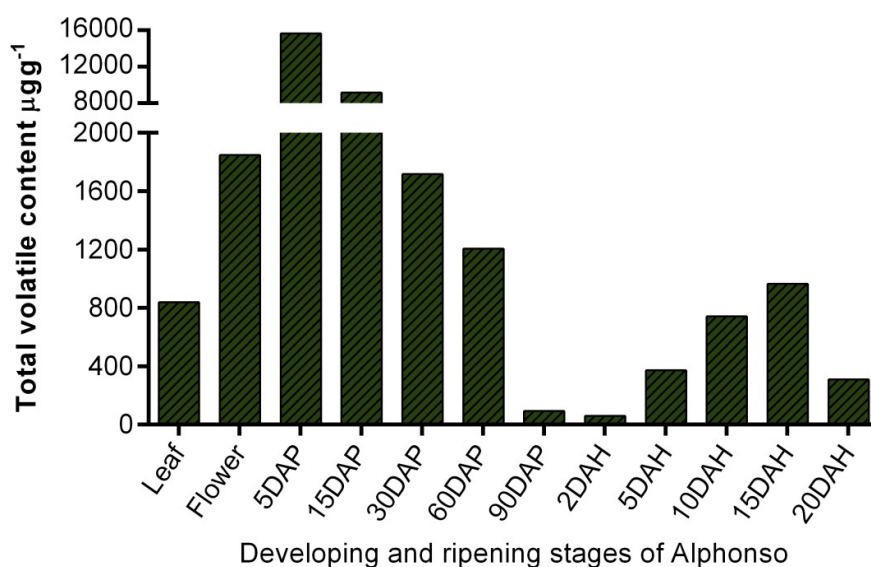


**Figure 1.8 Total volatile content of various Alphonso tissues**

Further, qualitative and quantitative analysis of these compounds revealed few stages as important time points in the development and ripening of the Alphonso fruit. One such stage was 5DAP which contributed the highest amount of volatiles to the fruit closely followed by 15DAP and these two were collectively termed as ‘jump start’ stage as the concentration of total volatiles gradually decreased in the further stages (Figure 1.8). Lactones and furanones which are vital flavorants of ripe Alphonso fruits (Wilson et al., 1990) showed *de novo* appearance at 10 DAH and the highest share to 15DAH stage. This was in agreement with the previous organoleptic analysis (Gholap et al., 1986) which suggested 15 DAH as the perfect ripe stage with the highest lactone content. In Alphonso, over-ripening was characterized by reduction in the quantities of terpenes and lactones and increase in the furanones (Pandit et al., 2009b).

## 1.6 Molecular characterization of mango genes

Development and ripening of any fruit is characterized by a coordinated series of many genetic, metabolic and physiological events. Such processes are largely studied targeting the genes that are directly or indirectly involved in these events. Such earlier attempt in the fruits *viz.* strawberry (Aharoni and O'Connell, 2002), banana (Mbeguie-A-Mbeguie et al., 2009), pineapple (Moyle et al., 2006) and melon (Nagasawa et al., 2005) have exemplified the role of varied fruit specific genes in their ripening.

### 1.6.1 Differential expression of genes during development and ripening of mango

Molecular biology of mango has a very recent history with a share of bunch of studies mainly targeted to various aspects of ripening. Pioneering study reported *in vitro* translation of total RNA from unripe and ripe mango fruits, these translated products showed differential patterns in both the stages, thus indicating ripening specific expression of various genes (Lopez-Gomez and Gomez-Lim, 1993). Further, genetic transformation of *ACC oxidase* gene in somatic proembryos of mango has been carried out but did not report phenotypic effect of the transformation (Cruz-Hernandez et al., 1996). Differential expression of five genes *viz.* PRL1 protein, transcription initiation factor, CCR4 protein and 18S and 23S rRNA encoding genes

from Alphonso and Totapuri mango cultivars was reported, wherein all the five genes were found to be regulatory elements and did not show any direct relation to ripening related events (Saiprasad et al., 2004). Fruit ripening and softening related genes viz. *pectate lyase* and *expansin* were characterized from Dashehari mango, these genes showed fruit and ripening specific expression which was inhibited/delayed upon 1-MCP treatment to fruits (Chourasia et al., 2006a; Sane et al., 2005). This study also confirmed application of 1-MCP in delaying mango ripening. Relative quantification of eighteen genes from Alphonso mango was studied through fruit development and ripening, which for the first time reported various genes related to terpene metabolism (*Isopentenyl pyrophosphate isomerase*, *geranyl pyrophosphate synthase*, *geranyl geranyl pyrophosphate synthase* and *farnasyl pyrophosphate synthase*). Terpene is an important and most abundant class of aroma volatiles in all the mango cultivars. Relative quantification of these genes showed their differential expression during various stages and was correlated to their volatile content (Pandit et al., 2010). Similarly, various other genes related to stress response, ethylene response, protein synthesis and turnover viz. *Isochorismate hydrolase*, *Glucosyl transferase*, *Monodehydrogenase ascorbate reductase*, *Methyl transferase*, *Small heat shock protein*, *Metallothionein*, *Chitinase*, *Ethylene response factor*, *Lipoxygenase* and *Ubiquitin-protein ligase* were studied for their relative expression through various stages of development and ripening of Alphonso mango (Pandit et al., 2010). Mango fruits are enriched source of various vitamins. Emphasizing their importance a key gene encoding hydroxyphenylpyruvate dioxygenase involved in tocopherol biosynthesis was isolated and characterized from Dashehari mango (Singh et al., 2011). Transcript analysis of this gene suggested its ripening related expression in fruits and was positively influenced by ethylene and abscisic acid treatments. Though all these studies flourished good knowledge in the field of mango molecular biology, they remain restricted to one or the other biosynthetic pathway or ripening related event.

Advancement of analytical techniques such as RNA sequencing (RNAseq) or next generation sequencing (NGS) in molecular biology provided way to study thousands of genes simultaneously during complex events of fruit ripening. In recent years RNAseq data from Langra, Kent, Zill and Dashehari mango has been reported, which identified 30509, 33142, 54207 and 74312 unique transcripts from these

cultivars, respectively (Azim et al., 2014; Dautt-Castro et al., 2015; Srivastava et al., 2016; Wu et al., 2014b). Huge data generated in these studies was further utilized to identify differentially expressed genes from raw and ripe fruits of Kent and Dashehari mangoes, which revealed many differences in their transcriptomic profiles and suggested cultivar specific variations in gene expression.

## 1.6.2 Aroma volatile biosynthesis in mango

### 1.6.2.1 Terpene backbone biosynthesis

‘Terpene hydrocarbon’ is a well studied class of plant secondary metabolites mainly due to its role in various biochemical processes such as attracting and guiding the pollinators, protecting the vital reproductive parts of plants from enemies and direct or indirect defence (Dudareva et al., 2004). Apart from this, they are key odorants of flowers and fruits. Aroma of mango fruits is known to be invariably dominated by terpenes. Monoterpenes and sesquiterpene biosynthesis take place in plastids and cytosol, respectively (Bouvier et al., 2005). Though their locations of biosynthesis are different, both are synthesized from isopentenyl diphosphate (IPP) and dimethylallyl diphosphate (DMAPP). These IPP and DMAPP are synthesized in plastids as well as cytosol by MEP and MVP pathways, respectively (Figure 1.9). Further, enzymatic condensation of IPP and DMAPP results in synthesis of geranyl diphosphate, farnesyl diphosphate and geranyl geranyl diphosphate and the reactions are catalysed by GPPS, FPPS and GGPPS, respectively as represented in Figure 1.10. These genes involved in biosynthesis of terpene backbones have been well studied from many other plant species such as *Mentha x piperita*, *Antirrhinum majus* and *Humulus lupulus* (Burke et al., 1999; Szkopińska and Plochocka, 2005; Tholl et al., 2004; Wang and Dixon, 2009).

Mango flavor being dominated by terpenes, studying the terpene biosynthesis in mango would be a productive approach to understand its metabolism. Only one such study has been reported till date in which three isoprenyl diphosphate synthase genes (IDS) which provide branch point for the synthesis of monoterpenes and sesquiterpenes were isolated and characterized from Alphonso mango (Kulkarni et al., 2012). Real time analysis of *MiGPS1*, *MiGPS2* and *MiFPS* genes during ripening stages depicted increased transcript level during mid ripe and complete ripe stages

which showed good correlation with monoterpene and sesquiterpene profiles of ripening Alphonso mango. Recently, Transcriptomic studies have also reported presence and differential expression of these genes till isoprenoid diphosphate biosynthesis but failed to report terminal gene homologs for monoterpene, sesquiterpene and diterpene synthases from mango (Dautt-Castro et al., 2015; Srivastava et al., 2016).

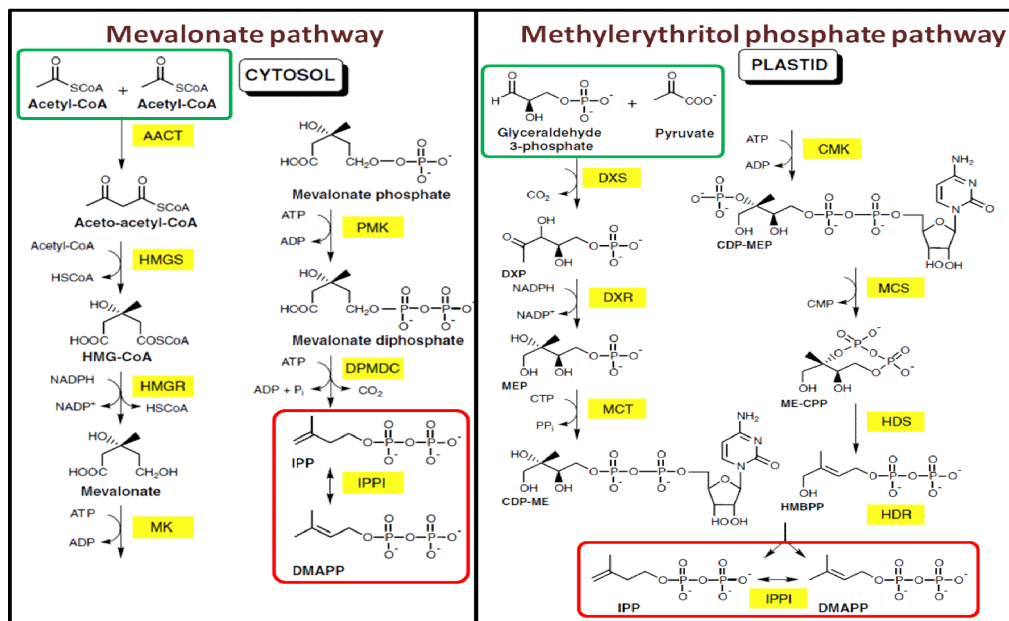


**Figure 1.9 Cytosolic and plastidial IPP and DMAPP biosynthesis pathways**

Source: (Bouvier et al., 2005)

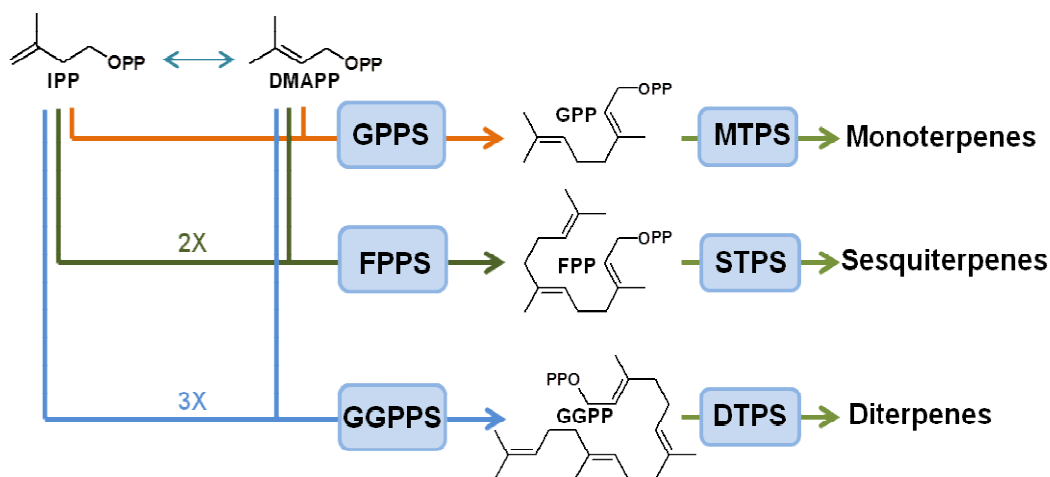


**Figure 1.10 Terpene biosynthesis pathway**

### 1.6.2.2 Fruity and caramel aroma of mango: Biosynthesis of Furanones

Furaneol and mesifuran are two furanones and showed their ripening specific appearance during mango ripening. Furaneol has long history as a principle odor compound of pineapple and its odor has been described as of 'burnt pineapple' by the researchers (Flath and Forrey, 1970). It has also been reported as an important aroma component of strawberry and tomato (Schwab and Roscher, 1997). This compound is known to impart sweet fruity odor and also has low odor detection threshold due to which smaller quantities of this compound are enough to impart a characteristic note to the fruits (Wilson et al., 1990). Biosynthesis of furaneol has been studied only from strawberry and tomato which revealed that D-fructose-1,6-diphosphate is first converted by an unknown enzyme into an unstable intermediate, 4-hydroxy-5-methyl-2-methylene-3(2H)-furanone (HMMF), further this HMFF is converted into furaneol by an enzyme enone oxidoreductase as described in Figure 1.11 (Klein et al., 2007; Raab et al., 2006). Enone oxidoreductase from strawberry also showed its highest expression during late ripening stages and correlated with furaneol content during these stages (Raab et al., 2006).

Alphonso fruit flavor analysis during ripening revealed *de novo* appearance of furaneol (4-hydroxy-2,5-dimethyl-3(2H)-furanone) and its methyl derivative mesifuran (2,5-dimethyl-4-methoxy-3(2H)-furanone) (Pandit et al., 2009b). Considering it as vital flavor contributor to ripe Alphonso fruits, an enone oxidoreductase from Alphonso was isolated and characterized (Kulkarni et al., 2013a), which showed sequence similarity to alkenal/enone oxidoreductase from cucumber and enone oxidoreductases from tomato and strawberry. Recombinant protein catalyzed biosynthesis of furaneol from D-fructose-1,6-diphosphate with NADH as reducing agent. Further, mango enone oxidoreductase (*MiEO*) showed reducing activity towards highly reactive carbonyls such as 3-buten-2-one and 1-penten-3-one similar to the oxidoreductase from cucumber leaves (Yamauchi et al., 2011).

Mesifuran is another important furanone detected from mango during ripening which is accountable for caramel like notes. Mesifuran biosynthesis has been investigated in strawberry for the first time, wherein *O-methyltransferase (FaOMT)*

catylsed synthesis of mesifuran from furaneol. Also, real time PCR analysis showed good correlation of its transcripts and mesifuran levels in ripening strawberries (Wein et al., 2002).

Similar methyltransferase homolog from Alphonso mango (*MiOMTS*) was isolated and characterized. Recombinant enzyme showed conversion of furaneol to mesifuran by utilizing SAM (S-adenosyl-L-methionine) as methyl donor (Figure 1.11). At the same time *in vitro* studies of recombinant protein coded by this *MiOMTS* also showed conversion of protocatechuic aldehyde to vanillin confirming its activity towards various substrates. Significant increase in the mesifuran was evinced in ethylene treated Alphonso mangoes during ripening and qPCR analysis of *O-methyltransferase* in ethylene treated mangoes also showed significant rise in its transcripts compared to untreated mangoes confirming ethylene driven transcriptional regulation of this gene (Chidley et al., 2016b).

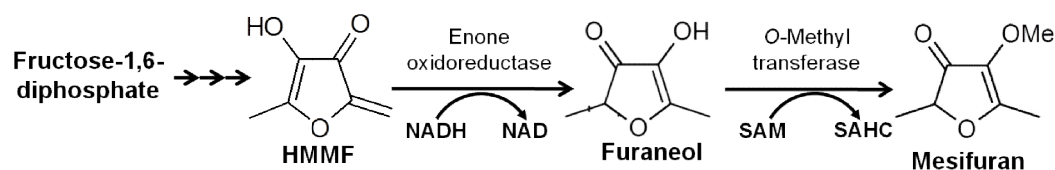


**Figure 1.11 Furanone biosynthesis**

### 1.6.2.3 Ester biosynthesis

Various esters have been reported from variety of fruits and known to contribute sweet aroma to ripened fruits. Kensington Pride, Baladi and Cuban mango cultivars showed significant amounts of ethyl butanoate amid various aroma volatiles (Bartley and Schwede, 1987; Engel and Tressl, 1983). Similarly, Keitt and Tommy Atkins mango cultivars showed presence of ethyl acetate and various C5, C6, C7, C8 and C10 esters. These esters are synthesized from aldehydes of different chain lengths originating from diverse metabolic pathways and converted to corresponding alcohols by activity of alcohol dehydrogenase (ADH). Further esters are synthesized from these alcohols upon action of alcohol acyltransferase (AAT) along with acetylCoA (Pérez et al., 1996) as described in Figure 1.12. Three different transcript variants of ADH have been reported from Dashehari mango, wherein ADH1 and 2 transcripts

were abundant during initial stages of ripening, whereas ADH3 was abundant during early fruit developing stages. All the three ADH variants from Dashehari mango showed positive response towards ethylene treatment whereas their response towards abscisic acid was different (Singh et al., 2010). This study analyzed ADH from mango in detail but further functional analysis is needed. Though AAT from mango is not functionally characterized various studies showed its involvement in esters synthesis from various fruits (Pérez et al., 1996). A study in transgenic melon showed decreased AAT activities, which resulted in 22 % decrease in the content of esters, while alcohol and aldehyde content was found to be increased (Shan et al., 2012).

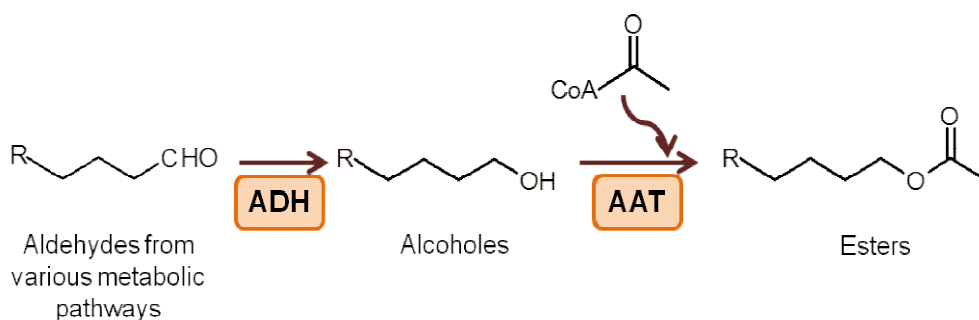


**Figure 1.12 Ester biosynthesis pathway**

#### 1.6.2.4 Mysterious lactone biosynthesis

Aroma volatile analysis of mango revealed ripening specific appearance of furanones and lactones, which can be considered as marker metabolites of mango ripening. Interestingly 14 different lactones have been reported from Alphonso, which is the highest number of lactones known from any single fruit (Idstein and Schreier, 1985; Wilson et al., 1990). Although lactones exhibit qualitative abundance, they are present at lower concentrations in Alphonso but have high impact on overall flavor of Alphonso due to their lower odor detection threshold. Further, lactones are known to impart sweet fruity flavor which is the characteristic feature of fully ripe fruit (Wilson et al., 1990). Though lactones are important constituent of fruit flavor their biosynthesis pathway is still unknown and further detailed study at metabolite and molecular level is required.



Metabolite and molecular studies have given useful insights in to mango flavor. Cultivar specific aroma volatiles and their modulation during fruit development and ripening have been well explored. Similarly, various molecular studies have characterized few biosynthetic pathways in mango by means of gene isolation, qPCR and *in vitro* analysis. Surprisingly, none of the studies focused on functional characterization and *in planta* approach. Cultivar specific transcriptomic studies to identify key genes and their functional characterization are required to understand mango flavor biogenesis *in toto*.

## Genesis of thesis and its organization

Decades of efforts involved in understanding the mango flavor revealed substantial findings through various mango cultivars across the globe. Plant Molecular Biology group at CSIR- National Chemical Laboratory, Pune, India has been working to reveal secrets of mango flavor and its biogenesis. The journey started with the ISSR marker and aroma volatile study to understand molecular and metabolite diversity amid various mango cultivars, which revealed qualitative abundance of aroma volatiles in Alphonso (Pandit et al., 2009a; Pandit et al., 2007). Further studies were undertaken to reveal changes in the aroma volatiles during fruit development and ripening, at various geographic locations and upon exogenous ethylene treatment in Alphonso (Chidley et al., 2013; Kulkarni et al., 2012; Pandit et al., 2009b). Molecular studies were also carried out which depicted biosynthesis of furanones and precursors for terpene metabolism from Alphonso mango (Chidley et al., 2016b; Kulkarni et al., 2013a).

Possessing this valuable knowledge about mango flavor biogenesis and aspiration to discover something novel, I initiated my Ph.D. work to identify novel genes involved in mango ripening and flavor biogenesis, in particular to get insight into unanswered lactone biosynthesis pathway.

The present thesis has been organized in following manner

**Chapter 1:** General Introduction and Review of Literature

**Chapter 2:** Changes in fatty acid composition during fruit development and ripening of three mango cultivars (Alphonso, Pairi and Kent) varying in lactone content

**Chapter 3:** Isolation and characterization of *9-lipoxygenase* and *epoxide hydrolase2* genes: Insight into lactone biosynthesis in mango fruit (*Mangifera indica* L.)

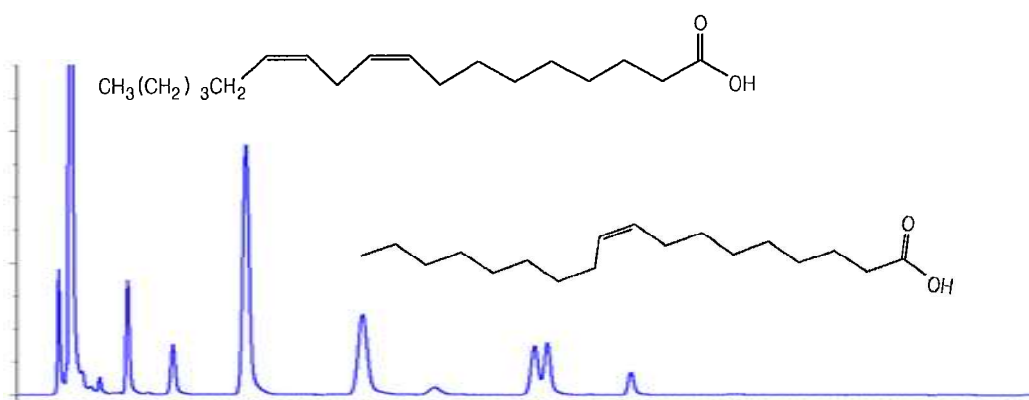
**Chapter 4:** Transcriptional transitions in Alphonso mango (*Mangifera indica* L.) during fruit development and ripening explain distinct aroma and shelf life characteristics

**Summary and future directions**

**Bibliography**



## Chapter 2



Changes in fatty acid composition during fruit development and ripening of three mango cultivars (Alphonso, Pairi and Kent) varying in lactone content

Contents from this chapter have been published as data article in  
Data in Brief (2016); 9, 480-491



## **Chapter 2 Changes in fatty acid composition during fruit development and ripening of three mango cultivars (Alphonso, Pairi and Kent) varying in lactone content**

### **2.1 Introduction**

Fruits have always remained integral part of human diet due to their nutritional quality wrapped together with delicious taste and aroma. Fruits are a good source of all the seven nutrients required by human beings *viz.* carbohydrates, proteins, fatty acids, dietary fibres, minerals, vitamins and water. Various diet studies have therefore, suggested daily consumption of fruits as a part of healthy diet (Sachdeva et al., 2013; Willett et al., 1995). Fatty acids are the important component of fruits as they are involved in multiple cellular, physiological, protective and defensive mechanisms. Apart from this fruits are good source of essential fatty acids from consumer point of view.

Mango (*Mangifera indica* L.) is vastly preferred among all the fruits due to its nutritional composition, sweet taste and creamy, fruity aroma (Tharanathan et al., 2006b). A detailed study on mango volatiles (Pandit et al., 2009a; Pandit et al., 2009b), sugar content (Castrillo et al., 1992) and ripening related changes (Yashoda et al., 2006) has been carried out. However, studies targeting fatty acid composition of mango are relatively less attempted. Fatty acid analysis of Alphonso, Neelam, Langra, Totapuri and Rajapuri cultivars at ripe stage suggested abundance of palmitic acid, palmitoleic acid and oleic acid in ripe pulp of all these cultivars than rest of the fatty acids (Bandyopadhyay and Gholap, 1973a). This study was closely followed by another attempt wherein a correlation between fatty acid composition and organoleptic properties of Alphonso mango fruits was stated (Bandyopadhyay and Gholap, 1973b; Gholap and Bandyopadhyay, 1975). An earlier report on lipid content of peel and pulp of five mango cultivars (Pathak and Sarada, 1974) gave initial insights about the lipid content of mango, where the total lipid content ranged between 0.75-1.7% for peel and 0.8-1.36% for pulp of ripe mango. Similarly fatty acid analysis of ripe Kent mango reflected abundance of palmitic, palmitoleic and  $\alpha$ -linolenic acids (Pott et al., 2003). A study on lipid content of seed (kernel) from

various mango varieties of Thailand (Sonwai and Ponprachanuvut, 2014) and African Bush mango (Olawale, 2010) displayed mango seeds as a rich source of lipids.

All the studies carried out till date to estimate fatty acid content of mango pulp, peel and seed reported relative quantification of individual fatty acids (percent of fatty acid from total fatty acid content). Relative quantification becomes ambiguous as the method is based on number of compounds identified and quantified in the respective study. Thus, the absolute quantification of individual fatty acids has been focused in the present study.

Fatty acids are well known precursors for a class of aroma volatiles called green leaf volatiles (GLVs) which include hexanal, trans-2-hexenal, trans-2-octanal, heptanal, 2-nonenal and 1-penten-3-one (Goff and Klee, 2006). These compounds are responsible for green grassy aroma (Matsui, 2006) and their presence was reported during early stages of Alphonso fruit development (Pandit et al., 2009b). Lactones is another group of aroma volatiles synthesized from fatty acids and contribute creamy, caramel, peach or coconut like aroma based on the type of  $\gamma$  or  $\delta$  lactone (Xi et al., 2012). Lactones have been shown to be ripening specific compounds and their qualitative and quantitative variation amid various mango cultivars as well as pulp and skin of Alphonso mango have been reported (Chidley et al., 2013; Pandit et al., 2009a).

As lactones have a significant share in the flavor character of Alphonso mango, analysis of their precursor i.e. fatty acids during the development and ripening of Alphonso mango will shade light on their biosynthesis. In this view, present study was undertaken for detailed profiling of fatty acids through various developing and ripening stages of three mango cultivars *viz.* Alphonso (lactone rich cultivar), Pairi and Kent (lactone less cultivars) (Pandit et al., 2009a) to understand their nutritional and flavor related importance.

## 2.2 Materials and methods

### 2.2.1 Plant material

*Mangifera indica* L. (Anacardiaceae) fruits of cv. Alphonso and cv. Pairi were collected from mango orchards at the Mango Research Sub Centre (16.528336 N, 73.344790 E), Deogad and of cv. Kent from mango orchards at the Regional Fruit Research Station (15.856849 N, 73.653387 E), Vengurle, both affiliated to Dr. Balasaheb Sawant Konkan Agricultural University, Dapoli, Maharashtra, India. Developing stages of all the three mango cultivars were collected at 15, 30 and 60 days after pollination (DAP) and at mature raw stage (90 DAP for cvs. Alphonso and Pairi, 110 DAP for cv. Kent). Fruits at these developing stages were harvested, pulp (mesocarp) and skin (exocarp) separated immediately, snap frozen in liquid nitrogen and stored at  $-80^{\circ}\text{C}$  until further use. A set of 12 fruits each for all the three cultivars were additionally harvested at their respective mature raw stage and kept in the hay containing boxes at ambient temperature for ripening. Three cultivars showed variation in the ripening duration, hence four ripening stages as table green, mid ripe, ripe and over ripe based on the skin color, aroma and fruit softness (each stage is represented by days after harvest i.e. DAH for cv. Alphonso as 5, 10, 15 and 20 days; for cv. Pairi as 4, 6, 8 and 10 days and for cv. Kent as 5, 8, 10 and 13 days, respectively) were used for further analysis. At each ripening stage fruits for each cultivar were removed from the box, pulp and skin were separated, frozen in liquid nitrogen and stored at  $-80^{\circ}\text{C}$  till further use.

### 2.2.2 Transesterification of fatty acids

Fatty acid methyl esters (FAMES) were synthesized by transesterification reaction in methanolic HCl. 500 mg of the tissue was finely crushed in liquid nitrogen and added to the 5 ml methanol containing 3M HCl, 25 $\mu\text{g}$  butylated hydroxytoluene (BHT) as an antioxidant and 250  $\mu\text{g}$  tridecanoic acid as an internal standard. Transesterification was carried out at  $80^{\circ}\text{C}$  in water bath for 2hrs to synthesize FAMES. After incubation reaction mixture was cooled on ice and FAMES were extracted twice in 2ml n-Hexane. n-Hexane layer was completely evaporated in vacuum evaporator, FAMES were reconstituted in 250 $\mu\text{l}$  chloroform and used for GC-MS and GC-FID analysis.

### 2.2.3 Extraction of aroma volatiles

Aroma volatiles were extracted from 2 g pulp and skin of completely ripe fruits of all the 3 cultivars by solvent extraction method using 10 ml dichloromethane (DCM) with appropriate concentration of nonyl acetate as an internal standard. Extraction was carried out for 30 min at 28 °C in a shaker. DCM was decanted and centrifuged at 10,000 rpm at RT to remove remaining tissue debris. The supernatant was dehydrated with anhydrous sodium sulphate and concentrated to 1 ml using vacuum evaporator. After overnight incubation at -80 °C the extracts were centrifuged at 10,000 rpm at 4 °C for 15 min to pellet out high molecular weight lipids. The extracts were further concentrated to 100 µl and stored at -20 °C till used for GC analysis.

### 2.2.4 Gas chromatography analysis

#### 2.2.4.1 Identification and quantification of FAMES

Gas chromatographic analysis was carried out on 7890B GC system Agilent Technologies coupled with Agilent 5977A MSD (Agilent Technologies, CA, USA). 1 µl of chloroform reconstituted FAMES were injected for GC-MSD analysis. Method for the gas chromatographic separation of fatty acid structural isoforms was standardized, for better resolution of fatty acids 75 m long SP<sup>TM</sup> 2560 (Supelco, USA) column with 0.18 mm i.d. and 0.14 µm film thickness was used. Helium was used as the carrier gas with 1 ml min<sup>-1</sup> flow. Initial oven temperature was kept at 130 °C and held for 5 min, followed by a ramp of 10 °C min<sup>-1</sup> till 230 °C with hold at 230 °C for 20 min. Injector temperature was maintained at 250 °C, source, quadrupole and transfer line temperatures were 150 °C, 180 °C and 250 °C, respectively. Mass spectra were obtained by Agilent MSD at 70eV on scan mode with scanning time of 0.2s for range of m/z 30-400. FAMES were identified by matching generated spectra with NIST 2011 and Wiley 10<sup>th</sup> edition mass spectral libraries. Identified compounds were confirmed by matching retention time and spectra of authentic standards procured from Sigma Aldrich (St. Louis, MO, USA). Identified compounds were quantified by GC-FID. Similar chromatographic conditions were maintained for GC-FID with detector temperature at 250 °C. Absolute quantification was done using internal standard by normalizing concentrations of all the FAMES with that of tridecanoic acid methyl ester.



#### 2.2.4.2 Qualitative and quantitative analysis of lactones

GC-MS and GC-FID analysis for lactones was carried out on similar instrument used for analysis of FAMES. Aroma volatiles were separated on GsBP-5MS (General Separation Technologies, Newark, DE, USA) capillary column (30 m × 0.32 mm i.d. × 0.25 µm film thickness). Other chromatographic conditions were maintained as mentioned earlier in our previous studies (Kulkarni et al., 2012). Since fatty acids are known to be the precursors for lactone biosynthesis, qualitative and quantitative analysis for lactones alone was carried out in the present study. Lactones were identified by matching generated spectra with NIST 2011 and Wiley 10<sup>th</sup> edition mass spectral libraries. Identified compounds were confirmed by matching retention time and spectra of authentic standards procured from Sigma Aldrich (St. Louis, MO, USA). Absolute quantification was done using internal standard by normalizing concentrations of all the lactones with that of known concentration of nonyl acetate.

#### 2.2.5 Statistical analysis

To validate data statistically tissue for each developing and ripening stages were collected from fruits of 3 independent trees for cv. Alphonso and 2 independent trees each for cv. Pairi and cv. Kent. These were considered as biological replicates. Extraction of FAMES and volatiles was carried out twice for each tissue as technical replicates followed by duplicate GC-FID runs of each extracts as analytical replicates. Fisher's LSD test was performed separately for pulp and skin at  $p \leq 0.05$  by ANOVA for comparative analysis of quantity of each fatty acid during various developing and ripening stages from each cultivar. Also comparison was done for each fatty acid at individual stage among the three cultivars using StatView software, version 5.0 (SAS Institute Inc., Cary, NC, USA). Similarly, ANOVA was carried out for lactone content of ripe pulp and skin from the three cultivars. Correlation analysis of total lactone content with individual fatty acid content and individual lactone content with individual fatty acid content from the pulp and the skin of three cultivars at ripe stage was studied using StatView software. Principle component analysis for whole data set of fatty acid content was carried out using Systat statistical software (Version11, Richmond, CA, USA).

## 2.3 Results

### 2.3.1 Fatty acid composition of mango pulp and skin

Total 17 different fatty acids were identified (Figure 2.1 and Figure 2.2) and quantified from the pulp and the skin tissues (Table 2.1, Table 2.2 and Figure 2.3) at various stages of development and ripening from three mango cultivars *viz.* Alphonso, Pairi and Kent. Collectively pulp and skin showed presence of 6 saturated fatty acids (myristic, palmitic, stearic, arachidic, behenic and lignoceric acid) having carbon chain length ranging from C14 to C24 at all the developing and ripening stages. Total four unsaturated fatty acids were detected through all the stages of pulp and skin of which two were mono-unsaturated (palmitoleic and oleic acid) and remaining two were poly-unsaturated *viz.* linoleic acid (LA) and  $\alpha$ -linolenic acid (ALA). Seven unusual fatty acids were identified with respect to chain length, position of unsaturation and their abundance in nature. Odd chain fatty acids were 2, 4-heptadienoic acid and 10-heptadecenoic acid of which the later was present only in the pulp of all the three cultivars. Similarly, 9, 12-hexadecadienoic acid and 9, 15-octadecadienoic acids were exclusively present in the pulp tissue. Three unusual mono-unsaturated fatty acids with unsaturation at C11 *viz.* 11-hexadecenoic acid, 11-octadecenoic acid and 11-eicosenoic acid were detected in the analysis and showed presence in the pulp as well as the skin of all the cultivars.

### 2.3.2 Variation in total fatty acid content of three mango cultivars

Quantitative analysis of all the fatty acids showed their variable contribution at each stage of the pulp and the skin of all the three cultivars as shown in the histogram (Figure 2.3). Increase in the total fatty acid content was observed in the pulp and the skin tissue of all the three cultivars as the ripening progressed. Total fatty acid content of Alphonso pulp was the lowest ( $2.85 \text{ mgg}^{-1}$ ) at table green stage and the highest ( $11.10 \text{ mgg}^{-1}$ ) at over ripe stage. The lowest fatty acid content in Pairi and Kent pulp was at mature raw ( $2.17 \text{ mgg}^{-1}$ ) and 60 DAP ( $1.12 \text{ mgg}^{-1}$ ) stages, and the highest content was at table green ( $5.17 \text{ mgg}^{-1}$ ) and over ripe ( $3.39 \text{ mgg}^{-1}$ ) stages, respectively. At ripe stage, total fatty acid content of Alphonso and Pairi pulp were 3.05 and 1.46 folds more than that in Kent, respectively. Skin of all the cultivars was rich in fatty acid content than the pulp at all the stages of development and ripening.

Total fatty acid content in Alphonso skin ranged from 5.48 to 11.93  $\text{mgg}^{-1}$ , whereas for Pairi and Kent skin the values ranged between 7.64 to 13.09  $\text{mgg}^{-1}$  and 4.33 to 9.03  $\text{mgg}^{-1}$ , respectively.

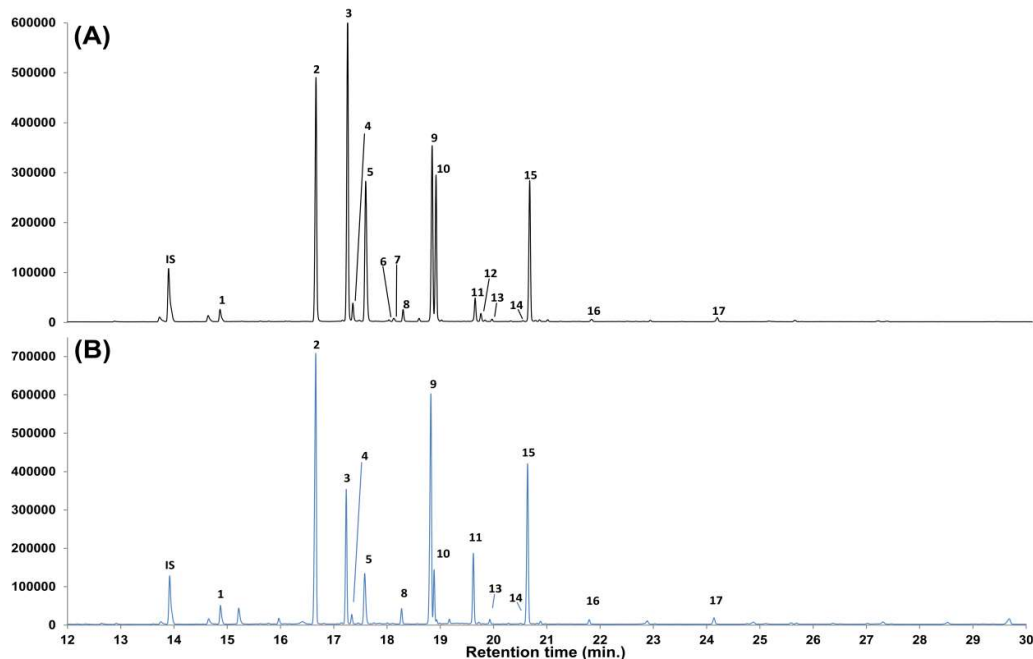


**Figure 2.1 Representative fatty acid chromatograms**

Representative chromatograms of fatty acids from mango pulp (a) and skin (b). Peak labels represent, compounds as IS: Internal standard, 1: Myristic acid, 2: Palmitic acid, 3: Palmitoleic acid, 4: 11-Hexadecenoic acid, 5: 2, 4-Heptadienoic acid, 6: 10-Heptadecenoic acid, 7: 9, 12-Hexadecadienoic acid, 8: Stearic acid, 9: Oleic acid, 10: 11-Octadecenoic acid, 11: Linoleic acid, 12: 9, 15-Octadecadienoic acid, 13: Arachidic acid, 14: 11-Eicosenoic acid, 15:  $\alpha$ -Linolenic acid, 16: Behenic acid, 17: Lignoceric acid

Total saturated fatty acids from pulp (Figure 2.4) showed high levels during initial developmental stages i.e. 15DAP and 30DAP which decreased till mature raw stage for Pairi, 60 DAP for Kent and table green stage for Alphonso. Thereafter they increased till over ripe stage with their highest content 3.10, 1.10 and 0.84  $\text{mgg}^{-1}$  for Alphonso, Pairi and Kent, respectively (Figure 2.4). Skin shared more saturated fatty acid content than the pulp of respective cultivars at each stage. Alphonso and Pairi skin possessed the lowest saturated fatty acid content at 15 DAP and high levels at over ripe stage. Amid all the skin tissues analysed, Kent skin at mid ripe stage had the lowest (1.45  $\text{mgg}^{-1}$ ) saturated fatty acid content (Figure 2.4). Total unsaturated fatty acid content from the pulp of all the three cultivars was more than the total saturated fatty acid content at their respective stages (fold change varied between 1.5 and 3.5).

The highest unsaturated fatty acid content was evinced from Alphonso pulp at over ripe stage (Figure 2.4) which was 2.04 and 3.13 fold more than the highest levels of Pairi (table green) and Kent (over ripe) pulp, respectively. Total unsaturated fatty acid content from Kent and Alphonso pulp increased during ripening, whereas decreased in case of Pairi (table green) to over ripe stage). Skin displayed high levels of total unsaturated fatty acids than the pulp at each stage of development and ripening of all the three mango cultivars and the highest level was clearly observed in Pairi skin (8.87 mgg<sup>-1</sup>) at its ripe stage (Figure 2.4). Moreover, Pairi skin impressively displayed high level of total unsaturated fatty acids at every stage of development and ripening as compared to Alphonso and Kent skin.

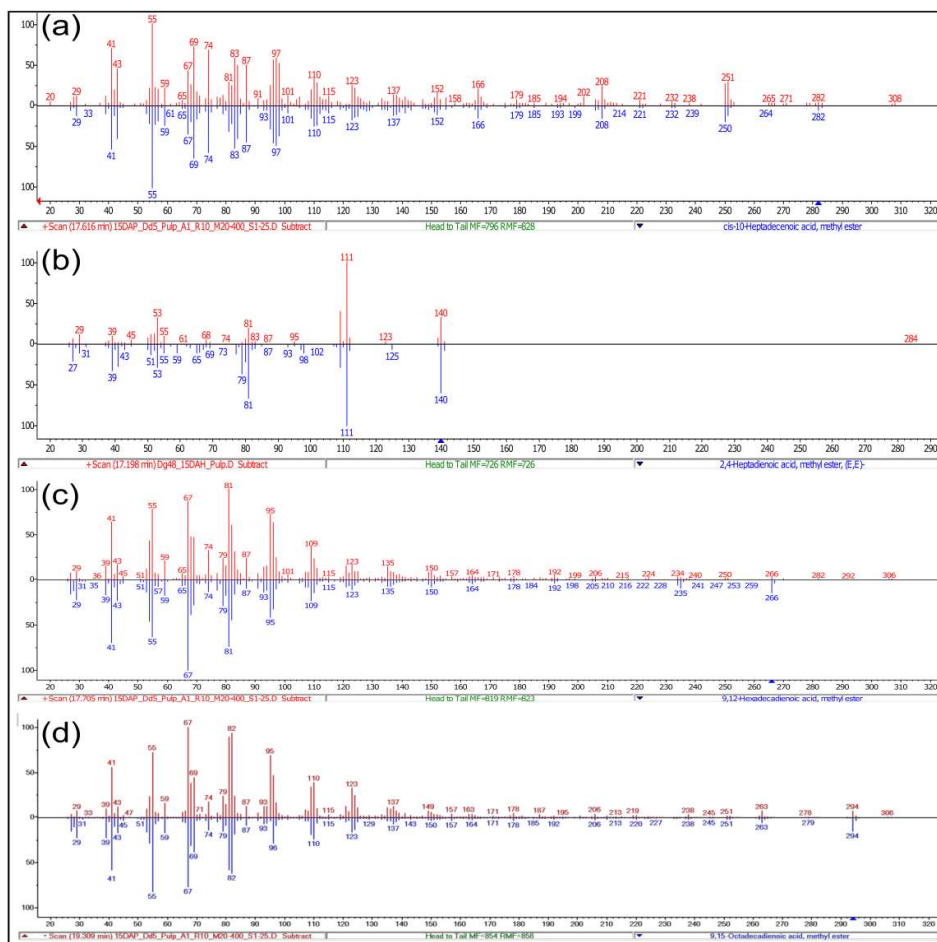


**Figure 2.2 MS spectra of odd chain and unusual fatty acid methyl esters**

Head to tail alignment of spectra for 10-Heptadecenoic acid (a), 9, 12 Hexadecadienoic acid (c) and 9, 15 Octadecadienoic acid (d). Spectra in red color represent experimental spectra while spectra in blue color represent standard spectra from NIST 2011 library.





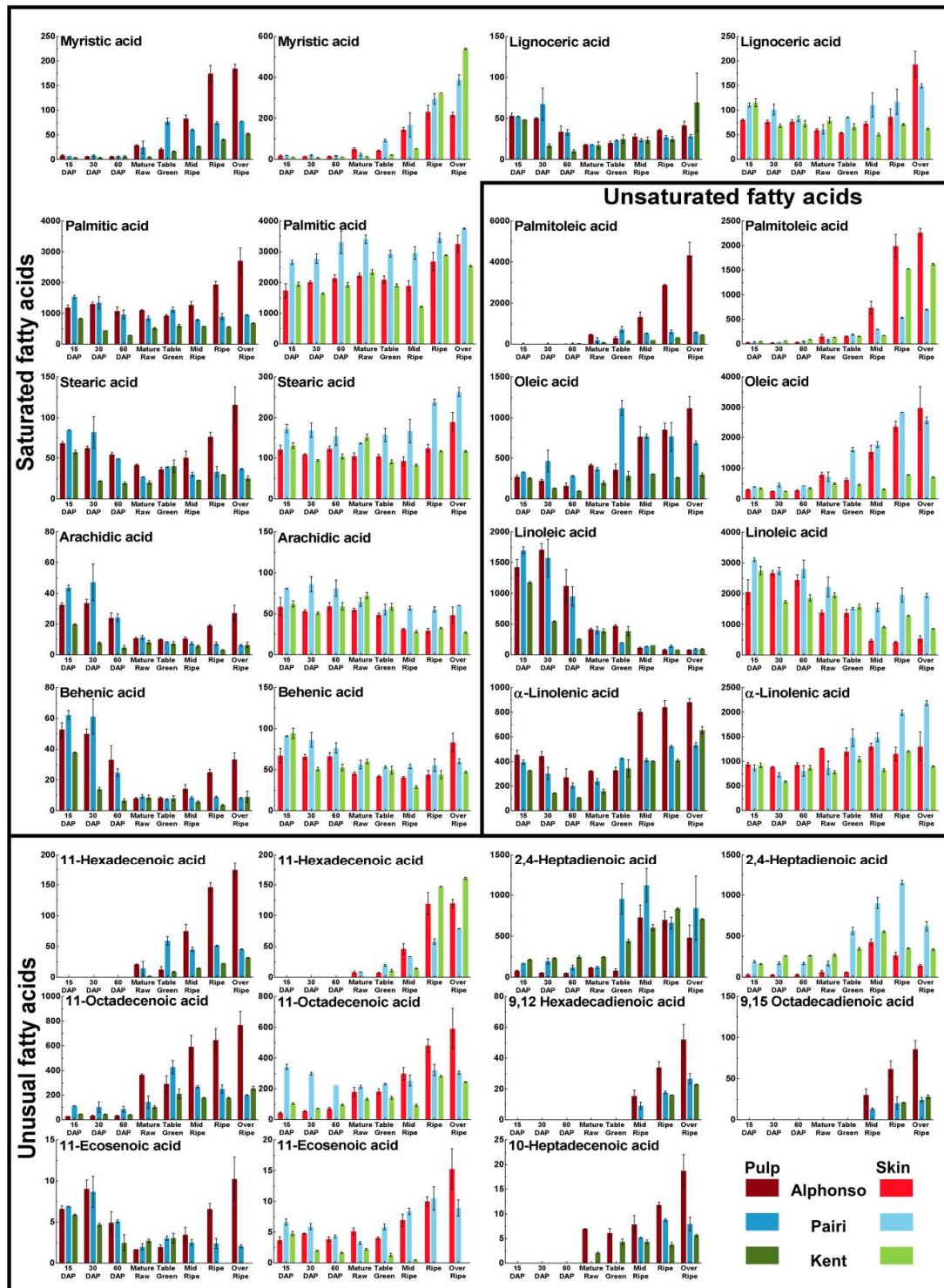


**Figure 2.3 Fatty acid histogram**

Content ( $\mu\text{g g}^{-1}$ ) of individual fatty acid from pulp and skin through various developing and ripening stages of Alphonso, Pairi and Kent mango cultivars. Vertical bars at each data point represent standard error of measurement calculated for the biological replicates used in the study.

### 2.3.3 Saturated fatty acids

Total 6 saturated fatty acids were present in pulp as well as skin of all the three cultivars, out of which palmitic acid was found to be the most abundant. Palmitic acid shared its high concentration in the pulp at 15 DAP stage for Pairi (1534  $\mu\text{gg}^{-1}$ ) and Kent (830  $\mu\text{gg}^{-1}$ ) and at over ripe stage of Alphonso (2705  $\mu\text{gg}^{-1}$ ). Skin had higher share of palmitic acid than pulp. The highest palmitic acid content was observed in over ripe skin of Pairi (3756  $\mu\text{gg}^{-1}$ ), closely followed by its ripe skin (3460  $\mu\text{gg}^{-1}$ ) (Table 2.2). Myristic acid content of pulp was low during developing stages but showed significant increase during the ripening stages. Among all the stages of pulp, level of myristic acid varied between 3.8 to 184.41  $\mu\text{gg}^{-1}$  (Table 2.1).

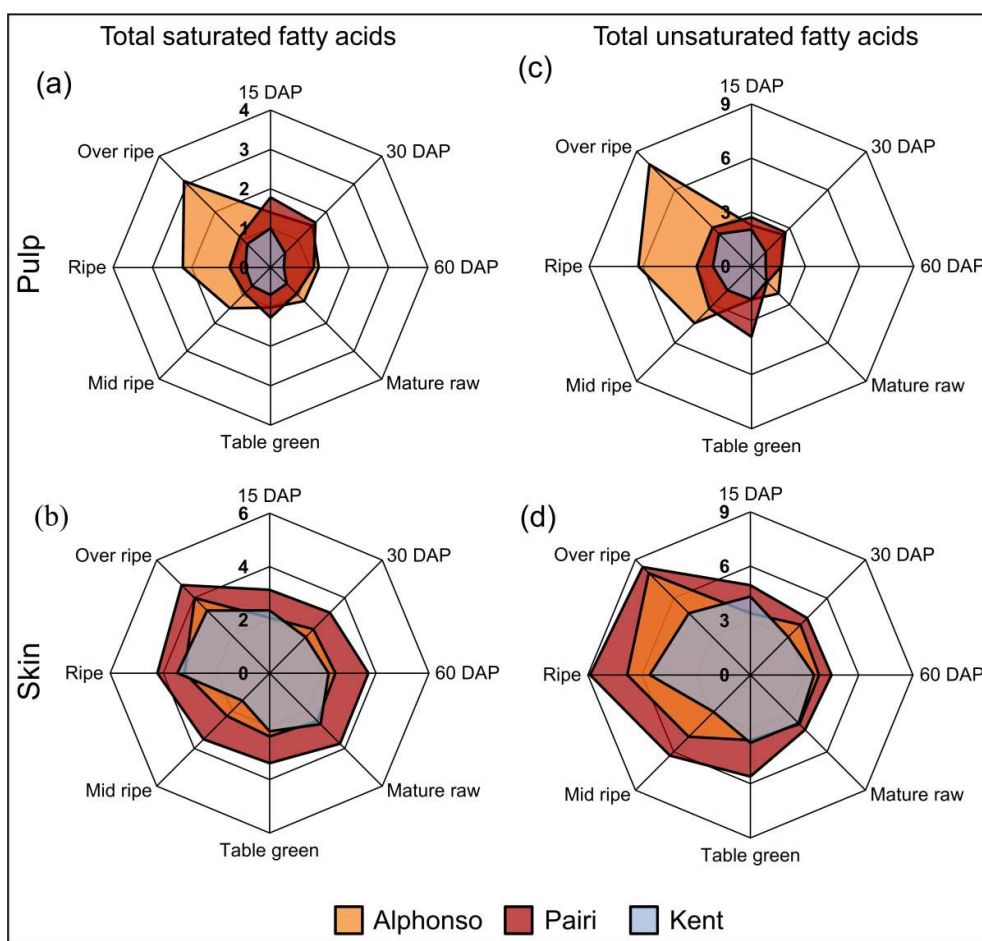


**Figure 2.4 Radar plot representing contribution (mgg<sup>-1</sup>) of total fatty acids**

Total saturated fatty acids from pulp (a), total saturated fatty acids from skin (b), total unsaturated fatty acids from pulp (c) and total unsaturated fatty acids from skin (d) at various developing and ripening stages of Alphonso, Pairi and Kent mango cultivars.



Moreover, myristic acid levels in Alphonso pulp were significantly higher than those in the Pairi and Kent pulp during mid ripe, ripe and over ripe stages. Myristic acid content in the skin significantly increased during ripening; wherein Kent skin possessed significantly high levels than that of Alphonso and Pairi during ripe and over ripe stages. Stearic acid levels in the pulp of Pairi and Kent were maximum during the early developmental stages i.e. 15 DAP and 30 DAP, which significantly decreased further till over ripe stage. In case of Alphonso pulp stearic acid content significantly decreased from 15 DAP ( $67.97 \mu\text{gg}^{-1}$ ) to table green stage ( $36.07 \mu\text{gg}^{-1}$ ) which again increased significantly till over ripe stage ( $115.93 \mu\text{gg}^{-1}$ ). Stearic acid content from skin tissues of Alphonso and Pairi showed no significant increase during developing and early ripening stages, which increased significantly at over ripe stage, respectively. Kent skin had the highest stearic acid content at mature raw stage amid its developing and ripening stages. Pairi skin possessed high levels of stearic acid than that in Alphonso and Kent skin tissues at all the stages, respectively. Long chain saturated fatty acids *viz.* arachidic, behenic and lignoceric acids were low abundance fatty acids in pulp with their highest share during early developmental stages. In skin arachidic acid showed high levels during early developmental stages of all the three cultivars, while behenic acid had its highest content at 15 DAP of Pairi and Kent and over ripe stage of Alphonso. Lignoceric acid content in the skin was the highest at over ripe stage for Alphonso and Pairi, while Kent had its highest content at 15 DAP stage.

### 2.3.4 Unsaturated fatty acids

Varieties of unsaturated fatty acids were evinced from the pulp and the skin of three mango cultivars. Six mono-unsaturated fatty acids, four di-unsaturated fatty acids and one tri-unsaturated fatty acid were detected in the analysis, out of which seven were unusual fatty acids. Unsaturated fatty acids fall amid the class of n-3, n-4, n-5, n-6, n-7 and n-9 fatty acids and are known to have nutritional and physiological importance.

#### 2.3.4.1 Mono-unsaturated fatty acids

Among the 6 mono-unsaturated fatty acids, oleic acid (9-octadecenoic acid), 11-octadecenoic acid and palmitoleic acid (9-hexadecenoic acid) were abundant and showed their highest share during the ripening stages of the pulp and the skin of all

the three cultivars. Palmitoleic acid content significantly increased during the ripening stages in the pulp as well as the skin tissues of all the cultivars. It was the most abundant fatty acid in Alphonso pulp ( $4325 \mu\text{gg}^{-1}$ ) at over ripe stage which was 7.3 and 9.5 folds more than that in the over ripe pulp of Pairi and Kent, respectively. At ripe stage palmitoleic acid contributed 33.9% to the total fatty acid pool of Alphonso pulp which was 4.8 and 9.1 folds higher than that in the pulp of Pairi and Kent, respectively. However, Alphonso skin had low share of palmitoleic acid compared to the pulp at respective ripening stage. Pairi had almost similar levels of palmitoleic acid at ripe and over ripe stages for the pulp and the skin. Kent skin possessed more palmitoleic acid than the pulp during ripe and over ripe stages. Oleic acid (9-octadecenoic acid), the second abundant mono-unsaturated fatty acid which serves as the substrate for LA and ALA biosynthesis in plants was detected with elevated levels in the pulp and the skin during ripening stages of all the cultivars. Kent showed relatively lower content of oleic acid in the pulp and the skin than those of Pairi and Alphonso. Utmost levels of oleic acid in the pulp ( $1117 \mu\text{gg}^{-1}$ ) and the skin ( $2982 \mu\text{gg}^{-1}$ ) of Alphonso were detected at over ripe stage, whereas in case of Kent the highest levels in the pulp ( $304 \mu\text{gg}^{-1}$ ) and the Skin ( $778 \mu\text{gg}^{-1}$ ) were detected at mid ripe and ripe stage, respectively. For Pairi, peak levels of oleic acid were detected in the table green pulp ( $1119 \mu\text{gg}^{-1}$ ) and the ripe skin ( $2847 \mu\text{gg}^{-1}$ ), respectively.

Three mono-unsaturated fatty acids with unsaturation at C11 viz. 11-hexadecenoic acid, 11-octadecenoic acid and 11-eicosenoic acid were detected from the pulp and the skin of all the three cultivars. 11-hexadecenoic acid showed *de novo* appearance with significant increase during ripening. Its abundance was detected in Alphonso pulp and skin as well as in Kent skin. 11-octadecenoic acid was detected in the developing and the ripening tissues of all the three cultivars. Alphonso pulp and skin showed increase in its content during fruit development and ripening stages. However, the pulp and the skin tissue of Pairi and Kent fruits displayed varied pattern of its content during development and ripening. 11-hexadecenoic acid and 11-octadecenoic acid abundance was relatively very low compared to their isomers with unsaturation at C9 i.e. palmitoleic acid and oleic acid, respectively. Though 9-eicosenoic acid was not detected in the analysis, 11-eicosenoic acid showed its presence in the pulp as well as in the skin albeit with low abundance (maximum- $15.24 \mu\text{gg}^{-1}$ ) during developmental and ripening stages. Decreased levels of 11-eicosenoic

acid were detected during development and ripening of Pairi pulp while it was not detected in the late ripening stages of the pulp and the skin of Kent. Another unusual odd chain fatty acid i.e. 10-heptadecenoic acid was detected exclusively in the ripening pulp of all the three cultivars. Its maximum level was detected in the Alphonso ( $18.69 \mu\text{gg}^{-1}$ ) at over ripe stage.

#### 2.3.4.2 Poly-unsaturated fatty acids

Among various poly-unsaturated fatty acids four di-unsaturated and only one tri-unsaturated fatty acids were detected from mango. 9, 12-hexadecadienoic acid (n-4) and 9, 15-octadecadienoic acid (n-3) were detected utterly in the pulp of the three cultivars during ripening stages. Though rise in their levels were noted in late ripening stages, their amounts remained less than  $52.02 \mu\text{gg}^{-1}$  and  $85.94 \mu\text{gg}^{-1}$  for 9, 12-hexadecadienoic acid and 9, 15-octadecadienoic acid, respectively (Table 2.1). Another odd chain fatty acid, 2, 4-heptadienoic acid was detected in pulp as well as skin of all the three cultivars with significantly increasing levels during development and ripening. Pairi and Kent had higher levels of 2, 4-heptadienoic acid than Alphonso in the pulp and the skin.

Among the developing stages of all the three mango cultivars, LA/ 9, 12-octadecadienoic acid (n-6) was the highest contributor and shared 37-41% of total fatty acids of the pulp as well as the skin at 15 DAP stage. Levels of LA were high at 15 DAP stage in the pulp ( $1425$ ,  $1699$  and  $1178 \mu\text{gg}^{-1}$ ) as well as in the skin ( $2054$ ,  $3104$  and  $2749 \mu\text{gg}^{-1}$ ) from Alphonso, Pairi and Kent, respectively which reduced significantly through development and ripening. The lowest level of LA ( $79.46 \mu\text{gg}^{-1}$ ) was detected in Alphonso pulp at over ripe stage.

The only tri-unsaturated fatty acid detected in the present study was ALA/ 9, 12, 15-octadecatrienoic acid (n-3), which is an essential fatty acid. ALA was detected in the pulp and the skin of all the three cultivars. Decrease in the ALA content was detected from early developmental stage to mature raw stage followed by a significant increase till over ripe stage except for Kent skin. Amid pulp, the highest amount of ALA was evinced from Alphonso ( $881 \mu\text{gg}^{-1}$ ) while for the skin Pairi displayed the highest content ( $2181 \mu\text{gg}^{-1}$ ) at the over ripe stage. At ripe stage, Alphonso pulp

contained  $840 \mu\text{gg}^{-1}$  of ALA which was 1.6 and 2.05 fold higher than that of Pairi and Kent pulp, respectively at the same stage.

### 2.3.5 Principle component analysis

Quantitative variation of 17 different fatty acids in the pulp and the skin through development and ripening of Alphonso, Pairi and Kent cultivars was examined by principle component analysis (PCA). First 3 principle components achieved 83.5% of total variance of which the first two components accounted together for 74% of the noticed variance (Figure 2.5). PC1 had high positive loadings for all the saturated fatty acids along with oleic, linoleic, linolenic and 11-eicosanoic acid. Palmitoleic, 11-hexadecenoic and 11-octadecenoic acid had positive loading with lower scale, while rest had intermediate positive loadings for PC1. PC2 had the highest positive loading for palmitoleic acid followed by 11-hexadecenoic and 11-octadecenoic acid. Lignoceric, stearic, palmitic, 11-eicosenoic and linolenic acid showed low positive loading to PC2. Linoleic, arachidic and behenic acid had negative loading for PC2 and high positive loading for PC1. Ripening and pulp specific fatty acids such as 9, 12-hexadecadienoic acid, 9, 15-octadecadienoic acid, 2, 4-heptadienoic and 10-heptadecenoic acid had negative loading across PC1 and high positive loadings across PC2. Based on these loadings, clear separation of ripening and developing stages across PC1 and separation of pulp and skin tissues across PC2 was evinced in the score plot (Figure 2.5), except for few overlapping stages. Thus, stages for ripening pulp, ripening skin, developing pulp and developing skin were separated in four different quadrants of the score plot. Mid ripe, ripe and over ripe stages of Alphonso pulp can be clearly seen separating from the ripening stages of the pulp of Pairi and Kent cultivars in the same quadrant due to high accumulation of palmitoleic acid in Alphonso pulp during ripening. Similarly, ripe and over ripe stages of Pairi skin and over ripe stage of Alphonso skin showed high positive loading to PC1 than other ripening stages of the skin from the three cultivars which could be credited to its high ALA content. All the developing stages of the pulp and the skin for all the three cultivars clustered in the third and the fourth quadrants with negative loadings for PC2 due to their higher content of linoleic acid.

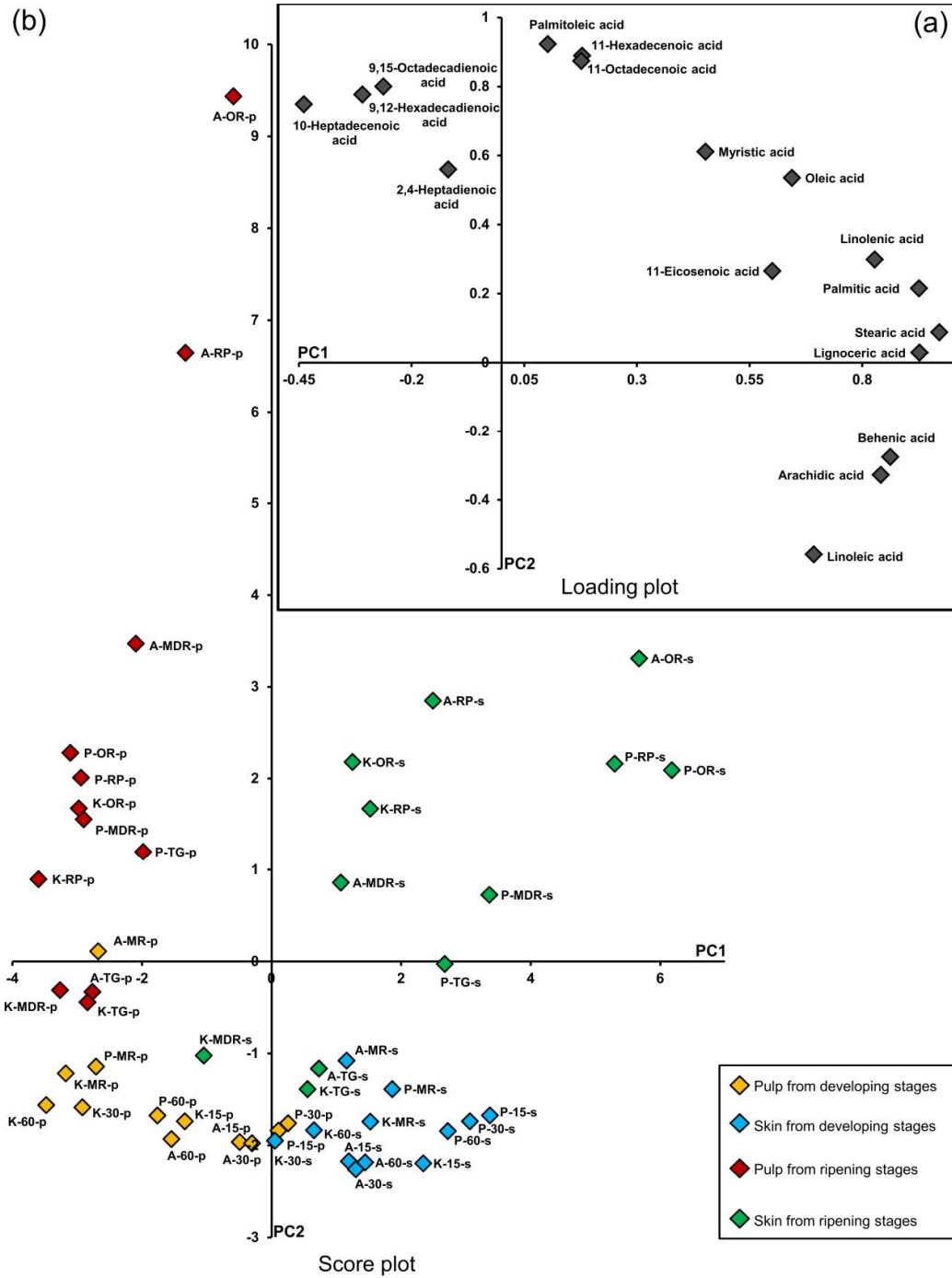


**Figure 2.5 Loading plot (a) and Score plot (b) of PCA**

Principle component analysis of 17 different fatty acids in the pulp and skin through various stages of fruit development and ripening from three mango cultivars, Alphonso, Pairi and Kent. Average values from biological replicates for each fatty acid were considered for the analysis. For the score plot (b) data labels represent, cultivars as A: Alphonso, P: Pairi and K: Kent, tissues as p: pulp and s: skin and stages as 15: 15DAP, 30: 30DAP, 60: 60DAP, MR: mature raw, TG: table green, MDR: mid ripe, R: ripe and OR: over ripe.

### 2.3.6 Lactone content of three cultivars at ripe stage

Lactone content of pulp and skin of Alphonso, Pairi and Kent cultivars was analysed at ripe stage i.e. the highest lactone containing stage according to our previous study (Pandit et al., 2009b). Total 7 lactones were detected and quantified (Table 2.3) in the volatile analysis of the ripe pulp and skin of the three cultivars.

**Table 2.3 Lactone content of ripe fruit**

Lactone content ( $\mu\text{g g}^{-1}$  tissue) of pulp and skin of Alphonso, Pairi and Kent at ripe stage.

Lactone	Alphonso pulp	Alphonso skin	Pairi pulp	Pairi skin	Kent pulp	Kent skin
$\gamma$ -butyrolactone	1.39±0.16	0.17±0.01	0.30±0.03	0.09±0.01	Trace <sup>a</sup>	Trace <sup>a</sup>
$\gamma$ -hexalactone	1.45±0.16	0.28±0.01	0.12±0.04	n.d.	n.d.	n.d.
$\delta$ -hexalactone	1.07±0.17	0.13±0.02	0.71±0.05	0.26±0.01	n.d.	n.d.
$\gamma$ -octalactone	2.16±0.20	1.49±0.09	0.07±0.01	0.28±0.03	n.d.	n.d.
$\delta$ -octalactone	0.65±0.05	0.15±0.002	0.11±0.03	0.14±0.01	n.d.	n.d.
$\gamma$ -decalactone	0.32±0.28	0.33±0.04	n.d.	0.35±0.06	n.d.	n.d.
$\delta$ -decalactone	0.09±0.01	0.61±0.20	n.d.	n.d.	n.d.	n.d.
<b>Total</b>	7.12	3.16	1.3	1.12	n.d.	n.d.

<sup>a</sup> Compound detected in traces in GC-MS analysis but not detected in GC-FID analysis

All the 7 lactones were present in the Alphonso pulp and skin, amid these  $\gamma$ -octalactone had the highest contribution compared to the other lactones. However, Pairi pulp was devoid of  $\gamma$ - and  $\delta$ -decalactones while the skin was devoid of  $\gamma$ -hexalactone and  $\delta$ -decalactone. In Pairi  $\delta$ -hexalactone and  $\gamma$ -decalactone were the major contributors amid all lactones from pulp and skin, respectively. Kent showed only traces of  $\gamma$ -butyrolactone, while rest of the lactones were not detected from pulp and skin. Total lactone content was the highest in case of Alphonso pulp ( $7.12 \mu\text{g g}^{-1}$ ) followed by Alphonso skin ( $3.16 \mu\text{g g}^{-1}$ ). Though Pairi was considered as lactone less cultivar, Pairi showed low but detectable levels of lactones viz.  $1.30 \mu\text{g g}^{-1}$  and  $1.12 \mu\text{g g}^{-1}$  in pulp and skin, respectively.

## 2.4 Discussion

### 2.4.1 Origin of unusual fatty acids

Various unusual fatty acids were detected in the present study. Three fatty acids with unsaturation at C11 *viz.* 11-hexadecenoic acid, 11-octadecenoic acid and 11-eicosenoic acid were detected from the pulp and the skin of all the three cultivars. Such unusual unsaturation could be because of existence of  $\Delta 11$  desaturase (Kleiman and Paynewahl, 1984) which synthesizes these compounds from their respective saturated fatty acids *viz.* 16:0, 18:0 and 20:0, respectively. Another probable pathway of biosynthesis of 11-hexadecenoic acid is by activity of  $\Delta 9$  desaturase on myristic acid and further elongation. Whereas 11-octadecenoic acid (*cis*-vaccenic acid) can be synthesized from palmitoleic acid after elongation (Shibahara et al., 1989; Tsevegsuren et al., 2003) and its presence has been reported from 17 different fruits (Shibahara et al., 1987). Similarly, 11-eicosenoic acid is known to be present in different plant seeds and nut oils. It is one of the abundant fatty acids in the seed oil of *Brassicaceae* family (Romanus et al., 2008) and it is also probably synthesized from oleic acid after additional elongation step. One odd chain mono-unsaturated fatty acid i.e. 10-heptadecenoic acid was also identified in the present study. Such presence of 10-heptadecenoic acid was also evinced from *Androsace septentrionalis* seed oil (Tsevegsuren et al., 2003) but biosynthetic pathway for this odd chain (C17) fatty acid is not known and thus, insists further research.

Pulp specific unusual di-unsaturated fatty acids *viz.* 9, 12-hexadecadienoic acid and 9, 15-octadecadienoic acid were evinced in the analysis. Such presence of 9, 12-hexadecadienoic acid has been reported from various plants. Biosynthesis of this fatty acid might be the result of activity of  $\Delta 12$  desaturase which accepts oleic acid as well as palmitoleic acid as substrate and synthesizes linoleic and 9, 12-hexadecadienoic acid, respectively (Tsevegsuren et al., 2003). Similarly, first report on presence of 9, 15-octadecadienoic acid was from mango pulp which proposed its synthesis either by the action of  $\Delta 15$  desaturase which acts on oleic acid (non-natural substrate for  $\Delta 15$  desaturase) or by the action of its another isoform which does not depend on the unsaturation at  $\omega 6$  (Shibahara et al., 1993).

Another odd chain di-unsaturated unusual fatty acid i.e. 2, 4-heptadienoic acid was evinced from pulp as well as skin tissues of three cultivars with notable level during ripening. Synthesis of 2, 4-heptadienoic acid was reported in yeast (*Sporobolomyces odorus*) to study the synthesis of lactones by biotransformation while feeding labelled  $\alpha$ -linolenic acid, which resulted in synthesis of radio labelled 2, 4-heptadienoic acid along with the  $\delta$ -jasmin lactone and (Z,Z)-dodeca-6,9-dieno-4-lactone. Though exact biosynthetic pathway of this odd chain fatty acid is not known, it is proposed that its synthesis might be the result of fragmentation of even chain fatty acid ( $\alpha$ -linolenic acid) in to two odd chain fragments (Haffner et al., 1996).

### 2.4.2 Fatty acids from mango fruit and their nutritional significance

Qualitative and quantitative analysis from three mango cultivars showed differential composition of fatty acids through various stages of mango fruit development and ripening. During analysis, perfect amalgamation of saturated, mono-unsaturated and poly-unsaturated fatty acids was observed. Developing stages were rich in saturated fats along with high levels of  $\omega$ -6 linoleic acid, whereas ripening stages were enriched by mono-unsaturated fatty acids and  $\omega$ -3 linolenic acid with reduced level of linoleic acid. Saturated fatty acids are good source of energy due to their high calorific values but are associated with coronary disorder as they tend to increase level of LDL-cholesterol and therefore, should be consumed in lower amounts. However, dietary intake of mono-unsaturated and poly-unsaturated fatty acid is recommended as they increase the level of HDL-cholesterol and reduce LDL-cholesterol from blood stream (Ulbricht and Southgate, 1991). At each stage of mango fruit development and ripening total unsaturated fatty acids exceeded total saturated fatty acids in pulp as well as in skin (Figure 2.4) making mango fruit good source of unsaturated fatty acids. Mono-unsaturated fatty acids like oleic acid and palmitoleic acid are known to be antithrombotic than saturated fatty acids (Reaven et al., 1991; Willett et al., 1995). Increased levels of these mono-unsaturated fatty acids during mango fruit ripening make it more ideal for consumption.

Humans are known to have evolved on diet condition which contained  $\omega$ 6/ $\omega$ 3 essential fatty acid (EFA) ratio nearing 1 and is considered as good intake of essential fatty acids. Consumption of fatty acids with high  $\omega$ 6/ $\omega$ 3 ratio is associated with



susceptibility to many diseases like cardiovascular diseases, cancer, inflammatory and autoimmune diseases. However, intake of EFA with lower  $\omega 6/\omega 3$  ratio decreases risk of these diseases (Simopoulos, 2002). Present analysis revealed increased level of  $\omega$ -3 fatty acid and reduced level of  $\omega$ -6 fatty acid during mango fruit ripening, which lead to the ratio of  $\omega 6/\omega 3 \leq 1$  at ripe stage (Table 2.4). Thus, ripened mango becomes perfect source of essential fatty acids.

Similarly, mango skin showed higher levels of all the fatty acids except few unusual fatty acids which were pulp specific. However, the skin of mango especially from ripening stages is not consumed and is discarded as waste of mango food processing industries (Ajila et al., 2007). Utilization of such unused mango skin has been studied for its pectin content (Berardini et al., 2005) and polyphenol, vitamin E and C, fiber and carotenoids content (Ashoush and Gadallah, 2011). Although skin is an enriched source of essential fatty acids, it has remained unnoticed till now and thus, can be utilized for oil extraction.

**Table 2.4 Flavor and nutritional perspective of fatty acids**

Table representing total lactone content ( $\mu\text{g g}^{-1}$ ), palmitic acid/palmitoleic acid (16:0/C16:1) ratio and linoleic acid/linolenic acid ( $\omega 6/\omega 3$ ) in pulp and skin at ripe stage of Alphonso, Pairi and Kent mango cultivars. Values shown are average of biological replicates sampled for the study. Difference between the tissues was significant ( $p \leq 0.05$ ) if the alphabets (a, b, c....) after the quantity of the lactone are different.

Ripe tissue	Flavor		Nutrition
	Total lactone content	C16:0/C16:1	LA/ALA ( $\omega 6/\omega 3$ )
Alphonso pulp	7.12 <sup>d</sup>	0.67	0.1
Pairi pulp	1.30 <sup>b</sup>	1.49	0.27
Kent pulp	nd <sup>a</sup>	1.78	0.2
Alphonso skin	3.16 <sup>c</sup>	1.35	0.37
Pairi skin	1.12 <sup>b</sup>	6.48	0.98
Kent skin	nd <sup>a</sup>	1.89	1.06

### 2.4.3 Fatty acid content and flavor qualities of mango cultivars

Flavor is the combined perception of taste, aroma, texture and visual appearance of food. Lactones- an important class of aroma volatiles; contribute fruity, creamy, coconut and peach like notes to mango flavor and are derived from fatty acid

metabolism. Though exact biosynthetic pathway for lactone is not known, these compounds are supposed to be synthesized from unsaturated fatty acids (Goff and Klee, 2006; Haffner et al., 1996; Xi et al., 2012). Thus, presence of high unsaturated fatty acids content in Alphonso pulp might play a crucial role in its flavor generation through increased lactone content. Moreover, they might as well contribute to the pulp texture by means of viscosity and lubricity. Studies on human and animal behaviour suggested that “fatty” may be one of the taste attributes other than well known five tastes (Mattes, 2009a). Thus high fatty acid content in Alphonso pulp than Pairi and Kent cultivars might be one of the important features responsible for highly favoured nature of Alphonso mango.

Development of sweet, fruity aroma of ripened fruits has earlier been correlated to the conversion of palmitic acid to palmitoleic acid (Bandyopadhyay and Gholap, 1973b; Gholap and Bandyopadhyay, 1975). In the present study, we have attempted to correlate this conversion to lactone content of the three cultivars. This is mainly because unsaturated fatty acids are considered to be precursor for lactone biosynthesis. In case of ripe Alphonso pulp the lowest (0.67) palmitic acid/palmitoleic acid (C16/C16:1) ratio and maximum lactone content was observed ( $7.12 \mu\text{g g}^{-1}$ ). Whereas, in Pairi pulp C16:0/C16:1 ratio was  $\sim 1.5$  and moderate levels of lactones ( $1.30 \mu\text{g g}^{-1}$ ) were detected. In this study volatile extraction was carried out from the pulp and the skin separately, whereas in our previous work (Pandit et al., 2009a) whole fruit (pulp and skin together) was used for volatile extraction. Also sensitivity of GC-MS instrument used in both the study was different. These might be the reasons for detection of lactones in Pairi in the present study. In case of Kent pulp this ratio was high (1.78) and lactones were not detected (Table 2.4). Similar correlation can be seen in the skin of Alphonso and Kent except that of Pairi where C16:0/C16:1 was very high (6.48) still lactones were detected. This could be because of overall high fatty acid content of Pairi skin and excessive accumulation of palmitic acid ( $\sim 1.2$  fold higher) than Alphonso and Kent skin at ripe stage.

In the correlation analysis between total lactone content and individual fatty acid content from ripe pulp and skin of three cultivars, palmitoleic acid, 11-octadecenoic acid and 9,15-octadecadienoic acid showed strong correlation ( $r = 0.847, 0.954$  and  $0.76$ , respectively) as shown in the correlation analysis (Table 2.5).

This signifies the probable role of conversion of palmitic acid to palmitoleic acid and palmitoleic acid to 11-ocadecenoic acid in the increased lactone content.

**Table 2.5 Correlation analysis 1**

Correlation analysis of total lactone content ( $\mu\text{g g}^{-1}$  tissue) and individual fatty acid content from the pulp and the skin tissues of Alphonso, Pairi and Kent cultivars at ripe stage. Values represent correlation coefficient ( $r$ ), Values in bold represent strong positive correlation ( $0.7 \leq r$ ) between fatty acid and lactone.

Fatty acid	Correlation coefficient
Myristic acid	-0.008
Palmitic acid	0.064
Stearic acid	-0.064
Arachidic acid	-0.043
Behenic acid	0.027
Lignoceric acid	-0.144
Palmitoleic acid	<b>0.847</b>
11-Hexadecenoic acid	0.547
10-Heptadecenoic acid	0.633
Oleic acid	0.078
11-Octadecenoic acid	<b>0.954</b>
11-Eicosenoic acid	0.477
9,12-Hexadecadienoic acid	0.645
Linoleic acid	-0.385
9,15-Octadecadienoic acid	<b>0.76</b>
2,4-Heptadienoic acid	-0.099
Linolenic acid	-0.053

Similarly, correlation analysis between individual lactone content and individual fatty acid from ripe pulp and skin of three cultivars showed strong correlations with unsaturated fatty acids as shown in the Table 2.6.  $\gamma$ -butyrolactone and  $\gamma$ -hexalactone showed strong correlations with palmitoleic acid, 10-heptadecenoic acid, 11- octadecenoic acid, 9, 12- hexadecadienoic acid and 9, 15- octadecadienoic acid.  $\delta$ -hexalactone showed strong correlations with 10-heptadecenoic acid, 9, 12- hexadecadienoic acid and 9, 15- octadecadienoic acid.  $\gamma$  and  $\delta$ - octalactone showed strong correlations with palmitoleic acid and 11- octadecenoic acid, additionally  $\delta$ - octalactone had strong correlation with 10-heptadecenoic acid, 9, 12- hexadecadienoic acid and 9, 15- octadecadienoic acid.  $\gamma$ -decalactone own strong correlations with 11- octadecenoic acid and 11- eicosenoic acid, whereas  $\delta$ - decalactone showed moderate correlation ( $0.3 \leq r \leq 0.7$ ) with

palmitoleic acid, 11- octadecenoic acid and 11-eicosenoic acid. Though such correlation can be seen at substrate level, genes involved in lactone biosynthesis and their transcript levels may also play an important role in differential accumulation of lactones in these tissues. However, lack of information about lactone biosynthesis restricts further discussion and in depth study needs to be aimed to identify probable lactone biosynthetic pathway in mango fruit.

### Table 2.6 Correlation analysis 2

Correlation analysis of individual lactone and individual fatty acid content from the pulp and the skin tissues of Alphonso, Pairi and Kent cultivars at ripe stage. Values represent correlation coefficient (r), Values in bold represents strong positive correlation ( $0.7 \leq r$ ) between fatty acid and lactone content.

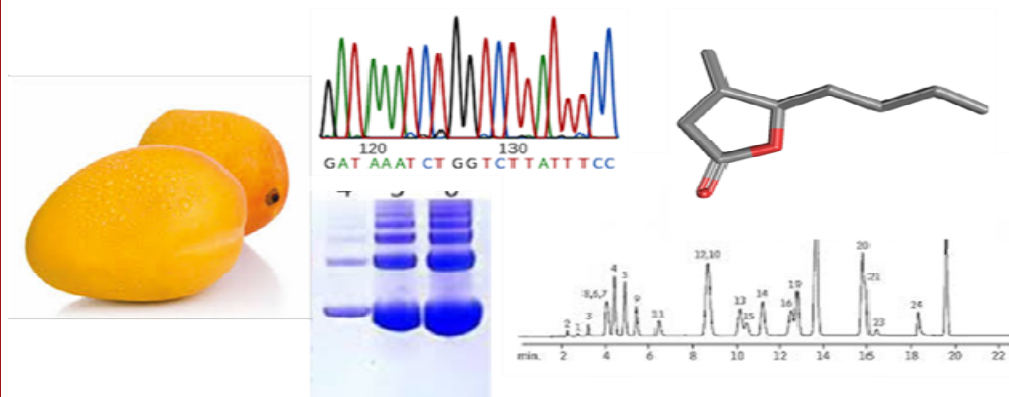
Lactone	Palmitoleic acid	10-Hepta decenoic acid	11-Octa decenoic acid	11- Eicosenoic acid	9,12- Hexadeca dienoic acid	9,15- Octadeca dienoic acid
$\gamma$ -Butyrolactone	<b>0.752</b>	<b>0.813</b>	<b>0.828</b>	0.229	<b>0.823</b>	<b>0.91</b>
$\gamma$ -Hexalactone	<b>0.832</b>	<b>0.73</b>	<b>0.885</b>	0.259	<b>0.77</b>	<b>0.878</b>
$\delta$ -Hexalactone	0.487	<b>0.9</b>	0.622	0.202	<b>0.808</b>	<b>0.825</b>
$\gamma$ -Octalactone	<b>0.888</b>	0.416	<b>0.974</b>	0.566	0.457	0.592
$\delta$ -Octalactone	<b>0.77</b>	<b>0.706</b>	<b>0.893</b>	0.405	<b>0.724</b>	<b>0.836</b>
$\gamma$ -Decalactone	0.496	-0.058	<b>0.748</b>	<b>0.953</b>	-0.035	0.118
$\delta$ -Decalactone	0.452	-0.283	0.472	0.558	-0.287	-0.22

## 2.5 Conclusion

In conclusion, fatty acid content of fruits from three mango cultivars at various stages displayed significant variation. Overall mango fruit possessed high fatty acid nutritional value during various stages of fruit development and ripening. The pulp and the skin of the ripening mango fruits are good source of  $\omega$ -3, mono and di-unsaturated essential fatty acids with relatively lower share of saturated fatty acids. Present study also gives insights in to the probable fatty acid precursors for lactone biosynthesis in mango. The study has also explored high fatty acid content of mango skin which can be an ideal raw material for nutritionally enriched food products.



## Chapter 3



Isolation and characterization of 9-*lipoxygenase* and *epoxide hydrolase 2* genes: Insight into lactone biosynthesis in mango fruit (*Mangifera indica* L.)

The contents of this chapter have been published as full length article in *Phytochemistry* (2017); DOI:10.1016/j.phytochem.2017.03.002



## Chapter 3 Isolation and characterization of 9-lipoxygenase and epoxide hydrolase 2 genes: Insight into lactone biosynthesis in mango fruit (*Mangifera indica* L.)

### 3.1 Introduction

Acceptability and preference of food items is based on human organoleptic perception, which is a combined impression of visual appearance, texture, aroma and taste of a specific item. A collective olfaction of aroma and taste through retronasal and orthonasal receptors and taste buds decides flavor of the food. It is well known that aroma compounds mainly contribute to the flavor of the food. Most of the aroma related studies have been carried out on various fruits, as they possess unique aroma with large diversity in their respective flavor profile.

Aroma volatile analysis of *Mangifera indica* L. (Anacardiaceae) has shown presence of variety of compounds viz. alkanes, alkenes, aldehydes, alcohols, monoterpenes, sesquiterpenes, oxygenated monoterpenes, oxygenated sesquiterpenes, non-terpene hydrocarbons, furanones and lactones (Dar et al., 2016; Idstein and Schreier, 1985; Pandit et al., 2009b). Alphonso, one of the most favoured and exported Indian mango cultivars has revealed qualitative abundance and blend of volatiles among various Indian and non Indian mango cultivars analysed (Pandit et al., 2009a). Among these groups of volatile compounds lactones and furanones are notably important due to their ripening specific temporal and spatial appearance in mango fruits (Pandit et al., 2009b). Volatile blend of Alphonso mango showed presence of fourteen different lactones (Idstein and Schreier, 1985; Wilson et al., 1990). Structurally these lactones are cyclic esters characterized by a closed ring consisting of four or five carbon atoms and a single oxygen atom, with a ketone group (C=O) in one of the carbons adjacent to oxygen in the ring. Lactones impart sweet fruity flavor, a characteristic feature of fully ripened mango fruit (Wilson et al., 1990). Despite the structural and functional characterization of these vital flavor metabolites, the pathway of their biosynthesis remains elusive.

Earlier attempts to identify probable precursors of lactone biosynthesis, even if in other organisms, can form a basis to reveal lactone biosynthesis in mango. For example, studies in various yeasts, moulds and bacteria suggest that fatty acids and keto acids might be the precursors at initial steps of lactone biosynthesis. The hydroxy fatty acids then synthesized (probably upon microbial reduction) from various  $\gamma$  and  $\delta$  keto acids (C8 – C12) could be converted into lactones by simple heating (Muys et al., 1962). Deuterium labelling studies in yeast (*Sporobolomyces odorus*) have revealed involvement of unsaturated fatty acids such as linolenic acid as precursors for  $\delta$ -Jasmin lactone and (Z,Z)-Dodeca-6,9-dieno-4-lactone synthesis (Haffner et al., 1996). Also, our studies as detailed in Chapter 2 describe dynamic nature of various fatty acids in developing and ripening stages of fruits of Alphonso, Pairi and Kent cultivars of mango and correlation of certain unsaturated fatty acid levels with that of lactones in these cultivars. Metabolism of epoxy octadecanoic acid by epoxide hydrolase (EH) for production of  $\gamma$ -decalactone and  $\gamma$ -dodecalactone has also been proposed through deuterium labelling studies in *Sporidiobolus salmonicolor* (Haffner and Tressl, 1998). Further, a study in nectarines has illustrated that administration of  $^{18}\text{O}$  labelled epoxy acid-5 (9-10 epoxy heptadecanoic acid) produced undecano-4-lactone. This important observation has suggested possible involvement of epoxy fatty acids in lactone production by the activity of EH (Schottler and Boland, 1996). Comparative EST analysis from ripening *Prunus persica* L. Batsch has later supported *EH* as the key gene responsible for lactone biosynthesis (Vecchiotti et al., 2009). These epoxy fatty acids in plants are synthesized by the activity of peroxygenase (PGX) enzyme (Fuchs and Schwab, 2013; Meesapyodsuk and Qiu, 2011). A report in Oat PGX (*AsPGX1*) revealed that it catalyzes epoxidation of oleic acid with the cumene hydroperoxide as an oxidant. Similarly, *AsPGX1* utilizes products of 9-lipoxygenase (9LOX) viz. 9-hydroperoxy-octadecadienoic (9-HOPD) and 9-hydroperoxy-octadecatrienoic (9-HOPT) acids as oxygen donor (Meesapyodsuk and Qiu, 2011) generating their respective monohydroxy fatty acids. Also, involvement of lipoxygenase (LOX) to form oxygenated chiral fatty acids leading to production of  $\gamma$  and  $\delta$  lactones upon beta oxidation has been reported (Cardillo et al., 1989). Significance of hydroxy fatty acid synthesized from products of 9LOX i.e. hydroperoxy fatty acid in the formation of lactone is also reported (Huang and Schwab, 2011).



These initial efforts insinuate involvement of LOX and EH enzymes in lactone biosynthesis. The present chapter therefore, focuses on isolation and transcript profiling of *9-lipoxygenase (Mi9LOX)*, *epoxide hydrolase 2 (MiEH2)*, *peroxygenase (MiPGXI)*, *hydroperoxide lyase (MiHPL)* and *acyl-CoA-oxidase (MiACO)* genes during various developmental and ripening stages in fruit of Alphonso, Pairi and Kent cultivars having differential levels of lactones. Further, molecular and biochemical characterization of *Mi9LOX* and *MiEH2* in mango fruit and probable role of these two enzymes in lactone biosynthesis have been investigated based on their over-expression by agroinfiltration approach followed by metabolite analysis.

## 3.2 Materials and methods

### 3.2.1 Plant material

All the tissues of fruit development and ripening stages for Alphonso, Pairi and Kent mango cultivars were similar as collected for the fatty acid analysis described in Chapter 2 (Section 2.2.1). In addition for transient expression studies ethylene treated fruits were collected as described earlier (Chidley et al., 2013). For ethylene treatment 20 mature raw fruits of Alphonso mango were collected from mango orchard of Dr. Balasaheb Sawant Konkan Agriculture University at Dapoli, Maharashtra, India (17.747823 N, 73.184961 E). These fruits stacked in plastic crates were further kept inside a closed chamber (3 m × 3 m × 3 m) and ethylene gas was sprayed inside the closed chamber to a final concentration of 100 ppm. The chamber was closed for 24 h and maintained at 30 °C and 85–90% humidity. Post ethylene treatment fruits were kept in hay containing boxes and allowed to ripen at ambient temperature. At 3DAH stage these fruits were used for the transient expression study.

### 3.2.2 RNA isolation and cDNA synthesis

Total RNA was isolated for all the tissues sampled for current study using RNeasy Plus mini kit (Quiagen, Venlo, The Netherlands). Two microgram of total RNA was reverse transcribed for synthesis of cDNA using High Capacity cDNA reverse transcription kit (Applied Biosystem, Carlsbad, CA, USA).

### 3.2.3 Isolation of open reading frames of *Mi9LOX*, *MiHPL*, *MiPGX1*, *MiEH2* and *MiACO*

Full length gene sequences of *peroxygenase (PGX)*, *hydroperoxide lyase (HPL)* and *acyl-CoA-oxidase (ACO)* were isolated from Alphonso mango using degenerate primer (Table 3.1) approach. RACE reactions with gene specific primers (Table 3.1) were carried out to obtain ends of *PGX*, *HPL* and *ACO* cDNAs. The terminal primers (Table 3.1) were designed for each gene and the full-length genes were isolated and sequenced. These were blasted against the NCBI database for respective genes.

For isolation of partial gene sequence of *EH2* from Alphonso mango, degenerate primers *viz.* EHDeF1 and EHDeR4 (Table 3.1) were designed by homology based approach aligning nucleotide sequences of *EH2* from other plant species available in NCBI database. Amplification was carried out using ripe stage cDNA as template. Amplicon with expected size was purified from agarose gel, cloned in pGEM-T easy vector (Promega, Madison, WI, USA) and sequenced to confirm partial cDNA sequence of *EH2*. Gene specific primers, EHRCF2 and EHRCR1 (Table 3.1) were designed from the obtained sequence and used for rapid amplification of cDNA ends (RACE) to acquire the 5' and 3' ends using the SMART™ RACE cDNA Amplification Kit (Clontech, CA, USA). Those amplicons were cloned and sequenced to design terminal gene specific primers, EHtrF1 and EHtrR1 (Table 3.1) for the isolation of complete open reading frame (ORF) of *EH2*. For isolation of *9LOX*, gene specific primers were designed from its available partial gene sequence (EU513272.1) from our previous study (Pandit et al., 2010). The same protocol as that of isolation of *EH2* ORF was further followed using LF1 and LR1 primers (Table 3.1) to obtain cDNA ends and terminal primers LOX\_TF1 and LOX\_TR1 (Table 3.1) to amplify complete ORF of *9LOX*. Ripe mango cDNA as template and Advantage2 polymerase mix (Clontech, CA, USA) were used to get complete ORFs of both the genes (*MiEH2* and *Mi9LOX*) from mango, cloned in to pGEM-T easy vector and transformed in to *E. coli* (Top 10) cells. In both the cases presence of complete ORF was confirmed by sequencing plasmid inserts from number of positive colonies for each. Encoded proteins from these genes and other plant *9LOX*, *13LOX*, *EH1* and *EH2* from NCBI database were used for phylogenetic

analysis. Neighbour joining tree was constructed by bootstrap test (1000 replicates) using MEGA 5.05.

### 3.2.4 Quantitative real-time PCR

Quantitative real-time PCR was performed using Fast Start Universal SYBR Green master mix (Roche Inc. Indianapolis, Indiana, USA) and *elongation factor 1 $\alpha$*  (*EF1 $\alpha$* ) as an endogenous control employing the primers reported earlier (Pandit et al., 2010). Transcripts of *Mi9LOX*, *MiEH2*, *MiPGX1*, *MiHPL* and *MiACO* were amplified using gene specific primers (Table 3.1) and quantification was done by ViiA™ 7 Real-Time PCR System (Applied Biosystems) having thermal cycle program of initial denaturation at 95 °C for 10 min with subsequent 40 cycles of 95 °C for 3 sec and 60 °C for 30 sec followed by a dissociation curve analysis of transcripts. The analysis was carried out for pulp and skin tissues from all the developing and ripening stages of Alphonso, Pairi and Kent mango fruits.

Transcripts of *Mi9LOX* and *MiEH2* were also analysed in a similar way from the test and the control tissues obtained from transient over-expression experiments to understand changes in the transcript profiles upon *Agrobacterium* infiltration.

### 3.2.5 Cloning and recombinant expression of *Mi9LOX* and *MiEH2* in *E. coli*

The full-length sequences of *Mi9LOX* and *MiEH2* amplified from the ripe Alphonso fruit cDNA using the Q5 High fidelity DNA polymerase (New England Biolabs Inc., Ipswich, MA, USA) and Advantage2 polymerase mix, respectively and the relevant terminal primers LOXpET101D F1/LOXpET101D R1 and EHTOPO\_F1/EHTOPO\_R1 (Table 3.1) were cloned in the pET101D and pEXP5-CT/TOPO expression vectors (Invitrogen), respectively. After confirming the correct orientation of the insert and the presence of an uninterrupted reading frame by sequencing, the recombinant plasmids of *Mi9LOX* and *MiEH2* were transformed in the BL21(DE3) pLysS Rosetta cells (Novagen, Madison, WI, USA), for recombinant gene expression.

**Table 3.1 List of primers used in the study**

Primers used in gene isolation, cloning and real time analysis. Classes represented as A: degenerate primers, B: gene specific primers to carry out RACE reaction, C: terminal primers, D: primers for bacterial expression cloning, E: primers for transient expression cloning in pBI121, F: Primers used in real time analysis

Gene	Primer	Class	Primer Sequence
<i>Mi9LOX</i>	LF1	B	GGGATCCGGACAATGGCAAACC
	LR1	B	GAAGCTATCCATATGATTATGGTGC
	LOX_TF1	C	ATGGGGACAGTGGTGTGATGAAG
	LOX_TR1	C	CTAAATTGAAACACTGTTTGAATTCC
	LOXpET101DF1	D	CACCATGGGGACAGTGGTGTGATGAAG
	LOXpET101DR1	D	AATTGAAACACTGTTTGAATTCTTTG
	LOXpBI121F1	E	AAAAAAGGATCCATGGGGACAGTGGTGTGATGAAG
	LOXpBI121R1	E	AAAAAAGGATCCCTAAATTGAAACACTGTTTGAATTCC
	LOXRTF4	F	GACAAGAAAGATGAGCCCTGGTGGC
	LOXRTR4	F	AAATTGACAGCAGCATGGAGAGCGG
<i>MiEH2</i>	EHDDeF1	A	CTYTGGTAYTCVTGGCG
	EHDDeR4	A	CCHRYCCATGGHSC
	EHRCF2	B	GTGGCTTCGGTGATACTGACGC
	EHRCR1	B	CCTGATCAGAGGCAACGACGTC
	EHtrF1	C	ATGGAAGATATACAGCACAGAATTGTG
	EHtrR1	C	TCAGAACTTCTGAAAAAAGTTGTATATG
	EHTOPO_F1	D	ATGGAAGATATACAGCACAGAATT
	EHTOPO_R1	D	GAACTTCTGAAAAAAGTTGTATATG
	EHpBI121F1	E	AAAAAAGGATCCATGGAAGATATACAGCACAGAATTGTG
	EHpBI121R1	E	AAAAAAGGATCCTCAGAACTTCTGAAAAAAGTTGTATATGTGC
	EHRTF4	F	CCTTGGGCCGGGAGTCAAATAAAGG
	EHRTR4	F	AATGGCACATCTCGCTTGAACCCAC
	<i>MiPGX1</i>	PGX_De_F	A
PGX_De_R		A	AMTCRAACAARCTMCCATC
PGX_RC_F		B	GGGATCATTTACCCTGGGAGAC
PGX_RC_R		B	CCCCTTACTTGCAATCCAGCC
MiPGX_Tr_F		C	ATGGACGGGGATGCAATGGCAACC
MiPGX_Tr_R		C	TTAAATCATCTTAGCTGCAGCGCCTGC
MiPGX1_RT_F1		F	AAGGAAGGTACATGCCTGCAAACCT
MiPGX1_RT_R1		F	CGGTTTCCCTCAGTCATGTCCCAA
<i>MiHPL</i>		HPL_RC_F	B
	HPL_RC_R	B	CCTCGTTGCACCACCTCG
	MiHPL_Tr_F	C	ATGATGATCAAATCCATGAGC
	MiHPL_Tr_R	C	TCATTTTGCCTTTTCAACGGCTG
	MiHPL_RT_F	F	TGAGCCACAACACGCTAAGA
	MiHPL_RT_R	F	AAGCCTGCAGAACCCTTCTC
<i>MiACO1</i>	MiACO_De_F	A	CTKGARACCACTGCAACWTTTGATC
	MiACO_De_R	A	CCAYTCACYAACRAAYCTGAAAGCATA
	MiACO_RC_F	B	TGGTGGCCTGGTGGATTGGGTAAAAG
	MiACO_RC_R	B	TGACGAACATACACCATAGTGCCATAAA
	MiACO1_TF	C	ATGGCTGGCGTTGATTATCTTGCTGACG
	MiACO1_TR	C	TCAGAGTCTTGCTGTTCCGGAGCTGTTG
	MiACO1_RT_F1	F	ACCTCTACGAGGAAGCTTGAAGGA
	MiACO1_RT_R1	F	AGAGTCTTGCTGTTCCGGAGCTGTTG
<i>MiEF1<math>\alpha</math></i>	EF1_F	F	AATACGACTCACTATAGGGCAAGCAG
	EF1_R	F	ATACGACTCACTATAGGGCTCCTTCTC

Starter culture was initiated in 20 ml terrific broth (TB) with  $100 \mu\text{gml}^{-1}$  ampicillin and grown at  $37^\circ\text{C}$  with 180 rpm for 24 hrs. Expression culture was started with 1L TB medium inoculated with 1% final concentration of starter culture with  $100 \mu\text{gml}^{-1}$  ampicillin at  $37^\circ\text{C}$  with 180 rpm shaking speed. Expression of recombinant protein was induced by 0.2 mM IPTG at 0.6  $\text{OD}_{600}$ . After induction expression culture was kept at  $16^\circ\text{C}$ , 120 rpm for 12 to 14 hrs and cells were harvested by centrifugation, resuspended in 100 mM phosphate buffer, pH 7 with 20 mM imidazole. The cells were lysed by sonication and the 6x-His tagged recombinant proteins were purified on Ni-NTA matrix (Invitrogen) wherein non-specifically bound proteins were removed by low molarity imidazole containing phosphate buffer washes. Recombinant proteins were eluted in 100 mM phosphate buffer with 250 mM imidazole (pH 7). In case of eluted *Mi9LOX*, low molecular weight contaminant proteins were removed by passing eluted fractions through Amicon Ultra centrifugal filters with NMWL 50 kDa membrane (Merck Millipore, Darmstadt, Germany). Purified recombinant proteins were checked by SDS-PAGE for their purity.

### 3.2.6 Enzyme assays of recombinant *Mi9LOX* and *MiEH2*

*Mi9LOX* activity assay was initially performed in 250  $\mu\text{l}$  final volume of 100 mM phosphate citrate buffer, pH 7.0 containing 200  $\mu\text{M}$  substrate i.e. linoleic acid (LA) or  $\alpha$ -linolenic acid (ALA) and 0.005% Tween20 at  $30^\circ\text{C}$ . The activity was measured by formation of the conjugated diene at 234 nm, applying an extinction coefficient  $25000 \text{M}^{-1}\text{cm}^{-1}$  for both the substrates.  $A_{234}$  at 0<sup>th</sup> min for each reaction was considered as blank and subtracted from  $A_{234}$  for given time (t). Similar activity assay was carried out for both the substrates with protein expressed from an empty vector. Optimum pH and temperature of the recombinant protein were determined by calculating *Mi9LOX* activity either at varied range of pH in phosphate citrate buffer at  $30^\circ\text{C}$  or in phosphate citrate buffer, pH 7 at various temperatures, respectively. After spectrophotometric measurement of catalytic activity of *Mi9LOX*, products were extracted in chloroform: methanol (2:1); completely dried in vacuum evaporator and reconstituted in methanol. These assay extracts were then used for UPLC coupled Q Exactive orbitrap HRMS (Thermo Scientific, Waltham, MA, USA) analysis for the product confirmation. Extracted compounds from the assay reactions were separated by water (A): methanol (B) solvent gradient, at 0 min with 70% (A)/30% (B); 0-2 min

50% (A)/50% (B); 2-12 min 0% (A)/100% (B), held for 2 min and again back to 70% (A)/30% (B) in 3 min with 2 min hold at flow rate 500  $\mu\text{l min}^{-1}$ .

Recombinant *MiEH2* activity assay was carried out in 500  $\mu\text{l}$  assay reaction in similar way as that of *Mi9LOX* using substrates *cis*-stilbene oxide (CSO), *trans*-stilbene oxide (TSO) and 12(13) epoxide of linoleic acid [(12) 13 EpOME]. Temperature and pH optimization was also carried out in a similar way. Products formed in the assay were extracted in chloroform: methanol (2:1); evaporated till dryness, reconstituted in 200  $\mu\text{l}$  methanol and HRMS analysis was carried out by accurate mass (molecular ion) identification. Identified products from assay reaction were confirmed with the mass and retention time indices of authentic standards *R,R* hydrobenzoin and *meso* hydrobenzoin. Extracted compounds from CSO and TSO assay reactions were separated by water (A): methanol (B) solvent gradient, 0-1 min with 80% (A)/20% (B); 1-2 min 60% (A)/40% (B); 2-4 min 40% (A)/60% (B); 4-11 min 20% (A)/80% (B); 11-16 min 0% (A)/100% (B), held for 2 min and again back to 80% (A)/20% (B) in 3 min with 2 min hold at flow rate 500  $\mu\text{l min}^{-1}$ . Compounds from assay reactions of 12(13) EpOME were separated by using similar gradient program as that for *Mi9LOX* assay reaction. Graphs plotted with standard compounds were used for quantitative analysis of CSO and TSO products generated by recombinant *MiEH2*. Full scans for both the programs were acquired on positive ion mode with AGC target value of 1E6, resolution of 70,000 at scan range 100 -500  $m/z$ , and maximum ion injection time (IT) of 250 ms.

### 3.2.7 Transient over expression of *Mi9LOX* and *MiEH2* in Alphonso mango fruits

The sequences of *Mi9LOX* and *MiEH2* were cloned separately at *Bam*HI restriction site in pBI121 plant expression vector between CaMV 35S promoter and *GusA* gene using terminal primers (Table 3.1). The resulted correctly oriented construct (A) pBI121+ *Mi9LOX*, construct (B) pBI121+ *MiEH2* and (C) pBI121 empty vector were transformed in *Agrobacterium tumefaciens* GV3101 strain for transient expression studies. Separate *A. tumefaciens* cultures (5 mL) were initiated for each construct from individual colonies in YEB medium (0.5% beef extract, 0.1% yeast extract, 0.5% peptone, 0.5% sucrose, 2 mM  $\text{MgSO}_4$ ) with 100  $\mu\text{gml}^{-1}$  rifampicin and

kanamycin antibiotics and incubated overnight at 28 °C. This culture was transferred to 50 ml induction medium, (YEB with 20 mM acetosyringone and 10 mM MES, pH 5.6) with 100 µgml<sup>-1</sup> rifampicin and kanamycin antibiotics, and again grown overnight. Cultures were then recovered by centrifugation and re-suspended in infiltration medium (10 mM MgCl<sub>2</sub>, 10 mM MES, 200 mM acetosyringone, pH 5.6) till optical density reached to 1.0. This suspension was again incubated at 28 °C with gentle agitation for 2 hr. Over-expression studies for *Mi9LOX* and *MiEH2* were carried out by *Agrobacterium* mediated infiltration in ethylene treated mango fruits at 3DAH stage by using hypodermic syringe. Equal volumes of (A) or (B) and (C) were used for infiltration in the two halves of the same mango fruit separated by fruit stone. During initial trials it was confirmed that, *Agrobacterium* mediated infiltration did not spread beyond fruit stone. Thus, control (C) and test (A/B) over-expressions were carried out in the same fruit. Five distinct mango fruits, each were used for the over-expression study of *Mi9LOX* and *MiEH2*. Infiltrated fruits were kept at 25 °C for 2 days in 12 hr dark and light conditions each. After 2 days; a part from each of the fruit halves was checked by Gus staining (Kapila et al., 1997; Spolaore et al., 2001) to confirm expression of *Mi9LOX* and *MiEH2* each under 35S promoter along with *GusA* and remaining part of the fruit pulp was stored in -80 °C until used for the lactone analysis by gas chromatography.

### 3.2.8 Qualitative and quantitative analysis of metabolites

Aroma volatile extraction was carried out from 5g of each tissue obtained from the transient over expression experiment by solvent extraction method as mentioned in Chapter 2 (Section 2.2.3). To understand the effect of transient over expression of *Mi9LOX* and *MiEH2* on lactone biosynthesis, qualitative and quantitative analysis of lactones alone was carried out in the present study in similar fashion as described in Chapter 2 (Section 2.2.4.2).

Qualitative and quantitative analysis of *Mi9LOX* and *MiEH2* products from tissues obtained after transient over expression was carried out on UPLC coupled Q-Exactive orbitrap HRMS (Thermo Scientific, Waltham, MA, USA) in a similar way done for the *Mi9LOX* and *MiEH2* assay products. Extraction of these intermediate compounds was carried out from 0.5 g tissue obtained from the transient over

expression experiment. Tissue was crushed in liquid nitrogen and added to 2ml of 80% methanol, vortexed and sonicated for 5 min and fatty acid intermediates were extracted in 1 ml of hexane. Hexane layer was removed and evaporated to complete dryness and metabolites were reconstituted in 100 µl of 100% methanol and further used for HRMS analysis.

### 3.2.9 Statistical analysis

Experiments for each developing and ripening stages were performed from fruits of 3 independent trees for cv. Alphonso and 2 independent trees each for cv. Pairi and cv. Kent. These were considered as biological replicates. Quantitative real time PCR analysis was carried out in triplicate for each biological replicate from Alphonso, Pairi and Kent cultivars. ANOVA was carried out for comparison of *Mi9LOX*, *MiEH2*, *MiPGX1*, *MiHPL* and *MiACO* transcripts at various fruit development and ripening stages from pulp and skin tissues of Alphonso, Pairi and Kent cultivars using Stat View software, version 5.0 (SAS Institute Inc., Cary, NC, USA). Extraction of volatiles in transient over expression studies was carried out twice for each tissue as technical replicates followed by duplicate GC-FID runs of each extract as analytical replicates. Fisher's LSD test was performed at  $p \leq 0.05$  and  $p \leq 0.1$  by ANOVA for comparative analysis of lactone content in control and test tissues in transient expression analysis using Stat View software, version 5.0 (SAS Institute Inc., Cary, NC, USA).

## 3.3 Results

### 3.3.1 *In silico* analysis of isolated genes from *Mangifera indica* L.

*EH* from mango depicted ORF of 957 nucleotides with 74 and 241 nucleotides long 5' and 3' UTR regions, respectively. While in case of *LOX*, ORF of 2526 nucleotides with only 3' UTR (167 nucleotides) was evident. These mango genes showed similarity with linoleate *9-lipoxygenase* and soluble *EH2* reported from other plant species with maximum similarity with *Citrus sinensis* (80%) and *Prunus persica* (75%), respectively. Further phylogenetic analysis of encoded protein sequences of *LOX* and *EH* genes in our study along with the other plant 9LOX, 13LOX, EH1 and EH2 sequences reported in the NCBI database showed four distinct clusters in



cladogram each representing 9LOX, 13LOX, EH1 and EH2, respectively (Figure 3.1); wherein mango LOX and EH grouped in clads of other plant 9LOX and EH2, respectively. Hence these were named as *Mi9LOX* (Appendix 1; KX090178) and *MiEH2* (Appendix 1; KX090179), respectively.

The other three genes from mango, viz. *peroxygenase*, *hydroperoxide lyase* and *acyl-CoA-oxidase* upon *in silico* analysis showed presence of complete ORF's of 708, 1485 and 1995 bp, respectively. Sequence analysis of respective genes confirmed their maximum similarities with reported sequences of *peroxygenase* (80%), *hydroperoxide lyase* (76%) and *acyl-CoA-oxidase* (86%) from *Citrus sinensis* and thus named as *MiPGXI* (Appendix 1; KX090180), *MiHPL* (Appendix 1; KX090181) and *MiACO* (Appendix 1; KX090182), respectively.

### 3.3.2 Expression of *Mi9LOX*, *MiHPL*, *MiPGXI*, *MiEH2* and *MiACO* in fruits of three mango cultivars

Transcript abundance of five candidate genes, viz. *Mi9LOX*, *MiHPL*, *MiPGXI*, *MiEH2* and *MiACO* was studied in pulp and skin tissues of fruit of Alphonso, Pairi and Kent cultivars at various stages of fruit development and ripening. Transcript levels of the individual genes from three cultivars at their maxima were not significantly different; however their differential expression was evinced at various ripening stages and in pulp and skin tissues of the three cultivars. Transcript level of each gene at its maximum expression was considered as 1 and its relative expression in the pulp and the skin of various stages was represented across cultivars (Figure 3.2 and Figure 3.3). All the three cultivars showed ripening specific appearance of *Mi9LOX*, *MiPGXI* and *MiACO* transcripts (Figure 3.2 and Figure 3.3). Relative quantification of *MiPGXI* showed optimum transcripts at mid ripe stage in the pulp as well as the skin tissues of Alphonso and Pairi cultivars, which later reduced significantly till over ripe stage. Whereas, *MiPGXI* transcript level in the pulp and the skin tissues of Kent cultivar increased continuously from table green stage to over ripe stage. *MiPGXI* transcript abundance from the skin tissue of Kent was very low compared to that in the pulp tissue. However, *MiPGXI* expression level was almost similar in the case of pulp and skin tissues of Pairi and 25% low in the case of Alphonso pulp than the skin tissue.

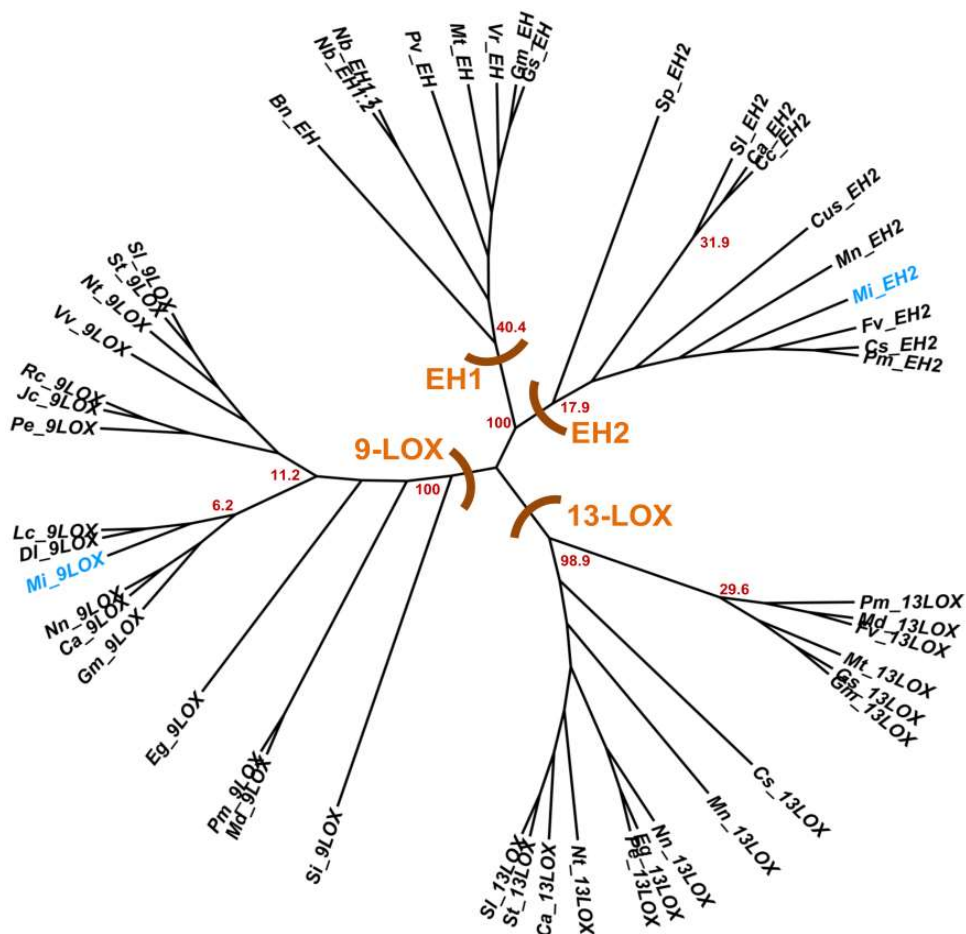


**Figure 3.1 Phylogenetic analysis of lipoxygenase and epoxide hydrolase genes**

Cladogram representing phylogenetic analysis by neighbor-joining of encoded proteins by *Mi9LOX* and *MiEH2* (blue color) genes with that of other plant 9LOX, 13LOX, EH1 and EH2 sequences. Node label represents name of the enzyme followed by two letters representing initials of botanical name of the plant. The numbers (red color) at the branch nodes signify the bootstrap scores acquired after 1000 trials. Details of sequence of plant species, enzyme and NCBI accession in parenthesis are as follows; *Nicotiana benthamiana*\_EH1.2 (ACE82566), *Nicotiana benthamiana*\_EH1.1 (ACE82565), *Phaseolus vulgaris*\_EH (AKJ75509), *Glycine max*\_EH (CAA55294), *Medicago truncatula*\_EH (XP\_003626202), *Glycine soja*\_EH (KHN43314), *Vigna radiata*\_EH (AIJ27456), *Brassica napus*\_EH (NP\_001302895), *Citrus sinensis*\_EH2 (XP\_006489040), *Prunus mume*\_EH2 (XP\_016647751), *Cicer arietinum*\_EH2 (XP\_004508197), *Fragaria vesca*\_EH2 (XP\_004290776), *Cajanus cajan*\_EH2 (KYP58120), *Cucumis sativus*\_EH2 (XP\_004134492), *Solanum lycopersicum*\_EH2 (XP\_004252913), *Solanum pennellii*\_EH2 (XP\_015077274), *Morus notabilis*\_EH2 (XP\_010105136), *Vitis vinifera*\_9LOX (XP\_010659859), *Malus domestica*\_9LOX (NP\_001281030), *Prunus mume*\_9LOX (XP\_008246456), *Glycine max*\_9LOX (XP\_003521704), *Solanum tuberosum*\_9LOX (NP\_001274916), *Nicotiana tabacum*\_9LOX (XP\_016433823), *Dimocarpus longan*\_9LOX (ANF89411), *Corylus avellana*\_9LOX (CAD10740), *Litchi chinensis*\_9LOX (AEQ30071), *Populus euphratica*\_9LOX (XP\_011023610), *Eucalyptus grandis*\_9LOX (XP\_010025195), *Jatropha curcas*\_9LOX (XP\_012089053), *Ricinus communis*\_9LOX (XP\_002512386), *Solanum lycopersicum*\_9LOX (XP\_004244890), *Sesamum indicum*\_9LOX (XP\_011087404), *Nelumbo nucifera*\_9LOX (XP\_010256003), *Malus domestica*\_13LOX (NP\_001280985), *Prunus mume*\_13LOX (XP\_008228181), *Medicago truncatula*\_13LOX (XP\_003627308), *Solanum tuberosum*\_13LOX (NP\_001275115), *Glycine soja*\_13LOX (KHN39622), *Fragaria vesca*\_13LOX (XP\_004303702), *Morus notabilis*\_13LOX (XP\_010086794), *Eucalyptus grandis*\_13LOX (XP\_010033729), *Populus euphratica*\_13LOX (XP\_011035732), *Nelumbo nucifera*\_13LOX (XP\_010273845), *Capsicum annuum*\_13LOX (NP\_001311748), *Nicotiana tabacum*\_13LOX (XP\_016495606), *Citrus sinensis*\_13LOX (XP\_006465905), *Solanum lycopersicum*\_13LOX (AAB65767), *Glycine max*\_13LOX (XP\_014624448).

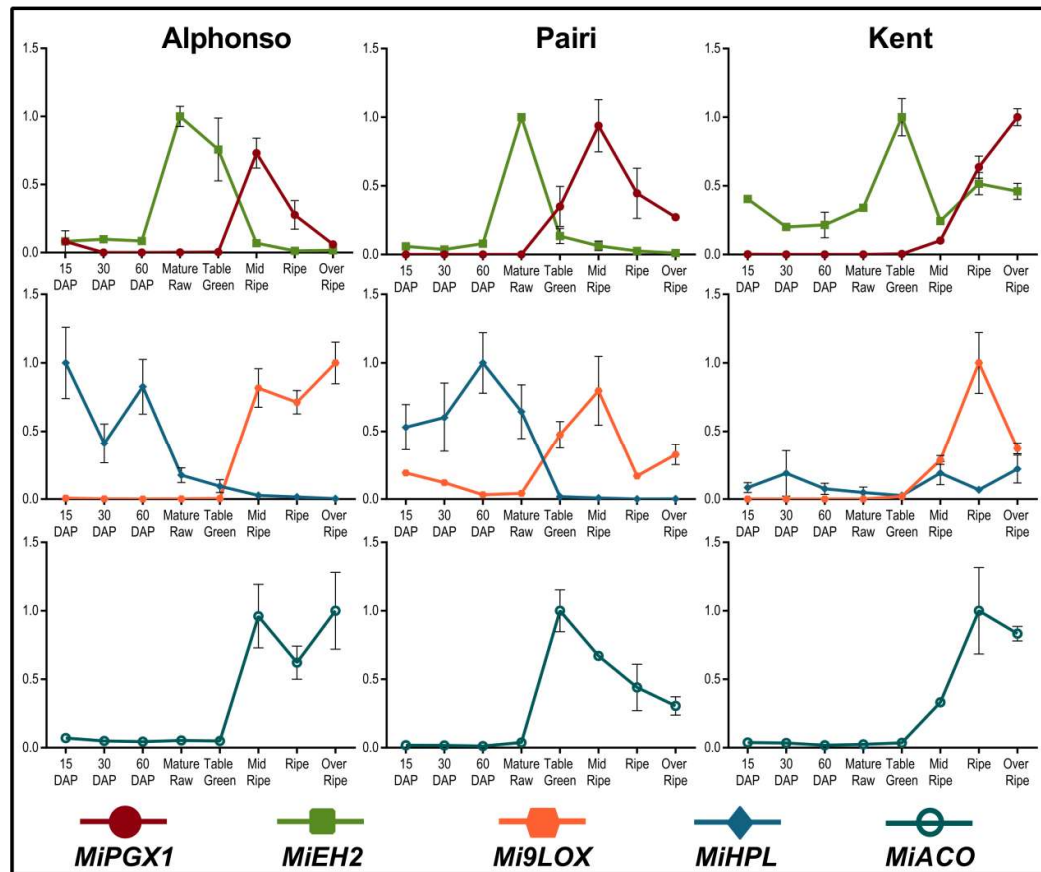


**Figure 3.2 qPCR analysis from pulp tissue**

Transcript profiles of *Mi9LOX*, *MiHPL*, *MiPGX1*, *MiEH2* and *MiACO* from pulp tissue of various fruit development and ripening stages of Alphonso, Pairi and Kent mango cultivars. Vertical bars at each data point represent standard error in the relative quantification among the biological replicates. X axis represents fruit development and ripening stages and Y axis represents relative transcript abundance.

*MiEH2* transcripts in Alphonso were found to be the highest during mature raw and table green stages of the pulp and the skin tissues. These levels were almost 50% lower in the skin tissue as compared to the pulp. In case of Pairi *MiEH2* transcripts were optimum at mature raw stage of the pulp tissue, which reduced by 60% at 60 DAP stage of the skin compared to the pulp. Interestingly, the pulp and the skin tissues of Kent showed expression of *MiEH2* throughout the developing and ripening stages. *MiHPL* transcripts were abundant in the developing tissues of Alphonso and Pairi, which further reduced to nearing zero at post table green stage. In case of Kent *MiHPL* transcripts were present throughout the developing and the ripening stages of the pulp and the skin tissues. Relative transcript profiles of *Mi9LOX* and *MiACO* from Alphonso pulp revealed their high abundance through mid ripe stage to over ripe stage, whereas, slight reduction in their level was observed at post

mid ripe stage in case of the skin tissue. *Mi9LOX* and *MiACO* transcripts from Pairi pulp and skin tissues showed their maximum level at table green stage except for optimum level for *Mi9LOX* at mid ripe stage of Pairi pulp. Reduction in the *Mi9LOX* and *MiACO* level was evinced in further ripening stages of Pairi tissues. In the case of Kent pulp, *Mi9LOX* and *MiACO* transcript abundance was the highest at ripe stage, whereas in case of Kent skin tissue transcript level was higher at over ripe stage. Interestingly, co-expression of *MiPGX1* and *MiEH2* was observed for short duration in Alphonso fruits from table green stage to ripe stage (10 days) and in Pairi fruits from mature raw stage to ripe stage (8 days). While in case of Kent fruits co-expression of *MiPGX1* and *MiEH2* was noted throughout the ripening stages.

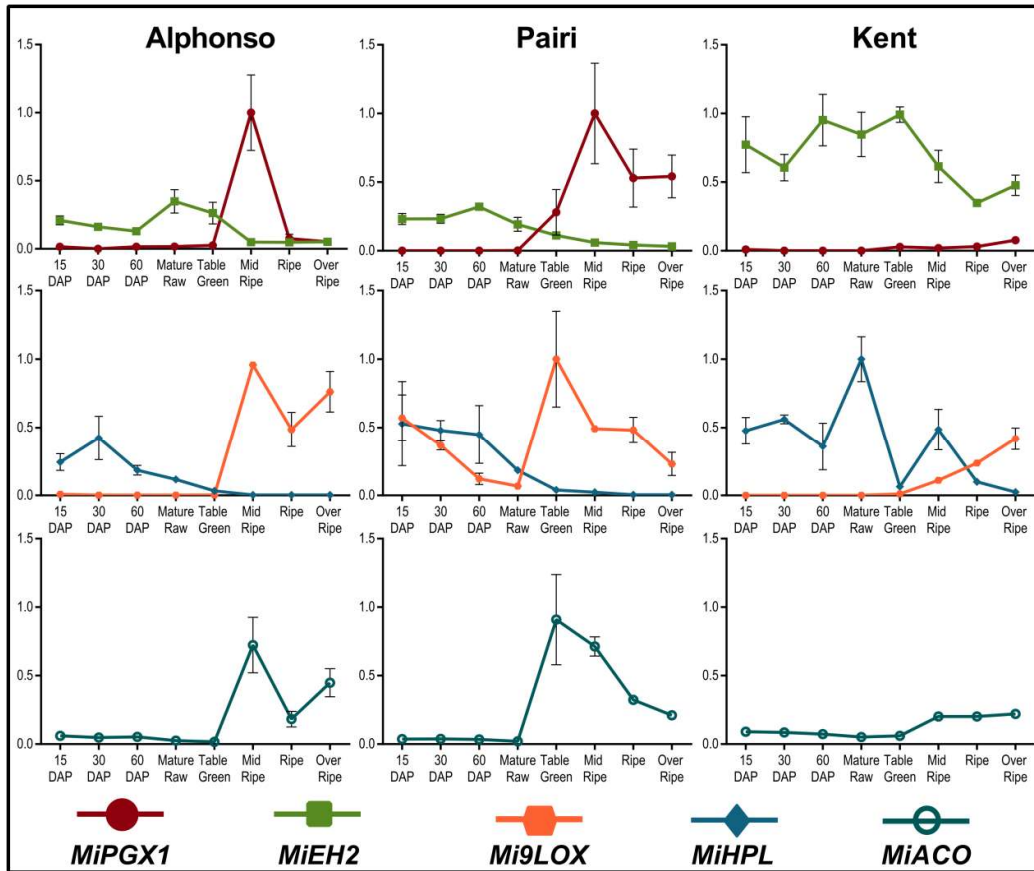


**Figure 3.3 qPCR analysis from skin tissue**

Transcript profiles of *Mi9LOX*, *MiHPL*, *MiPGX1*, *MiEH2* and *MiACO* from skin tissue of various fruit development and ripening stages of Alphonso, Pairi and Kent mango cultivars. Vertical bars at each data point represent standard error in the relative quantification among the biological replicates. X axis represents fruit development and ripening stages and Y axis represents relative transcript abundance.

### 3.3.3 Heterologous expression and catalytic activities of proteins encoded by *Mi9LOX* and *MiEH2*

The *Mi9LOX* gene from Alphonso mango encoded protein of 841 aa with calculated molecular weight of ~96.3 kDa and 78% similarity with 9LOX of *Litchi chinensis*. Presence of conserved substrate binding and oxygen binding domains (Santino et al., 2005) were also revealed when the amino acid sequence alignment and secondary structure prediction of *Mi9LOX* was performed with that of *Glycin max* (PDB- 2iuj), *Vitis vinifera*, *Solanum lycopersicum* and *Litchi chinensis* using ESript 3.0 software (Figure 3.4).

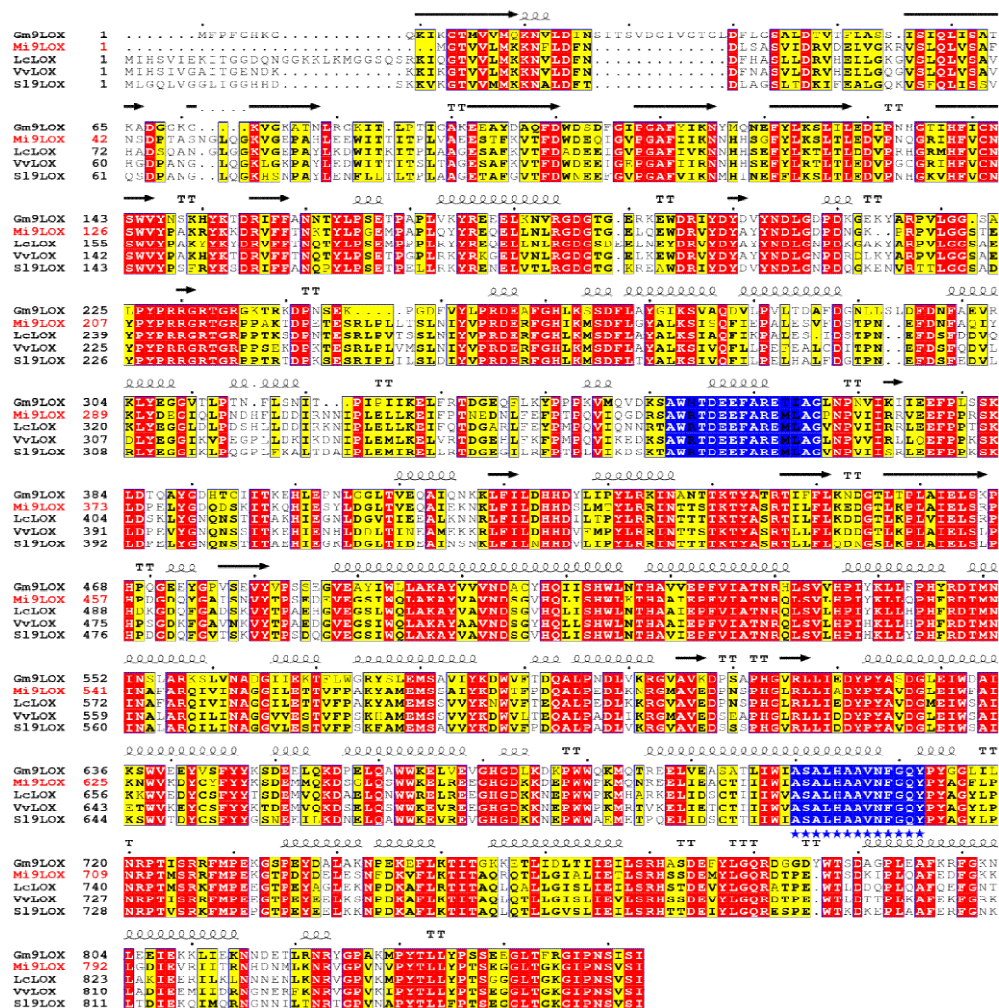


**Figure 3.4 Secondary structure prediction of *Mi9LOX***

Alignment of *Mi9LOX* protein sequence with other lipoxygenases from *Glycin max* (PDB- 2iuj), *Litchi chinensis* (AEQ30071), *Vitis vinifera* (AGU28274) and *Solanum lycopersicum* (NP\_001234856). Amino acids highlighted in blue color represent conserved substrate binding domain and amino acids highlighted in blue with underlined blue stars represent conserved oxygen binding domain.

*MiEH2* from Alphonso mango encoded 318 aa long protein with calculated molecular weight of ~35.9 kDa and 81% similarity with predicted bifunctional epoxide hydrolase 2 from *Citrus sinensis*. Further secondary structure prediction and alignment of *MiEH2* with epoxide hydrolases from other plants, viz. *Solanum tuberosum* (PDB-2cjp), *Citrus sinensis* and *Nicotiana benthamiana* showed conserved catalytic residues (Figure 3.5) (Bellevik et al., 2002b).

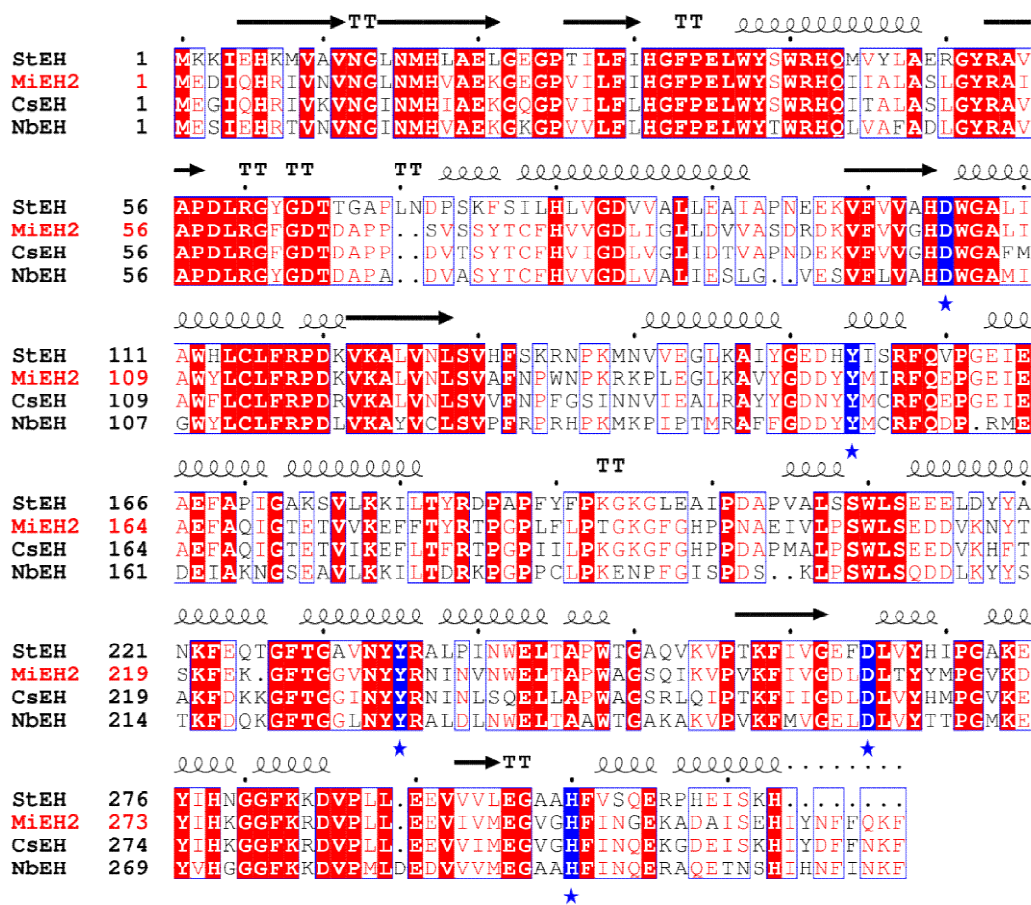


**Figure 3.5 Secondary structure prediction of *MiEH2***

Alignment of *MiEH2* protein sequence with other epoxide hydrolases from *Solanum tuberosum* (PDB-2cjp), *Citrus sinensis* (XP\_006489041) and *Nicotiana benthamiana* (ACE82566). Amino acids highlighted in blue color represent conserved catalytic residues from enzyme active site.

The encoded protein sequences of *Mi9LOX* and *MiEH2* were also analysed on PROtein SOLubility evaluator (PROSO) to understand solubility of the expressed recombinant proteins. Both, *Mi9LOX* and *MiEH2* belonged to the solubility class with probability of 0.696 and 0.506, respectively. SDS-PAGE analysis indicated recombinant *MiEH2* protein purity to be good (Figure 3.6a) to carry out enzymatic

activity studies, whereas *Mi9LOX* eluted fractions had low molecular weight nonspecific proteins, which were eliminated by further purification step (Figure 3.6b and Figure 3.6c).

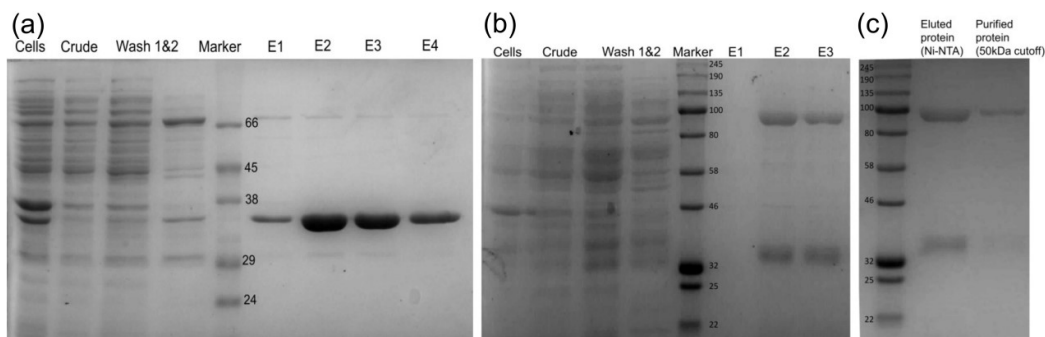


**Figure 3.6 Purified recombinant *Mi9LOX* and *MiEH2***

CBB stained SDS-PAGE gels representing purified recombinant proteins *MiEH2* (a) and *Mi9LOX* (b) by Ni-NTA affinity purification and purified fraction of *Mi9LOX* after passing through 50 kDa cut-off column (c).

The enzymatic activity of purified recombinant *Mi9LOX* using linoleic acid (LA) and linolenic acid (ALA) as substrates revealed formation of 9HpODE and 9HpOTrE products, respectively (Figure 3.7). Biochemical characterization of *Mi9LOX* revealed considerably high activity between pH 6 to 8 with optima at pH 6.5 and over 40% reduction in the activity at pH 5 and 9 (Figure 3.8). Activity profile of *Mi9LOX* at varied temperatures showed stable activity of the enzyme between 37 to 45 °C, with temperature optima at 37.0 °C (Table 3.2) while 75 and 69% reduction in the activity at 35 and 50 °C, respectively. The enzyme kinetics for *Mi9LOX* with LA and ALA revealed more affinity towards ALA than LA based on the calculated Km values (Table 3.2) from *in vitro* studies. Similarly,  $V_{max}/K_m$  values of recombinant *Mi9LOX* showed higher catalytic efficiency with ALA than LA (Table 3.2).

Purified recombinant *MiEH2* showed activity towards *cis*-Stilbene oxide (CSO), *trans*-Stilbene oxide (TSO) and 12(13) EpOME [12(13) epoxide of octadecamonoenoic acid/12(13) epoxide of linoleic acid] (Figure 3.9) indicating its efficiency to utilize and hydrolyse aromatic and fatty acid epoxides. Biochemical characterization revealed stable activity of *MiEH2* between pH 7 to 8 with optima at pH 8 and >40% reduction in activity below pH 6 and above pH 9. Activity profile of *MiEH2* at varied temperatures showed optima at 45 °C; while >40% reduction in the

activity between 25 to 40 °C. Over 50% reduction in the activity was noted at 50 °C with complete inactivation at 60 °C and above (Figure 3.8). The *MiEH2* revealed higher  $K_m$  and lower  $V_{max}/K_m$  value for CSO than TSO suggesting higher affinity and catalytic efficiency towards TSO (Table 3.2). Assay of *MiEH2* with 12(13) EpOME as substrate produced 12(13) DiHOME (12, 13 dihydroxy octadecamonoenoic acid) as a product (Figure 3.9) confirming utilization of fatty acid epoxides as substrates.  $V_{max}/K_m$  value for 12(13) EpOME suggested its intermediate catalytic efficiency towards fatty acid substrates with respect to CSO and TSO (Table 3.2).

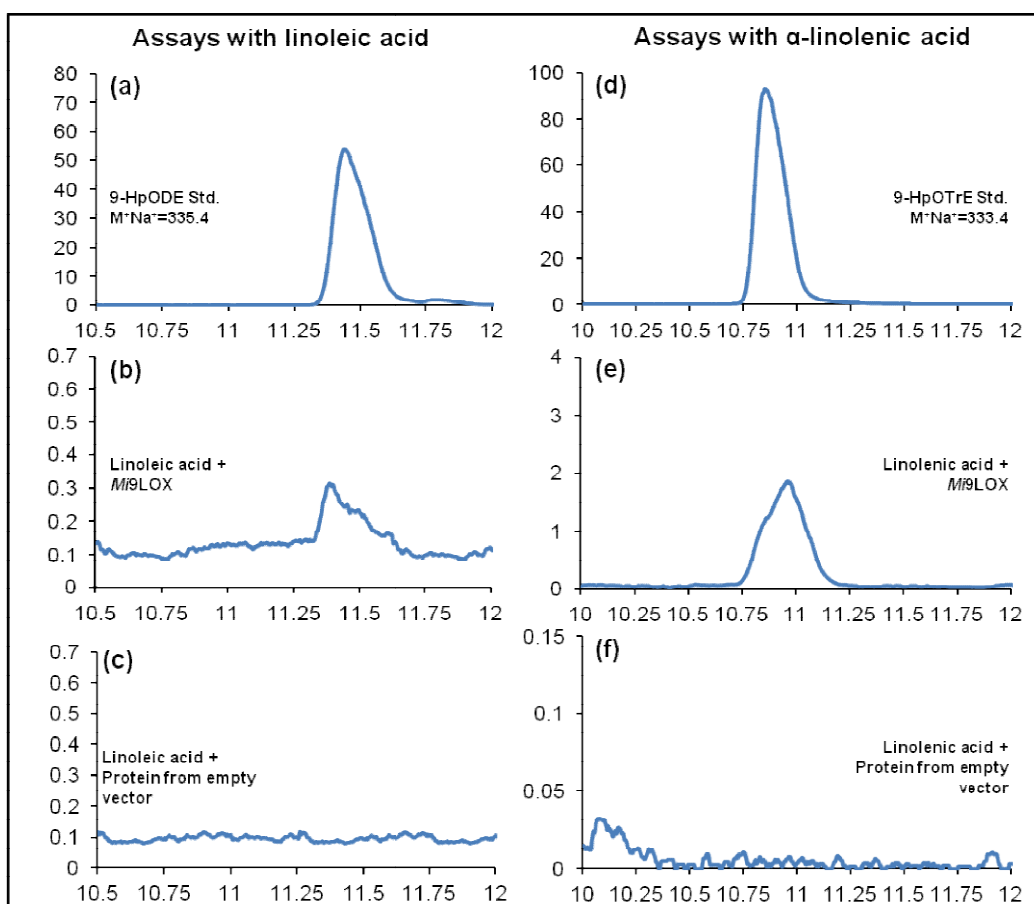


**Figure 3.7 Recombinant enzyme activities of *Mi9LOX***

Extracted ion chromatograms from HRMS analysis for product identification of *Mi9LOX* assay reactions, HpODE standard (a); HpOTrE standard (d); products formed in assay reactions of *Mi9LOX* with substrate linoleic acid (b) and linolenic acid (e). (c) and (f) represent assay reactions for the protein expressed from empty vector with substrates linoleic acid and linolenic acid, respectively. X-axis represents retention time (min) and Y-axis represents relative intensity.



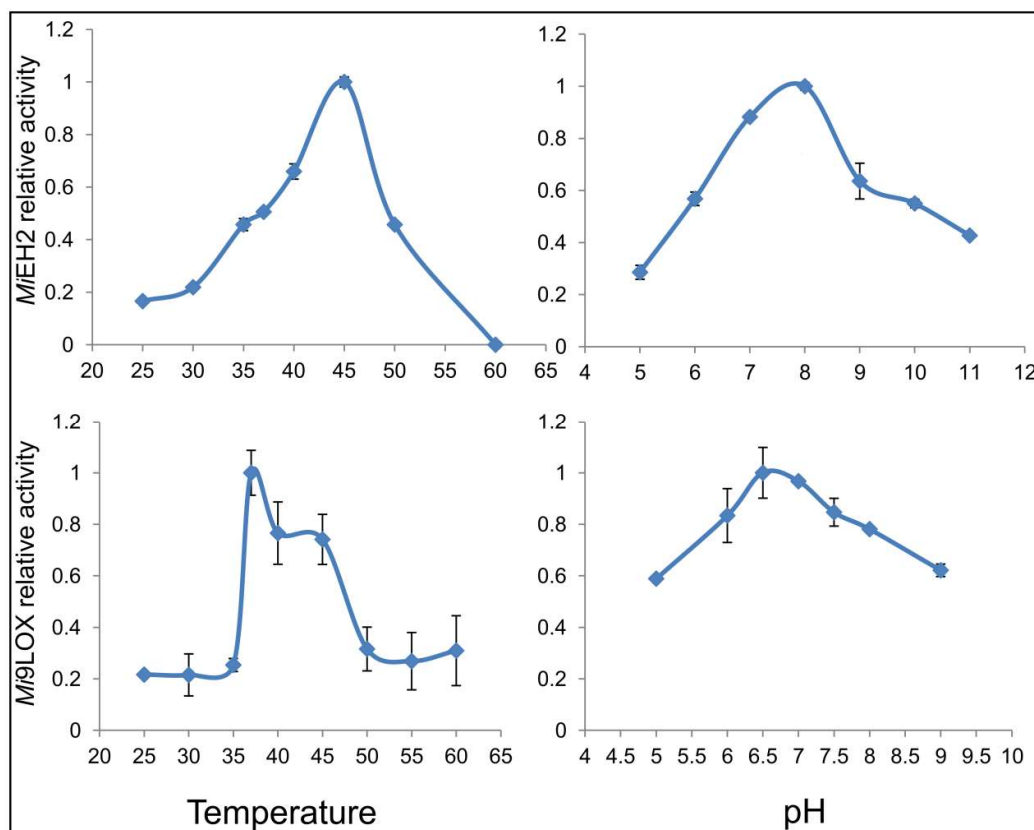


**Figure 3.8 Biochemical characterisation of *Mi9LOX* and *MiEH2***

Line graphs representing changes in the activity of *Mi9LOX* and *MiEH2* at different pH and temperatures.

**Table 3.2 Biochemical characterization and enzyme kinetics**

Enzymes	<i>Mi9LOX</i>		<i>MiEH2</i>		
	LA	ALA	CSO	TSO	12(13) EpOME
<b>V<sub>max</sub> (<math>\mu\text{M min}^{-1}\text{mg}^{-1}</math>)</b>	611.11 $\pm$ 55.55	279.84 $\pm$ 5.87	26.53 $\pm$ 4.81	1055.55 $\pm$ 55.55	26.70 $\pm$ 0.04
<b>K<sub>m</sub> (mM)</b>	0.35 $\pm$ 0.03	0.06 $\pm$ 8E <sup>-5</sup>	0.17 $\pm$ 0.04	0.11 $\pm$ 0.003	0.004 $\pm$ 4.49 E <sup>-5</sup>
<b>V<sub>max</sub>/K<sub>m</sub> min<sup>-1</sup>mg<sup>-1</sup>)</b>	1.73	4.56	0.16	9.34	6.19
<b>Optimum temperature</b>	37°C	37°C	45°C	45°C	—
<b>Optimum pH</b>	6.5	6.5	8	8	—

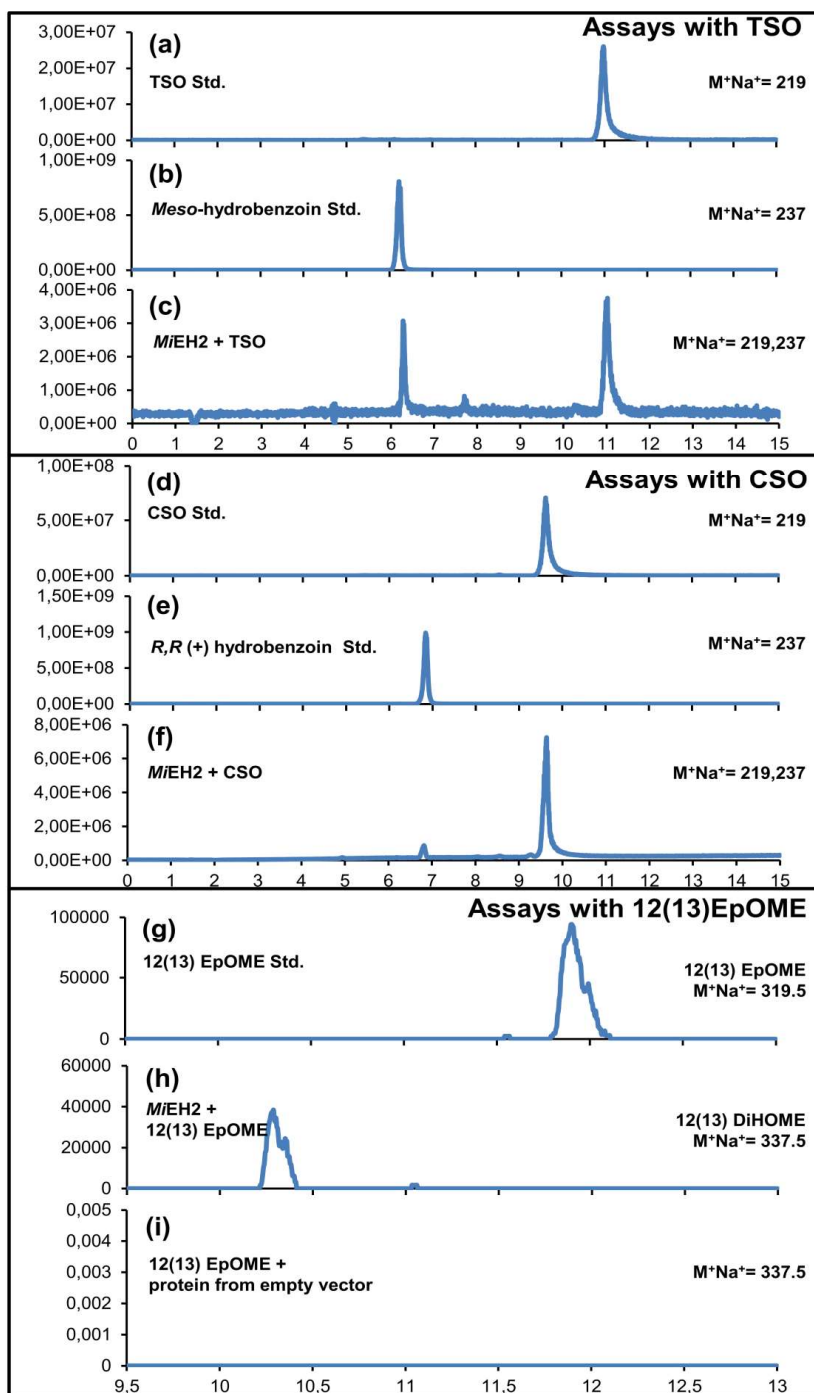


**Figure 3.9 Recombinant enzyme activities of *MiEH2***

Extracted ion chromatograms from HRMS analysis for product identification of *MiEH2* assay reactions, standards: TSO (a), meso hydrobenzoin (b), CSO (d), *R, R (+)* hydrobenzoin (e) and 12(13) EpOME (g). Chromatogram representing product formation by *MiEH2* with substrates TSO (c), CSO (f) and 12(13) EpOME (h). Assay reaction of protein expressed from empty vector with 12(13)EpOME substrate (i). X axis represents retention time (min) and Y axis represents relative intensity.

### 3.3.4 Transient over-expression of *Mi9LOX* and *MiEH2* resulted in elevated lactone levels in mango fruit

*Agrobacterium* inoculation for test and control constructs was carried out in two halves of the same ethylene treated fruits as described (Figure 3.10a), while Figure 3.10b depicts a part of fruit checked by Gus staining to confirm expression of *GusA* along with the *Mi9LOX* or *MiEH2* after two days of *Agrobacterium* infiltration. The remaining tissue was used for the analysis of lactone content and gene expression to avoid error due to indigenous variation in lactone content and gene expression.

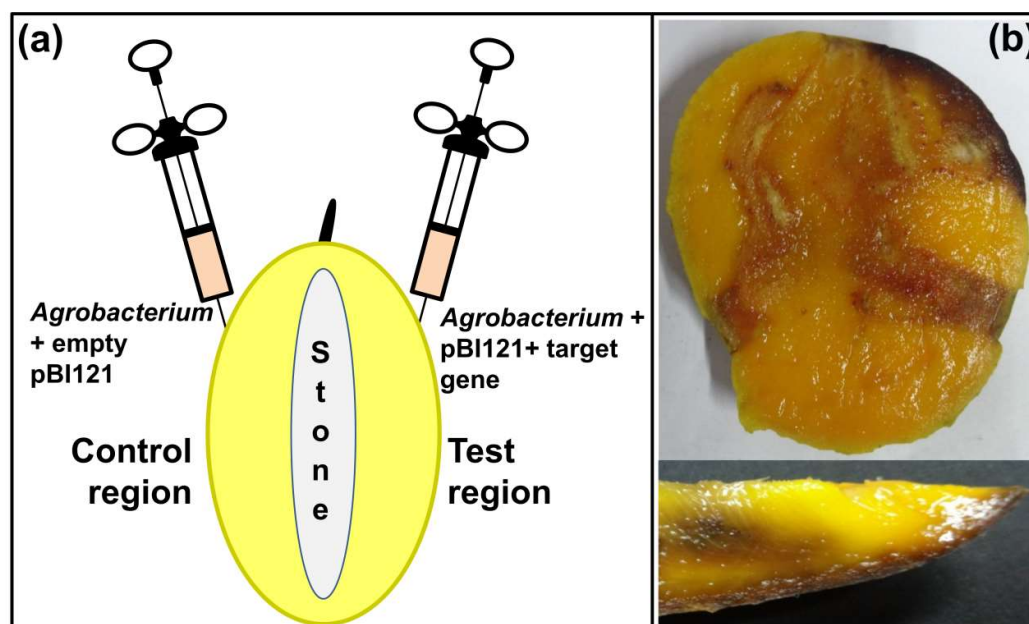


**Figure 3.10 Agroinfiltration and Gus staining**

Diagrammatic representation of Agroinfiltration of empty pBI121 and pBI121+ target gene constructs in two different regions of the same mango fruit separated by fruit stone (a). Representative pictures of Alphonso mango fruit after Agroinfiltration and Gus staining (b)

*Mi9LOX* and *MiEH2* transcripts from test tissues upon *Agrobacterium* infiltration showed significant increase of 1.73 and 8.3-fold, respectively as compared to the control tissues (Figure 3.11a). Intermediate metabolite analysis of these tissues by HRMS revealed significant increase of 1.9 folds in the 9HpOTrE upon *Mi9LOX* over-expression (Figure 3.11b), whereas 9HpODE was not detected in the present analysis from control as well as test tissues. *MiEH2* over-expression resulted in significant increase (2.57 folds) in the DHSAs (DiHydroxy Stearic Acid) concentration (Figure 3.11c). Another peak at mass 335.2, probably equivalent to exact mass of

DiHODE ( $M^+Na^+$ ) was also detected with significant increase (2.62 fold) in the test tissue as compared to the control.

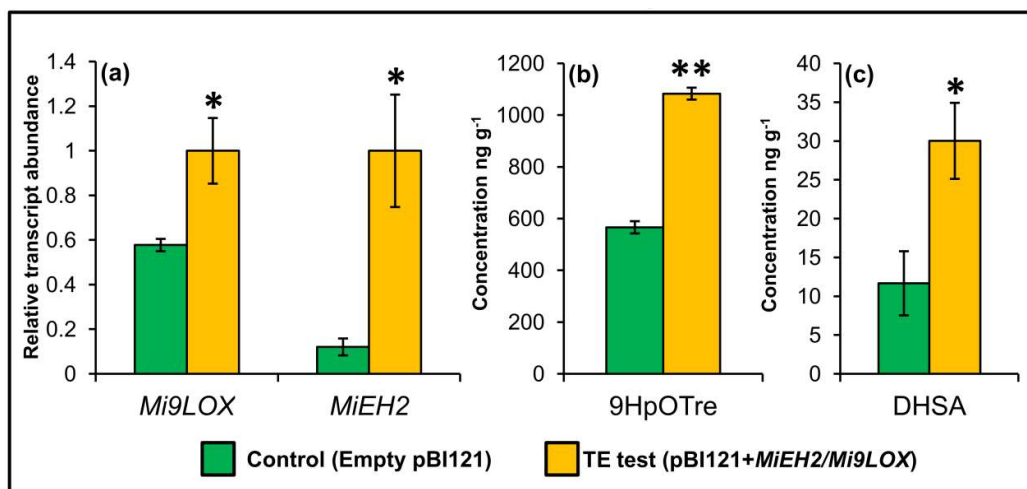


**Figure 3.11 Effect of transient over expression on transcripts and metabolites**

Histogram representing changes in the *Mi9LOX* and *MiEH2* transcripts level in the control and test tissues after agroinfiltration (a). Histogram representing changes in the 9HpOTre (9-Hydroperoxy Octadeca Trienoic Acid) and DHSA (Di-Hydroxy Stearic Acid) content with respect to control upon transient over expression of *Mi9LOX* (b) and *MiEH2* (c), respectively. Vertical bars represent standard error in the values of lactones from used data set, significance is represented as single star if  $p \leq 0.1$  and two stars if  $p \leq 0.05$

Volatile metabolite analysis by GC-MS of all these tissues indicated presence of eight lactones viz.  $\gamma$ -butyrolactone,  $\delta$ -valerolactone,  $\gamma$ -hexalactone,  $\delta$ -hexalactone,  $\gamma$ -octalactone,  $\delta$ -octalactone,  $\gamma$ -decalactone and  $\delta$ -decalactone while quantitative analysis by GC-FID showed increased levels of few lactones in both the sets (Figure 3.12a and Figure 3.12b). *Mi9LOX* transient over-expression resulted in significant increase at  $p$ -value  $\leq 0.1$  in the  $\delta$ -valerolactone ( $0.075 \mu\text{gg}^{-1}$  to  $0.082 \mu\text{gg}^{-1}$ ) and  $\delta$ -decalactone ( $0.043 \mu\text{gg}^{-1}$  to  $0.064 \mu\text{gg}^{-1}$ ) content (Figure 3.12a). While *MiEH2* transient over-expression depicted significant increase at  $p$ -value  $\leq 0.1$  in  $\delta$ -valerolactone ( $0.09 \mu\text{gg}^{-1}$  to  $0.13 \mu\text{gg}^{-1}$ ) and  $\gamma$ -hexalactone ( $0.37 \mu\text{gg}^{-1}$  to  $0.72 \mu\text{gg}^{-1}$ ) and highly significant increase at  $p$ -value  $\leq 0.05$  in  $\delta$ -hexalactone ( $0.53 \mu\text{gg}^{-1}$  to  $1.04 \mu\text{gg}^{-1}$ ) compared to that in the control tissue (Figure 3.12b).

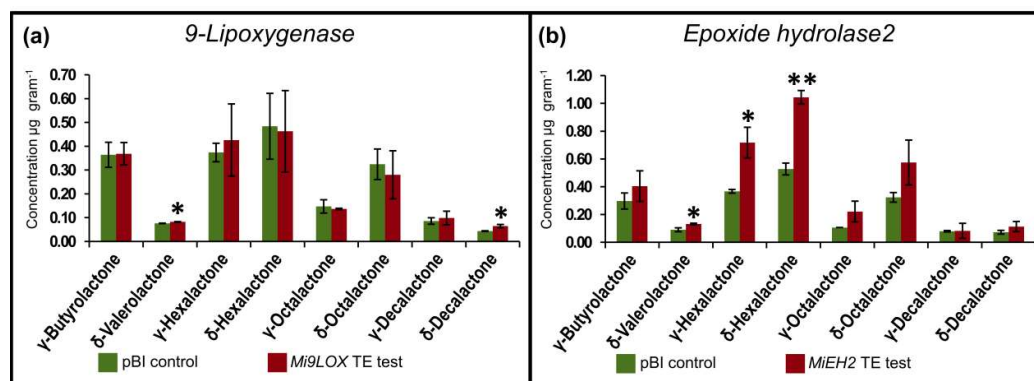


**Figure 3.12 Changes in the lactone content upon transient over expression**

Histogram representing changes in the lactone content with respect to control upon transient over expression of *Mi9LOX* (a) and *MiEH2* (b). Vertical bars represent standard error in the values of lactones from used data set, significance is represented as single star if  $p \leq 0.1$  and two stars if  $p \leq 0.05$

## 3.4 Discussion

### 3.4.1 *Mi9LOX* and *MiEH2* reveal catalytic properties similar to those of other plant 9LOX and EH2 enzymes

*Lipoxygenase* gene family, omnipresent to plant and animal kingdom comprises *9LOX* and *13LOX* as the most abundant classes (Feussner and Wasternack, 2002). The recombinant *Mi9LOX* protein characterized in the present study revealed optimum pH and temperature as well as thermal inactivation properties similar to that of other reported *9LOX* enzymes (Baysal and Demirdöven, 2007; Huang and Schwab, 2011; Padilla et al., 2012; Santino et al., 2005). However, more affinity of *Mi9LOX* towards ALA than LA similar to that of olive *9LOX* (Padilla et al., 2012) suggested probable tuning of this enzyme to *in vivo* availability of the substrate, as increased ALA content was observed during ripening of mango fruit (Chapter 2).

*Epoxide hydrolase* genes fall in to two classes *EH1* and *EH2*, which catalyse hydrolysis of aromatic epoxides and epoxides of fatty acids as well as aromatic compounds, respectively (Huang and Schwab, 2013; Wijekoon et al., 2008). The *MiEH2* in our study exhibited its promiscuous nature towards utilization of variety of substrates. It showed activity on CSO, TSO and 12(13) EpOME, however, more affinity towards TSO similar to EH2 reported from other plant species was observed (Bellevik et al., 2002a; Bellevik et al., 2002b; Huang and Schwab, 2013).

### 3.4.2 Role of *Mi9LOX* and *MiEH2* in biosynthesis of lactones in Alphonso mango

The hydroperoxy and hydroxy fatty acids produced by *Mi9LOX* and *MiEH2* upon catalytic conversion of  $\Delta^9$  unsaturated fatty acids (LA and ALA) and epoxy fatty acids, respectively are the potential precursors for lactone biosynthesis (Cardillo et al., 1989; Haffner and Tressl, 1998). We performed transient over expression of *Mi9LOX* and *MiEH2* through *Agrobacterium* infiltration experiment to get insights in to role of these genes in *de novo* biosynthesis of lactones in ripened mango fruits. Ethylene treated fruits were found to be ideal for transient expression to avoid the risk of bacterial and fungal infection owing to fruit injury during infiltration. Moreover, accelerated ripening and early appearance of lactones with no quantitative variation in Alphonso mango fruits upon exogenous ethylene treatment is known from our earlier studies (Chidley et al., 2013). Transient expression has been established as an efficient tool for functional characterization of genes (Orzaez et al., 2006; Spolaore et al., 2001) and clearly depicts its efficiency in the present study. Over expression of *Mi9LOX* and *MiEH2* resulted in the significant increase in the content of their products 9HpOTrE and DHSAs, respectively from the test tissue compared to the control. This confirms increased *Mi9LOX* and *MiEH2* enzyme activity in the tissue of transient over expression of the respective genes; although the actual enzyme levels could not be assayed due to insufficient tissue availability. Further significant increase in the lactone content specifically  $\delta$ -valerolactone (1.46 fold),  $\gamma$ -hexalactone (1.96 fold) and  $\delta$ -hexalactone (1.98 fold) after *MiEH2* over expression and,  $\delta$ -valerolactone (1.08 fold) and  $\delta$ -decalactone (1.48 fold) content upon *Mi9LOX* over expression, respectively was evinced, which confirms involvement of these genes in the lactone biosynthesis from mango fruit. Relatively less increase in  $\delta$ -valerolactone content upon *Mi9LOX* over expression might be because of less *Mi9LOX* transcripts post infiltration compared to *MiEH2* transcripts (Figure 3.11a). Similarly, 9LOX is much upstream to the final product lactone and conversion of its products i.e. hydroperoxy fatty acids to hydroxy fatty acids by peroxygenase could be rate limiting.

### 3.4.3 Temporal expression of *Mi9LOX*, *MiHPL*, *MiPGXI*, *MiEH2* and *MiACO* genes correlates with variable lactone content in fruit of mango cultivars

Lactone content varies amid the fruits of different mango cultivars (Pandit et al 2009a). To get real insights of lactone biosynthesis in mango, three cultivars viz. Kent, Pairi and Alphonso with no, low (pulp,  $1.3 \mu\text{gg}^{-1}$ ; skin,  $1.12 \mu\text{gg}^{-1}$ ) and high (pulp,  $7.12 \mu\text{gg}^{-1}$ ; skin,  $3.16 \mu\text{gg}^{-1}$ ) lactone content, respectively were compared (Chapter 2). In Alphonso pulp and skin tissues the highest transcript abundance of *Mi9LOX*, *MiPGXI* and *MiACO* was observed at mid ripe stage (10 DAH stage), which correlates with our earlier report of the first appearance of lactones at 10 DAH stage during Alphonso mango ripening (Kulkarni et al., 2012; Pandit et al., 2009b). In case of Pairi high abundance of *Mi9LOX* and *MiPGXI* transcripts detected at mid ripe stage but higher level of *MiACO* transcripts seen at table green stage (Figure 3.2 and Figure 3.3) indicates early onset of fatty acid degradation before the high abundance of *Mi9LOX* and *MiPGXI* transcripts. This probably makes reduced fatty acid substrate availability for lipoxygenase and peroxygenase resulting in low lactone content in Pairi fruits. Further significant reduction of *MiHPL* transcripts in these ripening tissues of Alphonso and Pairi suggests supply of hydroperoxy fatty acid pool to peroxygenase instead of HPL pathway. Previous studies on Alphonso have affirmed this by abundance of products of HPL pathway in the fruit developing stages than in the ripening stages (Pandit et al., 2009b). Contrary to this in Kent higher expression of *Mi9LOX*, *MiPGXI* and *MiACO* during the late ripening stages (ripe and over ripe stages) indicates delayed events for lactone biosynthesis (Figure 3.2 and Figure 3.3). Moreover, presence of *MiHPL* transcripts during fruit ripening signifies its co-expression with lipoxygenase diverting pool of hydroperoxy fatty acid to HPL pathway instead of peroxygenase pathway. This probably reasons the lactone less nature of Kent fruit.

Thus, altogether higher expression of *Mi9LOX*, *MiPGXI* and *MiACO* at mid ripe stage with adjournment of HPL pathway may result in high lactone content in Alphonso fruits. Early onset of fatty acid degradation may lead to low lactone content in Pairi. While delayed expression of *Mi9LOX*, *MiPGXI* and *MiACO* and depletion of hydroperoxy fatty acids by HPL pathway in combination with lower fatty acid content

(Chapter 2) may be the reason for no lactone content of Kent cultivar. In addition to this, variable *in vivo* conditions in the fruit of three cultivars might be responsible for differential catalytic efficiency of respective enzymes (though similar transcript abundance at respective maxima) leading to variation in lactone content. Further structural studies of these enzymes and *in vivo* substrate-product analysis using tracer technology might give better clarity about lactone biosynthesis in mango.

### 3.4.4 Proposed lactone biosynthesis pathway in mango

Based on present results and available information probable pathway of lactone biosynthesis can be proposed in mango fruit (Figure 3.13). *MiEH2* and *Mi9LOX* are part of mono-oxygenase (peroxygenase) and di-oxygenase (lipoxygenase) pathways, respectively (steps A1 and B2; Figure 3.13).

#### Probable pathway of lactone biosynthesis in mango fruit

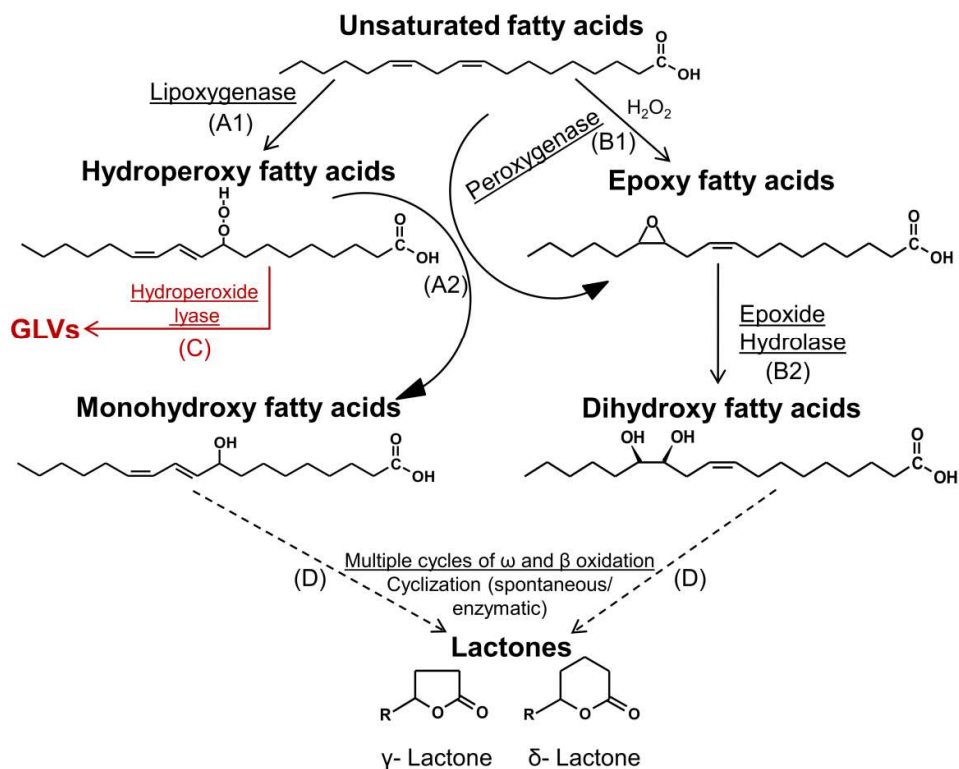


**Figure 3.13 Proposed lactone biosynthesis pathway in mango fruit**

Proposed pathway of lactone biosynthesis in mango fruit, words in bold represent metabolites; words underlined represent enzymes; A1, A2, B1, B2 and D steps are favourable for lactone biosynthesis. Step C; red in color suggests unfavoured step for lactone biosynthesis.



Products of lipoxygenase are diverted to multiple pathways including hydroperoxide lyase (HPL) pathway (step C; Figure 3.13), which produces C6 aldehydes and ketones responsible for fresh green leafy aroma volatiles (Huang and Schwab, 2011, 2012). This may divert hydroperoxy fatty acid pool to HPL pathway which is an unfavourable step for lactone biosynthesis. Products of lipoxygenase are also diverted to peroxygenase pathway. It is known that peroxygenase catalyzes epoxidation of unsaturated fatty acids using reactive oxygen (step B1; Figure 3.13). Similarly it also utilizes hydroperoxy fatty acids as co-substrates or oxygen donor to produce epoxy and monohydroxy fatty acids (step A2; Figure 3.13) (Babot et al., 2013; Fuchs and Schwab, 2013; Meesapyodsuk and Qiu, 2011). These epoxy fatty acids are further catalyzed by epoxide hydrolase to produce dihydroxy fatty acids (step B2; Figure 3.13). In fungi the importance of fatty acid degradation in production of lactones from monohydroxy and dihydroxy fatty acids are well reported (Cardillo et al., 1989; Endrizzi et al., 1996; Haffner and Tressl, 1998; Schottler and Boland, 1996). Also in peach fruit post harvest temperatures influenced lactone content by regulation of *acyl-CoA-oxidase*, an important gene from  $\beta$  oxidation pathway of fatty acid degradation (step D; Figure 3.13) (Xi et al., 2012). These findings insinuate that along with the *lipoxygenase* (*Mi9LOX*) and *epoxide hydrolase* (*MiEH2*), other genes viz. *peroxygenase* (*MiPGX1*), *hydroperoxide lyase* (*MiHPL*) and *acyl-CoA-oxidase* (*MiACO*) also play important role in lactone biosynthesis in mango (Figure 3.13).

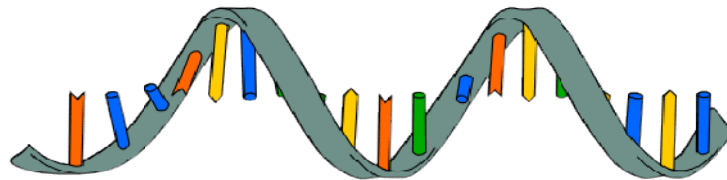
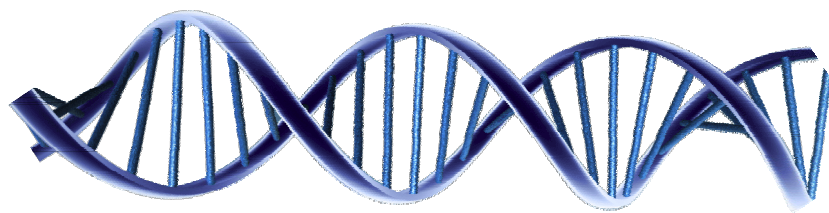
### 3.5 Conclusion

The genes encoding *Mi9LOX*, *MiEH2*, *MiHPL*, *MiPGX1* and *MiACO* were isolated from mango fruit. Variable lactone content of Alphonso, Pairi and Kent mango cultivars was elucidated by the expression analysis of these five genes during various fruit development and ripening stages of pulp and skin tissues of all the three cultivars. Among these *Mi9LOX* and *MiEH2* were characterized from Alphonso fruit, which divulged metabolism of unsaturated fatty acids leading to production of hydroperoxy fatty acids and hydroxy fatty acids, respectively. Increased lactone content upon transient over-expression of *Mi9LOX* and *MiEH2* ascertained their probable role in lactone biosynthesis in mango fruit. Finally, probable lactone biosynthesis pathway in mango was proposed.





## Chapter 4



Transcriptional transitions in Alphonso mango (*Mangifera indica* L.) during fruit development and ripening explain distinct aroma and shelf life characteristics



## **Chapter 4    Transcriptional transitions in Alphonso mango (*Mangifera indica* L.) during fruit development and ripening explain distinct aroma and shelf life characteristics**

### **4.1 Introduction**

Mango (*Mangifera indica* L.) is one of the popular and highly favoured fruit. Global mango production has been reported to be 43.3 million metric tons in 2013 preceding banana, apples, grapes and oranges. (<https://www.statista.com/statistics/237064/top-world-producers-of-selected-fresh-fruit-by-value-2009/>). There are thousands of mango cultivars worldwide, amid which Alphonso, Keitt, Kent, Lilli, Zill, Osteen, Haden, Kesar, Pairi, Dashehari, Langra and Banganapalli are well known. These varieties vary in their fruit color, size, shape, flavor, taste and ripening period and pattern. To understand composition and biosynthesis of their unique flavor and complex ripening process, various studies have been carried out at metabolic (Gil et al., 2000; Pandit et al., 2009a), proteomic (de Magalhães Andrade et al., 2012; Fasoli and Righetti, 2013; Renuse et al., 2012), genetic (Chidley et al., 2016b; Kulkarni et al., 2013a; Kulkarni et al., 2013b; Martínez et al., 2001; Pandit et al., 2010; Pandit et al., 2007; Sane et al., 2005; Singh et al., 2011) and post harvest processing (Chidley et al., 2016a; Chidley et al., 2013; González-Aguilar et al., 2007; Hofman et al., 1997; Jiang and Joyce, 2000) levels. Whole genome sequencing and RNA sequencing (RNAseq) are the two important high throughput technologies adopted recently to understand complex cellular and physiological processes in fruits such as citrus (Wu et al., 2014a), tomato (Consortium, 2012), and strawberry (Shulaev et al., 2011) while domestication and diseases tolerance in citrus (Martinelli et al., 2012; Wu et al., 2014a). Although mango genome sequence is not yet available, few recent studies have described the transcriptomic analysis of various tissues of few mango cultivars. The first report from Zill mango (Wu et al., 2014b) provided extensive transcriptomic and proteomic profiling from pulp and skin tissues of four fruit developing stages using pooled RNA but not stage specific and differentially expressed transcripts. Another study of leaf transcriptome and chloroplast genome sequencing from cultivar Langra provided information about the production of many bioactive compounds (Azim et al., 2014). Transcriptome analysis from two (raw and ripe) and three (raw,

mid ripe and ripe) stages of Kent (Dautt-Castro et al., 2015) and Dashehari fruit pulp (Srivastava et al., 2016), respectively gave important insights in to the ripening process and flavor biogenesis in these mango cultivars.

India is the highest producer and exporter of mango with 40.6% share in international mango market (<http://www.fao.org>). Amongst Indian mango cultivars Alphonso is globally favored and highly exported mango due to its unique and attractive flavor, low fiber containing pulp and high carotene content (Tharanathan et al., 2006a; Veda et al., 2007). Ripening duration of Alphonso mango is 15 days from harvest, which is the highest amid all mango cultivars, *viz.* ripening duration for Kent and Dashehari mango fruit is 10 and 6 days, respectively (Dautt-Castro et al., 2015; Srivastava et al., 2016). Fruit ripening in Alphonso mango progresses from skin towards stone leading to attractive skin color and easy monitoring of ripening progress. On the other hand various mango varieties, *viz.* Haden, Keitt, Kent, Tommy Atkins (National Mango Board, USA; <http://www.mango.org>) and Dashehari (Srivastava et al., 2016) show polarity of their ripening from fruit stone to skin making it difficult to identify ripened fruits. Longer ripening duration and shelf life of Alphonso mango provides sufficient time for its transportation. Mechanisms underlying these unique properties of Alphonso mango need to be explored in depth at spatial and temporal level of fruit development and ripening using transcriptomic, proteomic and metabolomic approaches as they can be correlated to the specific phenotype. Present study focuses on the transcriptome analysis of Alphonso mango through eight different tissues such as flower, whole fruit at 30 and 60 DAP (Days After Pollination), pulp and skin of 90 DAP fruit (mature raw fruit) and pulp from three fruit ripening stages *i.e.* 5 DAH (Days After Harvest): table green stage; 10 DAH: mid ripe stage and 15 DAH: ripe stage to analyze various fruit developing and ripening processes in Alphonso mango.

## 4.2 Materials and methods

### 4.2.1 Plant material

Flower and fruits of cv. Alphonso were collected from three individual biological replicates from the Mango Research Sub Centre, Deogad (16.528336 N, 73.344790 E)

affiliated to Dr. Balasaheb Sawant Konkan Agricultural University, Dapoli, Maharashtra, India. Flowers from inflorescence were collected and snap frozen. Fruits from developing stages were collected at 30, 60 and 90 days after pollination (DAP). Fruits from 30 and 60DAP were analysed as whole fruit in the present study after removing fruit stone, whereas at mature raw stage (90 DAP) pulp (mesocarp) and skin (exocarp) were separated, snap frozen in liquid nitrogen and stored at  $-80^{\circ}\text{C}$  until further use. A set of fruits were additionally harvested at their mature raw stage and kept in the hay containing boxes at ambient temperature for ripening and only pulp tissue for ripening stages as table green, mid ripe and ripe were collected at 5, 10 and 15 days after harvest (DAH), respectively. At each ripening stage fruits were removed from the box, pulp and skin were separated and pulp was frozen in liquid nitrogen and stored at  $-80^{\circ}\text{C}$  till further use.

#### **4.2.2 RNA isolation and cDNA synthesis**

Total RNA isolation was carried out for all the tissues sampled for current study using RNeasy Plus mini kit (Quiagen, Venlo, The Netherlands). RNA quality as 260 nm/280 nm ratio was checked using Nanodrop (Thermo Fisher Scientific, Waltham, Massachusetts, USA) and RNA integrity was checked using Bioanalyzer (BioRad). Two microgram of total RNA was used to carry out reverse transcription for synthesis of cDNA using High Capacity cDNA reverse transcription kit (Applied Biosystem, Carlsbad, CA, USA).

#### **4.2.3 Library preparation and sequencing**

One microgram of total RNA from each stage was used to prepare 8 individual libraries from sampled tissues. mRNA purification was carried out using polyT oligo beads. The purified mRNA was fragmented in the range of 100 to 140 bases with optimum at around 120 bases from which the cDNA was synthesized. End repair, A-Tailing, Adapter ligation and the library preparation were performed using Tru Seq RNA sample preparation kit v2 (Illumina) as per manufacturer's instructions. PCR enrichment was performed for 15 cycles and the sample was validated on the bioanalyzer. Libraries were sequenced in a Paired End 100 base run, using TruSeq SBS Kit v3-HS (Catalog No.: FC-401-3001) for sequencing on the Illumina

HiSeq1000 platform at Centre for Cellular and Molecular Platforms (C-CAMP), Bangalore according to manufacturer's recommended protocols ([http://www.illumina.com/systems/hiseq\\_systems/hiseq\\_2000\\_1000/kits.ilmn](http://www.illumina.com/systems/hiseq_systems/hiseq_2000_1000/kits.ilmn)).

#### 4.2.4 Bioinformatic data analysis

Paired end RNA sequencing was performed using Illumina Hiseq 2000. Quality check on raw data files was performed using FastQC computational tool (<http://www.bioinformatics.babraham.ac.uk/projects/fastqc/>). Adapter free, good quality reads ( $Q \geq 30$ ; min read length=85) were obtained using Cutadapt (Martin, 2011). Alphonso transcriptome for each stage was assembled using Velvet-Oases (Schulz et al., 2012) with K-mers 67, 75, 83 and merging them at 27 k-mer. Additionally, a merged transcriptome was also generated using k-mer 55. Further, for all the merged assembled transcripts Transdecoder was used (<https://transdecoder.github.io/>) to extract potential candidate coding regions within transcripts. Partial cds were discarded and only those transcripts with start and stop codon were made non redundant based upon sequence identity cut-off 90% using CD-HIT-est (Li and Godzik, 2006) and used for downstream analyses.

Further, merged full length transcripts (from merged assembly) were used as reference to map back all the raw reads from each stage using default parameters of Bowtie (Langmead et al., 2009). DESeq2 was used to identify differentially expressed transcripts (Love et al., 2014) and were filtered based upon  $p$ -value  $\leq 0.05$  and expression value  $>0$ . All those transcripts having mapping count zero were excluded for further analysis such as in identification of uniquely expressed transcripts in a particular stage or a specific set of stages (e.g. developing and ripening stages). Unique and common list of transcripts were represented using Venny (<http://bioinfogp.cnb.csic.es/tools/venny/>). Full length transcripts (from merged assembly) were used as reference for differential expression analysis using DESeq2 (Love et al., 2014).

Annotation, enzyme code distribution and GO mapping and interproscan were carried out in the BLAST2GO 3.1.3 workbench (Biobam Bioinformatics S.L., Valencia, Spain) as described in the user manual (Conesa et al., 2005). GO



enrichment analysis was carried out in given test and reference sets by Fisher's exact test in BLAST2GO with  $p$ -value (0.001) and FDR filters.

### 4.2.5 Quantitative real-time PCR

Quantitative real-time PCR was performed using Fast Start Universal SYBR Green master mix (Roche Inc. Indianapolis, Indiana, USA) and *elongation factor 1 $\alpha$*  (*EF1 $\alpha$* ) as an endogenous control employing the primers reported earlier (Pandit et al., 2010). Various transcripts selected from transcriptome data were amplified using gene specific primers (Appendix 2) and quantification was done by ViiA™ 7 Real-Time PCR System (Applied Biosystems) having thermal cycle program of initial denaturation at 95 °C for 10 min with subsequent 40 cycles of 95 °C for 3sec and 60 °C for 30 sec followed by a dissociation curve analysis of transcripts. Relative quantification ( $\Delta\Delta$ CT method) and statistical analysis was carried out using DataAssist™ v3.01 software (Applied Biosystem, Carlsbad, CA, USA).

## 4.3 Results

### 4.3.1 Alphonso mango transcriptome

Alphonso mango transcriptome was screened through 8 tissue samples. To map differentially expressed transcripts a merged assembly was generated from the reads of all the tissues, which reflected upon overall Alphonso mango flower and fruit transcriptome. For each tissue read numbers were more than 100 million, which were assembled using k-mers 67, 75 and 83 separately and then merged for individual tissue. Average number of unique transcripts post assembly was 76,043 and with n-50 and n-80 values as 1,835 and 1,008 bp, respectively (Annexure 1\_Supplementary file 1). The minimum and maximum lengths of transcript from these assemblies were 100 and 17342 bp, respectively (Annexure 1\_Supplementary file 1). Average number of transcripts was 11,925 upon filtering for redundancy and identifying candidate coding regions with maximum 90% identity and minimum 70% coverage (Table 4.1).

**Table 4.1 Number of non redundant transcripts/sample**

Assembly	No of NR transcripts
Flower	15778
30 DAP	14622
60 DAP	14090
90 DAP pulp	9382
90 DAP skin	12664
5 DAH	10084
10 DAH	9748
15 DAH	9032

Unique transcripts from each assembled and filtered tissue were subjected to BLASTx against the non-redundant dataset from NCBI ([www.ncbi.nlm.nih.gov](http://www.ncbi.nlm.nih.gov)). From total of 20,755 unique transcripts from merged assembly, 92.22% transcripts were annotated while, 954 transcripts (4.59%) coded for hypothetical proteins and 659 (3.17%) remained unidentified. BLASTx statistics revealed maximum hits from *Citrus sinensis* and *C. clementina* followed by *Theobroma cacao*, *Jatropha curcas*, *Vitis venifera* and *Ricinus communis* (Figure 4.1a). Total 74,330 GO terms related to various biological processes (BP), molecular functions (MF) and cellular components (CC) were assigned to these 20,755 unique transcripts. Metabolic, cellular and single organism processes followed by biological regulation and localization were the most abundant terms under the BP category, binding and catalytic activity related terms under MF while, organelle, membrane and macromolecular complex terms under CC, respectively (Figure 4.1b, Figure 4.2 ).

Unique transcripts were assigned enzyme commission (EC) number to identify involvement of these transcripts in various BPs. Total 4,611 ECs were assigned from oxidoreductase, transferase, hydrolase, ligase, lyase and isomerase, wherein, transferases were the most abundant followed by hydrolases in all the eight tissues (Figure 4.3). These assigned ECs represented 142 known pathways from KEGG database (<http://www.genome.jp/kegg/pathway.html>), which are potentially functional in Alphonso mango fruit development and ripening. Most of these pathways were saturated with higher number of annotations from transcriptome data e.g. metabolism

of starch, sucrose and various amino acids including methionine and biosynthesis pathway of ethylene, phenylpropanoids and flavonoids (Appendix 3).

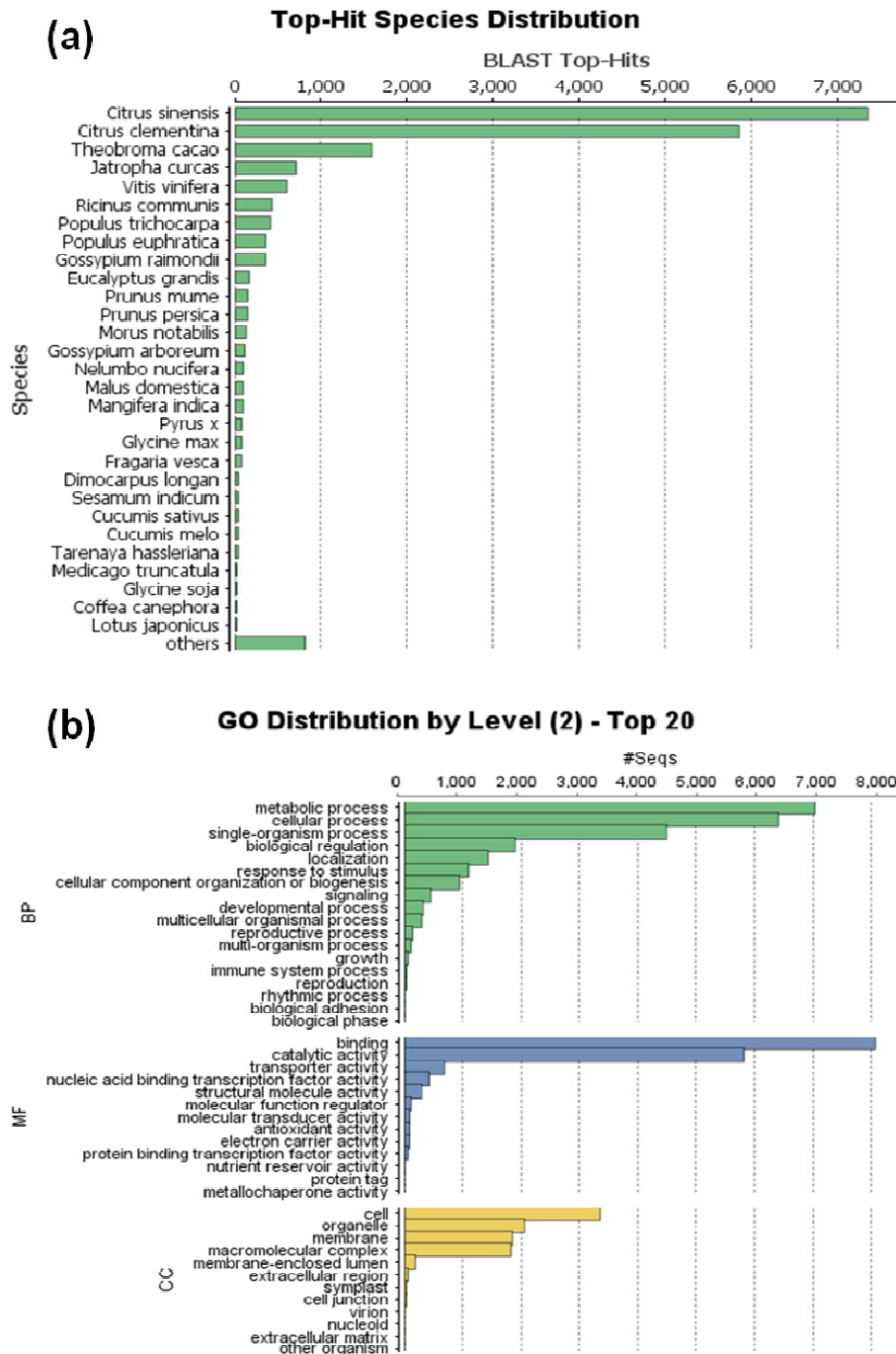


**Figure 4.1 Blast2GO statistics**

Blast statistics showing distribution of top hit species (a) and distribution of top gene ontologies from BP: biological processes, MF: molecular functions and CC: cellular components (b)

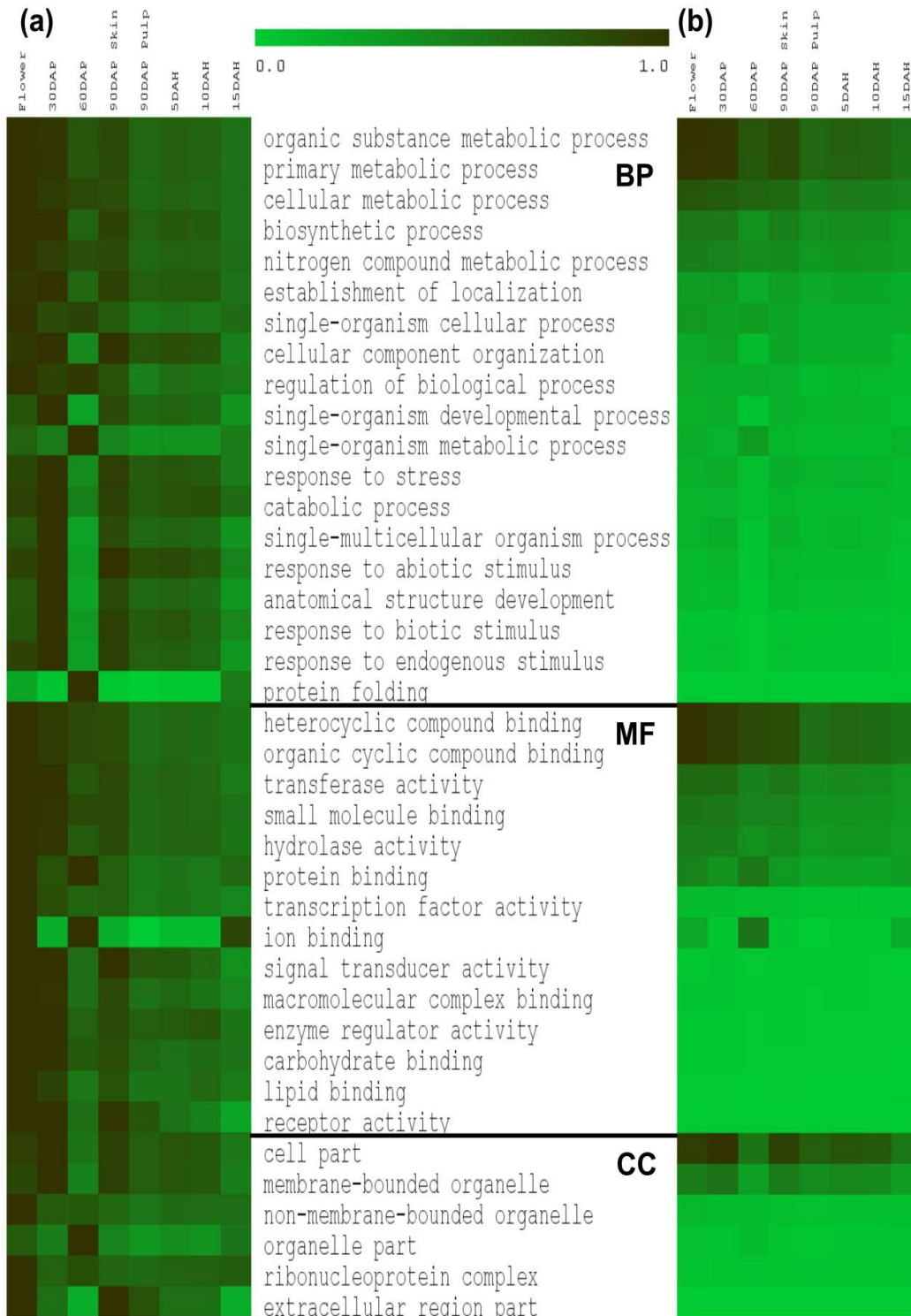


**Figure 4.2 Heatmap representing expression profiles of various gene ontologies** Biological process (BP), molecular function (MF) and cellular components (CC) in different tissues analysed were represented. Stage wise normalization (a) for each GO and global normalization (b) for each GO category presented.

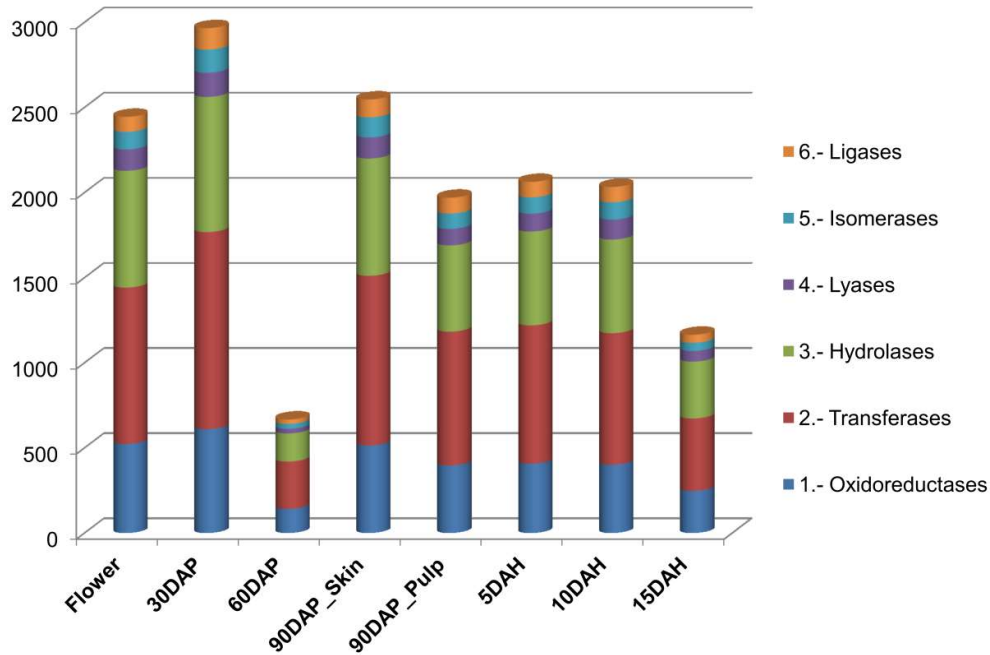


**Figure 4.3 Enzyme code distribution**

Number of transcripts (Y-axis) coding for six classes of enzymes through various stages of Alphonso mango fruit development and ripening (X-axis)

### 4.3.2 Transcriptome changes through flower to fruit and fruit development to ripening

Variations in the transcriptome were studied using number of parameters, such as differentially expressed transcripts, transcripts distinctive to a stage and gene ontology enrichment during flower to fruit transition and through process of fruit development and ripening.

#### 4.3.2.1 Differentially expressed transcripts

Comparison between adjacent tissue stages was carried out to identify differentially expressed transcripts at each stage of fruit development and ripening (Table 4.2, Annexure 1\_Supplementary file 2). Between flower to fruit of 30DAP, 524 transcripts were down regulated while 181 were up regulated. Amid the down regulated transcripts alpha-amylase and subtilisin inhibitor-like (contig\_6593), carbonic anhydrase (contig\_5377), chitinase (contig\_4907) and maternal effect embryo arrest 59 (contig\_4949) were with the highest fold change, while homeodomain-like protein (contig\_12912 and 12913), cytochrome p450 - cyp72a219-like (contig\_4083), heat

shock cognate 70 kDa protein (contig\_5948) and inositol-3-phosphate synthase (contig\_9620) were highly up regulated. Transition from 30 DAP to 60 DAP resulted in up regulation of 73 and down regulation of 7 transcripts. Important down regulated transcripts were, n-acetyltransferase (contig\_1261), 9-*cis*-epoxycarotenoid dioxygenase (contig\_1680), protein reversion-to-ethylene sensitivity (contig\_9164) and ethylene receptor 2 (contig\_6147). While important up regulated transcripts were nucleotide sugar transporter family protein (contig\_6337), beta-xylosyltransferase (contig\_4150), various cellulose synthase catalytic subunits and laccases.

**Table 4.2 Number of differentially expressed transcripts**

<b>Comparison</b>	<b>Up regulated</b>	<b>Down regulated</b>
30DAP vs Flower	181	524
60DAP vs 30DAP	73	7
90DAP pulp vs 60DAP	31	158
90DAP skin vs 60DAP	4	93
90DAP skin vs 90DAP pulp	54	4
5DAH vs 90DAP pulp	42	52
10DAH vs 5DAH	191	418
15DAH vs 10DAH	30	12

Comparison between 60 DAP fruit tissue with 90 DAP pulp and skin tissue, respectively revealed down regulation of beta-xylosyltransferase, beta-d-xylosidase, cellulose synthase and galacturonosyl transferase; whereas spx and exs domain-containing protein was up regulated in 90 DAP pulp and skin both. Up regulation of homeobox protein sbh1, gdsl esterase lipase, caffeoyl shikimate esterase, hydroperoxide lyase, udp-rhamnose:rhamnosyl transferase and pectinesterase inhibitor was evinced from 90 DAP pulp tissue compared to that in 60 DAP fruit tissue. Evaluation of differentially expressed transcripts between pulp and skin of 90 DAP revealed very few transcripts down regulated in skin with none of them showing change more than 2-fold, while 54 transcripts were up regulated in 90 DAP skin tissue including the important ones as DNA mismatch repair protein msh5, acyl carrier protein, amino-acid permease, calcium-transporting ATPase, isoflavone reductase and various disease resistance proteins.

During ripening of Alphonso pulp from 90 DAP to 5 DAH, 42 transcripts were up regulated (>2-fold) including methyltransferase, amino-acid permease, chloroplastic 9-*cis*-epoxycarotenoid dioxygenase, beta-galactosidase and protein phosphatase mainly, whereas 52 transcripts were down regulated, important ones being few disease resistance proteins, peroxidase, sucrose synthase and glycerol-3-phosphate dehydrogenase. The highest level of differential expression was evinced through transition from 5 DAH to 10 DAH among all the ripening tissues, wherein 418 transcripts were down and 191 were up regulated. Prominently down regulated transcripts were phospholipase A LCAT3, sugar phosphate exchanger, auxin-responsive protein IAA9, abscisate  $\beta$ -glucosyltransferase and membrane-associated kinase regulator with more than 3-fold change, while up regulated were aspartic proteinase nepenthesin, UDP-glucose 6-dehydrogenase, 1-aminocyclopropane-1-carboxylate oxidase, peroxidase, bidirectional sugar transporter sweet1-like, omega-6 fatty acid desaturase and squalene monooxygenase. During the transition from 10 DAH to 15 DAH stage increased phosphate metabolism was evident. Total 30 transcripts were up regulated mainly including phospholipase-d, inorganic pyrophosphatase, phosphate transporter, transcription factor glk2 and DNA translocase, whereas 12 transcripts were down regulated and important ones were aspartic protease, plastocyanin-like domain protein, annexin d2-like and glucuronosyltransferase (>2-fold).

#### 4.3.2.2 Idiosyncratic transcripts for the stage

Various transcripts unique to each of these stages (Figure 4.4, Table 4.3 and Annexure 1\_Supplementary file 3) representing multiple stage specific processes were identified during this comparative analysis, Total of 388 transcripts were identified as unique to flower tissue which mostly included various transcription and translation factors, late embryogenesis abundant proteins, stress-sensitive and dehydration-responsive element-binding protein-1b and various ribosomal proteins. Similarly distinct transcripts specific to fruit developing and ripening stages were identified, wherein 1,090 and 27 transcripts were idiosyncratic to the fruit developing and ripening stages, respectively (Annexure 1\_Supplementary file 3). Various auxin and gibberellin induced and regulated proteins, many proteins responsible for various vacuole activities, multiple disease resistance proteins and various terpene synthases were

distinct to the developing stages. Transcripts coding for multiple transcription and translation factors during Alphonso fruit development were also detected. Interestingly multiple ethylene responsive transcription factors along with the protein reversion-to-ethylene sensitivity were uniquely revealed in the developing stages. Whereas, NIN-like protein, respiratory burst oxidase homolog protein d-like, rhamnogalacturonate lyase b-like, lectin receptor kinase, gag protein and methionine Y-lyase were exclusive to the Alphonso ripening stages. Similarly, WRKY transcription factor 43, b3 domain-containing val3 and ap2 ERF domain-containing transcription factors were uniquely identified from the ripening stages. Many hypothetical and uncharacterized proteins were also found to be Alphonso ripening specific and their characterization might help to reveal ripening process in Alphonso.

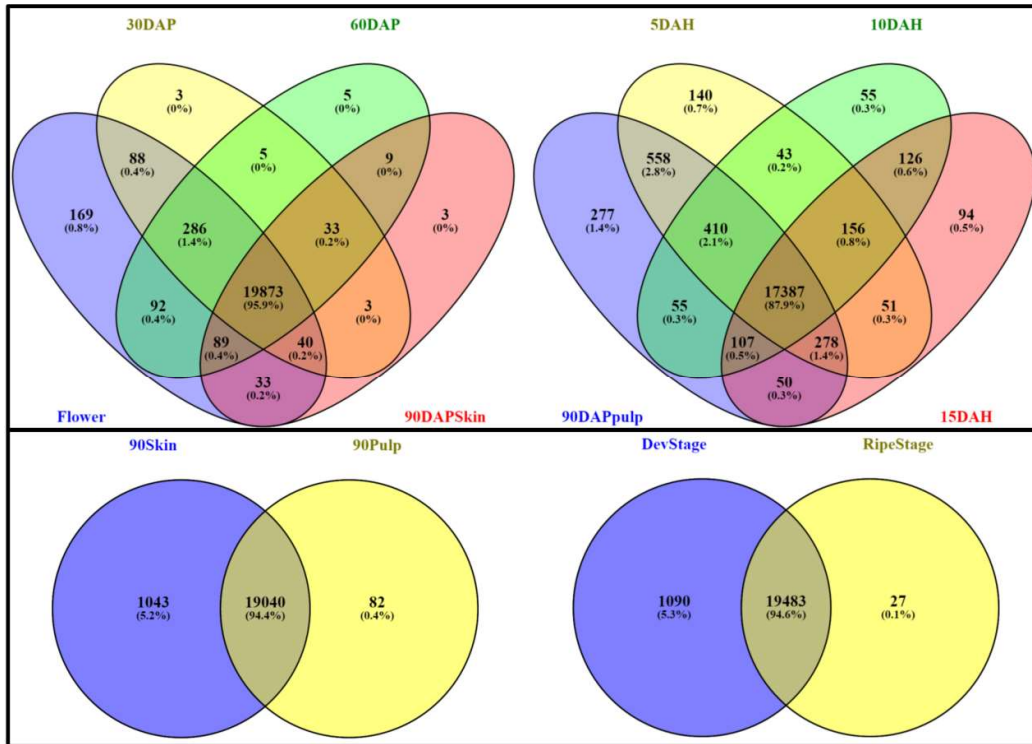


**Figure 4.4 Distribution of common and distinct transcripts**

Venn diagrams representing common and distinct transcripts through various stages



**Table 4.3** Number of distinct transcripts for a stage amid various comparisons

Comparison	Stage/s	No. of unique transcripts
30DAP vs Flower	Flower	383
	30DAP	44
60DAP vs 30DAP	30DAP	134
	60DAP	195
90DAP pulp vs 60DAP	60DAP	1306
	90DAP pulp	36
90DAPskin vs 60DAP	60DAP	388
	90DAP skin	79
90DAP skin vs 90DAP pulp	90DAP pulp	82
	90DAP skin	1043
5DAH vs 90DAP pulp	90DAP pulp	489
	5DAH	390
10DAH vs 5DAH	5DAH	1027
	10DAH	343
15DAH vs 10DAH	10DAH	563
	15DAH	473
Development vs Ripening	Development	1090
	Ripening	27

#### 4.3.2.3 Gene ontology (GO) enrichment

Fisher's exact test was performed to understand over and down represented GOs ( $p$ -value  $\leq 0.001$ ) during the transition, which gave an overall picture of the Alphonso mango development and ripening (Figure 4.5). During the flower to 30 DAP fruit transition certain GOs were overexpressed, such as post-embryonic developmental and anatomical structure morphogenesis process, response to abiotic stimulus and various plastid and thylakoid processes. At the same time hydrolysis of *O*-glycosyl compounds and UDP-glycosyltransferase activity along with the methyltransferase, sucrose metabolic and lipid biosynthetic activities coding GOs were down represented. 30 to 60 DAP transition described enriched GOs for starch and sucrose metabolic process, fatty acid, cellulose and vitamin biosynthetic processes, protein glycosylation, response to oxidative stress and heat along with HSP binding. During the same event cell differentiation, growth and cell death in addition to the anatomical structure morphogenesis, secondary metabolic process and response to biotic stimulus coding GOs were observed to be decreased.

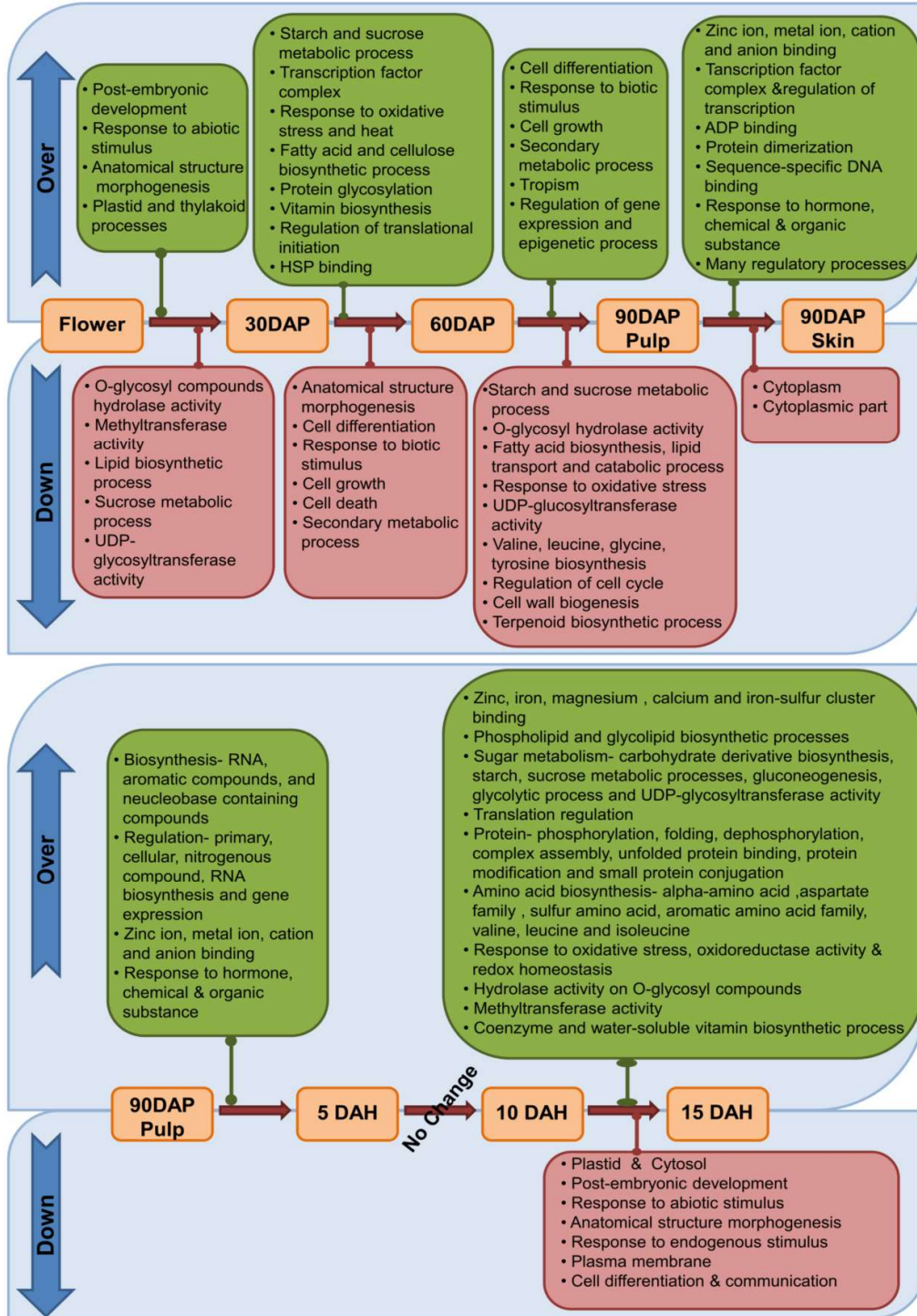


**Figure 4.5 Gene ontology enrichment**

Over and down expressed gene ontologies (GO) between stages of development and ripening

Comparison between 60 DAP fruit and 90 DAP pulp revealed over represented GOs for cell differentiation and cell growth, response to biotic stimulus, secondary metabolic process, tropism and regulation of gene expression. While, starch and sucrose metabolic processes, *O*-glycosyl hydrolase UDP-glucosyltransferase activities, fatty acid biosynthesis and catabolic processes along with the lipid transport, various amino acid and terpenoid biosynthesis and cell wall biogenesis were down represented. 90 DAP pulp and skin tissues showed over expression of various ion, ADP and sequence-specific DNA binding activities along with the response to hormone, chemical and organic substances in the skin tissue; whereas only cytoplasm and cytoplasmic part related GOs were found to be down expressed in the skin compared to that in the pulp at 90 DAP.

Transition of 90 DAP pulp and 5 DAH pulp revealed only over representation of GOs such as biosynthesis of RNA, aromatic compounds, and nucleobase containing compounds; binding of various ions; regulation of primary, cellular, nitrogenous compounds, RNA biosynthesis processes and gene expression and response to hormone, chemical and organic substance. Surprisingly none of the GOs showed significant enrichment during the transition from 5 to 10 DAH and reflected as the stationary phase of Alphonso mango ripening. 10 DAH (mid ripe stage) to 15 DAH (ripe stage) transition showed over expression of many GOs such as binding of various ions; phospholipid, glycolipid, amino acid, co-enzyme and water soluble vitamin biosynthetic processes; methyltransferase, UDP-glycosyltransferase and *O*-glycosyl hydrolase activities; starch, sucrose metabolic processes, gluconeogenesis and glycolytic process; protein phosphorylation, dephosphorylation, folding, protein modification and small protein conjugation along with the regulation and response to oxidative stress, oxidoreductase activity and redox homeostasis. While GOs related to plastid and cytosol; post embryonic development; response to abiotic and endogenous stimulus; anatomical structure morphogenesis, plasma membrane, cell differentiation and communication were down represented.

### 4.3.3 Spatial changes in transcriptome at 90 DAP

In case of Alphonso mango, 90 DAP stage is a mature raw stage of the fruit and is considered as the right stage of fruit harvest (0 Days After Harvest) for further

artificial ripening of the fruit (Pandit et al., 2009b). Hence transcriptome analysis of skin and pulp were separately carried out at this stage. Overall 90 DAP skin was found to be metabolically more active compared to the 90 DAP pulp with respect to differentially expressed genes (Annexure 1\_Supplementary file 2), unique genes (Annexure 1\_Supplementary file 3) and enriched GOs (Figure 4.5). In the skin 54 transcripts were up regulated whereas only 4 were down regulated compared to the pulp. Among the up regulated transcripts isoflavone reductase, transcription and translation regulatory proteins, hydrolases, methyltransferase etc. were more prominent. Whereas four down regulated transcripts were membrane and cytoplasm related GOs. Unique transcripts upon comparison between 90 DAP pulp and skin showed carotene and xanthophylls biosynthesis related contigs, beta-carotene hydroxylase and anthocyanidin 3-o-glucosyltransferase, flavor related various terpene synthases and ripening related contigs such as ethylene-responsive transcription factors, pectate lyase, pectin esterase and cellulase as unique to skin compared to pulp. These findings highlight initiation of Alphonso ripening process from skin and its probable progress towards fruit stone, which is the important characteristic of Alphonso mango.

#### 4.3.4 Genes involved in the flavor biogenesis in Alphonso mango

Quantitatively mono-terpenes are abundant in Alphonso followed by sesqui-terpenes (Pandit et al., 2009a; Pandit et al., 2009b). Present data revealed 6 contigs coding for mono-terpene synthases (*limonene synthase1*, *limonene synthase2*, *beta ocimine synthase1*, *beta ocimine synthase2*, *isoprene synthase1* and *isoprene synthase2*), 5 contigs coding for the sesquiterpene synthases (*germacreneD synthase1*, *germacreneD synthase2*, *nerolidol synthase1*, *nerolidol synthase2* and *alpha farnesene synthase*) and 3 contigs coding for the di-terpene synthases (*ent-kaurene synthase* and *casbene synthase (E,E)-geranillinalool synthase*). Phylogenetic analysis (Figure 4.6) of these genes along with the other plant terpene synthases (TPS) showed distribution of these genes in to the TPS-a, TPS-b, TPS-e and TPS-f clades, respectively (Sallaud et al., 2009).

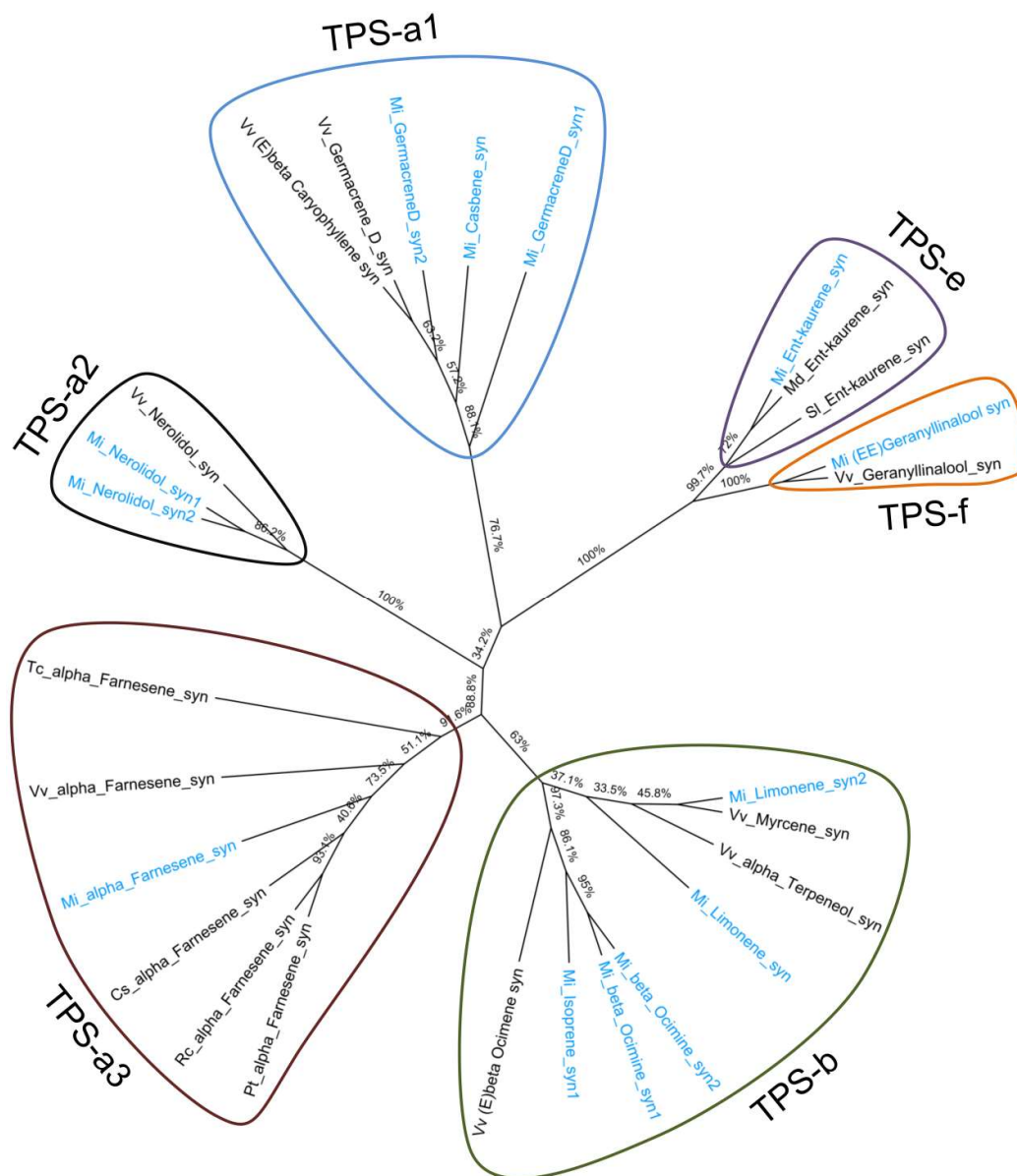


**Figure 4.6 Phylogenetic analysis of terpene synthases**

Cladogram representing phylogenetic analysis by neighbor-joining of encoded proteins by various terpene synthases from present study (blue color) along with the terpene synthases from other Angiosperm plants. Node label represents name of the enzyme followed by two letters representing initials of botanical name of the plant. Details of sequence of plant species, enzyme and NCBI accession in parenthesis are as follows *Vitis vinifera* (E)-beta-caryophyllene synthase (ADR74192.1), *Vitis vinifera* germacrene D synthase (ADR74198.1), *Vitis vinifera* nerolidol synthase (ADR74211.1), *Vitis vinifera* (E,E)-geranyl linalool synthase (ADR74219.1), *Malus domestica* ent-kaurene synthase (AFG18184.1), *Solanum lycopersicum* ent-kaurene synthase (AEP82778.1), *Vitis vinifera* (E)-beta-ocimene synthase (ADR74204.1), *Vitis vinifera* Alphaterpeneol synthase (ADR74202.1), *Vitis vinifera* myrcene synthase (NP\_001268009), *Citrus sinensis* alpha-farnesene synthase (XP\_006467948.1) *Populus trichocarpa* alpha-farnesene synthase (XP\_002317269.2), *Ricinus communis* alpha-farnesene synthase (XP\_015574261.1), *Theobroma cacao* alpha-farnesene synthase (EOY28527.1) and *Vitis vinifera* alpha\_farnesene synthase (NP\_001268183.1)

Furaneol and mesifuran are the two furanones from Alphonso mango and their synthesis by *enone oxidoreductase (EO)* and *O-methyltransferase (OMTS)*, respectively are described earlier (Chidley et al., 2016b; Kulkarni et al., 2013a). Multiple contigs coding for *quinone oxidoreductase* and *O-methyltransferases* were detected in the present analysis. Phylogenetic analysis of these contigs with the characterized genes revealed another similar transcript variant for the *MiEO* (Figure 4.7), whereas none of the contigs showed similarity to the *MiOMTS* (Figure 4.8). Green grassy aroma of unripe fruits is due to the C6 volatiles formed during the lipoxygenase and hydroperoxide lyase (HPL) pathways. In the present study single contig coding for the *hydroperoxide lyase* and 6 contigs coding for the *13-lipoxygenase* were detected. Involvement of *9-lipoxygenase (Mi9LOX)* and epoxide *hydrolase 2 (MiEH2)* in the biogenesis of lactones from Alphonso mango has also been confirmed (Chapter 3). One more transcript encoding *9-lipoxygenase* similar to that of the characterized *Mi9LOX* (Figure 4.9) and 3 contigs coding for *epoxide hydrolase 2* grouping with the *MiEH2* (Figure 4.10) were additionally detected in the present study. Three more novel contigs coding for *epoxide hydrolase* were also detected but neither grouped with the other *EH1* or *EH2* from different plant species (Figure 4.10).

Differential expression of all these flavor related genes was analysed in terms of transcript abundance in flower and fruit developing and ripening stages (Figure 4.11). Amid these contigs coding for various TPS were abundant in flower and during early developing stages. Interestingly, many contigs coding for EH (contigs 8280, 3904, 3901, 14123 and 8281), LOX (contigs 18105, 12748, 12747 and 12385) and EO (contigs 8026, 5618, 15594, 14137 and 13600) were found to be ripening specific and might be playing crucial role in generating unique aroma volatiles during Alphonso fruit ripening.

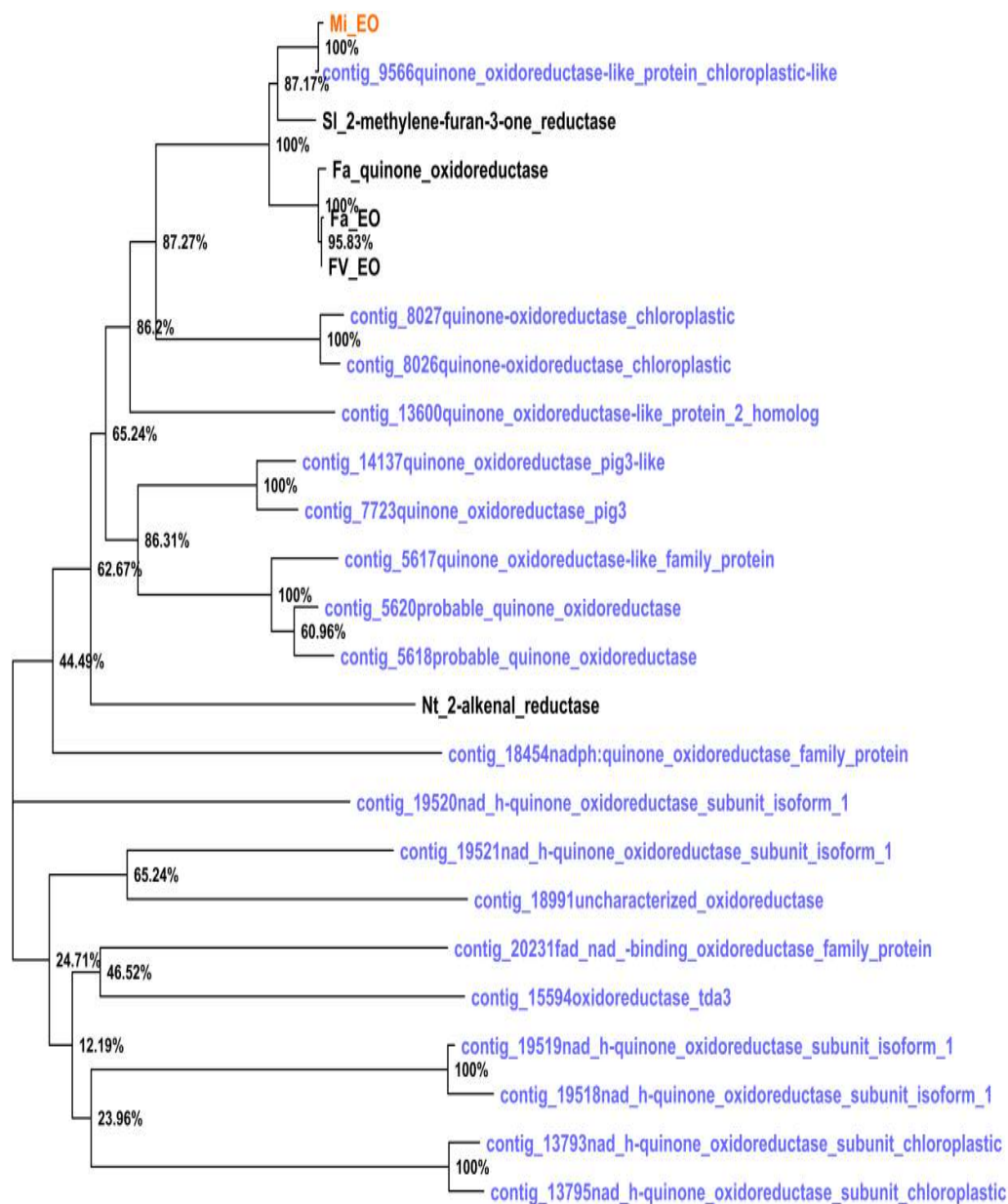


**Figure 4.7 Phylogenetic analysis of transcripts encoding enone oxidoreductase**

Phylogenetic analysis by neighbor-joining of encoded proteins by Enone oxidoreductase (gi|387135418) involved in the biosynthesis of furaneol from *Mangifera indica* (orange color) and other contigs representing quinone oxidoreductases from present study (blue color) along with the other characterized oxidoreductases (black color) from *Nicotiana tabacum* 2-alkenal\_reductase (gi|75206691), *Fragaria vesca* Enone oxidoreductase (gi|613785129), *Solanum lycopersicum* 2-methylene-furan-3-one\_reductase (gi|823630988), *Fragaria* × *Ananassa*\_ Enone\_Oxidoreductase (gi|480312155) and *Fragaria* × *Ananassa*\_ quinone\_oxidoreductase (gi|29468088)

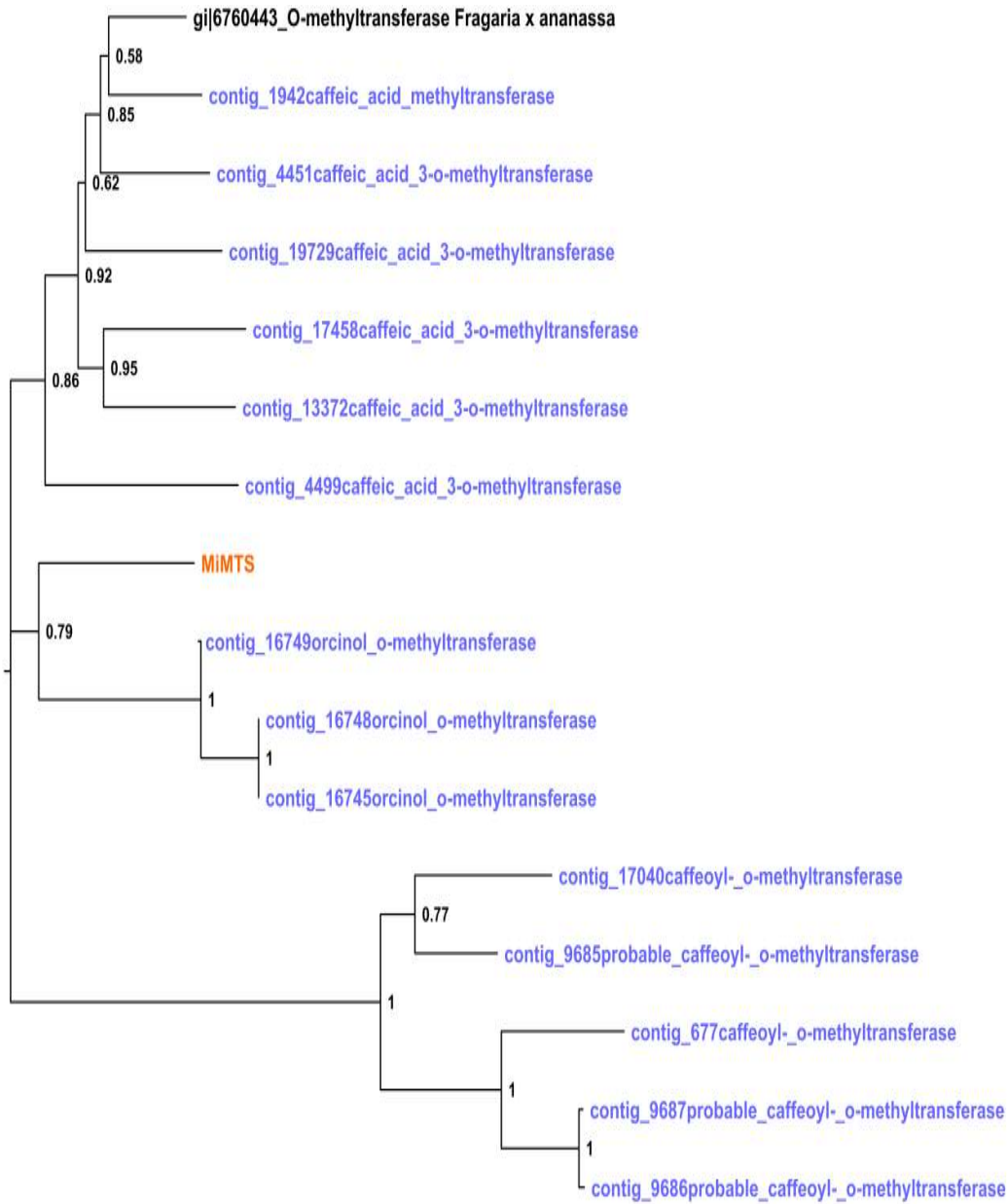


**Figure 4.8 Phylogenetic analysis of transcripts encoding O-methyltransferase**

Phylogenetic analysis by neighbor-joining of encoded proteins by *O-methyltransferase* (KP993176) involved in the biosynthesis of mesifuran from *Mangifera indica* (orange color) along with the characterized *O-methyltransferase* (black color) from *Fragaria x ananassa* (AAF28353) and other contigs representing *O-methyltransferase* from present study (blue color).



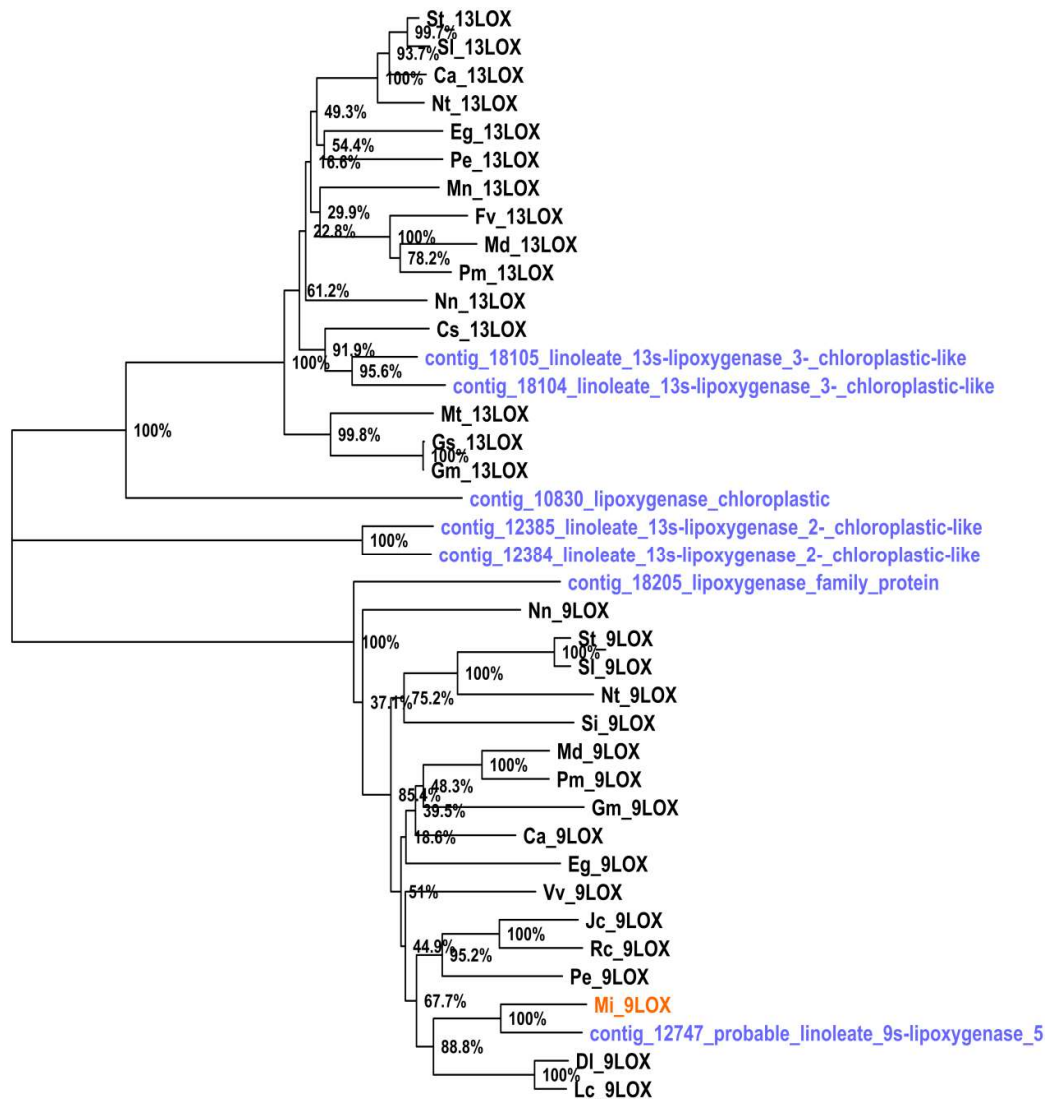


**Figure 4.9 Phylogenetic analysis of transcripts encoding lipoxygenase**

Phylogenetic analysis by neighbor-joining of encoded proteins by *9-lipoxygenase* (KX090178) involved in the biosynthesis of aroma volatiles from *Mangifera indica* (orange color) and other contigs representing *lipoxygenases* from present study (blue color) along with the other plant 9 and 13lipoxygenases (black color) from *Vitis vinifera* 9LOX (XP\_010659859), *Malus domestica* 9LOX (NP\_001281030), *Prunus mume* 9LOX (XP\_008246456), *Glycine max* 9LOX (XP\_003521704), *Solanum tuberosum* 9LOX (NP\_001274916), *Nicotiana tabacum* 9LOX (XP\_016433823), *Dimocarpus longan* 9LOX (ANF89411), *Corylus avellana* 9LOX (CAD10740), *Litchi chinensis* 9LOX (AEQ30071), *Populus euphratica* 9LOX (XP\_011023610), *Eucalyptus grandis* 9LOX (XP\_010025195), *Jatropha curcas* 9LOX (XP\_012089053), *Ricinus communis* 9LOX (XP\_002512386), *Solanum lycopersicum* 9LOX (XP\_004244890), *Sesamum indicum* 9LOX (XP\_011087404), *Nelumbo nucifera* 9LOX (XP\_010256003), *Malus domestica* 13LOX (NP\_001280985), *Prunus mume* 13LOX (XP\_008228181), *Medicago truncatula* 13LOX (XP\_003627308), *Solanum tuberosum* 13LOX (NP\_001275115), *Glycine soja* 13LOX (KHN39622), *Fragaria vesca* 13LOX (XP\_004303702), *Morus notabilis* 13LOX (XP\_010086794), *Eucalyptus grandis* 13LOX (XP\_010033729), *Populus euphratica* 13LOX (XP\_011035732), *Nelumbo nucifera* 13LOX (XP\_010273845), *Capsicum annuum* 13LOX (NP\_001311748), *Nicotiana tabacum* 13LOX (XP\_016495606), *Citrus sinensis* 13LOX (XP\_006465905), *Solanum lycopersicum* 13LOX (AAB65767), *Glycine max* 13LOX (XP\_014624448).

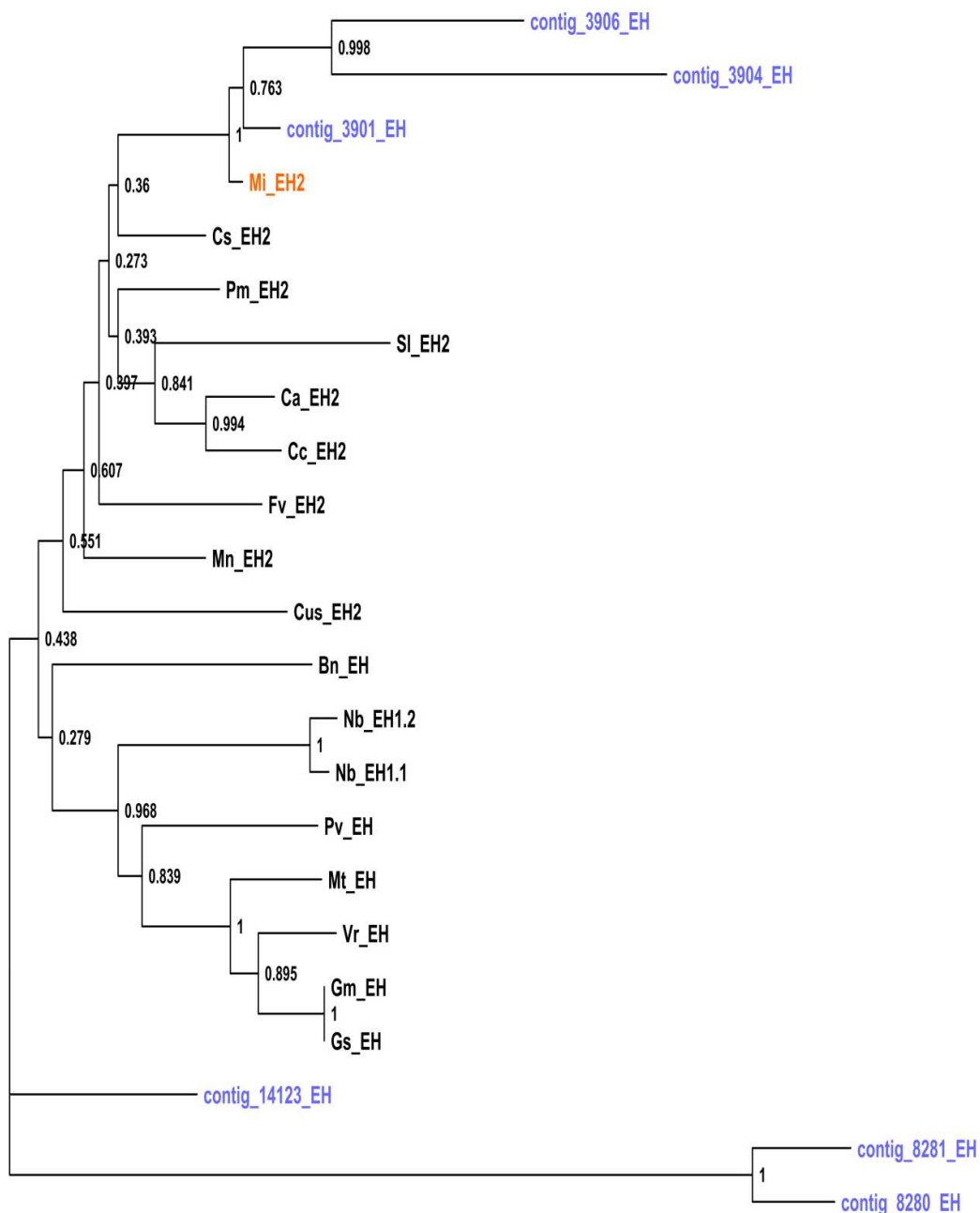


**Figure 4.10 Phylogenetic analysis of transcripts encoding epoxide hydrolase**

Phylogenetic analysis by neighbor-joining of encoded proteins by *epoxide hydrolase 2* (KX090179) involved in the biosynthesis of aroma volatile lactones from *Mangifera indica* (orange color) and other contigs representing *epoxide hydrolases* from present study (blue color) along with the other plant *epoxide hydrolases* (black color) from *Nicotiana benthamiana*\_EH1.2 (ACE82566), *Nicotiana benthamiana*\_EH1.1 (ACE82565), *Phaseolus vulgaris*\_EH (AKJ75509), *Glycine max*\_EH (CAA55294), *Medicago truncatula*\_EH (XP\_003626202), *Glycine soja*\_EH (KHN43314), *Vigna radiata*\_EH (AIJ27456), *Brassica napus*\_EH (NP\_001302895), *Citrus sinensis*\_EH2 (XP\_006489040), *Prunus mume*\_EH2 (XP\_016647751), *Cicer arietinum*\_EH2 (XP\_004508197), *Fragaria vesca*\_EH2 (XP\_004290776), *Cajanus cajan*\_EH2 (KYP58120), *Cucumis sativus*\_EH2 (XP\_004134492), *Solanum lycopersicum*\_EH2 (XP\_004252913) and *Morus notabilis*\_EH2 (XP\_010105136).

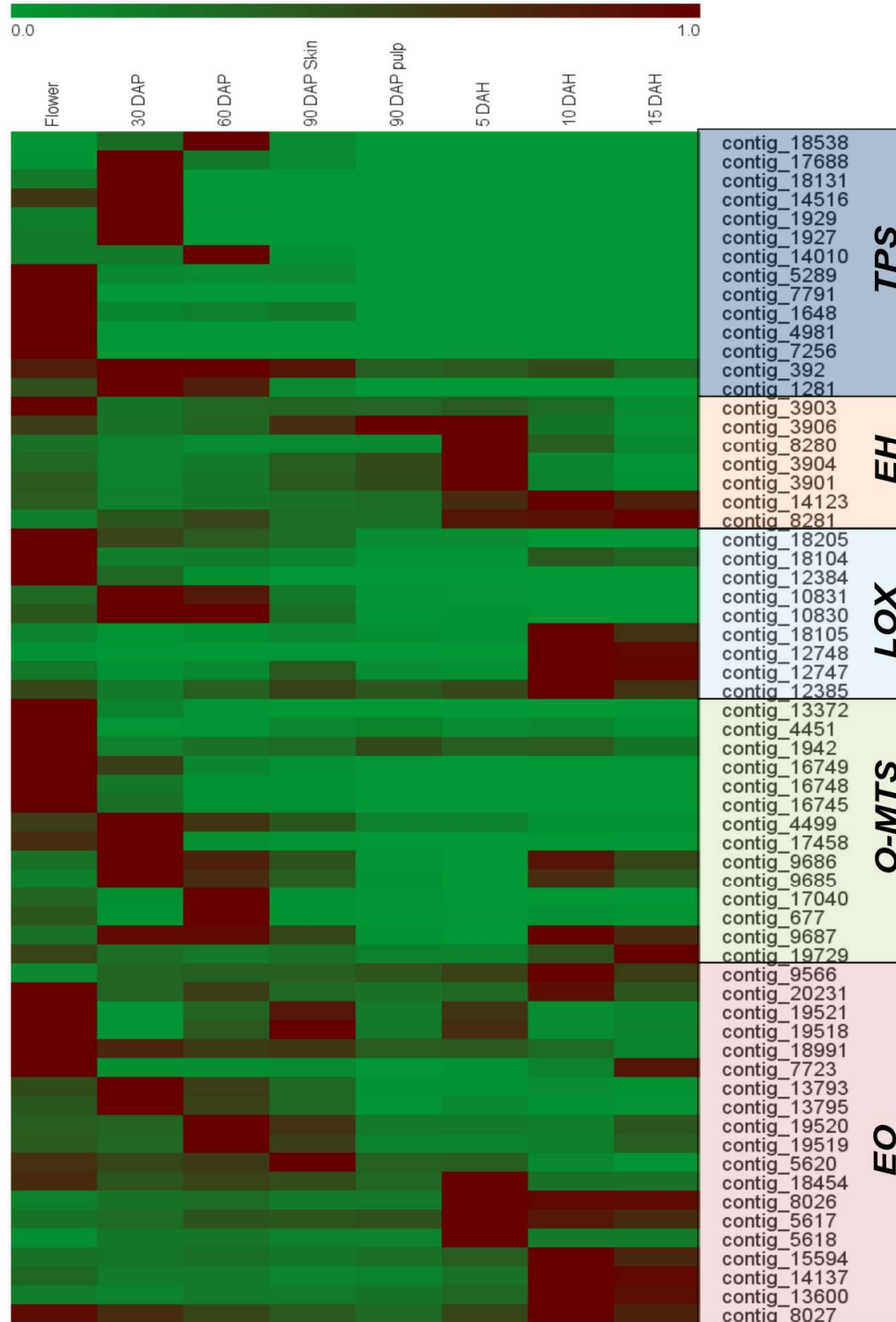


**Figure 4.11 Heat map representing differential expression of flavor related genes**

Heat map representing differential expression of various contigs coding for genes involved in aroma biosynthesis (TPS: terpene synthase, EH: epoxide hydrolase, LOX: lipoxygenase, O-MTS: O-methyltransferase and EO: enone oxidoreductase) through various stages.

### 4.3.5 Glycosidases and cell wall degrading enzymes from Alphonso mango

Glycosidases are involved in variety of functions such as hydrolysis of complex carbohydrates (storage and structural) to mono-saccharides, removal of sugars from various glycans including glycosidically bound aroma volatiles which serve as storage pool for the aroma compounds. In the present study many glycosidases were detected acting on various sugars i.e. glucose, galactose, mannose, fructose, xylose, fucose and rhamnose. Among these, class glucosidase with the highest number of contigs (51 contigs) was observed to be containing 28 and 21 contigs coding for glucan  $\beta$ -glucosidase and general  $\beta$ -glucosidase, respectively. Two contigs coding for  $\alpha$ -glucosidases were identified of which one coded for glucan  $\alpha$ -glucosidase and the other for general  $\alpha$ -glucosidase. Among these, at 30 DAP stage contig\_7442 and contig\_7857 were found to be down regulated (>3-fold) compared to those in flower. Contig\_16888 was down regulated whereas contig\_17138 was upregulated at 10 DAH than those in 5 DAH. At 15 DAH contig\_9072 was down regulated (1.5-fold) compared to that in 10 DAH. Among the galactosidase class, 9 contigs encoding  $\alpha$ -galactosidase and 21 contigs encoding  $\beta$ -galactosidase were detected. Two of these were down regulated (contig\_1095 and contig\_1096) in 30 DAP compared to those in flower. Contig\_3844 was down regulated in 90 DAP pulp compared to 60 DAP. Transition from 90 DAP to 5 DAH reflected in to up regulation of contig\_3844 (2.72-fold) whereas, contig\_1525 coding for  $\alpha$ -galactosidase was found to be down regulated in 10 DAH compared to that in 5 DAH. In the mannosidase class, 5  $\alpha$ -mannosidase and 8 endo- $\beta$ -mannosidase coding contigs were identified out of which two encoding for endo-beta-mannosidase (contig\_15554 and contig\_15558) were down regulated in 10 DAH compared to 5 DAH, rest didn't show differential regulation. Among 2  $\alpha$ -xylosidase and 5  $\beta$ -xylosidase from Alphonso mango only contig\_1633 showed differential regulation which was up regulated in 60 DAP compared to 30 DAP and was further down regulated in both the 90 DAP tissues. Two transcripts coding for the acid beta-fructofuranosidase (contig\_12501 and contig\_12502) were detected but did not show any differential regulation in various tissues analysed. Also, 7 contigs coding for the alpha-l-fucosidase were identified from Alphonso mango but did not show differential regulation.

Degradation of plant cell wall components, namely cellulose, hemi-cellulose and pectin by cellulases and glucanases in ripening fruits is responsible for the fruit softness. Cellulases encoding five contigs were identified amid which one coded for acidic cellulase and found to be abundant during flower and early fruit developing stages. Total 18 contigs encoding glucanase were detected of which contig\_4148 was up regulated in flower compared to 30 DAP, where as 4 transcripts (contig\_9268, contig\_19283, contig\_9267 and contig\_17145) were down regulated (>2-fold) in 10 DAH compared to 5 DAH. Pectin is another component of fruit cell wall and is degraded by a set of enzymes *viz.* pectate lyase (PL), pectin esterase (PE), polygalacturonase (PG) and rhamnogalacturonate lyase. In the present study 17 PL, 25 PG and 10 PE coding transcripts were detected. However, only few were differentially expressed, for example, only PL contig\_7696 was down regulated in 30 DAP fruit compared to flower and PL contig\_9578 was up regulated in 10 DAH fruit than 5 DAH. PG non-catalytic subunit jp650 coding contig\_9895 was down regulated in 5 DAH pulp than in 90 DAP pulp, whereas PG contig\_3471 was down regulated and PG contig\_1614 up regulated in 10 DAH compared to 5 DAH stage. Also, PE contig\_7997 was down regulated and contig\_9162 was up regulated in 30 DAP stage compared to flower. Similarly, 8 transcripts encoding rhamnogalacturonate lyase were detected of which two (contig\_7745 and contig\_7746) were distinct to the ripening stages (Annexure 1\_Supplementary file 3).

#### **4.3.6 Transcriptome analysis identified novel enzyme inhibitors from Alphonso mango**

We identified various classes of enzyme inhibitors (Appendix 4 and Figure 4.12) such as  $\alpha$ - amylase inhibitor (2 contigs), inhibitor of proliferation pds5, apoptosis inhibitor (2 contigs), bax inhibitor (4 contigs), lipid transfer protein inhibitor (6 contigs), various kinase inhibitors (16 contigs), cysteine proteinases inhibitor (4 contigs), inter-alpha-trypsin inhibitor (3 contigs), serine protease inhibitor, kunitz family trypsin and protease inhibitor, guanosine nucleotide diphosphate dissociation inhibitor , nf-kappa-b inhibitor (2 contigs), pectinesterase inhibitor (12 contigs), polygalacturonase inhibitor, proteasome inhibitor, protein transport inhibitor (4 contigs), protein phosphatase inhibitor and rho gdp-dissociation protein inhibitor (4 contigs).

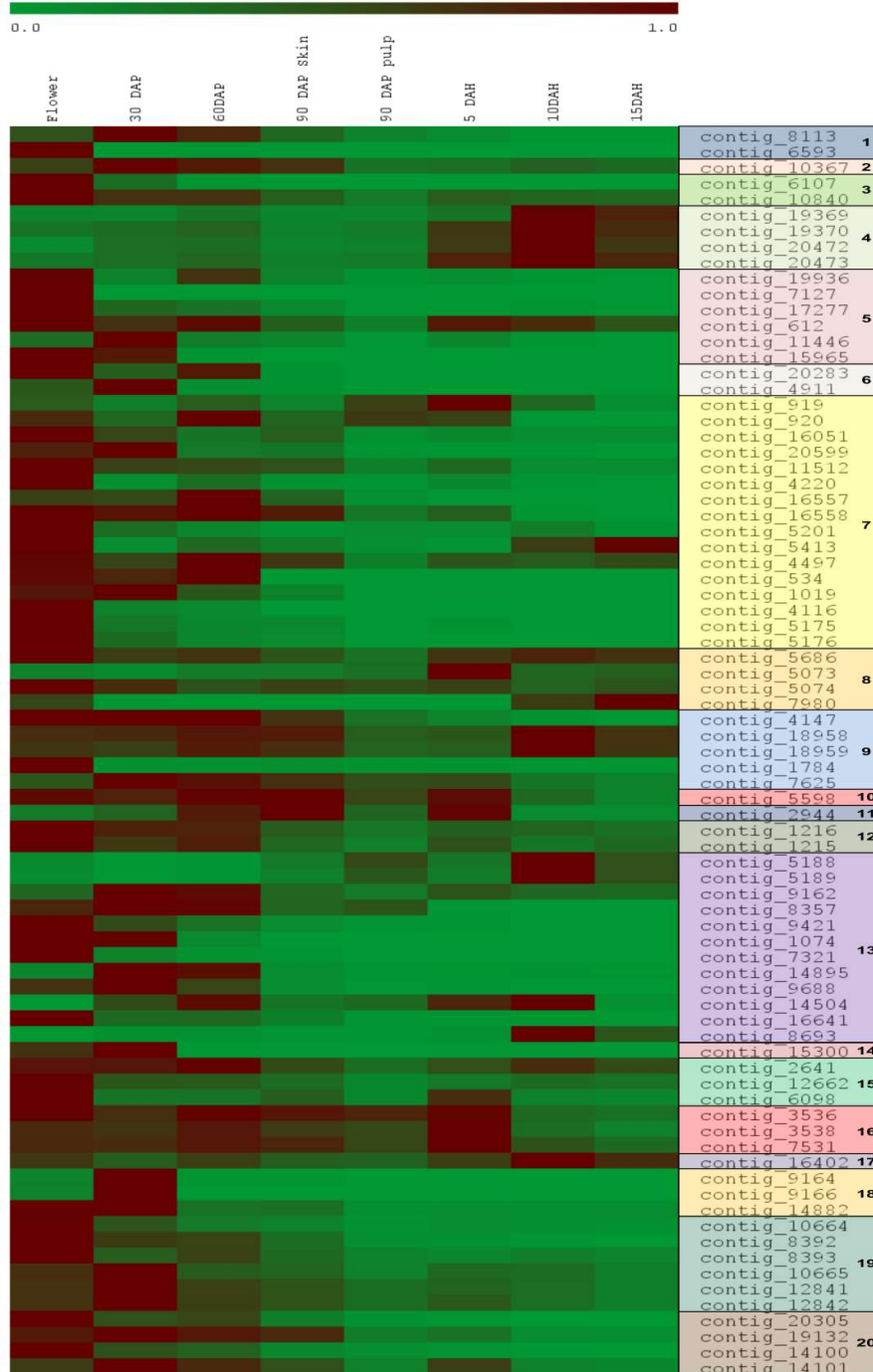


**Figure 4.12 Heat map representing differential expression of various inhibitors**

Various contigs coding for 20 different groups of inhibitors. Description for group 1-20 as follows, 1: alpha-amylase inhibitor, 2: androgen induced inhibitor of proliferation pds5, 3:apoptosis inhibitor, 4:bax inhibitor, 5:bifunctional inhibitor of lipid-transfer protein seed storage, 6:cell wall and vascular inhibitor of beta-fructosidase, 7:kinase inhibitor, 8:cysteine proteinase inhibitor , 9:trypsin inhibitor, 10:guanosine nucleotide diphosphate dissociation inhibitor, 11:macrophage migration inhibitory factor, 12:nf-kappa-b inhibitor, 13:pectinesterase inhibitor, 14:polygalacturonase inhibiting protein, 15:phosphoprotein phosphatase inhibitors, 16:plasminogen activator inhibitor 1 rna-binding, 17:proteasome inhibitor, 18:protein reversion to ethylene sensitivity, 19:protein transport inhibitor and 20:rho gdp-dissociation inhibitor.

Along with these, contigs coding for protein reversion-to-ethylene sensitivity (3 contigs), cell wall and vascular inhibitor of beta-fructosidase (2 contigs) and macrophage migration inhibitory factor were also identified from Alphonso transcriptome. These inhibitors showed their differential regulation during fruit development and ripening (Figure 4.12). Most of the inhibitors were found to be expressing throughout all the stages except for the group 4 (coding for bax inhibitor), which were abundant only during fruit ripening stages of Alphonso mango and probably played important role in ripening physiology of Alphonso mango.

### **4.3.7 Transcriptome validation through qPCR**

Transcriptomic data was validated by qPCR analysis of 38 genes selected from various metabolic pathways such as carbohydrate metabolism (cellulose synthase, chitinase and pectate lyase), fatty acid metabolism (omega 3 fatty acyl desaturase, omega 6 fatty acyl desaturase, glyceraldehyde-3-phosphate acyl transferase, alcohol dehydrogenase and long chain fatty acyl CoA ligase), terpene metabolism (mono-terpene synthases, sesqui-terpene synthases and di-terpene synthases) and proteins such as ethylene responsive factors and disease resistance proteins. Various transcript variants of these genes were selected wherever available to confirm the accuracy of assembly. qPCR analysis revealed similar differential expression pattern of these transcripts through all the eight stages. Transcript variants confirmed the accurate assembly and showed differential expression of these variants from each other through various tissues analysed (Figure 4.13 and Figure 4.14).

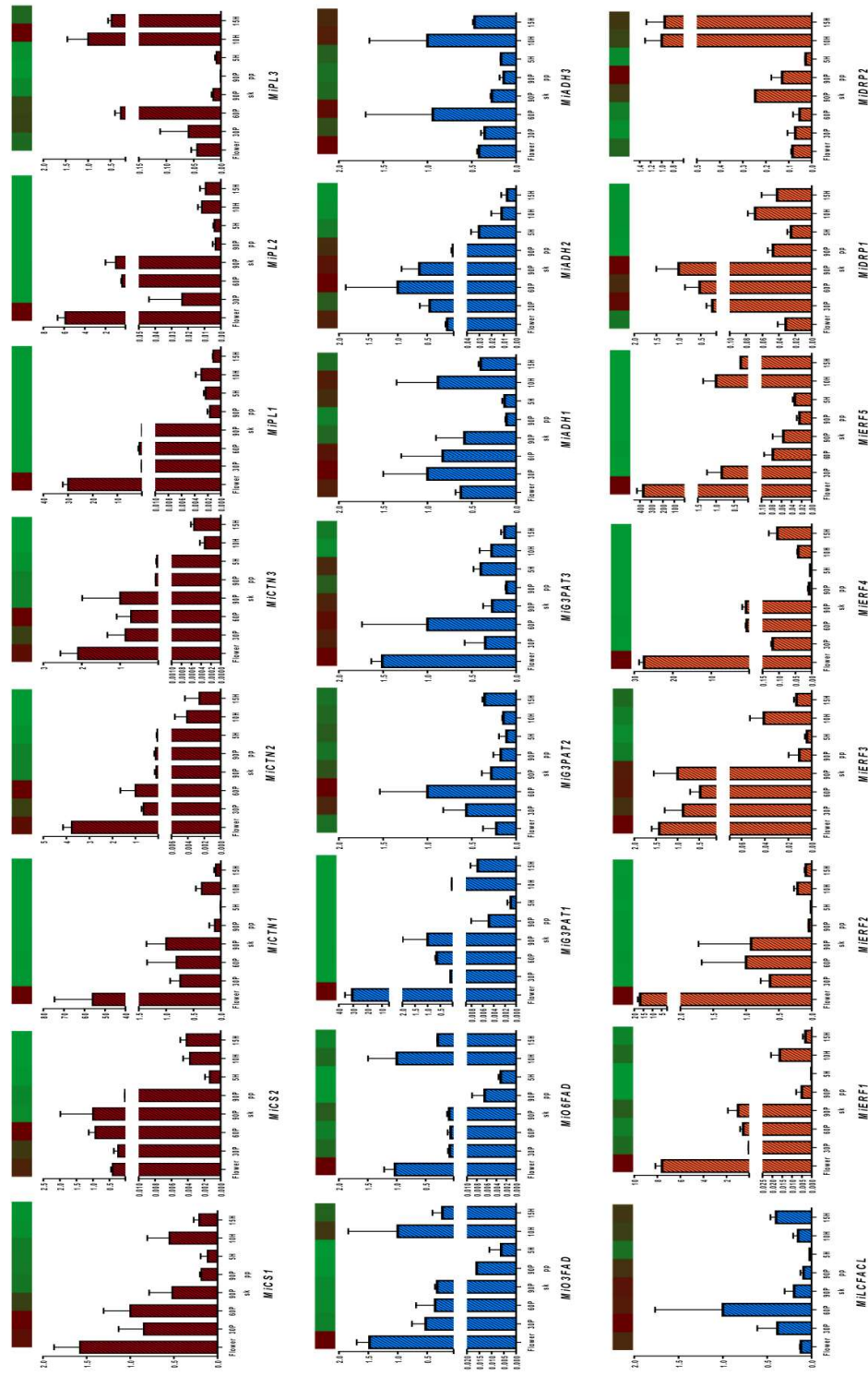


**Figure 4.13 Real time validation data of various transcripts**

qPCR analysis of various genes (obtained through RNAseq data) from carbohydrate (red) and lipid (blue) metabolism as well as ethylene responsive factors and disease resistance proteins (orange) through various tissues. Vertical bars at each data point represent standard error in the relative quantification among the biological replicates. X-axis represents fruit development and ripening stages and Y-axis represents relative transcript abundance. Heat map above each histogram represents RNAseq data for the same transcript.



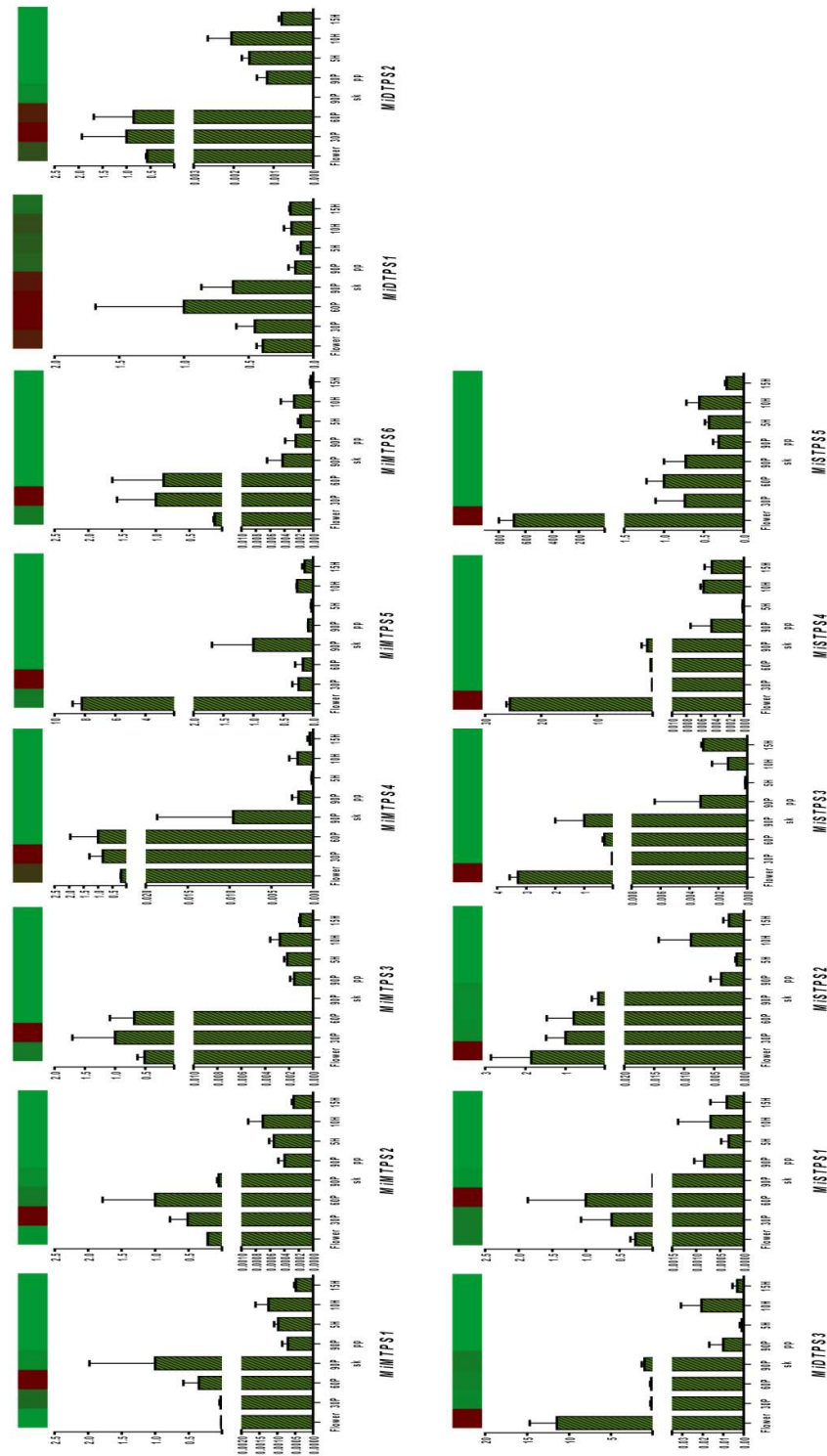


**Figure 4.14** Real time validation of various transcripts from terpene metabolism qPCR analysis for genes from terpene metabolism (green) through various tissues. Vertical bars at each data point represent standard error in the relative quantification among the biological replicates. X-axis represents fruit development and ripening stages and Y-axis represents relative transcript abundance. Heat map above each histogram represents RNAseq data for the same transcript.

## 4.4 Discussion

Recently transcriptome studies on mango cultivars namely, Zill (Wu et al., 2014b), Langra (Azim et al., 2014), Kent (Dautt-Castro et al., 2015) and Dashehari (Srivastava et al., 2016) have put forth important information regarding fruit and leaf physiology. These studies have identified genes encoding multiple enzymes involved in various pathways of primary and secondary metabolism such as, citrate cycle, glycolysis and gluconeogenesis from carbohydrate metabolism; fatty acid biosynthesis, beta oxidation and salicylic acid biosynthesis from fatty acid metabolism; biosynthesis and degradation of various amino acids as well as ethylene biosynthesis from methionine. Genes involved in the flavonoid biosynthesis, vitamin biosynthesis ( $\beta$ -carotene and  $\alpha$ -tocopherols) as well as terpenoid backbone synthesis (mevalonate pathway) have also been well explored. In the present study genes involved in all these pathways were identified and their differential expression was also evident through various stages of the Alphonso mango fruit development and ripening (Annexure 1\_Supplementary file 2). In addition present study revealed some novel findings highlighting better understanding of various processes involved in mango fruit development and ripening and some unique to most favoured Alphonso mango fruit, which are discussed below.

### 4.4.1 Novel flavor related genes from Alphonso mango transcriptome

Quantitative abundance of terpenes in mangos is well known (Pandit et al., 2009a; Pandit et al., 2009b), transcriptome and gene expression studies in mango have explored the terpene biosynthesis pathway till GPP, FPP and GGPP synthesis (Azim et al., 2014; Dautt-Castro et al., 2015; Kulkarni et al., 2013b; Srivastava et al., 2016; Wu et al., 2014b). Here 6, 5 and 3 genes encoding mono-terpene synthases (MTPS), sesqui- terpene synthases (STPS) and di-terpene synthases (DTPS), respectively involved in biosynthesis of specific terpene molecules have been identified (Figure 1.10 from Chapter 1). These genes were abundant in the flower tissue followed by 30 DAP. Further, the transcript abundance of many of these terpene synthase genes in the present study has been depicted to be idiosyncratic to the developing stages leading to their least expression in the ripening stages of Alphonso fruit (Figure 4.14 and Annexure 1\_Supplementary file 3). Previous aroma volatile analysis from Alphonso

mango supports this observation wherein flower had the highest concentration of mono- terpenes, oxygenated mono- terpenes and sesqui- terpenes which decreased through the fruit development (Pandit et al., 2009b).

Another flavor related pathway is lipoxygenase (LOX) followed by HPL pathway (Baysal and Demirdöven, 2007; Huang and Schwab, 2011, 2012), which produces C6 GLVs and lactones through peroxygenase pathway (Chapter 3). Transcriptome analyzed from Kent and Dashehari mangos reported presence of 6 and 5 genes coding for the LOX family, respectively (Dautt-Castro et al., 2015; Srivastava et al., 2016). Here detailed annotation of Alphonso mango *LOX* genes has been reported, wherein 2 code for the *9-LOX* and 6 for the *13-LOX*. *Peroxygenase* and *epoxide hydrolase (EH)* genes have been well studied for biosynthesis of cutin biopolymer (Blee and Schuber, 1993) and defence related compounds (Masui et al., 1989; Ohta et al., 1990), while results from Chapter 3 have shown involvement of these genes in the production of lactones . In spite of their biological significance none of the previous transcriptome studies in mango identified presence of peroxygenase and epoxide hydrolase genes. On the contrary in the current study various contigs coding for novel EH (3 contigs), EH2 (4 contigs) and peroxygenase (3 contigs) were detected. Similarly, multiple transcripts encoding *enone oxidoreductase* and *O-methyltransferase*, having role in furanone biosynthesis (Chidley et al., 2016b; Kulkarni et al., 2013a) were also identified and expression profiles of many of them were shown to be ripening specific (Figure 4.11). Abundance and ripening related expression of large number of these unique flavor related genes in Alphonso mango (Figure 4.11) signifies their role in synthesis of diverse aroma volatiles and their unique blend giving sweet and fruity flavor in Alphonso as shown by our previous studies (Kulkarni et al., 2012; Pandit et al., 2009b).

#### **4.4.2 Possible role of various enzyme inhibitors in slow ripening and longer shelf life of Alphonso mango fruit**

Fruit ripening is a complex physiological process and can be characterized by means of fruit softening due to changes in the cell wall structure (Atkinson et al., 2012; Gross and Sams, 1984; Lunn et al., 2013), increased sugar content by polysaccharide hydrolysis (Chidley et al., 2016a) and changes in the aroma volatiles (Pandit et al.,

2009b). Starch and pectin are the major storage and structural polysaccharides in the mango fruit, respectively. Various hydrolases and lyases are known to carry out polysaccharide and cell wall hydrolysis (Ali et al., 2004; Atkinson et al., 2012; Chourasia et al., 2006b; Fischer and Bennett, 1991; Lizada, 1993; Peroni et al., 2008) while amylases degrade the starch in to soluble sugars during ripening. We identified 4  $\alpha$ -amylase, 3 isoamylase and 1, 3  $\beta$ -amylase coding transcripts. Only one transcript coding for  $\alpha$ -amylase (contig\_1439) was down regulated through flower to 30 DAP fruit transition while others were expressed throughout the fruit developing and ripening stages. On the other hand, transcriptome analysis of Kent mango revealed identification of 4  $\beta$ -amylase and 3  $\alpha$ -amylase transcripts out of which only 2  $\beta$ -amylase coding transcripts were found to be up regulated in ripe tissue, none of the other showed differential expression (Dautt-Castro et al., 2015).

Secondly, in the present study large number of PL, PG and PE encoding transcripts known to be responsible for degradation of complex heteropolysaccharide, pectin (Ali et al., 2004) were detected (Appendix 5). Most of these were steady in their expression and only few were differentially expressed in Alphonso mango. These results are in contrast to the observations from the Kent (Dautt-Castro et al., 2015) and Dashehari (Srivastava et al., 2016) mango transcriptomic data in terms of number of unigenes detected and their differential regulation. In case of Dashehari mango 4 PL and none of the PE or PG were up regulated, whereas in Kent mango 4 PL, 6 PE and 6 PG coding unigenes were reported to be up regulated. These results signify controlled steady activity of pectin degradation leading to slow and balanced transitions in Alphonso fruit ripening physiology and may be one of the reasons for its longer shelf life.

Third interesting observation was, 79 contigs coding for 20 different inhibitor classes were also identified from Alphonso mango (Figure 4.12). Surprisingly, only 3 unigenes coding for the cysteine proteinase inhibitor were reported from Langra leaf transcriptome, while no presence of such inhibitors from Zill (Wu et al., 2014b), Kent (Dautt-Castro et al., 2015) and Dashehari (Srivastava et al., 2016) mango transcriptomes was reported. Overall Alphonso mango transcriptome was observed to be rich in these inhibitors throughout the fruit development and ripening.

Thus, presence of large number of amylase, PL, PE and PG transcripts with very few of them differentially regulated, perpetual expression of most of the starch and cell wall hydrolyzing transcripts along with the persistent presence of inhibitors for amylase, pectinesterase (Figure 4.15), polygalacturonase and ethylene sensitivity can be cumulatively suggested to play a crucial role in controlled and slow ripening and longer fruit shelf life of Alphonso mango.

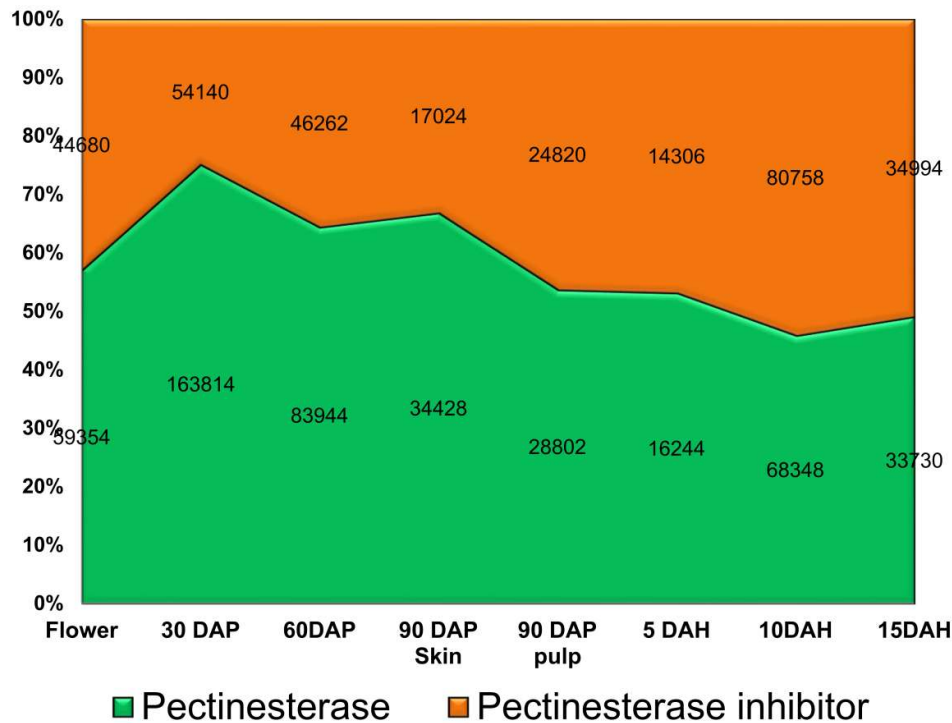


**Figure 4.15 Balance between pectinesterase enzyme and its inhibitor**

Summary of transcripts coding for pectinesterase and pectinesterase inhibitor at various stages. Numbers at each stage in green and orange zone represent sum of total transcripts coded by various contigs of pectinesterase and pectinesterase inhibitor, respectively.

Additionally oxidative burst, oxidoreductase activities and oxidative stress related gene ontologies were observed during the ripening. These factors are responsible for the generation of reactive oxygen species and lead to cell death and fruit damage. Such reactive oxygen species induced cell death is suppressed by Bax inhibitor and was well studied in *Arabidopsis thaliana* (Kawai-Yamada et al., 2004). Four contigs coding for Bax inhibitor in Alphonso mango showed ripening specific expression probably responsible for preventing cell death in ripening fruits and thus longer shelf life. Further detailed study on these inhibitors might help to understand

jelly formation in Dashehari mangos due to excessive ripening and spongy tissue formation due to uneven ripening in Alphonso mangos (Shivashankar et al., 2007; Srivastav et al., 2015).

#### **4.4.3 Defence mechanism in Alphonso from flower to fruit**

Ripened fruits are prone to be attacked by various pathogens (Coates and Johnson, 1997). A well distinct defence mechanism was observed in Alphonso mango wherein various defence related proteins (227 contigs) and chitinases (19 contigs) acting on fungal cell wall (Daulagala, 2014) were differentially regulated (Annexure 1\_Supplementary file 2). Chitinases were found to be accumulated in the flower and in the early fruit developing stages. Insect driven pollination has the risk of fungal infection to flower and further spore accumulation around ovary causing internal infection to the fruit. This might be restricted by the presence of various chitinases in Alphonso mango. Similarly various disease resistance proteins might play role during fruit development and ripening process to defend infections.

#### **4.5 Conclusion**

Transcriptome of Alphonso mango analysed through eight stages of flower to fruit development and ripening transitions revealed various differentially regulated and stage specific genes. Unique transcript profiles probably responsible for distinct and favourable characteristics of Alphonso mango fruit such as flavor, color, ripening duration, skin to stone ripening pattern and longer shelf life were identified and analysed. This study provides large data sets for further functional validation of fruit ripening process.

## Summary and Future Directions

Alphonso mango the only fruit which shows the highest diversity in its lactone content was analyzed along with low lactone containing and lactoneless cultivars Pairi and Kent, respectively at metabolite and molecular level. Further transcriptome of Alphonso mango was analyzed across eight different stages to identify novel transcripts and pathways involved in the Alphonso mango ripening and flavor biogenesis. Results obtained from the present thesis work and their future directions are summarized below.

### Fatty acid profiles of three mango cultivars

Fatty acid profiling was performed to identify probable precursors for lactone biosynthesis. A total of 17 different fatty acids were identified and quantified from pulp and skin tissues at various stages of mango fruit development and ripening from three cultivars *viz.* Alphonso, Pairi and Kent with high, low and no lactone content at ripe stage, respectively. Present analysis revealed increase in the unsaturated fatty acid content in pulp and skin during fruit ripening, making fruits more nutritious with addition of considerable levels of  $\alpha$ -linolenic acid in all the cultivars and ratio of  $\omega 6/\omega 3 \leq 1$  at ripe stage suggesting ripened mango fruits as perfect source of essential fatty acids. Study also emphasizes fatty acid rich nature of mango skin, which remains unused from mango food processing industries and can be utilized for nutritional enrichment of other food products. In the present data, a decrease in C16:0/C16:1 ratio and increase in the fatty acid derived flavor compounds, lactones, were evinced from Alphonso pulp and skin and Pairi pulp. Similarly, palmitoleic acid, 11-octadecenoic acid and 9, 15- octadecadienoic acid showed strong correlation with total lactone content from the ripe pulp and skin tissues of three cultivars, whereas various unsaturated fatty acids showed strong correlation with content of all the eight lactones individually.

### Lactone biosynthesis in mango

Quantitative real-time analysis of *9-lipoxygenase (Mi9LOX)*, *epoxide hydrolase 2 (MiEH2)*, *peroxygenase (MiPGX1)*, *hydroperoxide lyase (MiHPL)* and *acyl-CoA-oxidase (MiACO)* genes during various developmental and ripening stages in fruit of

Alphonso, Pairi and Kent cultivars with high, low and no lactone content and explains their variable lactone content. Study also covers isolation, recombinant protein characterization and transient over-expression of *Mi9LOX* and *MiEH2* genes in mango fruits. Recombinant *Mi9LOX* utilized linoleic and linolenic acids, while *MiEH2* utilized aromatic and fatty acid epoxides as their respective substrates depicting their role in fatty acid metabolism. Significant increase in concentration of  $\delta$ -valerolactone and  $\delta$ -decalactone upon *Mi9LOX* over-expression and that of  $\delta$ -valerolactone,  $\gamma$ -hexalactone and  $\delta$ -hexalactone upon *MiEH2* over-expression further suggested probable involvement of these genes in lactone biosynthesis in mango.

### **Transcriptome analysis of Alphonso mango**

Transcriptome of Alphonso mango was analysed through Illumina sequencing from eight stages of fruit development and ripening including flowers. Total transcriptome data generated from all the eight stages ranged from 65.45 – 143 Mb. About 20,755 unique transcripts were identified from Alphonso mango and 92.22% of them were annotated. 4,611 unique transcripts were assigned Enzyme Commission number which code for 142 biological pathways. Differential regulation ( $p$ -value  $\leq 0.05$ ) of thousands of unique transcripts was observed through various stages of Alphonso fruit development and ripening. Novel transcripts coding for genes involved in monoterpene, sesquiterpene and diterpene biosynthesis were identified along with various flavor related genes involved in ripening specific furanone and lactone biosynthesis. Further, differential expression of various genes in 90 DAP skin and pulp reveals polarity of Alphonso ripening from skin towards fruit stone. Cell wall modifying enzymes were encoded by large number of transcripts. Only few of them were found to be differentially regulated and most of these remained steady through all the stages. Simultaneously, their activities were regulated by various inhibitors encoded by the set of transcripts throughout Alphonso fruit development and ripening. The present study reveals the secret of slow ripening and longer shelf life of Alphonso mango with identification of 79 novel transcripts coding for various inhibitors for the enzymes involved in the fruit softening and other metabolic activities.



---

## Future Directions

The results from present thesis work revealed many novel features of mango ripening and flavor biogenesis such as  $\omega$ -3 fatty acid rich nature of ripening mangoes especially mango skin, possible precursor fatty acids and key genes involved in lactone biogenesis and various novel transcripts related to flavor biogenesis, transcriptional factors and various inhibitor playing their role in unique aroma and long shelf life of Alphonso mango. Thus, present work with these useful insights may provide foundation for future research work and its industrial application, which is discussed below.

- **$\omega$ -3 fatty acid rich food products**

Nutritionally important  $\omega$ -3 fatty acid ( $\alpha$ -linolenic acid) rich nature of mango skin, which remains unused from food processing industries suggests its utilization by various industries to produce nutritionally enriched food products.

- **Metabolite labeling studies**

Fatty acids showing strong correlation with various lactones should be further analyzed with isotope labeling and their infiltration in mango fruits to identify exact precursor and intermediates for each lactone in its biosynthesis.

- ***In planta* studies**

Various genes involved in proposed lactone biosynthesis pathway from mango can be studied in model plants such as *Arabidopsis* or *Nicotiana* for further functional characterization.

- **Addressing spongy tissue formation in Alphonso mango**

Alphonso is a well known famous mango cultivar but its export is sometimes affected due to physiological disorders such as spongy tissue formation. Various ripening related enzymes, transcription factors and inhibitors were

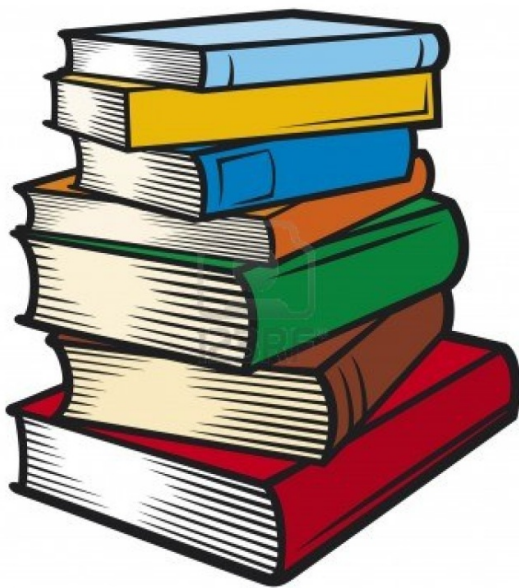
identified from Alphonso mango transcriptome. Further analysis of these transcripts will be helpful to address this physiological disorder.

- **Functional studies on novel inhibitors**

Functional studies on various novel inhibitors will help to understand slow ripening and longer shelf life of Alphonso mango. These inhibitors can also be used as future markers in various mango breeding programs for the selection of slowly ripening new mango variety with longer shelf life.



# Bibliography





---

## Bibliography

- Aharoni, A., O'Connell, A. P., 2002. Gene expression analysis of strawberry achene and receptacle maturation using DNA microarrays. *Journal of Experimental Botany* 53, 2073-2087.
- Ajila, C. M., Bhat, S. G., Prasada Rao, U. J. S., 2007. Valuable components of raw and ripe peels from two Indian mango varieties. *Food Chemistry* 102, 1006-1011.
- Ali, Z. M., Chin, L.-H., Lazan, H., 2004. A comparative study on wall degrading enzymes, pectin modifications and softening during ripening of selected tropical fruits. *Plant Science* 167, 317-327.
- Almora, K., Pino, J. A., Hernandez, M., Duarte, C., González, J., Roncal, E., 2004. Evaluation of volatiles from ripening papaya (*Carica papaya* L., var. Maradol roja). *Food Chemistry* 86, 127-130.
- Andrade, E. H. A., Maia, J. G. S., Zoghbi, M. G. B., 2000. Aroma volatile constituents of Brazilian varieties of mango fruit. *Journal of food composition and analysis* 13, 27-33
- Ashoush, I. S., Gadallah, M. G. E., 2011. Utilization of mango peels and seed kernels powders as sources of phytochemicals in biscuit. *World Journal of Dairy & Food Science* 6, 35-42.
- Atkinson, R. G., Sutherland, P. W., Johnston, S. L., Gunaseelan, K., Hallett, I. C., Mitra, D., Brummell, D. A., Schröder, R., Johnston, J. W., Schaffer, R. J., 2012. Down-regulation of polygalacturonase1 alters firmness, tensile strength and water loss in apple (*Malus x domestica*) fruit. *BMC plant biology* 12, 129-142.
- Aubert, C., Günata, Z., Ambid, C., Baumes, R., 2003. Changes in physicochemical characteristics and volatile constituents of yellow and white fleshed nectarines during maturation and artificial ripening. *Journal of Agricultural and Food Chemistry* 51, 3083-3091.
- Azim, M. K., Khan, I. A., Zhang, Y., 2014. Characterization of mango (*Mangifera indica* L.) transcriptome and chloroplast genome. *Plant molecular biology* 85, 193-208.

- Babot, E. D., del Rio, J. C., Kalum, L., Martinez, A. T., Gutierrez, A., 2013. Oxyfunctionalization of aliphatic compounds by a recombinant peroxygenase from *Coprinosia cinerea*. *Biotechnology and Bioengineering* 110, 2323-2332.
- Bandyopadhyay, C., Gholap, A. S., 1973a. Changes in fatty-acids in ripening mango pulp (variety Alphonso). *Journal of Agricultural and Food Chemistry* 21, 496-497.
- Bandyopadhyay, C., Gholap, A. S., 1973b. Relationship of aroma and flavor characteristics of mango (*Mangifera indica* L.) to fatty-acid composition. *Journal of the Science of Food and Agriculture* 24, 1497-1503.
- Bandyopadhyay, C., Gholap, A. S., 1973c. Relationship of aroma and flavour characteristics of mango (*Mangifera indica* L.) to fatty acid composition. *Journal of the Science of Food and Agriculture* 24, 1497-1503.
- Bapat, V. A., Trivedi, P. K., Ghosh, A., Sane, V. A., Ganapathi, T. R., Nath, P., 2010. Ripening of fleshy fruit: molecular insight and the role of ethylene. *Biotechnology advances* 28, 94-107.
- Bartley, J. P., Schwede, A., 1987. Volatile flavor components in the headspace of the Australian or "Bowen" mango. *Journal of Food Science* 52, 353-355.
- Bashir, H. A., Abu-Goukh, A.-B. A., 2003. Compositional changes during guava fruit ripening. *Food Chemistry* 80, 557-563.
- Baysal, T., Demirdöven, A., 2007. Lipoxygenase in fruits and vegetables: A review. *Enzyme and Microbial Technology* 40, 491-496.
- Bell, E. A., Boehnke, P., Harrison, T. M., Mao, W. L., 2015. Potentially biogenic carbon preserved in a 4.1 billion-year-old zircon. *Proceedings of the National Academy of Sciences* 112, 14518-14521.
- Bellevik, S., Summerer, S., Meijer, J., 2002a. Overexpression of *Arabidopsis thaliana* soluble epoxide hydrolase 1 in *Pichia pastoris* and characterisation of the recombinant enzyme. *Protein Expression and Purification* 26, 65-70.
- Bellevik, S., Zhang, J. M., Meijer, J., 2002b. *Brassica napus* soluble epoxide hydrolase (BNSEH1) - Cloning and characterization of the recombinant enzyme expressed in *Pichia pastoris*. *European Journal of Biochemistry* 269, 5295-5302.

- Berardini, N., Knodler, M., Schieber, A., Carle, R., 2005. Utilization of mango peels as a source of pectin and polyphenolics. *Innovative Food Science & Emerging Technologies* 6, 442-452.
- Berger, R. G., 2007. *Flavours and fragrances: chemistry, bioprocessing and sustainability*. Springer Science & Business Media, Germany.
- Berger, R. G., Drawert, F., Kollmannsberger, H., Nitz, S., Schraufstetter, B., 1985. Novel volatiles in pineapple fruit and their sensory properties. *Journal of Agricultural and Food Chemistry* 33, 232-235.
- Berger, R. G., Drawert, F., Nitz, S., 1983. Sesquiterpene hydrocarbons in pineapple fruit. *Journal of Agricultural and Food Chemistry* 31, 1237-1239.
- Bernal, J. D., 1951. *The physical basis of life*. Routledge and Paul, London.
- Berry, R., Shaw, P., Tatum, J., Wilson III, C., 1983. Citrus oil flavor and composition studies. *Food Technology* 37, 88.
- Biale, J. B., Young, R. E., Olmstead, A. J., 1954. Fruit respiration and ethylene production. *Plant physiology* 29, 168-174.
- Blee, E., Schuber, F., 1993. Biosynthesis of cutin monomers: involvement of a lipoxygenase/ peroxygenase pathway. *The Plant Journal* 4, 113-123.
- Bouvier, F., Rahier, A., Camara, B., 2005. Biogenesis, molecular regulation and function of plant isoprenoids. *Progress in Lipid Research* 44, 357-429.
- Bouzayen, M., Latché, A., Nath, P., Pech, J.-C., 2010. Mechanism of fruit ripening. *Plant developmental biology-Biotechnological perspectives*. Springer, 319-339.
- Brady, C. J., 1987. Fruit Ripening. *Annual Review of Plant Physiology* 38, 155-178.
- Brückner, B., Wyllie, S. G., 2008. *Fruit and vegetable flavour: recent advances and future prospects*. CRS Press, Boca Raton/New York.
- Brummell, D. A., Harpster, M. H., 2001. Cell wall metabolism in fruit softening and quality and its manipulation in transgenic plants. *Plant molecular biology* 47, 311-339.
- Burke, C. C., Wildung, M. R., Croteau, R., 1999. Geranyl diphosphate synthase: Cloning, expression, and characterization of this prenyltransferase as a heterodimer. *Proceedings of the National Academy of Sciences* 96, 13062-13067.

- Bushdid, C., Magnasco, M. O., Vosshall, L. B., Keller, A., 2014. Humans can discriminate more than 1 trillion olfactory stimuli. *Science* 343, 1370-1372.
- Cardillo, R., Fronza, G., Fuganti, C., Grasselli, P., Nepoti, V., Barbeni, M., Guarda, P. A., 1989. On the mode of conversion of racemic, c14-c19, gamma-hydroxy alkene fatty-acids into c7-c11, optically-active gamma-lactones and delta-lactones in *Cladosporium suaveolens*. *Journal of Organic Chemistry* 54, 4979-4980.
- Castrillo, M., Kruger, N. J., Whatley, F. R., 1992. Sucrose metabolism in mango fruit during ripening. *Plant Science* 84, 45-51.
- Chidley, H. G., Deshpande, A. B., Oak, P. S., Pujari, K. H., Giri, A. P., Gupta, V. S., 2016a. Effect of postharvest ethylene treatment on sugar content, glycosidase activity and its gene expression in mango fruit. *Journal of the Science of Food and Agriculture* 97, 1624-1633.
- Chidley, H. G., Kulkarni, R. S., Pujari, K. H., Giri, A. P., Gupta, V. S., 2013. Spatial and temporal changes in the volatile profile of Alphonso mango upon exogenous ethylene treatment. *Food Chemistry* 136, 585-594.
- Chidley, H. G., Oak, P. S., Deshpande, A. B., Pujari, K. H., Giri, A. P., Gupta, V. S., 2016b. Molecular Cloning and Characterization of *O*-Methyltransferase from Mango Fruit (*Mangifera indica* cv. Alphonso). *Molecular Biotechnology* 58, 340-350.
- Chourasia, A., Sane, V. A., Nath, P., 2006a. Differential expression of pectate lyase during ethylene-induced postharvest softening of mango (*Mangifera indica* var. Dashehari). *Physiologia Plantarum* 128, 546-555.
- Chourasia, A., Sane, V. A., Nath, P., 2006b. Differential expression of pectate lyase during ethylene-induced postharvest softening of mango (*Mangifera indica* var. Dashehari). *Physiologia Plantarum* 128, 546-555.
- Chyau, C.-C., Ko, P.-T., Chang, C.-H., Mau, J.-L., 2003. Free and glycosidically bound aroma compounds in lychee (*Litchi chinensis* Sonn.). *Food Chemistry* 80, 387-392.
- Coates, L., Johnson, G., 1997. Postharvest diseases of fruit and vegetables. *Plant pathogens and plant diseases*, 533-548.



- Conesa, A., Götz, S., García-Gómez, J. M., Terol, J., Talón, M., Robles, M., 2005. Blast2GO: a universal tool for annotation, visualization and analysis in functional genomics research. *Bioinformatics* 21, 3674-3676.
- Consortium, T. G., 2012. The tomato genome sequence provides insights into fleshy fruit evolution. *Nature* 485, 635-641.
- Cruz-Hernandez, A., Gómez-Lim, M. A., Litz, R., 1996. Transformation of mango somatic embryos. V International Mango Symposium 455, 292-298.
- Dar, S. M., Oak, P., Chidley, H., Deshpande, A., Giri, A., Gupta, V., 2016. Chapter 19 - Nutrient and Flavor Content of Mango (*Mangifera indica* L.) Cultivars: An Appurtenance to the List of Staple Foods. In: Preedy, M. S. J., Simmonds, V. R. (Eds.), *Nutritional Composition of Fruit Cultivars*. Academic Press, San Diego, 445-467.
- Daulagala, P., 2014. Expression of chitinase with antifungal activities in ripening Banana fruit. *Tropical plant research* 1, 72-79.
- Dautt-Castro, M., Ochoa-Leyva, A., Contreras-Vergara, C. A., Pacheco-Sanchez, M. A., Casas-Flores, S., Sanchez-Flores, A., Kuhn, D. N., Islas-Osuna, M. A., 2015. Mango (*Mangifera indica* L.) cv. Kent fruit mesocarp de novo transcriptome assembly identifies gene families important for ripening. *Frontiers in plant science* 6, 1-12.
- de Magalhães Andrade, J., Toledo, T. T., Nogueira, S. B., Cordenunsi, B. R., Lajolo, F. M., do Nascimento, J. R. O., 2012. 2D-DIGE analysis of mango (*Mangifera indica* L.) fruit reveals major proteomic changes associated with ripening. *Journal of proteomics* 75, 3331-3341.
- Dixon, J., Hewett, E. W., 2000. Factors affecting apple aroma/flavour volatile concentration: a review. *New Zealand Journal of Crop and Horticultural Science* 28, 155-173.
- Dudareva, N., Pichersky, E., Gershenzon, J., 2004. Biochemistry of plant volatiles. *Plant physiology* 135, 1893-1902.
- Egea, I., Barsan, C., Bian, W., Purgatto, E., Latché, A., Chervin, C., Bouzayen, M., Pech, J.-C., 2010. Chromoplast differentiation: current status and perspectives. *Plant and Cell Physiology* 51, 1601-1611.

- Endrizzi, A., Pagot, Y., LeClainche, A., Nicaud, J. M., Belin, J. M., 1996. Production of lactones and peroxisomal beta-oxidation in yeasts. *Critical Reviews in Biotechnology* 16, 301-329.
- Engel, K. H., Tressl, R., 1983. Studies on the volatile components of two mango varieties. *Journal of Agricultural and Food Chemistry* 31, 796-801.
- Fasoli, E., Righetti, P. G., 2013. The peel and pulp of mango fruit: A proteomic samba. *Biochimica et Biophysica Acta (BBA)-Proteins and Proteomics* 1834, 2539-2545.
- Feussner, I., Wasternack, C., 2002. The lipoxygenase pathway. *Annual review of plant biology* 53, 275-297.
- Fischer, R. L., Bennett, A. B., 1991. Role of cell wall hydrolases in fruit ripening. *Annual review of plant biology* 42, 675-703.
- Flath, R., Forrey, R., Teranishi, R., 1969. High resolution vapor analysis for fruit variety and fruit product comparisons. *Journal of Food Science* 34, 382-386.
- Flath, R. A., Forrey, R. R., 1970. Volatile components of smooth cayenne pineapple. *Journal of Agricultural and Food Chemistry* 18, 306-309.
- Flath, R. A., Light, D. M., Jang, E. B., Mon, T. R., John, J. O., 1990. Headspace examination of volatile emissions from ripening papaya (*Carica papaya* L., Solo Variety). *Journal of Agricultural and Food Chemistry* 38, 1060-1063.
- Forney, C. F., Kalt, W., Jordan, M. A., 2000. The composition of strawberry aroma is influenced by cultivar, maturity, and storage. *HortScience* 35, 1022-1026.
- Fraser, P. D., Truesdale, M. R., Bird, C. R., Schuch, W., Bramley, P. M., 1994. Carotenoid biosynthesis during tomato fruit development (evidence for tissue-specific gene expression). *Plant physiology* 105, 405-413.
- Fuchs, C., Schwab, W., 2013. Epoxidation, hydroxylation and aromatization is catalyzed by a peroxygenase from *Solanum lycopersicum*. *Journal of Molecular Catalysis B-Enzymatic* 96, 52-60.
- Gholap, A. S., Bandyopadhyay, C., 1975. Contribution of lipid to aroma of ripening mango (*Mangifera indica* L.). *Journal of the American Oil Chemists Society* 52, 514-516.
- Gholap, A. S., Bandyopadhyay, C., 1977. Characterization of green aroma of raw mango (*Mangifera indica* L.). *Journal of the Science of Food and Agriculture* 28, 885-888.

- Gholap, A. S., Bandyopadhyay, C., Nadkarni, G. B., 1986. Aroma development in mango fruit. *Journal of Food Biochemistry* 10, 217-229.
- Gil, A. M., Duarte, I. F., Delgadillo, I., Colquhoun, I. J., Casuscelli, F., Humpfer, E., Spraul, M., 2000. Study of the compositional changes of mango during ripening by use of nuclear magnetic resonance spectroscopy. *Journal of Agricultural and Food Chemistry* 48, 1524-1536.
- Gilbert, J. M., Young, H., Ball, R. D., Murray, S. H., 1996. Volatile flavor compounds affecting consumer acceptability of kiwifruit. *Journal of Sensory Studies* 11, 247-259.
- Goff, S. A., Klee, H. J., 2006. Plant volatile compounds: sensory cues for health and nutritional value? *Science*;311(5762):815-9. 311, 815-819.
- Golding, J. B., Shearer, D., McGlasson, W. B., Wyllie, S. G., 1999. Relationships between respiration, ethylene, and aroma production in ripening banana. *Journal of Agricultural and Food Chemistry* 47, 1646-1651.
- González-Aguilar, G., Zavaleta-Gatica, R., Tiznado-Hernández, M., 2007. Improving postharvest quality of mango 'Haden' by UV-C treatment. *Postharvest Biology and Technology* 45, 108-116.
- Haffner, T., Nordsieck, A., Tressl, R., 1996. Biosynthesis of delta-Jasmin lactone(=(Z)-Dec-7-eno-5-lactone) and (Z,Z)-Dodeca-6,9-dieno-4-lactone in the yeast *Sporobolomyces odorus*. *Helvetica Chimica Acta* 79, 2088-2099.
- Haffner, T., Tressl, R., 1998. Stereospecific metabolism of isomeric epoxyoctadecanoic acids in the lactone-producing yeast *Sporidiobolus salmonicolor*. *Lipids* 33, 47-58.
- Hakala, M. A., Lapveteläinen, A. T., Kallio, H. P., 2002. Volatile compounds of selected strawberry varieties analyzed by purge-and-trap headspace GC-MS. *Journal of Agricultural and Food Chemistry* 50, 1133-1142.
- Heidlas, J., Lehr, M., Idstein, H., Schreier, P., 1984. Free and bound terpene compounds in papaya (*Carica papaya*, L.) fruit pulp. *Journal of Agricultural and Food Chemistry* 32, 1020-1021.
- Ho, C.-T., Zheng, X., Li, S., 2015. Tea aroma formation. *Food Science and Human Wellness* 4, 9-27.

- Hofman, P. J., Smith, L. G., Joyce, D. C., Johnson, G. I., Meiburg, G. F., 1997. Bagging of mango (*Mangifera indica* cv.Keitt') fruit influences fruit quality and mineral composition. *Postharvest Biology and Technology* 12, 83-91.
- Horvat, R. J., Chapman, G. W., Senter, S. D., Norton, J. D., Okie, W. R., Robertson, J. A., 1992. Comparison of the volatile compounds from several commercial plum cultivars. *Journal of the Science of Food and Agriculture* 60, 21-23.
- Huang, F.-C., Schwab, W., 2011. Cloning and characterization of a 9-lipoxygenase gene induced by pathogen attack from *Nicotiana benthamiana* for biotechnological application. *BMC Biotechnology* 11, 1-15.
- Huang, F.-C., Schwab, W., 2012. Overexpression of hydroperoxide lyase, peroxygenase and epoxide hydrolase in tobacco for the biotechnological production of flavours and polymer precursors. *Plant Biotechnology Journal* 10, 1099-1109.
- Huang, F.-C., Schwab, W., 2013. Molecular characterization of NbEH1 and NbEH2, two epoxide hydrolases from *Nicotiana benthamiana*. *Phytochemistry* 90, 6-15.
- Hunter, G. L. K., Bucek, W. A., Radford, T., 1974. Volatile components of canned Alphonso mango. *Journal of Food Science* 39, 900-903.
- Idstein, H., Schreier, P., 1985. Volatile constituents of alphonso mango (*Mangifera indica*). *Phytochemistry* 24, 2313-2316.
- Imsabai, W., Ketsa, S., van Doorn, W. G., 2006. Physiological and biochemical changes during banana ripening and finger drop. *Postharvest Biology and Technology* 39, 211-216.
- Jiang, Y., Joyce, D., 2000. Effects of 1-methylcyclopropene alone and in combination with polyethylene bags on the postharvest life of mango fruit. *Annals of Applied Biology* 137, 321-327.
- Jiang, Y., Song, J., Hui, Y., 2010. Fruits and fruit flavor: classification and biological characterization. In: Hui, Y. H. (Ed.), *Handbook of fruit and vegetable flavors*, vol. 1. John Wiley & Sons, Inc., 4-23.
- Johnson, J., Clydesdale, F., 1982. Perceived sweetness and redness in colored sucrose solutions. *Journal of Food Science* 47, 747-752.

- Kapila, J., DeRycke, R., VanMontagu, M., Angenon, G., 1997. An Agrobacterium-mediated transient gene expression system for intact leaves. *Plant Science* 122, 101-108.
- Kawai-Yamada, M., Ohori, Y., Uchimiya, H., 2004. Dissection of Arabidopsis Bax inhibitor-1 suppressing Bax-, hydrogen peroxide-, and salicylic acid-induced cell death. *The Plant Cell* 16, 21-32.
- Kleiman, R., Paynewahl, K. L., 1984. Fatty-acid composition of seed oils of the meliaceae, including one genus rich in *cis*-vaccenic acid. *Journal of the American Oil Chemists Society* 61, 1836-1838.
- Klein, D., Fink, B., Arold, B., Eisenreich, W., Schwab, W., 2007. Functional characterization of enone oxidoreductases from strawberry and tomato fruit. *Journal of Agricultural and Food Chemistry* 55, 6705-6711.
- Kulkarni, R., Chidley, H., Deshpande, A., Schmidt, A., Pujari, K., Giri, A., Gershenzon, J., Gupta, V., 2013a. An oxidoreductase from 'Alphonso' mango catalyzing biosynthesis of furaneol and reduction of reactive carbonyls. *SpringerPlus* 2, 494-502.
- Kulkarni, R., Pandit, S., Chidley, H., Nagel, R., Schmidt, A., Gershenzon, J., Pujari, K., Giri, A., Gupta, V., 2013b. Characterization of three novel isoprenyl diphosphate synthases from the terpenoid rich mango fruit. *Plant physiology and biochemistry* 71, 121-131.
- Kulkarni, R. S., Chidley, H. G., Pujari, K. H., Giri, A. P., Gupta, V. S., 2012. Geographic variation in the flavour volatiles of Alphonso mango. *Food Chemistry* 130, 58-66.
- Lalel, H. J. D., Singh, Z., Tan, S. C., 2003a. Distribution of aroma volatile compounds in different parts of mango fruit. *Journal of Horticultural Science & Biotechnology* 78, 131-138.
- Lalel, H. J. D., Singh, Z., Tan, S. C., 2003b. The role of ethylene in mango fruit aroma volatiles biosynthesis. *Journal of Horticultural Science & Biotechnology* 78, 485-496.
- Langmead, B., Trapnell, C., Pop, M., Salzberg, S. L., 2009. Ultrafast and memory-efficient alignment of short DNA sequences to the human genome. *Genome biology* 10, R25.21-R25.10.

- Lebrun, M., Plotto, A., Goodner, K., Ducamp, M. N., Baldwin, E., 2008. Discrimination of mango fruit maturity by volatiles using the electronic nose and gas chromatography. *Postharvest Biology and Technology* 48, 122-131.
- Li, W., Godzik, A., 2006. Cd-hit: a fast program for clustering and comparing large sets of protein or nucleotide sequences. *Bioinformatics* 22, 1658-1659.
- Lizada, C., 1993. Mango. In: Seymour, G., Taylor, J., Tucker, G. (Eds.), *Biochemistry of fruit ripening*. Chapman and Hall, London, 255-271.
- Lopez-Gomez, R., Gomez-Lim, M., 1993. Changes in mRNA and protein synthesis during ripening in mango fruit. *Journal of plant physiology* 141, 82-87.
- Love, M. I., Huber, W., Anders, S., 2014. Moderated estimation of fold change and dispersion for RNA-seq data with DESeq2. *Genome biology* 15, 1-21.
- Macleod, A. J., Detroconis, N. G., 1982. Volatile flavor components of mango fruit. *Phytochemistry* 21, 2523-2526.
- MacLeod, A. J., Macleod, G., Snyder, C. H., 1988. Volatile aroma constituents of mango (cv Kensington). *Phytochemistry* 27, 2189-2193.
- MacLeod, A. J., Pieris, N. M., 1984. Comparison of the volatile components of some mango cultivars. *Phytochemistry* 23, 361-366.
- Macleod, A. J., Snyder, C. H., 1985. Volatile components of two cultivars of mango from Florida. *Journal of Agricultural and Food Chemistry* 33, 380-384.
- Maia, J. G. S., Andrade, E. H. A., Zoghbi, M. D. B., 2004. Aroma volatiles from two fruit varieties of jackfruit (*Artocarpus heterophyllus* Lam.). *Food Chemistry* 85, 195-197.
- Malnic, B., Godfrey, P. A., Buck, L. B., 2004. The human olfactory receptor gene family. *Proceedings of the National Academy of Sciences* 101, 2584-2589.
- Martin, M., 2011. Cutadapt removes adapter sequences from high-throughput sequencing reads. *EMBnet. journal* 17, 10-12.
- Martinelli, F., Uratsu, S. L., Albrecht, U., Reagan, R. L., Phu, M. L., Britton, M., Buffalo, V., Fass, J., Leicht, E., Zhao, W., 2012. Transcriptome profiling of citrus fruit response to huanglongbing disease. *PloS one* 7, 1-16.
- Martínez, P. G., Gómez, R. L., Gómez-Lim, M. A., 2001. Identification of an ETR1-homologue from mango fruit expressing during fruit ripening and wounding. *Journal of plant physiology* 158, 101-108.

- Masui, H., Kondo, T., Kojima, M., 1989. An antifungal compound, 9, 12, 13-trihydroxy-(E)-10-octadecenoic acid, from *Colocasia antiquorum* inoculated with *Ceratocystis fimbriata*. *Phytochemistry* 28, 2613-2615.
- Matsui, K., 2006. Green leaf volatiles: hydroperoxide lyase pathway of oxylipin metabolism. *Current Opinion in Plant Biology* 9, 274-280.
- Mattes, R. D., 2009a. Is there a fatty acid taste? *Annual Review of Nutrition* 29, 305-327.
- Mattes, R. D., 2009b. Oral detection of short-, medium-, and long-chain free fatty acids in humans. *Chemical senses* 34, 145-150.
- Mbeguie-A-Mbeguie, D., Hubert, O., Baurens, F. C., Matsumoto, T., Chillet, M., Fils-Lycaon, B., Sidibe-Bocs, S., 2009. Expression patterns of cell wall-modifying genes from banana during fruit ripening and in relationship with finger drop. *Journal of Experimental Botany* 60, 2021-2034.
- Meesapyodsuk, D., Qiu, X., 2011. A peroxygenase pathway involved in the biosynthesis of epoxy fatty acids in oat. *Plant physiology* 157, 454-463.
- Mehinagic, E., Royer, G., Symoneaux, R., Jourjon, F., Prost, C., 2006. Characterization of odor-active volatiles in apples: Influence of cultivars and maturity stage. *Journal of Agricultural and Food Chemistry* 54, 2678-2687.
- Moyle, R., Ripi, J., Fairbairn, D. J., Botella, J. R., Crowe, M., 2006. The pineapple EST sequencing and microarray project. *Proceedings of the Vth International Pineapple Symposium*. International Society Horticultural Science, Leuven 1, 47-50.
- Muys, T. G., Jonge, A. P. D., Vanderven, B., 1962. Synthesis of optically active gamma- and delta-lactones by microbiological reduction. *Nature* 194, 995-996.
- Nagasawa, M., Mori, H., Shiratake, K., Yamaki, S., 2005. Isolation of cDNAs for genes expressed after/during fertilization and fruit set of melon (*Cucumis melo* L.). *Journal of the Japanese Society for Horticultural Science* 74, 23-30.
- Narain, N., Hsieh, T. C., Johnson, C. E., 1990. Dynamic headspace concentration and gas chromatography of volatile flavor components in peach. *Journal of Food Science* 55, 1303-1307.
- Ohta, H., Shida, K., Peng, Y.-L., Furusawa, I., Shishiyama, J., Aibara, S., Morita, Y., 1990. The occurrence of lipid hydroperoxide-decomposing activities in rice

- and the relationship of such activities to the formation of antifungal substances. *Plant and Cell Physiology* 31, 1117-1122.
- Olawale, O., 2010. Evaluation of lipids extracted from mango and melon seeds. *the Pacific Journal Science and Technology* 11, 508-510.
- Ong, B. T., Nazimah, S. A. H., Osman, A., Quek, S. Y., Voon, Y. Y., Hashim, D. M., Chew, P. M., Kong, Y. W., 2006. Chemical and flavour changes in jackfruit (*Artocarpus heterophyllus* Lam.) cultivar J3 during ripening. *Postharvest Biology and Technology* 40, 279-286.
- Orzaez, D., Mirabel, S., Wieland, W. H., Granell, A., 2006. Agroinjection of tomato fruits. A tool for rapid functional analysis of transgenes directly in fruit. *Plant physiology* 140, 3-11.
- Padilla, M. N., Luisa Hernandez, M., Sanz, C., Martinez-Rivas, J. M., 2012. Molecular cloning, functional characterization and transcriptional regulation of a 9-lipoxygenase gene from olive. *Phytochemistry* 74, 58-68.
- Pandit, S. S., Chidley, H. G., Kulkarni, R. S., Pujari, K. H., Giri, A. P., Gupta, V. S., 2009a. Cultivar relationships in mango based on fruit volatile profiles. *Food Chemistry* 114, 363-372.
- Pandit, S. S., Kulkarni, R. S., Chidley, H. G., Giri, A. P., Pujari, K. H., Kollner, T. G., Degenhardt, J., Gershenzon, J., Gupta, V. S., 2009b. Changes in volatile composition during fruit development and ripening of 'Alphonso' mango. *Journal of the Science of Food and Agriculture* 89, 2071-2081.
- Pandit, S. S., Kulkarni, R. S., Giri, A. P., Koellner, T. G., Degenhardt, J., Gershenzon, J., Gupta, V. S., 2010. Expression profiling of various genes during the fruit development and ripening of mango. *Plant Physiology and Biochemistry (Paris)* 48, 426-433.
- Pandit, S. S., Mitra, S., Giri, A. P., Pujari, K. H., Patil, B. P., Jambhale, N. D., Gupta, V. S., 2007. Genetic diversity analysis of mango cultivars using inter simple sequence repeat markers. *Current Science* 93, 1135-1141.
- Patel, H. K., 2014. The electronic nose: artificial olfaction technology. In: Elias, G. (Ed.). Springer, USA, 1-245.
- Pathak, S. R., Sarada, R., 1974. Lipids of mango (*Mangifera indica*). *Current Science* 43, 716-717.



- Paull, R. E., Chen, N. J., 1983. Postharvest variation in cell wall-degrading enzymes of papaya (*Carica papaya* L.) during fruit ripening. *Plant physiology* 72, 382-385.
- Pérez, A. G., Sanz, C., Olías, R., Ríos, J. J., Olías, J. M., 1996. Evolution of strawberry alcohol acyltransferase activity during fruit development and storage. *Journal of Agricultural and Food Chemistry* 44, 3286-3290.
- Peroni, F. H. G. a., Koike, C., Louro, R. P., Purgatto, E., do Nascimento, J. o. R. O., Lajolo, F. M., Cordenunsi, B. R., 2008. Mango starch degradation. II. The binding of  $\alpha$ -amylase and  $\beta$ -amylase to the starch granule. *Journal of Agricultural and Food Chemistry* 56, 7416-7421.
- Pesis, E., Fuchs, Y., Zauberman, G., 1978. Cellulase activity and fruit softening in avocado. *Plant physiology* 61, 416-419.
- Pino, J. A., Almora, K., Marbot, R., 2003. Volatile components of papaya (*Carica papaya* L., Maradol variety) fruit. *Flavour and Fragrance Journal* 18, 492-496.
- Pino, J. A., Mesa, J., Munoz, Y., Marti, M. P., Marbot, R., 2005. Volatile components from mango (*Mangifera indica* L.) cultivars. *Journal of Agricultural and Food Chemistry* 53, 2213-2223.
- Pott, I., Breithaupt, D. E., Carle, R., 2003. Detection of unusual carotenoid esters in fresh mango (*Mangifera indica* L. cv. 'Kent'). *Phytochemistry* 64, 825-829.
- Prasanna, V., Prabha, T., Tharanathan, R., 2007. Fruit ripening phenomena—an overview. *Critical reviews in food science and nutrition* 47, 1-19.
- Quijano, C. E., Salamanca, G., Pino, J. A., 2007. Aroma volatile constituents of Colombian varieties of mango (*Mangifera indica* L.). *Flavour and Fragrance Journal* 22, 401-406.
- Raab, T., López-Ráez, J. A., Klein, D., Caballero, J. L., Moyano, E., Schwab, W., Muñoz-Blanco, J., 2006. FaQR, required for the biosynthesis of the strawberry flavor compound 4-hydroxy-2, 5-dimethyl-3 (2H)-furanone, encodes an enone oxidoreductase. *The Plant Cell* 18, 1023-1037.
- Ravishankar, K., Anand, L., Dinesh, M., 2000. Assessment of genetic relatedness among mango cultivars of India using RAPD markers. *The Journal of Horticultural Science and Biotechnology* 75, 198-201.
- Reaven, P., Parthasarathy, S., Grasse, B. J., Miller, E., Almazan, F., Mattson, F. H., Khoo, J. C., Steinberg, D., Witztum, J. L., 1991. Feasibility of using an oleate-

- rich diet to reduce the susceptibility of low-density-lipoprotein to oxidative modification in humans. *American Journal of Clinical Nutrition* 54, 701-706.
- Renuse, S., Harsha, H., Kumar, P., Acharya, P. K., Sharma, J., Goel, R., Kumar, G. S. S., Raju, R., Prasad, T. K., Slotta, T., 2012. Proteomic analysis of an unsequenced plant—*Mangifera indica*. *Journal of proteomics* 75, 5793-5796.
- Romanus, K., Van Neer, W., Marinova, E., Verbeke, K., Luypaerts, A., Accardo, S., Hermans, I., Jacobs, P., De Vos, D., Waelkens, M., 2008. Brassicaceae seed oil identified as illuminant in Nilotic shells from a first millennium AD Coptic church in Bawit, Egypt. *Analytical and Bioanalytical Chemistry* 390, 783-793.
- Sachdeva, S., Sachdev, T., Sachdeva, R., 2013. Increasing fruit and vegetable consumption: Challenges and opportunities. *Indian Journal of Community Medicine* 38, 192-197.
- Saiprasad, G. V. S., Anand, L., Ravishankar, K. V., Mythili, J. B., Nagesh, M., Joshi, R., 2004. Isolation and characterization of mRNAs differentially expressed during ripening of mango fruits. *Indian Journal of Biotechnology* 3, 533-537.
- Sallaud, C., Rontein, D., Onillon, S., Jabès, F., Duffé, P., Giacalone, C., Thoraval, S., Escoffier, C., Herbette, G., Leonhardt, N., 2009. A novel pathway for sesquiterpene biosynthesis from Z, Z-farnesyl pyrophosphate in the wild tomato *Solanum habrochaites*. *The Plant Cell* 21, 301-317.
- Sánchez-Palomo, E., Diaz-Maroto, M. C., Perez-Coello, M. S., 2005. Rapid determination of volatile compounds in grapes by HS-SPME coupled with GC-MS. *Talanta* 66, 1152-1157.
- Sane, V. A., Chourasia, A., Nath, P., 2005. Softening in mango (*Mangifera indica* cv. Dashehari) is correlated with the expression of an early ethylene responsive, ripening related expansin gene, *MiExpA1*. *Postharvest Biology and Technology* 38, 223-230.
- Santino, A., Iannacone, R., Hughes, R., Casey, R., Mita, G., 2005. Cloning and characterisation of an almond 9-lipoxygenase expressed early during seed development. *Plant Science* 168, 699-706.
- Sanz, C., Pérez, A. G., Richardson, D. G., 1994. Simultaneous HPLC determination of 2, 5-dimethyl-4-hydroxy-3 (2H)-furanone and related flavor compounds in strawberries. *Journal of Food Science* 59, 139-141.

- Schottler, M., Boland, W., 1996. Biosynthesis of dodecano-4-lactone in ripening fruits: Crucial role of an epoxide-hydrolase in enantioselective generation of aroma components of the nectarine (*Prunus persica* var *nucipersica*) and the strawberry (*Fragaria ananassa*). *Helvetica Chimica Acta* 79, 1488-1496.
- Schulz, M. H., Zerbino, D. R., Vingron, M., Birney, E., 2012. Oases: robust de novo RNA-seq assembly across the dynamic range of expression levels. *Bioinformatics* 28, 1086-1092.
- Schwab, W., Roscher, R., 1997. 4-Hydroxy-3(2H)-furanones: Natural and maillard products. *Recent Research Developments in Phytochemistry* 1, 643-673.
- Shan, W., Zhao, C., Fan, J., Cong, H., Liang, S., Yu, X., 2012. Antisense suppression of alcohol acetyltransferase gene in ripening melon fruit alters volatile composition. *Scientia Horticulturae* 139, 96-101.
- Shibahara, A., Yamamoto, K., Nakayama, T., Kajimoto, G., 1987. *Cis*-vaccenic acid in pulp lipids of commonly available fruits. *Journal of the American Oil Chemists Society* 64, 397-401.
- Shibahara, A., Yamamoto, K., Shinkai, K., Nakayama, T., Kajimoto, G., 1993. *Cis*-9,*cis*-15-octadecadienoic acid - a novel fatty-acid found in higher-plants. *Biochimica Et Biophysica Acta* 1170, 245-252.
- Shibahara, A., Yamamoto, K., Takeoka, M., Kinoshita, A., Kajimoto, G., Nakayama, T., Noda, M., 1989. Application of a GC-MS method using deuterated fatty-acids for tracing *cis*-vaccenic acid biosynthesis in kaki pulp. *Lipids* 24, 488-493.
- Shivashankar, S., Ravindra, V., Louis, H., 2007. Biochemical changes in seed and mesocarp of mango (*Mangifera indica* L.) cv. 'Alphonso' and their significance during the development of spongy tissue. *The Journal of Horticultural Science and Biotechnology* 82, 35-40.
- Shulaev, V., Sargent, D. J., Crowhurst, R. N., Mockler, T. C., Folkerts, O., Delcher, A. L., Jaiswal, P., Mockaitis, K., Liston, A., Mane, S. P., 2011. The genome of woodland strawberry (*Fragaria vesca*). *Nature genetics* 43, 109-116.
- Simopoulos, A. P., 2002. The importance of the ratio of omega-6/omega-3 essential fatty acids. *Biomedicine & Pharmacotherapy* 56, 365-379.
- Singh, R. K., Ali, S. A., Nath, P., Sane, V. A., 2011. Activation of ethylene-responsive p-hydroxyphenylpyruvate dioxygenase leads to increased

- tocopherol levels during ripening in mango. *Journal of Experimental Botany* 62, 3375-3385.
- Singh, R. K., Sane, V. A., Misra, A., Ali, S. A., Nath, P., 2010. Differential expression of the mango alcohol dehydrogenase gene family during ripening. *Phytochemistry* 71, 1485-1494.
- Slavin, J. L., Lloyd, B., 2012. Health benefits of fruits and vegetables. *Advances in Nutrition: An International Review Journal* 3, 506-516.
- Sonwai, S., Ponprachanuvut, P., 2014. Studies of fatty acid composition, physicochemical and thermal properties, and crystallization behavior of mango kernel fats from various thai varieties. *Journal of Oleo Science* 63, 661-669.
- Spolaore, S., Trainotti, L., Casadoro, G., 2001. A simple protocol for transient gene expression in ripe fleshy fruit mediated by *Agrobacterium*. *Journal of Experimental Botany* 52, 845-850.
- Srivastav, M., Singh, S., Ajang, M., 2015. Evaluation of mango genotypes for jelly seed disorder. *Indian Journal of Horticulture* 72, 408-410.
- Srivastava, S., Singh, R. K., Pathak, G., Goel, R., Asif, M. H., Sane, A. P., Sane, V. A., 2016. Comparative transcriptome analysis of unripe and mid-ripe fruit of *Mangifera indica* (var.“Dashehari”) unravels ripening associated genes. *Scientific Reports* 6, 1-13.
- Szkopińska, A., Plochocka, D., 2005. Farnesyl diphosphate synthase; regulation of product specificity. *Acta Biochimica Polonica* 52, 45-55.
- Takeoka, G. R., Buttery, R. G., Teranishi, R., Flath, R. A., Guntert, M., 1991. Identification of additional pineapple volatiles. *Journal of Agricultural and Food Chemistry*, 1848-1851.
- Tamura, H., Boonbumrung, S., Yoshizawa, T., Varanyanond, W., 2001. The volatile constituents in the peel and pulp of a green Thai mango, Khieo Sawoei cultivar. *Food Science and Technology Research* 7, 72-77.
- Tharanathan, R., Yashoda, H., Prabha, T., 2006a. Mango (*Mangifera indica* L.),“The king of fruits”—An overview. *Food Reviews International* 22, 95-123.
- Tharanathan, R. N., Yashoda, H. M., Prabha, T. N., 2006b. Mango (*Mangifera indica* L.), "The king of fruits" - an overview. *Food Reviews International* 22, 95-123.

- Tholl, D., Kish, C. M., Orlova, I., Sherman, D., Gershenzon, J., Pichersky, E., Dudareva, N., 2004. Formation of monoterpenes in *Antirrhinum majus* and *Clarkia breweri* flowers involves heterodimeric geranyl diphosphate synthases. *Plant Cell* 16, 977-992.
- Tokitomo, Y., Steinhaus, M., BÜTTNER, A., Schieberle, P., 2005. Odor-active constituents in fresh pineapple (*Ananas comosus* [L.] Merr.) by quantitative and sensory evaluation. *Bioscience, biotechnology, and biochemistry* 69, 1323-1330.
- Tsevegsuren, N., Aitzetmuller, K., Vosman, K., 2003. Isomers of hexadecenoic and hexadecadienoic acids in *Androsace septentrionalis* (Primulaceae) seed oil. *Lipids* 38, 1173-1178.
- Ulbricht, T. L. V., Southgate, D. A. T., 1991. Coronary heart-disease - 7 dietary factors. *Lancet* 338, 985-992.
- Ulrich, D., Komes, D., Olbricht, K., Hoberg, E., 2007. Diversity of aroma patterns in wild and cultivated *Fragaria* accessions. *Genetic Resources and Crop Evolution* 54, 1185-1196.
- Vecchiotti, A., Lazzari, B., Ortugno, C., Bianchi, F., Malinverni, R., Caprera, A., Mignani, I., Pozzi, C., 2009. Comparative analysis of expressed sequence tags from tissues in ripening stages of peach (*Prunus persica* L. Batsch). *Tree Genetics & Genomes* 5, 377-391.
- Veda, S., Platel, K., Srinivasan, K., 2007. Varietal differences in the bioaccessibility of  $\beta$ -carotene from mango (*Mangifera indica*) and papaya (*Carica papaya*) fruits. *Journal of Agricultural and Food Chemistry* 55, 7931-7935.
- Wang, G. D., Dixon, R. A., 2009. Heterodimeric geranyl(geranyl)diphosphate synthase from hop (*Humulus lupulus*) and the evolution of monoterpene biosynthesis. *Proceedings of the National Academy of Sciences of the United States of America* 106, 9914-9919.
- Wein, M., Lavid, N., Lunkenbein, S., Lewinsohn, E., Schwab, W., Kaldenhoff, R., 2002. Isolation, cloning and expression of a multifunctional *O-methyltransferase* capable of forming 2, 5-dimethyl-4-methoxy-3 (2H)-furanone, one of the key aroma compounds in strawberry fruits. *The Plant Journal* 31, 755-765.

- Whitaker, R., Evans, D., 1987. Plant biotechnology and the production of flavor compounds. *Food Technology*, 86-101.
- Wijekoon, C. P., Goodwin, P. H., Hsiang, T., 2008. The involvement of two epoxide hydrolase genes, NbEH1.1 and NbEH1.2, of *Nicotiana benthamiana* in the interaction with *Colletotrichum destructivum*, *Colletotrichum orbiculare* or *Pseudomonas syringae* pv. tabaci. *Functional Plant Biology* 35, 1112-1122.
- Willett, W. C., Sacks, F., Trichopoulou, A., Drescher, G., Ferroluzzi, A., Helsing, E., Trichopoulos, D., 1995. Mediterranean diet pyramid - a cultural model for healthy eating. *American Journal of Clinical Nutrition* 61, 1402-1406.
- Wilson, C. W., Shaw, P. E., Knight, R. J., 1990. Importance of some lactones and 2,5-dimethyl-4-hydroxy-3(2h)-furanone to mango (*Mangifera indica* L.) aroma. *Journal of Agricultural and Food Chemistry* 38, 1556-1559.
- Wu, G. A., Prochnik, S., Jenkins, J., Salse, J., Hellsten, U., Murat, F., Perrier, X., Ruiz, M., Scalabrin, S., Terol, J., 2014a. Sequencing of diverse mandarin, pummelo and orange genomes reveals complex history of admixture during citrus domestication. *Nature biotechnology* 32, 656-662.
- Wu, H.-X., Jia, H.-M., Ma, X.-W., Wang, S.-B., Yao, Q.-S., Xu, W.-T., Zhou, Y.-G., Gao, Z.-S., Zhan, R.-L., 2014b. Transcriptome and proteomic analysis of mango (*Mangifera indica* Linn) fruits. *Journal of proteomics* 105, 19-30.
- Xi, W.-P., Zhang, B., Liang, L., Shen, J.-Y., Wei, W.-W., Xu, C.-J., Allan, A. C., Ferguson, I. B., Chen, K.-S., 2012. Postharvest temperature influences volatile lactone production via regulation of acyl-CoA oxidases in peach fruit. *Plant Cell and Environment* 35, 534-545.
- Yamauchi, Y., Hasegawa, A., Taninaka, A., Mizutani, M., Sugimoto, Y., 2011. NADPH-dependent reductases involved in the detoxification of reactive carbonyls in plants. *Journal of biological chemistry* 286, 6999-7009.
- Yashoda, H. M., Prabha, T. N., Tharanathan, R. N., 2006. Mango ripening: changes in cell wall constituents in relation to textural softening. *Journal of the Science of Food and Agriculture* 86, 713-721.



## Appendices

**Appendix 1:** cDNA sequences of *Mi9LOX*, *MiEH2*, *MiPGX1*, *MiHPL* and *MiACO*. Characters in bold and underlined represent 5' and 3' UTRs if any.

>KX090178[organism= *Mangifera indica*] *Mangifera indica* cultivar Alphonso 9-lipoxygenase mRNA, complete cds.

ATGGGGACAGTGGTGTGATGAAGAAGAATTTTTGGACTTCAATGACCTCAGTGCATCGGTTATTGATCG  
 TGTTGATGAACTGGTTGGTAAAAGAGTCTCTTTGCAGCTCGTTAGTGCTTTTAACTCTGACCCTACTGCAT  
 CAAATGGGCTGCAAGGAAAGGTTGGAGAGCCAGCACATTTGGAAGAGTGGATTACTACAATCACTCCTTTG  
 GTAGCAGAGGAATCGACATTCAAGGTCACATTTGATTGGGATGAACAGATTGGAGTTCAGGAGCATTTCAT  
 AATAAAGAACAATCATCACAGTGGATTTTACTTCAAATCTCTCACACTTGAGGATGTTCCCTAATCAGGGTC  
 GGATTCACCTTTGTATGCAACTCCTGGGTTTATCCTGCAAACGCTATAAGAAAGATCGCGTTTTCTTCACC  
 AACAAGACATACCTTCCAGGTGAAATGCCGGCACCATTACAATATTATAGAGAGCAAGAACTCCTAAACTT  
 GAGAGGAGATGGAAGTGGAGAGCTTCAAGAATGGGACAGAGTCTATGACTATGCGTACTATAATGATTTGG  
 GTGATCCGGACAATGGCAAACACGACCAGTTCTTGGAGGGTCTACTGAGTATCCTTATCCTCGTAGGGGA  
 AGAACAGGCAGACCACCAGCAAAAACAGATCCTGAGACTGAGAGCAGGCTGCCACTTCTGACGAGCTTAAA  
 CATCTATGTCCCAAGAGATGAGCGATTTGGTACATAAAAATGTCAGATTTTCTTGGTTATGCACTGAAAT  
 CCATATCTCAATTCATTGAGCCAGCGTTGGAATCTGTATTTGACAGCACCCCAAATGAATTTGACAACCTT  
 GCTCAAATATACAACTCTACGATGAAGGGATTGAGCTTCCCTAATGACCATTTTCTTGATGATATTAGAAA  
 TAATATCCCCTTAGAATTGCTCAAGGAGATTTTTCCAACCAATGAGGATAATCTCTTTGAATTTCCAACAC  
 CACAGGTGATCCAAGGGGATAGGTCTGCATGGAGAACCGATGAAGAGTTTGCAAGAGAAATGCTGGCTGGA  
 CCGAACCTGTGCATTCGCGGAGTTGAGGAATTCCTCCAAGAAGCAAGCTCGACCCTGAACTATATGG  
 TGATCAAGATAGTAAGATAACCAAACAGCACATAGAGAGCTACTTAGATGGGCTGACTGTAGAGCAGGCAA  
 TTGAGAAGAACAAGCTATTCATATTGGATCACCATGATTCCTGATGACATACTTGAGAAGGATAAACACT  
 ACTTCCACAAAGACTTATGCATCCAGGACAATCCTTTTTCTTAAAAGAGGATGGAACCTTTGAAACCACTGGC  
 AATTGAATTGAGCAGGCCACATCCTGATGGAGATCAATATGGTGCCATCAGCAACGTTTACACGCCATCAG  
 AAGATGAAGTGAAGGTTCCATATGGCAGCTGGCTAAAGCTTATGTGGCTGTAAATGACTCTGGTGTTCAT  
 CAGCTCATCAGCCACTGGTTGAAGACTCATGCAGCAATTGAGCCATTTGTGATAGCAACAAATCGGCAACT  
 GAGTGTGCTTACCCAATTTATAAGCTTCTGCAACCTCATTTCCGTGACACAATGAATATAAATGCGTTTTG  
 CTCGTGAGATCGTCATTAATGCGGGTGAATTTCTGGAACTACGGTTTTCCCTGCAAAGTATGCCATGGAA  
 ATGTCATCTGCAATCTACAAAGACTGGACTTTTCCAGATCAGGCACTTCTGAAGACCTCAAGAATAGAGG  
 AATGGCAGTTGAGGACCCCACTCTCCACATGGTCTTTCGCTACTGATAGCAGACTACCCATATGCTGTTG  
 ATGGGCTTGAAATCTGGTTTGAATAAAAAACTGGGTCAAAGACTATTGCTACTTCTACTACAAAAGCGAT  
 GAAATGATGCAAAGGATAGTGGACTGCAATCCTGGTGAAGGAACTACGCGAGGAGGGTCATGGTGACAA  
 GAAAGATGAGCCCTGGTGGCCTAAAATGCAAATCGTGAAGAGCTGATAGAGGCATGCACCATAATCATAT



GGATAGCTTCCGCTCTCCATGCTGCTGTCAATTTTGGACAGTATCCTTATGCAGGTTTCTCCCTAACCGT  
 CCAACTATGAGTCGAAGATTCATGCCTGAAAAGGAACTCCTGATTATGATGAGCTAGAGTCGAATTTTGA  
 CAAAGTGTTTCTGAAAACGATCACTGCTCAGCGGCAGACTCTTCTTGGCATTGCTCTTATAGAGACTTTGT  
 CAAGGCATTCATCGGATGAGATGTACCTGGGACAAAGAGACACACCTGAATGGACATCAGATAAAATCCCC  
 TTGCAAGCATTTCGAGGACTTCGAAAGAAATTGGGAGACATTGAAGTAAGAATCATAACAAGAAATCATGA  
 CAATATGCTCAAGAACCGCGTTGGCCCTGTCAATGTGCCATACACTTTGCTTTATCCTACCAGTGAAGGTG  
 GCCTTACTGGCAAAGGAATTCCAAACAGTGTTCATTTAGAGCTAAATTCTTCAGATACACATTATTAT  
TGTATTATATTGGAAATAAATGTACCCACTTTGATCTTCTTATATGGTTGTGACAAACATTGAATTAGTGC  
TGTAATAAAGCCATTTGTGATTGCAAGAGTAAAAAAAAAAAAAAAAAAAAAAAAAAAAAAAAAAGT

>KX090179 [organism= *Mangifera indica*] *Mangifera indica* cultivar  
 Alphonso epoxide hydrolase-2 mRNA, complete cds.

ACGCGGGGATATAACGCTACACAATCCACAGCTTTCAACTGCTCCAACAACGAACTTCAACCCAGAATCA  
GCGATGGAAGATATACAGCACAGAATTGTGAATGTCAATGGCTTAAACATGCACGTGGCAGAGAAAGGCGA  
 AGGTCCAGTCATTCTTTCATTACCGTTTTCCCGAACTGTGGTACTCCTGGCGGCATCAGATCATCGCCT  
 TGGCTTCCCTCGGCTACCGAGCCATTGCTCCGGATCTACGTGGCTTCGGTGATACTGACGCGCCGCCGTCT  
 GTCTCGAGTTACACGTGTTTCCACGTGGTGGGGACCTCATTGGACTTCTCGACGTCGTTGCCTCTGATCG  
 GGATAAGGTTTTCTGTGGTGGCCATGATTGGGGTGTCTTATTGCTTGGTACTTGTGCTTGTTTAGACCGG  
 ATAAGGTCAAAGCTTTGGTCAACTTGAGTGTTGCGTTTAAATCCCTGGAACCCCAAGAGGAAGCCACTTGAG  
 GGTGAAAGCTGTTTATGGTGACGATTATTACATGATCAGATTTTCAAGGAGCCTGGTGAGATAGAAGCTGA  
 GTTTGGCCAGATTGGTACTGAGACAGTTGTCAAGGAATTCTTTACATACAGGACACCTGGTCCTCTTTTTTC  
 TCCCTACAGGTAAAGGATTTGGACATCCCCCAAATGCTGAAATTGTCTTACCCTCTTGGCTATCAGAGGAT  
 GATGTTAAAAACTACACCAGCAAATTTGAGAAAGGCTTTACAGGAGGAGTGAACCTATTACCGTAATATAAA  
 CGTGAACCTGGAACTTACAGCTCCTTGGGCCGGGAGTCAAATAAAGGTTCTGTAAAGTTCATCGTGGGTG  
 ACCTGGACCTGACATATTATATGCCAGGAGTCAAGGATTACATACACAAAGGTGGGTTCAGCGAGATGTG  
 CCATTATTGGAAGAAGTGATTGTAATGGAAGGTGTAGGTCACTTCATTAATGGAGAAAAGGCTGATGCAAT  
 CAGTGAGCACATATACAACTTTTTTTCAGAAGTTCTGATATGTTATTTGGTTTTTAGTAGAGTTTTCACTTC  
ATTTGGGTTGTTTTGCGGCAGTGCAACAGGAGTTGTTAAGTATTTTATTTCAAGCATTATAAATTGATTTT  
GGGTTGTTTTTTCAGAGTTCAGAGTGAATGCTAGTTGTTTGAATAAGCCATGGTGTGTAATGGTGTATGT  
TTCAAATCGTATAATAAGTATGCCATTGTTGTCAAAAAAAAAAAAAAAAAAAAAAAAAAAAAAAAAAAGT

>KX090180 [organism= *Mangifera indica*] *Mangifera indica* cultivar Alphonso peroxygenase-1 mRNA, complete cds.

ATGGACGGGGATGCAATGGCAACCGAGGCTCCTTATGCACCAGTCACTTATGAGAGAAGAGTCCCCACTGACTTGGATGACAAAATTCCCAAGCCTTATATGCCAAGAGCACTGGAAGCTCCAGATCCGAGCCATCCAAATGAAACACAAGGGCACAATAATCACAACTGAGTGTGCTTCAGCAGCATGTAGCCTTTTTTGACCAAGATGACAATGGGATCATTTACCCTTGGGAGACTTATACAGGACTAAGAGCAATTGGTTTTCAACATGATAGTTTTCTGTGATATTGGCCTTTGTCACTCAACTTGGCACTGAGTTATCCTACTCTCCCCGGGTGGATCCCATCTCCTTTCTTACCCATTTACATACACAACATACACAAAGCAAAGCATGGCAGTGACTCAGGAACATATGACACGGAAGGAAGGTACATGCCTGCAAACCTGGAATTCATATTTAGCAAATATTCTCATAACAGTGCCTGGTAAGTTAACAATAGGAGAGCTTTGGGACATGACTGAGGGAAACCGTGTAGCAATGGACTTCTTTGGCTGGATTGCAAGTAAAGGGGAATGGCTTGTTTTTATACATTTTGGCGAGGGACGAGGAAGTTTTCTATCAAAGAAGCTGTGAGACCGTGTACGATGGTAGTTTGTGTTGAGTACTGTGCAAACTGAATGCAGGCGCTGCAGCTAAGATGATTTAA

>KX090181 [organism= *Mangifera indica*] *Mangifera indica* cultivar Alphonso hydroperoxide lyase mRNA, complete cds.

ATGATGATCAAATCCATGAGCTTAAGTCCCGGCATGCCATCTTCATCTTCACCCTTGTCTTCTCCACCTCCACTCTCCACCGCCTCACCGCCCGCCACTTCCCTCCCCTTCGCACAGTACCCGGATCCTACGGCTGGCCTTTGCTTGGCCCCATCTCTGACCGCCTTGACTACTTCTGGTTCAGGGTCCGGCTACCTTCTTTAAGAAGCGTATAGAGAAGCACAAAAGCACGGTGTTCGGAACAACATGCCGCCGACGTGGCCACTTTTTCTGGGTGTTAACCCGAATGTTATTGCTGTTCTTGACTGTAAGTCATTTTCGCATCTTTTTGATATGGAGATCGTGGAGAAGAAGAATATTCTTGTGGTGATTTTCATGCCTAGTGTCAAATTTACTGGAAATTTAAGAACTTGCCTTATCTTGATACTTCTGAGCCACAACACGCTAAGATCAAGAACTTCGTCCTTGACATTCTGAAACGCAGTTCAACAGTGTGGCTTACAGCGCTCAAGTCGAACCTCGACACATTGTTTGACACCATTGAAACGAATATCTCCGAGAAGGTTCTGCAGGCTTTTTATTCCCTTTACAAAATGCTTGTTCAACTTCCTCACAACGGCCATCGTTGGAGCTGATCCCACAACCGACCCTAACATCGCCGACTCCGGCTATGCCATGCTGGACAGCTGGCTCGCCCTACAGATCCTCCCCACCGTCAAATTTGGAATCTTACAGCCTCTTGAAGAGATTTTTCTTCACTCTTTTGCTTACCCTTTGCCCCCCGTAAGTGGAGGCTACAATAAGCTTTATAACTTCGTTGAAAAACAAGGCAACGAGGTGGCGCAACGAGGTGTCACCGAGTTTGGACTCACTAAAGAAGAAGCTACCCATAATTTGTTGTTTACGCTAGGCTTTAATGCCTTTTGGTGGGTTCTCTGTGTTTTTACCTACTTTAATCGGCACCATTGCTAGTGATAAACTGGAATACAGAAGAACTTAGAAAAGAAGTTAAAGAAAAAATTGGATCTTCAAGTTTGAATTTTGAGTCGGTCAAAGATTTGGAACCTTGTTCAGTCTTTTGTGTTATGAGACTTTGAGAGTCAACCCTCCGGTCCCTCTTTCAGTACGGCAGGCAAGGAAGGATTTTCAACTGAGTTCGCATGACTCGGTGTATGATATCAAGAAAGGTGAGTTGCTTTGTGGTACCAGTCTCAGATAATGAAAGACTCGAAGGTGTTTGAAGATCCAGAGACTTTTAAAGCGGAGAGGTTTATGGGTGAAAAAGGAAGAGAGCTGCTGAATTACTTGTACTGGTCAAACGGGCCACAGACTGGATCACCCACCGGGTCAATAAACAGTGTGCAGGTAAAGATGTGGTTACTCTGACGTCGTTTTTGATCGTTGCTTACATATTTCAAAGATATGAATCGATCAGTGGGAGCTCTTCTTCAATCACAGCCGTTGAAAAGGCAAAATGA

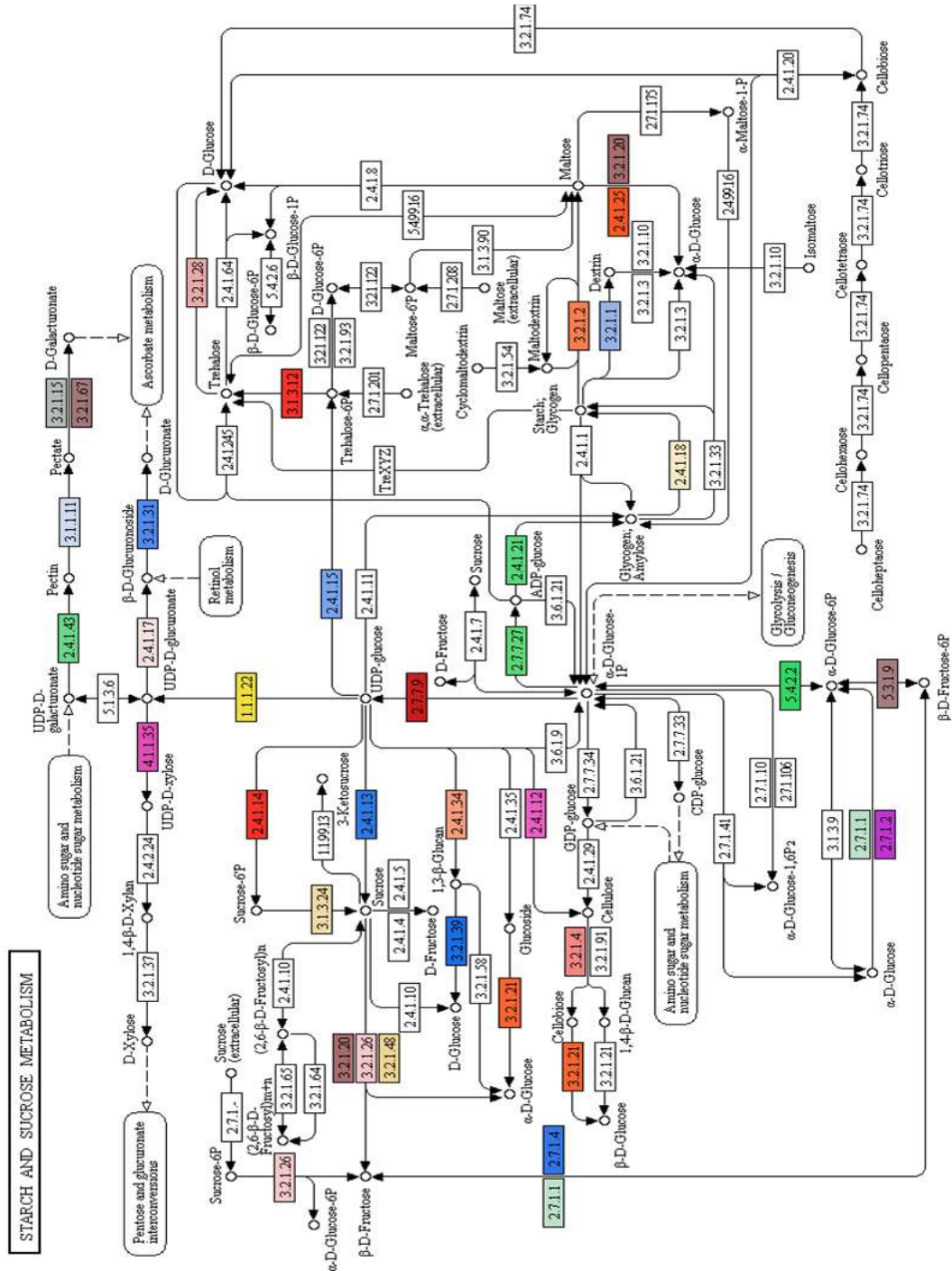
>KX090182 [organism= *Mangifera indica*] *Mangifera indica* cultivar Alphonso acyl-CoA-oxidase mRNA, complete cds.

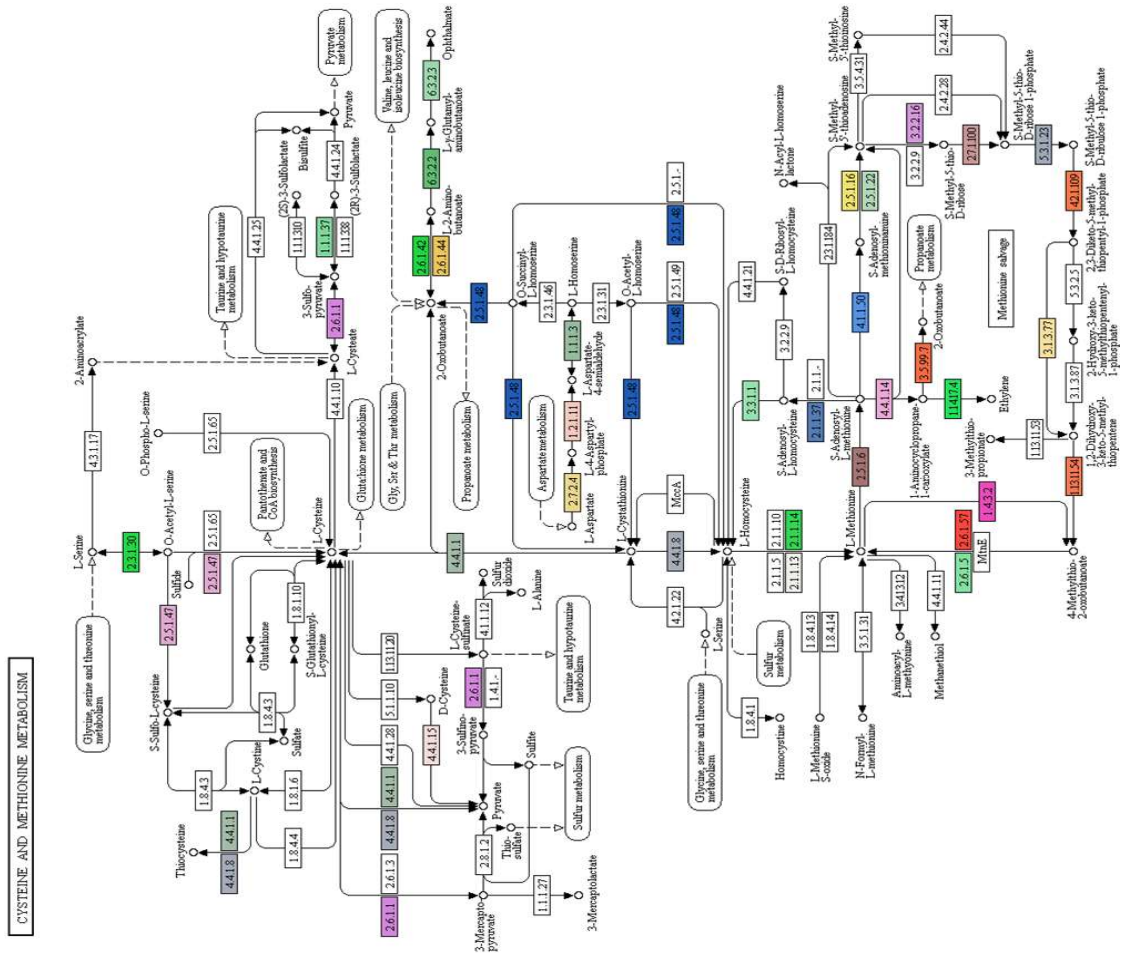
ATGGCTGGCGTTGATTATCTTGCTGACGAGAGGAACAAGGCGGAGTTCGATGTCAACGAGATGAAGATCGT  
CTGGGCCGGCTCTCGCCACGCCTTCGAACTCTCAGATCGGATTTCTCGACTCGTCGCCAGTGATCCGGCCT  
TTCGAAAGGATAACAGACCTATGCTAAGTAGGAAGGAGTTGTTTAAGAACACTCTGAGAAAGACGGCTCAT  
GCTTGGAACGGATTAATGAGCTCCGTCTAACTGAAGAAGAGGCCAATAAGCTAAGTTTTATGTTGATGA  
ACCTGCTTTTGC GGATCTTCATTGGGGAATGTTTGTGCCGGCTATAAAAAGGACAAGGGACTGATGAGCAGC  
ACCAGAAGTGGTTGCCATTGGCATATAAGATGCAAATAATCGGATGCTATGCACAACTGAGCTAGGTCAT  
GGCTCCAATGTTCAAGGGCTTGAAACCACTGCAACATTTGATCCTCAGACTGATGAGTTCATCATTACAG  
TCCTACACTGACTTCAAGCAAATGGTGGCCTGGTGGATTGGGTAAAGTTTCTACCCATGCTGTTGTTTATG  
CTCGTCTAATAACAGATGGCAAGGACCATGGAGTGCATGGTTTTATTGTTTCAGCTACGGAGCCTGGATGAT  
CACTCACCTCTTCTGGCATAATAGTTGGAGACATTGGAATGAAGTTTGGAAATGGGGCATATAAACTAT  
GGATAATGGTGTGTTTTGAGATTTGATCATGTGCGTATCCCTAGGAATCAAATGTTGATGCGGGTTTCAACA  
TTACAAGGGAAGGAAATATAACAATCAAATGTTCCCTCGGCAATTAGTTTTATGGCACTATGGTGTATGTT  
CGTCAAGTGATTGTATCTGATGCTTCTTATGCCCTATCACGAGCAGTTTGTATTGCCACAAGGTACAGTTG  
TGTTTCGTAGACAATTCGGTTCACAGAATGGTGGTGTGAGACCCAGGTGATTGATTACAAAACCTCAGCAA  
ATAGACTCTTCCCATTGCTTGCTTCTGCCTATGCTTTCAGATTTGTTAGTGAGTGGTTGAAATGGTTGTAT  
ACCGATGTGATGCAAAGATTGCAAGCTAATGATTTCTCAACATTGCCTGAGGCTCATGCATGTACCGCGGG  
TTTGAAGTCTCTGACTACTTCTGCCACAGCTGATGGGATTGAGGAATGTCGAAAATTATGTGGTGGCCATG  
GTTACTTGTGTAGCAGCGGACTTCCAGAATTTTGCAGTATATGTCCCTGCTTGTACATATGAAGGAGAC  
AACACTGTGCTACTTTTACAGGTTGCAAGGTTTCTCATGAAAACCTGTCTCTCAACTGGGGTCTGAAAGAA  
GCCTGTTGGGACAATATCTTACATGGAACAAGCGGAGCATTGATGAAATGTCGTTGTGAGGTTCAAAGAG  
CTGAGGATTGGTTAAAGCCTTCTGTAATACTGGAGGTTTTTGAAGCAAGGGCCACTAGGATGTCTGTTGCA  
TGTGCTCAAAACCTGAGCAAGTTCGCAAATCCAGAAGAGGGCTTTTTCAGAACTCTTAGCTGATTTAGTTGA  
GGCAGCAATTGCTCATTGCCAGTTAATTGTTGTTTCAAAGTTTATTGAGAAATTGCGACAAGACATACCTG  
GAAAGGGGGTGAACAAGTGTAGGAATGCTCTGCAACATTTATGCTTTGCATATTCTGCACAAAATCTG  
GGTGATTTTGTATCCACTGGCTGCATAACTTCCAAGCAAGCTTCACTTGCTAATGAGCAACTAAGGTCTTT  
GTATTCCCAGGTCCGTCTAATGCGGTTGCCCTTGTGATTCATTCAATTATACCGACCATTTTCTGGGAT  
CAGTCCTTGGCCGGTATGATGGAAACGTGTATCCAAACCTCTACGAGGAAGCTTGAAGGATCCTCTCAAT  
GATTCTGTTGTACCTGATGGCTACCATGAATACATCCGCCCATTTCTGAAACAACAGCTCCGAACAGCAAG  
ACTCTGA

**Appendix 2: Details of primers used in qPCR analysis (Chapter 4).**

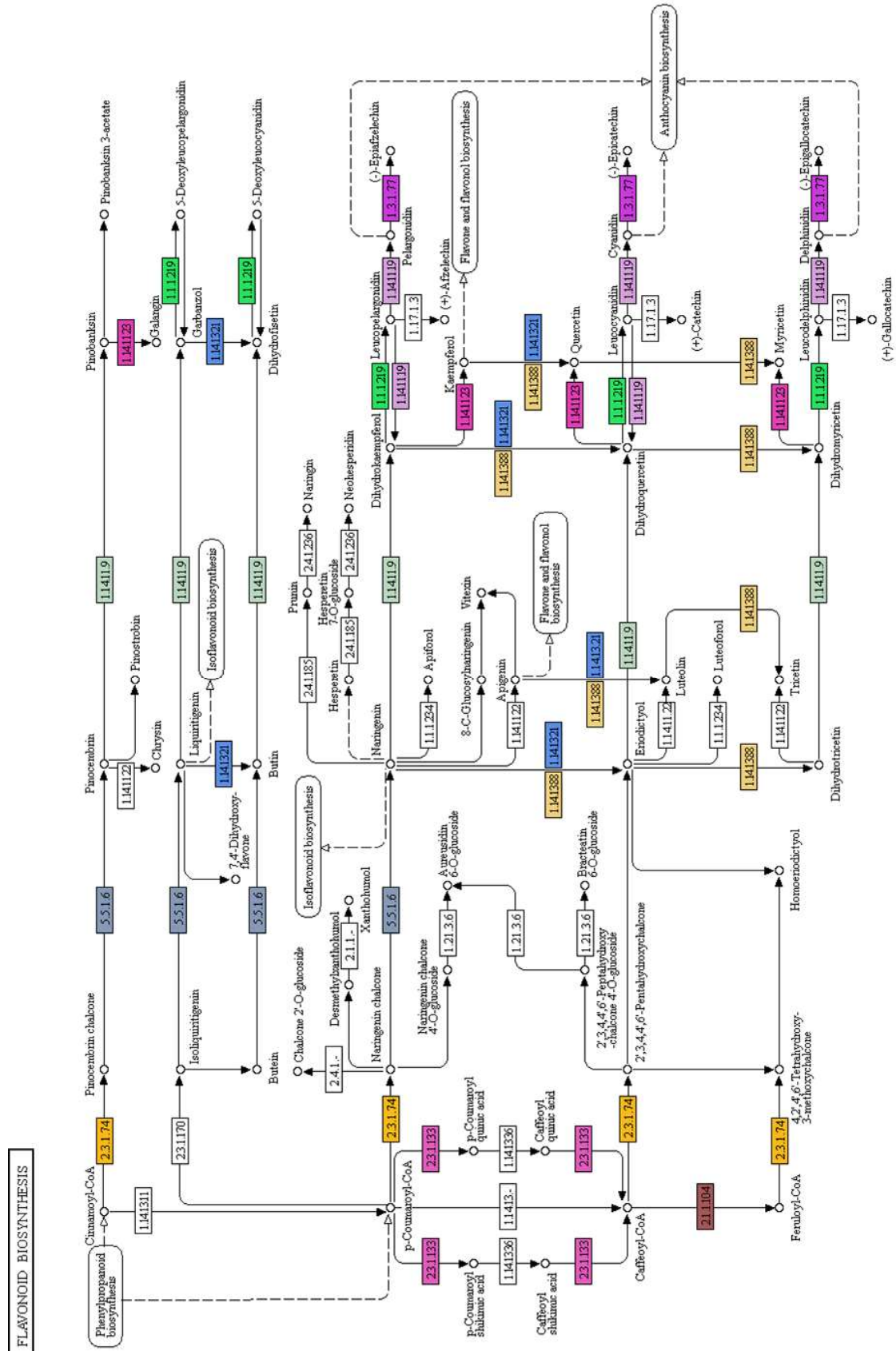
No.	Primer	Sequence	No.	Primer	Sequence
1	MiCS1_RT_F	TGCACCAAGTTCTGAGATGGGCT	39	MiERF3_RT_F	GTCGGACGCTGGAATGGGGATAG
2	MiCS1_RT_R	GGTGTAAAGCAAGCCTCTCAAGCCA	40	MiERF3_RT_R	TCCCCAAAACGGCGTATCCAAG
3	MiCS2_RT_F	AAAGGGAGTCCGAGAGTGGAGGG	41	MiERF4_RT_F	GCAAAATGGGCGAGCGGAGATACGA
4	MiCS2_RT_R	GCCACATGCACCTGCTTGTTCTT	42	MiERF4_RT_R	TTGAACCTCAGCGCCGCTTCATC
5	MiCTN1_RT_F	TGGGACTACCTGCGTCTCCTGAA	43	MiERF5_RT_F	CTGGTCAGTGTAGGATCGGCTCG
6	MiCTN1_RT_R	GCCTTGACCAGAGCATGACACCT	44	MiERF5_RT_R	CTGCCACTTTCCCATGGTCTT
7	MiCTN2_RT_F	GCAATGGCGATGACCACGAATCC	45	MiDRP1_RT_F	AGTGCCATTTTCAGTTCCTTCCA
8	MiCTN2_RT_R	AAAGCCTTTTGTGGCCACAGCC	46	MiDRP1_RT_R	CTCAACTGCATCAAGCTTCTAGCCA
9	MiCTN3_RT_F	TGTGGCTCAGCACAAGGTTTCT	47	MiDRP2_RT_F	ATTGTGGTGGCGTTCTCTAGCA
10	MiCTN3_RT_R	CTCCTTCTGGCCCTTGAGCTTCC	48	MiDRP2_RT_R	TATCCCTCTCTCGATCTTGCCCC
11	MiPL1_RT_F	AGCCATGGAAGTAACCCGGCAAG	49	MiMTPS1_RT_F	GCTTGCAACACCCTTGCTCCTTG
12	MiPL1_RT_R	CCTCCCTCGCACAGACAAACCTC	50	MiMTPS1_RT_R	GAGTGGTGGCTGAACACCAACC
13	MiPL2_RT_F	TACCATGTGAGGCGGTGGAGGTT	51	MiMTPS2_RT_F	GGCGATCGGCCAATTACCAACT
14	MiPL2_RT_R	CAGGACGGCTCATCACACCAGAA	52	MiMTPS2_RT_R	AGCGTCAGCCTCACTTCTTCTT
15	MiPL3_RT_F	CGGTCGAGGTGCCAGTGTTCATA	53	MiMTPS3_RT_F	GCGCTGATTGCTTCTGCATGGTT
16	MiPL3_RT_R	CCCTCACCATGGCATTTCCTCCT	54	MiMTPS3_RT_R	TACTGAGCCATCCTGGCCAGATTCA
17	MiO3FAD_RT_F	GCTGCGTTGCTTGCCGGTTTATC	55	MiMTPS4_RT_F	GGCATTGCAAGTGAAGCACGCAA
18	MiO3FAD_RT_R	GTCGTGACCATGGTATGCAGGT	56	MiMTPS4_RT_R	TTGGCAAGCTCGAGTAGACGGTG
19	MiO6FAD_RT_F	AGGCCTTTCTCAGCGGAATCTGG	57	MiMTPS5_RT_F	CGTGACAGCGACTACACCAACT
20	MiO6FAD_RT_R	TGAAGATGGTGCAGTGGAAACGG	58	MiMTPS5_RT_R	CTTCATCCACGTATCAGCCCGT
21	MiG3PAT1_RT_F	TGCACGCATAGGACCCTTTTGGA	59	MiMTPS6_RT_F	AAGCGTGGCAAGACACATGCAAA
22	MiG3PAT1_RT_R	GCCTTACGGTTCTAATCGGGGCT	60	MiMTPS6_RT_R	GAACCAACATGACTGCCCCCGAA
23	MiG3PAT2_RT_F	ATAAGGCATCGCCCAATGACCCC	61	MiDTPS1_RT_F	AGAGGTGGGTGACACAGTACAGG
24	MiG3PAT2_RT_R	TCGCAACACGACAGCACTCAGAA	62	MiDTPS1_RT_R	GCGGGCATCAGATAGTTCAGGGG
25	MiG3PAT3_RT_F	ACAACATGAGAAGGTTGCAGAACA	63	MiDTPS2_RT_F	TGGTTTCAAATGTCTTGCGGCGT
26	MiG3PAT3_RT_R	ACCGCCCTTCTCTCCAATTCT	64	MiDTPS2_RT_R	CCGTGCAATCTGAAGTGGGAAGC
27	MiADH1_RT_F	ATTTTGGCCATGAAGCGGGAGG	65	MiSTPS1_RT_F	GATGGCTTTACGCTCCGGCTTC
28	MiADH1_RT_R	AGTGACGACACTCCCTGCACTCT	66	MiSTPS1_RT_R	TTGCGTCATTTGCCAGTGTGACC
29	MiADH2_RT_F	ACTGACCTCCCTCTGTGGTTGA	67	MiSTPS2_RT_F	CTCCAGTGCCTCTGCTTGATCGT
30	MiADH2_RT_R	CAAACCCTGCCCTTCTCCATGA	68	MiSTPS2_RT_R	TGGGGTCTCTGAGCATTGAAGCA
31	MiADH3_RT_F	GTCTTGGTGCGGCATGGAATGTG	69	MiSTPS3_RT_F	TGAAACCCTAAAGCCACGGAAGCA
32	MiADH3_RT_R	TGCCCTCTGAGTTTAGCACCTTG	70	MiSTPS3_RT_R	CCCCTACTTTTGACGGACGACCA
33	MiLCFAFL_RT_F	AACTCGCAGTTTCTTCCCTGT	71	MiSTPS4_RT_F	AGCGACAAGGTGTACAAGGAGCA
34	MiLCFAFL_RT_R	CCGAGTTCCAAGCAAGCGCCTAT	72	MiSTPS4_RT_R	AGGCATGCTCCCATCAGTGAACC
35	MiERF1_RT_F	CCACCACCAACAGTGGCGATCAA	73	MiSTPS5_RT_F	AAGGAGTGCCTCTCTCCCAACC
36	MiERF1_RT_R	TCTTATCTCCGCCCCATTTC	74	MiSTPS5_RT_R	GAGACCTGGAAGCCGTTGGTTGT
37	MiERF2_RT_F	GAGAGCCACTCGATCAGCCACAA	75	MiSTPS6_RT_F	AGGACACAGAGGAACCGGCACAT
38	MiERF2_RT_R	TTACCCATGTGGGTTTCTCCGGC	76	MiSTPS6_RT_R	TCACCTCTCTAGCTCAGCCGT

**Appendix 3:** Important pathways, such as starch and sucrose metabolism, cysteine and methionine metabolism and ethylene biosynthesis, phenylpropanoid biosynthesis and flavonoid biosynthesis from KEGG database which are functional in Alphonso mango.











**Appendix 4:** List of transcripts encoding various inhibitors

<b>Contig</b>	<b>Annotation</b>
contig_8113	alpha-amylase inhibitor alpha subunit family protein
contig_6593	alpha-amylase subtilisin inhibitor-like
contig_10367	androgen induced inhibitor of proliferation pds5 isoform 1
contig_6107	apoptosis 1 inhibitor-like
contig_10840	apoptosis inhibitor 5-like
contig_19369	bax inhibitor 1-like
contig_19370	bax inhibitor 1-like
contig_20472	bax inhibitor 1-like
contig_20473	bax inhibitor 1-like
contig_19936	bifunctional inhibitor lipid-transfer protein seed storage 2s
contig_7127	bifunctional inhibitor lipid-transfer protein seed storage 2s
contig_17277	bifunctional inhibitor lipid-transfer protein seed storage 2s
contig_612	bifunctional inhibitor lipid-transfer protein seed storage 2s
contig_11446	bifunctional inhibitor lipid-transfer protein seed storage 2s
contig_15965	bifunctional inhibitor lipid-transfer protein seed storage 2s
contig_919	bri1 kinase inhibitor 1
contig_920	bri1 kinase inhibitor 1
contig_20283	cell wall and vascular inhibitor of beta-fructosidase
contig_4911	cell wall vacuolar inhibitor of fructosidase 2-like
contig_16051	cyclin-dependent kinase inhibitor 3-like
contig_20599	cyclin-dependent kinase inhibitor 3-like
contig_11512	cyclin-dependent kinase inhibitor 5-like
contig_4220	cyclin-dependent kinase inhibitor 7
contig_16557	cyclin-dependent kinase inhibitor 7-like isoform x2
contig_16558	cyclin-dependent kinase inhibitor 7-like isoform x2
contig_5201	cyclin-dependent protein kinase inhibitor sim-like
contig_5413	cyclin-dependent protein kinase inhibitor smr1
contig_4497	cyclin-dependent protein kinase inhibitor smr3
contig_534	cyclin-dependent protein kinase inhibitor smr3-like
contig_1019	cyclin-dependent protein kinase inhibitor smr3-like
contig_4116	cyclin-dependent protein kinase inhibitor smr3-like
contig_5175	cyclin-dependent protein kinase inhibitor smr3-like
contig_5176	cyclin-dependent protein kinase inhibitor smr3-like
contig_5686	cysteine proteinase inhibitor 12
contig_5073	cysteine proteinase inhibitor 6-like
contig_5074	cysteine proteinase inhibitor 6-like
contig_7980	cysteine proteinase inhibitor b-like
contig_5598	guanosine nucleotide diphosphate dissociation inhibitor 2
contig_4147	inter-alpha-trypsin inhibitor heavy chain-

---

<b>Contig</b>	<b>Annotation</b>
contig_18958	inter-alpha-trypsin inhibitor heavy chain h3 isoform x1
contig_18959	inter-alpha-trypsin inhibitor heavy chain h3 isoform x1
contig_1784	kunitz family trypsin and protease inhibitor protein
contig_2944	macrophage migration inhibitory factor homolog
contig_1216	nf-kappa-b inhibitor-like protein 2 isoform 1
contig_1215	nf-kappa-b inhibitor-like protein 2 isoform 2
contig_9162	pectinesterase pectinesterase inhibitor 26
contig_9688	pectinesterase pectinesterase inhibitor 51
contig_16641	pectinesterase pectinesterase inhibitor ppe8b-like
contig_2641	phosphoprotein phosphatase inhibitors
contig_12662	phosphoprotein phosphatase inhibitors
contig_8693	plant invertase pectin methylesterase inhibitor superfamily protein
contig_3536	plasminogen activator inhibitor 1 rna-binding
contig_3538	plasminogen activator inhibitor 1 rna-binding
contig_7531	plasminogen activator inhibitor 1 rna-binding
contig_15300	polygalacturonase inhibiting protein
contig_5188	probable pectinesterase pectinesterase inhibitor 12
contig_5189	probable pectinesterase pectinesterase inhibitor 12
contig_8357	probable pectinesterase pectinesterase inhibitor 34
contig_9421	probable pectinesterase pectinesterase inhibitor 34
contig_1074	probable pectinesterase pectinesterase inhibitor 40-like
contig_7321	probable pectinesterase pectinesterase inhibitor 47
contig_14895	probable pectinesterase pectinesterase inhibitor 51
contig_14504	probable pectinesterase pectinesterase inhibitor 7
contig_16402	probable proteasome inhibitor
contig_6098	protein phosphatase inhibitor 2 isoform x2
contig_9164	protein reversion-to-ethylene sensitivity1 isoform x2
contig_9166	protein reversion-to-ethylene sensitivity1 isoform x2
contig_14882	protein reversion-to-ethylene sensitivity1 isoform x2
contig_10664	protein transport inhibitor response 1
contig_8392	protein transport inhibitor response 1-like
contig_8393	protein transport inhibitor response 1-like
contig_10665	protein transport inhibitor response 1-like
contig_20305	rho gdp-dissociation inhibitor 1
contig_19132	rho gdp-dissociation inhibitor 1 family protein
contig_14100	rho gdp-dissociation inhibitor 1-like
contig_14101	rho gdp-dissociation inhibitor 1-like
contig_7625	serine protease inhibitor family protein
contig_12841	transport inhibitor response 1-like protein
contig_12842	transport inhibitor response 1-like protein

---

**Appendix 5:** Summary of contigs coding for pectate lyase (PL), pectinesterase (PE) and polygalacturonase (PG)

**Pectate lyase (PL)**

<b>Contig</b>	<b>Annotation</b>
contig_16459	pectate lyase
contig_9578	pectate lyase 22 precursor family protein
contig_9579	pectate lyase 22 precursor family protein
contig_17156	pectate lyase family protein
contig_7696	pectate lyase-like
contig_18874	pectate lyase-like
contig_488	probable pectate lyase 12
contig_773	probable pectate lyase 4
contig_17157	probable pectate lyase 4
contig_10554	probable pectate lyase 5
contig_10555	probable pectate lyase 5
contig_13983	probable pectate lyase 8
contig_13984	probable pectate lyase 8
contig_13985	probable pectate lyase 8
contig_13986	probable pectate lyase 8
contig_13987	probable pectate lyase 8
contig_13988	probable pectate lyase 8

**Pectinesterase (PE)**

<b>Contig</b>	<b>Annotation</b>
contig_11605	pectinesterase 3
contig_19630	pectinesterase 31
contig_5249	pectinesterase 63
contig_7997	pectinesterase 63
contig_11000	pectinesterase family protein
contig_8936	pectinesterase pectinesterase
contig_3139	probable pectinesterase 53
contig_8066	probable pectinesterase 67
contig_5524	probable pectinesterase 68-like
contig_11297	thermostable pectinesterase

**Polygalacturonase (PG)**

<b>Contig</b>	<b>Annotation</b>
contig_13192	polygalacturonase adpg2
contig_14447	polygalacturonase at1g48100
contig_14448	polygalacturonase at1g48100
contig_1614	polygalacturonase at1g48100-like
contig_7066	polygalacturonase at1g48100-like
contig_5206	polygalacturonase qrt3
contig_12817	polygalacturonase qrt3-like
contig_7503	polygalacturonase-like
contig_7792	polygalacturonase-like
contig_188	probable polygalacturonase
contig_3471	probable polygalacturonase
contig_5508	probable polygalacturonase
contig_5747	probable polygalacturonase
contig_6329	probable polygalacturonase
contig_7757	probable polygalacturonase
contig_7758	probable polygalacturonase
contig_7759	probable polygalacturonase
contig_10975	probable polygalacturonase
contig_18096	probable polygalacturonase
contig_20376	probable polygalacturonase
contig_4736	probable polygalacturonase at1g80170
contig_15509	probable polygalacturonase at1g80170 isoform x2
contig_7176	probable polygalacturonase at3g15720
contig_9895	probable polygalacturonase non-catalytic subunit jp650
contig_18002	probable polygalacturonase non-catalytic subunit jp650



## Curriculum Vitae

Ashish B. Deshpande

[ashishbdeshpande@gmail.com](mailto:ashishbdeshpande@gmail.com)

[https://www.researchgate.net/profile/Ashish\\_Deshpande5](https://www.researchgate.net/profile/Ashish_Deshpande5)

Mobile: +91-9028285341

CSIR - National Chemical Laboratory,  
Biochemical Sciences Division,  
Dr. Homi Bhabha Road, Pashan,  
Pune, Maharashtra-411008  
India

### Education

Degrees Obtained	Board/University	Marks obtained	Year
B.Sc. (Biotechnology, Biochemistry, Genetics)	Bangalore University	80.50%	2007
M.Sc. Biochemistry	Bangalore University	65.75%	2009
P.G. Diploma in Intellectual Property Rights Law	National Law School of India University, Bangalore	B+ Grade	2009
National Eligibility Test (NET)	CSIR-UGC	JRF+ Lectureship	June 2010
National Eligibility Test (NET)	CSIR-UGC	Lectureship	June 2011

**Ph.D. Thesis:** Mango (*Mangifera indica* L.) Flavor Biogenesis: Metabolic Profiling and Molecular Analysis (submitted to Academy of Scientific and Innovative Research, New Delhi, India., AcSIR)

## Research Experience

- Minor research project titled **“Study of esterase activity with respect to different phenotypes of pea (*Pisum Sativum* ) seed and effect of esterase on different substrates.”** sanctioned by UGC (University Grant Commission), Delhi, India. (Funding-Rs. 1,75,000/-) during lectureship (Not availed)
- Research experience at CSIR-NCL as JRF (2 years) and SRF (till date) on **“Molecular and biochemical analysis of mango flavor biogenesis”** project. Technical expertise achieved in molecular biology (Gene isolation, cloning, recombinant expression, transient expression, protein purification and enzyme kinetics), Metabolomics (Isolation of primary and secondary metabolites, GCMS and HRMS analysis of metabolites) and Transcriptomic analysis.

## Specialized Skills

- Extraction of primary and secondary metabolites
- Gas chromatography (GC-MS and GC-FID), Q-Exactive Orbitrap HRMS
- DNA and RNA isolation, cDNA synthesis and gene isolation
- Recombinant and expression cloning, recombinant expression in *E.coli*
- Transient expression by *Agrobacterium* mediated infiltration
- Purification of recombinant enzymes and enzyme assays
- Gene expression profiling- qPCR analysis
- Transcriptome analysis/ RNASeq data analysis
- Statistical analysis
- Teaching experience to graduate and post graduate students

---

## Publication Highlights

### Journal Publications

1. **Ashish B. Deshpande**, Hemangi G. Chidley, Pranjali S. Oak, Keshav H. Pujari, Ashok P. Giri, Vidya S. Gupta: *Data on changes in the fatty acid composition during fruit development and ripening of three mango cultivars (Alphonso, Pairi and Kent) varying in lactone content*. Data in Brief 09/2016; 9. DOI:10.1016/j.dib.2016.09.018
2. **Ashish B. Deshpande**, Hemangi G. Chidley, Pranjali S. Oak, Keshav H. Pujari, Ashok P. Giri, Vidya S. Gupta: *Isolation and characterization of 9-lipoxygenase and epoxide hydrolase 2 genes: Insight into lactone biosynthesis in mango fruit (Mangifera indica L.)*. Phytochemistry (In press). DOI:10.1016/j.phytochem.2017.03.002
3. Hemangi G. Chidley, **Ashish B. Deshpande**, Pranjali S. Oak, Keshav H. Pujari, Ashok P. Giri, Vidya S. Gupta: *Effect of postharvest ethylene treatment on sugar content, glycosidase activity and its gene expression in mango fruit: Effect of postharvest ethylene treatment on mango ripening*. Journal of the Science of Food and Agriculture 06/2016; DOI:10.1002/jsfa.7912
4. Hemangi G. Chidley, Pranjali S. Oak, **Ashish B. Deshpande**, Keshav H. Pujari, Ashok P. Giri, Vidya S. Gupta: *Molecular cloning and characterization of O-methyltransferase from mango fruit (Mangifera indica cv. Alphonso)*. Molecular Biotechnology 04/2016; 58(5). DOI:10.1007/s12033-016-9933-2
5. Ram Kulkarni, Hemangi Chidley, **Ashish Deshpande**, Axel Schmidt, Keshav Pujari, Ashok Giri, Jonathan Gershenzon, Vidya Gupta: *An oxidoreductase from 'Alphonso' mango catalyzing biosynthesis of furaneol and reduction of reactive carbonyls*. SpringerPlus 10/2013; 2(1). DOI:10.1186/2193-1801-2-494

### Book Chapters

1. Dar, S. M., Oak, P., Chidley, H., **Deshpande, A.**, Giri, A., Gupta, V., 2016. Chapter 19 - *Nutrient and Flavor Content of Mango (Mangifera indica L.) Cultivars: An Appurtenance to the List of Staple Foods* In: Nutritional Composition of Fruit Cultivars. (Eds. Preedy, Monique S.J. SimmondsVictor R.) Academic Press, San Diego, pp. 445-467.;



2. Gupta V. S., Giri A. P., Pandit S. S., Kulkarni R. S., Chidley H. G., **Deshpande A. B.**, Dar M. S. and Oak P. S., 2013, *Alphonso mango flavor: Blend and Biosynthesis*, In: *Biotechnology Beyond Borders* (Eds. MV Deshpande and J Ruiz-Herrera) CSIR-NCL, Pune, India, pp 103-121.

### Patents:

Sr. No	Title	Country	Application No
1	A nucleotide sequence of 9- <i>lipoxygenase</i> gene from mango	IN	201611011374
2	A nucleotide sequence of <i>epoxide hydrolase2</i> gene from mango	IN	201611011975
3	A nucleotide sequence of <i>o-methyl transferase</i> gene from Alphonso mango	IN	1795/DEL/2015
4	A nucleotide sequence of <i>o-methyl transferase</i> gene from Alphonso mango	WO	PCT/IN2016/050184

### Workshops and Conferences

- International Symposium on “Proteomics Beyond Ids... and 4<sup>th</sup> annual meeting of Proteomics Society (India)”; 22-24 November 2012 at CSIR-NCL, Pune
- National Seminar on “Exploring Strategies for Enhancement of Secondary Metabolites in Medicinal Plants”; 13-14 February 2013 at Department of Botany, University of Pune
- Symposium on “Accelerating Biology 2013”; 20-22 February 2013 at C-DAC, Pune
- Hands-on training: Implementing NGS for genomics and epigenetics studies; 24<sup>th</sup> -27<sup>th</sup> February 2014 at IISER, Pune
- A one day workshop on “ Insights in Biology 2025”; October 29, 2015 at CSIR-NCL, Pune

### Posters and Awards

- A poster titled “ **Study of lactone biosynthesis in Alphonso mango**” presented during 26- 27 February 2013, as a part of National Science Day celebrations 2013 at CSIR-NCL, Pune
- **NCL RF- Agnimitra Memorial Best Poster Award 2015** received in the area of Biological Sciences for the poster titled “**Recombinant and Transient Expression of Epoxide hydrolase gene from Alphonso Mango**” presented on 25<sup>th</sup> and 26<sup>th</sup> February 2015, as a part of National Science Day celebrations 2015 at CSIR-NCL, Pune